

The role of PTX3 in brain inflammation and repair

A thesis submitted to The University of Manchester for the degree of
Doctor of Philosophy in the Faculty of Life Sciences

2014

Beatriz Rodriguez Grande

List of contents

List of contents	2
List of figures	8
List of tables	11
Abbreviations	12
Abstract	17
Declaration	18
Copyright statement	19
Acknowledgements	21
Overview and justification of the use of alternative format.....	23
Authorship details	24
Chapter 1: Introduction	27
1.1 Brain inflammation in stroke	28
1.1.1 Ischaemic injury	29
1.1.1.1 The acute phase of ischaemic brain injury.....	29
1.1.1.1.1 Neurones.....	31
1.1.1.1.2 The blood-brain barrier	31
1.1.1.1.3 Endothelial cells	32
1.1.1.1.4 Pericytes	33
1.1.1.1.5 Astrocytes	33
1.1.1.1.6 Basement membrane	34
1.1.1.1.7 Oedema.....	35

1.1.1.1.8	Neutrophils	36
1.1.1.1.9	Microglia and macrophages	37
1.1.1.1.10	Cytokines: interleukin-1	38
1.1.1.2	Interplay between central and peripheral inflammatory responses	39
1.1.1.2.1	Central inflammation.....	39
1.1.1.2.2	Peripheral inflammation	40
1.1.1.3	Pro-/anti-inflammatory balance	41
1.1.1.3.1	Microglia and macrophage polarisation	41
1.1.1.3.2	Glial scar.....	42
1.1.1.4	Repair mechanisms	43
1.1.1.4.1	Angiogenesis	43
1.1.1.4.2	Neurogenesis	45
1.1.2	Remote damage.....	46
1.1.2.5	The substantia nigra.....	47
1.1.2.6	Neurotransmitters in the SN	48
1.1.2.7	Remote inflammation and remote neurodegeneration.....	49
1.1.3	The search for new targets for stroke treatment.....	50
1.2	Pentraxin 3	51
1.2.1	Pentraxins.....	51
1.2.2	PTX3 as a biomarker.....	52
1.2.3	PTX3 expression	52
1.2.4	PTX3 from gene to protein	53
1.2.5	PTX3 ligands and functions	56
1.2.5.8	Peripheral functions	56
1.2.5.8.1	Pathogen recognition	56

1.2.5.8.2	ECM stability and fertility	57
1.2.5.8.3	Neutrophil infiltration.....	57
1.2.5.8.4	Vascular events.....	58
1.2.5.8.5	Other peripheral functions	59
1.2.5.9	Central functions.....	60
1.3	Rationale for studying PTX3 in stroke	60
1.4	Aims and objectives	62
Aim 1.....		62
Objectives to aim 1.....		62
Aim 2.....		62
Objectives to aim 2.....		62
Chapter 2:	Supplementary Materials and Methods	63
2.1	Materials.....	64
2.2	Methods.....	64
2.2.1	PTX3 genotyping	64
2.2.2	Middle cerebral artery occlusion.....	64
2.2.3	Bromodeoxyuridine (BrdU) injections	65
2.2.4	Behavioural tests	65
2.2.4.1	Motor scores	66
2.2.4.2	Y maze test.....	66
2.2.4.3	Open field	66
2.2.5	Tissue collection.....	67
2.2.6	Cell or tissue processing.....	67
2.2.7	Enzyme-linked immunosorbent assay.....	68
2.2.8	Bicinchoninic acid assay	69

2.2.9	Immunofluorescence	69
2.2.10	Brain damage assessment.....	70
2.2.10.1	Cresyl violet staining	70
2.2.10.2	IgG staining.....	70
2.2.10.3	Calculation of brain damage	71
2.2.11	Cell cultures	71
2.2.11.1	Primary neuronal cultures.....	71
2.2.11.2	Mixed glial cultures	72
2.2.11.3	Mouse brain endothelial cell (MBEC) cultures	72
2.2.11.4	Neutrophil isolation	73
2.2.12	Cell treatments	74
2.2.13	Neutrophil transmigration and neurotoxicity assays.....	74
2.2.14	Lactate dehydrogenase assay	75
2.2.15	MTT assay.....	75
2.2.16	Microscopy/Image acquisition and image analysis.....	76
2.2.17	Statistical analysis	76
Chapter 3: The role of PTX3 in brain damage and inflammation after cerebral ischaemia (research article).....		78
Additional supplementary information to Chapter 3		79
Chapter 4: PTX3 in angiogenesis and neurogenesis (research article).....		81
Chapter 5: The role of PTX3 in post-stroke inflammation		82
5.1	Introduction.....	83
5.2	Materials and Methods	83
5.2.1	MCAo and brain sample processing	83
5.2.2	Neutrophil infiltration	84

5.2.3	Neutrophil neurotoxicity	84
5.2.4	Glial and vascular activation.....	84
5.3	Results.....	85
5.3.1	The role of PTX3 in neutrophil migration and toxicity	85
5.3.2	The role of PTX3 in vascular activation after MCAo.....	88
5.3.3	PTX3 in astrocytic activation after MCAo	89
5.3.4	The role of PTX3 in microglial/macrophage activation after MCAo	91
5.4	Discussion	92
Chapter 6: Loss of substance P and inflammation precede delayed neurodegeneration in the substantia nigra after cerebral ischaemia (research article)		
		96
Chapter 7: The role of PTX3 in remote inflammation and neurodegeneration after cerebral ischaemia (research article).....		
		97
Chapter 8: Discussion		
		98
8.1	Introduction.....	99
8.2	Interpretation of results	100
8.2.1	PTX3 expression.....	100
8.2.2	Neuroprotection and inflammation	100
8.2.3	Angiogenesis and neurogenesis	108
8.2.4	Functional outcome.....	111
8.2.5	Remote damage.....	112
8.3	Hypothesis about the mechanisms of action of PTX3	113
8.3.1	Aggregation/pH hypothesis.....	113
8.3.2	Concentration hypothesis	114
8.4	Limitations of the study	115
8.5	Future work.....	117

8.6	Conclusions and implications	120
Appendix 1	123
Materials	124
References	130

Word count: 53,878

List of figures

Chapter 1

Figure 1. Brain inflammatory response and its contribution to neurotoxicity	30
Figure 2. Common elements of angiogenesis and neurogenesis.....	44
Figure 3. Striato-nigral circuitry.....	48
Figure 4. Structure of PTX3 gene and protein	55

Chapter 3 (*page numbers correspond to the article, but not the thesis, pagination*)

Figure 1. Cerebral ischemia drives pentraxin-3 (PTX3) expression in the brain.....	12
Figure 2. Central, but not peripheral pentraxin-3 (PTX3) expression is interleukin-1 (IL-1) dependent after cerebral ischemia	14
Figure 3. Interleukin-1 (IL-1) but not ischemic, excitotoxic or oxidative stimuli induce PTX3 release <i>in vitro</i>	16
Figure 4. Lack of pentraxin-3 (PTX3) does not affect brain damage acutely after middle cerebral artery occlusion (MCAo).....	18
Figure 5. Pentraxin-3 (PTX3) knockout (KO) mice show increased blood-brain barrier (BBB) damage and edema, and impaired glial responses compared to wild type (WT) mice, 6 days after middle cerebral artery occlusion (MCAo)	20
Errata.....	25
Supplementary figure 1. Representative example showing a PCR gel used for genotyping of littermates.....	28
Supplementary figure 2. PTX3 ELISA on plasma samples from mice after 30min MCAo and 48 h reperfusion.....	28

Supplementary figure 3. Vascular density in WT and PTX3 KO mice	29
Supplementary figure 4. CD45-PTX3 immunostaining.....	29
Supplementary figure 5. Quantification of vascular and BBB proteins.....	30
Additional supplementary information to Chapter 3	
Figure 1. Neuroprotection by endogenous PTX3	80
Figure 2. Scar thickness and astrocytic proliferation in the scar are not altered by PTX3 6 days after MCAo	80
Chapter 4 (<i>page numbers correspond to the article, but not the thesis, pagination</i>)	
Figure 1. PTX3 KO mice have less vasculature in the striatum than WT mice during the recovery phase	9
Figure 2. Lack of PTX3 impairs angiogenesis 14 days after MCAo	10
Figure 3. VEGFR2 is reduced in PTX3 KO mice 14 days after MCAo	11
Figure 4. PTX3 deficiency impairs neurogenesis in the ischaemic brain 6 days after MCAo.....	12
Figure 5. NSPC proliferation is not altered by PTX3 deficiency 14 days after MCAo	13
Figure 6. PTX3 deficiency impairs <i>in vitro</i> neurogenesis.....	15
Figure 7. PTX3 KO mice have increased rotational bias 14 days after MCAo	16
Chapter 5	
Figure 1. PTX3 depletion promotes neutrophil recruitment 48 h after MCAo but prevents neutrophil recruitment 14 days after MCAo.....	86
Figure 2. Lack of PTX3 leads to decreased neutrophil transmigration but increased neutrophil toxicity in a cell-autonomous manner <i>in vitro</i>	87
Figure 3. PTX3 does not affect blood vessel activation after MCAo	88

Figure 4. Level of astrogliosis is not affected by lack of PTX3 48 h and 14 days after MCAo.....	90
Figure 5. Lack of PTX3 does not affect the amount of activated microglia 48 h or 14 days after MCAo	92
Chapter 6 (<i>page numbers correspond to the article, but not the thesis, pagination</i>)	
Figure 1. MCAo leads to ischemic damage in the striatum and focal loss of SP in the SN.....	9
Figure 2. Neuroinflammation is induced in the SN within 24 h reperfusion after MCAo.....	11
Figure 3. No significant cell loss occurs in the SN after 45 min MCAo during 24 h reperfusion.....	13
Figure 4. Mild focal cerebral ischemia results in loss of SP and inflammation in the SN without inducing significant neuronal damage	15
Figure 5. No changes in SP levels, inflammation or neuronal death are observed in the SN 4 h after mild (30 min) MCAo	17
Figure 6. Neuronal death is accompanied by sustained SP loss and inflammatory changes in the SN 6 days after mild MCAo.....	19
Figure 7. Dopaminergic neuronal loss follows inflammation and SP loss without worsening general motor function.....	21
Chapter 7 (<i>page numbers correspond to the article, but not the thesis, pagination</i>)	
Figure 1. Inflammatory response in the SN 48 h after MCAo	8
Figure 2. Neuronal death in the SN 48 h after MCAo	9
Figure 3. Inflammatory response in the SN 6 days after MCAo.....	11
Figure 4. Neuronal death in the SN 6 days after MCAo	13

List of tables

Table 1. Reagents	124
Table 2. Primary antibodies	126
Table 3. Secondary antibodies	127
Table 4. Equipment and software.....	127
Table 5. Cell media and buffers	128

Abbreviations

µl	Microlitres
aa	Aminoacids
Ab	Antibody
AD	Alzheimer's Disease
AP-1	Activator protein-1
APP	Acute phase protein
AQP-4	Aquaporin 4
BBB	Blood-brain barrier
BCA	Bicinchoninic acid
BDNF	Brain-derived neurotrophic factor
BrdU	Bromo deoxyuridine
BSA	Bovine serum albumin
CBF	Cerebral blood flow
CNS	Central nervous system
CoCl ₂	Cobalt chloride
CRP	C reactive protein
CSF	Cerebrospinal fluid
Cys	Cysteine
DAB	3,3'-diaminobenzidine
DAMPs	Danger-associated molecular patterns
DAPI	4',6-diamino-2-phenylindol

DCX	Doublecortin
DG	Deoxyglucose
DIV	Day <i>in vitro</i>
DMEM	Dulbecco's Modified Eagle Medium
DMSO	Dimethyl sulfoxide
DNA	Deoxyribonucleic acid
EC	Endothelial cells
ECA	External carotid artery
ECM	Extracellular matrix
EGF	Epidermal growth factor
ELISA	Enzyme-linked immunosorbent assay
ERK	Extracellular signal-regulated protein kinase
EtOH	Ethanol
FCS	Foetal calf serum
FC γ R	Fragment crystallisable γ receptor
FGF2	Fibroblast growth factor 2
FH	Factor H
FUDR	5,-fluoro-2-deoxyuridine
GABA	Gamma-amminobutyric acid
h	Hours
HC	Heavy chain
HIF	Hypoxia inducible factor
HRP	Horseradish peroxidase
HT	Heat treated
I α I	Inter α trypsin inhibitor

Iba1	Ionised calcium binding adaptor molecule 1
ICAM	Intercellular adhesion molecule
IFN	Interferon
Ig	Immunoglobulin
IgSF	Immunoglobulin superfamily
IκB	I kappa B
IKK	I kappa B kinase
IL	Interleukin
IL-1R	Interleukin 1 receptor
IL-1RA	Interleukin 1 receptor antagonist
i.p.	Intraperitoneal
IRAK	Interleukin 1 receptor-associated kinase
JNK	c-Jun N-terminal protein kinase
KDa	Kilodaltons
KO	Knockout
LDH	Lactate dehydrogenase
LPS	Lipopolysaccharide
MAPK	Mitogen-activated protein kinase
MBECs	Mouse brain endothelial cells
MBP	Myelin basic protein
MCA	Middle cerebral artery
MCAo	Middle cerebral artery occlusion
min	Minutes
ml	Mililitres
MMPs	Matrix metalloproteinases

MyD88	Myeloid differentiation factor 88
NET	Neutrophil extracellular trap
NeuN	Neuronal nuclei
NF IL-6	Nuclear factor interleukin 6
NF-κB	Nuclear factor kappa B
NK1	Neurokinin-1
NK1R	Neurokinin-1 tachykinin receptor
NMDA	N-methyl D-aspartate
NO	Nitric Oxide
NSPC	Neural stem progenitor cell
PAMPs	Pathogen-associated molecular patterns
PD	Parkinson's Disease
PECAM	Platelet endothelial cell adhesion molecule
PFA	Paraformaldehyde
PSGL-1	P-selectin glycoprotein 1
PTX	Pentraxin
ROS	Reactive oxygen species
RT	Room temperature
SAP	Serum Amyloid P component
SEM	Standard error of the mean
SJC	Sandra J. Campbell anti-granulocyte serum
SN	Substantia nigra
SNc	Substantia nigra compacta
SNr	Substantia nigra reticulata
SP	Substance P

SP1	Selective promoter factor 1
SVZ	Subventricular zone
TGF	Transforming growth factor
TH	Tyrosine hydroxylase
TJ	Tight junction
TNF	Tumour necrosis factor
TLR	Toll-like receptor
tPA	Tissue plasminogen activator
TSG	Tumour necrosis factor-stimulated gene
VCAM	Vascular cell adhesion molecule
VEGF	Vascular endothelial growth factor
VEGFR	Vascular endothelial growth factor receptor
v/v	Volume/volume
w/v	Weight/volume
WT	Wild type
ZO-1	Zonula occludens-1

Abstract

The University of Manchester

Beatriz Rodriguez Grande

Doctor of Philosophy

2014

The role of PTX3 in brain inflammation and repair

Pentraxin 3 (PTX3) is an acute phase protein which regulates peripheral inflammation and it has been suggested to have neuroprotective properties. Inflammation is commonly associated with poor outcome during diverse central nervous system (CNS) disorders, but the role of PTX3 in brain inflammation is completely unknown. We studied the role of PTX3 in brain inflammation and repair after stroke, a CNS disorder which is the third cause of death worldwide. To induce ischaemic stroke, we used the middle cerebral artery occlusion (MCAo) model and found that the pro-inflammatory cytokine interleukin (IL)-1 was the inducer of PTX3 expression in the brain. The analysis of markers of inflammation and repair up to 14 days after MCAo in wild type and PTX3 knockout (KO) mice revealed that, in general, lack of PTX3 has a negative effect on recovery after MCAo. PTX3 KO mice had delayed oedema resolution, defective glial scar, impaired microglial proliferation and reduced angiogenesis and neurogenesis. Therefore, PTX3 emerges as a target for stroke recovery and possibly other CNS inflammatory diseases. PTX3 was, however, not involved in remote neurodegeneration in the substantia nigra (SN) (an area of the brain remote but connected with the area affected by the stroke), but we observed that remote inflammation preceded remote neuronal death in the SN. Therefore, prevention of remote inflammation may help prevent remote neurodegeneration in the SN after stroke. This could have long term implications in SN neurodegeneration, which is a key pathological feature of Parkinson's disease.

Declaration

I declare that no portion of the work referred to in this thesis has been submitted in support of an application for another degree or qualification of this or any other university or other institute of learning.

Copyright statement

- i.** The author of this thesis (including any appendices and/or schedules to this thesis) owns certain copyright or related rights in it (the “Copyright”) and s/he has given The University of Manchester certain rights to use such Copyright, including for administrative purposes.
- ii.** Copies of this thesis, either in full or in extracts and whether in hard or electronic copy, may be made only in accordance with the Copyright, Designs and Patents Act 1988 (as amended) and regulations issued under it or, where appropriate, in accordance with licensing agreements which the University has from time to time. This page must form part of any such copies made.
- iii.** The ownership of certain Copyright, patents, designs, trade marks and other intellectual property (the “Intellectual Property”) and any reproductions of copyright works in the thesis, for example graphs and tables (“Reproductions”), which may be described in this thesis, may not be owned by the author and may be owned by third parties. Such Intellectual Property and Reproductions cannot and must not be made available for use without the prior written permission of the owner(s) of the relevant Intellectual Property and/or Reproductions.
- iv.** Further information on the conditions under which disclosure, publication and commercialisation of this thesis, the Copyright and any Intellectual Property and/or Reproductions described in it may take place is available in the University IP Policy (see <http://www.campus.manchester.ac.uk/medialibrary/policies/intellectual-property.pdf>), in any relevant Thesis restriction declarations deposited in the

University Library, The University Library's regulations (see <http://www.manchester.ac.uk/library/aboutus/regulations>) and in The University's policy on presentation of Theses

Acknowledgements

I would like to say a big thank you to my supervisors Emmanuel and Adam for all their patience and encouragement. I would like to thank Emmanuel for the detailed feedback in every set of results, every manuscript, abstract or poster I have had to prepare, and thanks for taking the time to correct even little things like grammar, orthography, etc. And thanks to Adam for his contagious enthusiasm towards Science, for teaching me such a wide range of techniques and taking the time to explain the scientific background of every experimental setp. Thanks to both of them for trusting me to supervise students, for giving me the freedom to organise my time and experiments, and for their useful advice on manuscript preparation and publication without which I would have not been able to write any paper, nor this thesis. Also thank you to my advisor Richard Grencis for his constant optimism and for providing a different perspective to my research.

Thanks also to everyone in the lab: all PIs and post-docs for always making interesting observations to strengthen my research (especially thanks to Sylvie for her encouragement and for being such an inspirational scientist); the technicians, always ready to give a hand whenever it was needed (thanks in particular to Kat Smedley for all the genotyping and re-genotyping) and all the other PhD students for sharing the ups and downs of research. Thanks to Katie, Hannah, Mike, Georgia, Natasha, Emily, Isaura, etc for all the fun in the lab, in the pub or in the netball court. Also thanks to the students I have supervised, for their contribution to the project and for their enthusiasm even towards routine experiments.

I would also like to thank Simon and Simone Collins for funding this project, for taking the time to follow closely the development of our research and, more broadly, for their interest in learning about the impact of biomedical research.

Finally, thanks to everyone that has made of my time in Manchester such a wonderful time, especially to Christina, Hannah and all my housemates, and thanks to my parents for encouraging me to study something that I really like, for understanding my decision to continue my education abroad and for their constant support in every step I take.

Overview and justification of the use of alternative format

Thesis chapters address the role of PTX3 and inflammation in damage and repair after cerebral ischaemia in different areas of the brain and different times of recovery. The first three chapters of results focus on the role of PTX3 in the ischaemic area up to one week (Chapter 3) or two weeks (Chapters 4 and 5) after the ischaemic event. Chapters 6 and 7 look at the role of PTX3 in remote brain injury after stroke: Chapter 6 contains the characterisation of remote damage (brain injury in a region that is connected to the primary area of damage) and inflammation after ischaemic stroke, and Chapter 7 details the role of PTX3 in remote damage and inflammation after ischaemic stroke.

Most of the results are already written in a research paper format, and a substantial part of the work has already been published. In order to avoid self-plagiarism, we considered the alternative format as the more appropriate way to present and discuss results in this thesis.

Page format, font style, font size and figure size from all publications have been adapted to the thesis format to improve readability. Reference format has also been modified to be consistent throughout the thesis, and all references are grouped in the References section, at the end of the thesis.

Authorship details

The results chapters contain the work of several authors. Here are the details of the contribution of each author to the work presented.

Chapter 1. Introduction.

Author: Beatriz Rodriguez-Grande

Chapter 2. Supplementary Materials and Methods.

Author: Beatriz Rodriguez-Grande

Chapter 3 (paper format). The role of PTX3 in brain damage and inflammation after cerebral ischaemia

Authors: Beatriz Rodriguez-Grande, Matimba Swana, Loan Nguyen, Pavlos Englezou, Samaneh Maysami, Stuart M. Allan, Nancy J. Rothwell, Cecilia Garlanda, Adam Denes and Emmanuel Pinteaux

A.D., B.R.-G., M.S., L.N., P.E. and S.M. performed the experimental work (see detailed distribution below). C.G. provided the PTX3 KO mice and PTX3 antiserum. S.M.A., N.J.R. and C.G. critically reviewed the manuscript and contributed research ideas and tools. E.P., A.D. and B.R.-G. wrote the paper. E.P. and A.D. supervised the project.

Chapter 4 (paper format): Pentraxin-3 in angiogenesis and neurogenesis

Authors: Beatriz Rodriguez-Grande, Lidiya Varghese, Adam Denes and Emmanuel Pinteaux.

B.R.-G., L.V. and A.D. performed the experimental work (see detailed distribution below). B.R.-G. wrote the paper. E.P. and A.D. supervised the project.

Chapter 5 (not in paper format). The role of PTX3 in post-stroke inflammation

Authors: Beatriz Rodriguez-Grande, Charlotte Allen, Adam Denes and Emmanuel Pinteaux.

B.R.-G. and C.A. performed the experimental work (see detailed distribution below).

B.R.-G. wrote the chapter. E.P. and A.D. supervised the project.

Chapter 6 (paper format). Loss of substance P and inflammation precede neurodegeneration in the substantia nigra after cerebral ischemia

Authors: Beatriz Rodriguez-Grande, Victoria Blackabey, Beatrice Gittens, Emmanuel Pinteaux and Adam Denes.

A.D., B.R.-G., V.B. and B.G. performed the experimental work (see detailed distribution below). E.P., A.D. and B.R.-G. wrote the paper. E.P. and A.D. supervised the project.

Chapter 7 (paper format). The role of PTX3 in remote inflammation and neurodegeneration after cerebral ischaemia

Authors: Beatriz Rodriguez-Grande, Adam Denes and Emmanuel Pinteaux.

B.R.-G performed the experimental work and wrote the paper. E.P. and A.D. supervised the project.

Chapter 8. Discussion.

Author: Beatriz Rodriguez-Grande.

A.D. and B.R.-G. performed the surgeries to provide the tissue. The whole thesis project was supervised by E.P. and A.D.

The detailed distribution of the experimental work is indicated in the tables below.

Author(s) of the experiments shown in each figure are indicated. Thesis author is highlighted in blue.

Chapter 3		
Fig.	Letter	Author
1	A	A.D.
	B	A.D.
	C	B.R.-G.
	D	A.D.
	E	A.D.
	F	A.D.
	G	A.D.
	H	B.R.-G.
2	A	A.D./M.S.
	B	A.D./M.S.
	C	A.D./P.E.
3	A	L.N.
	B	A.D./M.S.
	C	A.D./M.S.
	D	B.R.-G.
4	A	B.R.-G.
	B	B.R.-G.
	C	B.R.-G.
	D	B.R.-G.
5	A	B.R.-G.
	B	B.R.-G.
	C	B.R.-G.
	D	B.R.-G.
	E	B.R.-G.
	F	S.M.

Supplementary information to Chapter 3	
Fig.	Author
1	B.R.-G.
2	B.R.-G.
3	B.R.-G.
4	B.R.-G.
5	B.R.-G.

Additional supplementary information to Chapter 3	
Fig.	Author
1	B.R.-G.
2	B.R.-G.

Chapter 4		
Fig.	Letter	Author
1	A	L.V./B.R.-G.
	B	L.V.
2	A	L.V.
	B	L.V./B.R.-G.
	C	L.V./B.R.-G.
3	A	L.V.
	B	L.V.
4	A	B.R.-G.
	B	B.R.-G.
5	A	B.R.-G.
	B	B.R.-G.
	C	B.R.-G.
	D	B.R.-G.
6	A	F.M.-H.
	B	F.M.-H.
7	A	B.R.-G.
	B	B.R.-G.
	C	B.R.-G.
	D	B.R.-G.
	E	B.R.-G.

Chapter 5		
Fig.	Letter	Author
1	A	B.R.-G.
	B	B.R.-G.
	C	B.R.-G.
	D	B.R.-G.
2	A	C.A.
	B	C.A.
3	A	B.R.-G.
	B	B.R.-G.
	C	B.R.-G.
4	A	B.R.-G.
	B	B.R.-G.
5	A	B.R.-G.
	B	B.R.-G.

Chapter 6		
Fig.	Letter	Author
1	A	A.D./B.G.
	B	A.D./B.G.
	C	V.B.
	D	A.D./B.G.
2	A	V.B.
	B	V.B./B.R.-G.
	C	V.B.
	D	V.B.
3	A	V.B.
	B	B.R.-G.
	C	B.R.-G.
	D	B.R.-G.
4	A	B.R.-G.
	B	B.R.-G.
	C	B.R.-G.
	D	B.R.-G.
	E	B.R.-G.
5	A	B.R.-G.
	B	B.R.-G.
	C	B.R.-G.
	D	B.R.-G.
6	A	B.R.-G.
	B	B.R.-G.
	C	B.R.-G.
7	A	B.R.-G.
	B	B.R.-G.
	C	B.R.-G.

Chapter 7	
Fig.	Author
1	B.R.-G.
2	B.R.-G.
3	B.R.-G.
4	B.R.-G.

Chapter 1: Introduction

1.1 Brain inflammation in stroke

Inflammation is a response of our body to injury or infection, in which cellular and humoral components are mobilised to fight infectious agents, clear dying cells and cell debris and promote repair. Inflammatory mechanisms were first identified in peripheral tissues, but it is now clear that both central and systemic immune processes are involved in diseases of the brain. It is also known that insults that are considered sterile (such as ischaemic injury) drive an inflammatory response that shares several mechanisms with those induced by infection. In both central and peripheral tissues, uncontrolled or unresolved inflammation is detrimental both in acute conditions such as stroke, and chronic conditions such as neurodegenerative disease, atherosclerosis or arthritis, where inflammation is a main contributor to disease progression (Medzhitov, 2010; Nathan & Ding, 2010).

Stroke is the leading cause of disability and the third most common cause of death worldwide (Bousser, 2012) and, as the average age of the population increases, the incidence of stroke, which was estimated in 16 million per year worldwide in 2011 (Wissel *et al.*, 2011), is expected to increase sharply. The severity of post-stroke disability drastically hinders the quality of life of patients and their families, and stroke-related services take over a considerable amount of the budget from health institutions. Indeed, post-stroke care costs £ 8 bn per year in the UK alone (McArthur *et al.*, 2011). Inflammation has been shown to play a key role in stroke, correlating with stroke severity (Jin *et al.*, 2010; Lambertsen *et al.*, 2012). Several anti-inflammatory approaches have been tested to reduce brain injury after stroke. However, most of these approaches have not been successful in clinical settings and, to date, only tissue plasminogen activator (tPA), a thrombolytic molecule, is approved

for stroke treatment (Iadecola & Anrather, 2011). Therefore it is essential to get a better insight into the interplay between inflammation and stroke pathophysiology and repair in order to find more effective treatments.

1.1.1 Ischaemic injury

Stroke can be ischaemic or haemorrhagic. Ischaemic stroke occurs when blood flow is blocked by the obstruction of an artery supplying the brain. Haemorrhagic stroke occurs when arteries or blood vessels are broken and blood leaks into the brain parenchyma. As the majority of strokes are ischaemic (Smith *et al.*, 2013), we have focused our research on this stroke type. We have used the transient middle cerebral artery (MCA) occlusion (MCAo) model, which is an experimental rodent model to study ischaemic brain injury (Durukan & Tatlisumak, 2007). Occlusion of the MCA, the most common ischaemic stroke type in patients (Durukan & Tatlisumak, 2007), stops blood flow into the striatum, creating an initial core of ischaemic damage in that area which spreads over time even after the reperfusion of the tissue. Infarct size varies depending on the length of occlusion (Durukan & Tatlisumak, 2007). Below is a summary of our current understanding of how brain damage occurs after ischaemic stroke, how repair mechanisms are initiated and the role of inflammation in these processes.

1.1.1.1 The acute phase of ischaemic brain injury

The early stage after an injury is known as the acute phase. In addition to a systemic acute phase response, the CNS undergoes rapid changes after the ischaemic event. The first phenomenon leading to brain damage after cerebral ischaemia is the ischaemic cascade. When blood flow stops, the lack of oxygen and glucose (ischaemia) prevents

the production of adenosine tri-phosphate (ATP). This energy failure disables ionic pump function, producing an increase in intracellular levels of Na^+ and Ca^{2+} . Increase in concentration of cations promotes cell swelling, and excessive Ca^{2+} activates intracellular enzymes which can eventually lead to necrotic or apoptotic cell death (Lipton, 1999). Different cells of the central nervous system (CNS) have different degrees of resilience to ischaemia and they respond in different ways to the ischaemic insult and the associated inflammatory response. Figure 1 depicts some basic steps of the brain inflammatory response and how they further contribute to neuronal death.

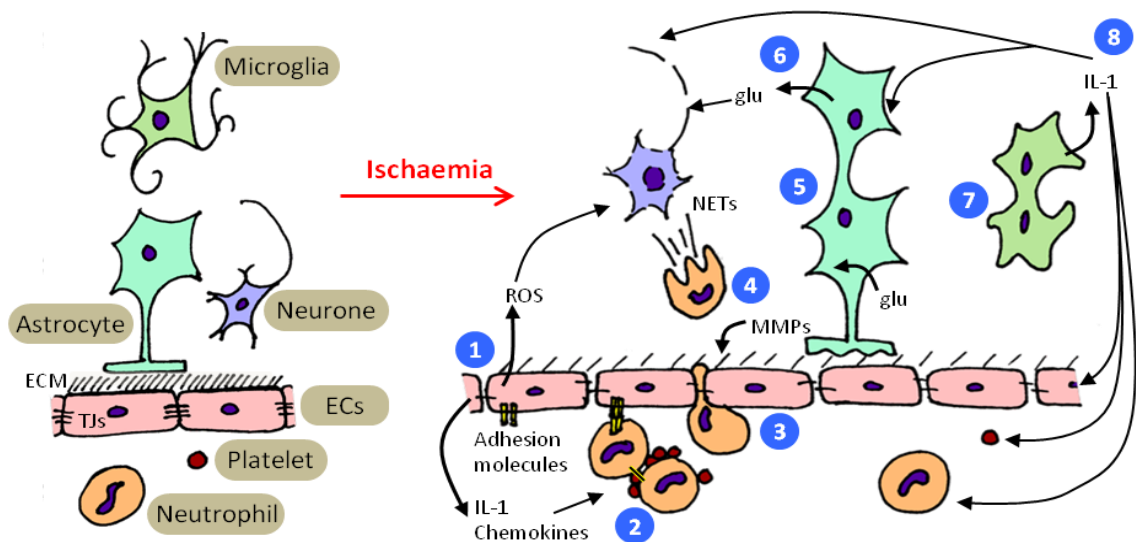


Figure 1. Brain inflammatory response and its contribution to neurotoxicity. Endothelial cells (ECs) are activated, expressing adhesion molecules and secreting reactive oxygen species (ROS), chemokines and proinflammatory cytokines such as interleukin (IL)-1 (1). Neutrophils and platelets are recruited and bind to adhesion molecules (2). Neutrophils infiltrate through the blood-brain barrier (BBB), loosened by a reduced amount of tight junction proteins (TJs) and extracellular matrix (ECM) degradation by matrix metalloproteinases (MMPs) (3). Neutrophil extracellular traps (NETs) further damage neurons (4), which are already affected by the ischaemic cascade. Astrocytes become activated, proliferate, and reduce excitotoxicity through intake of glutamate (glu) (5) until they undergo energy failure, in which case they

release glutamate and increase excitotoxicity (6). Activated microglia proliferate, acquire phagocytic activity and secrete large amounts of proinflammatory cytokines such as IL-1 (7), which amplifies the inflammatory response (8).

1.1.1.1.1 Neurones

Neurones are more sensitive to ischaemia than any other cell type in the brain and are therefore the first to undergo cell death (Lipton, 1999). Neuronal death happens quickly in the core of the infarct (the area depleted of blood supply) as a result of the ischaemic cascade detailed previously. Neurodegeneration is amplified by excitotoxicity, a process by which neuronal overexcitation leads to neuronal death: high levels of Na^+ retained in the cell alter glutamate transporters, forcing the release of glutamate into the extracellular space. Glutamate is an excitatory neurotransmitter and therefore it reinforces Ca^{2+} entry and thus facilitates the activation of apoptotic or necrotic pathways. Unlike in the infarct core, neuronal death does not happen immediately in the hypoperfused area around the infarct, called the penumbra. Collateral perfusion in the penumbra maintains neurones alive during the early stages after stroke, but those neurones do not have a healthy metabolic status and are prone to die if blood flow is not restored, or if other insults (such as glutamate-mediated excitotoxicity) arise (Moskowitz *et al.*, 2010). Neurones transmit information both within the brain and to the peripheral nervous system and thus brain damage can affect both central and peripheral functions, depending on the area of injury.

1.1.1.1.2 The blood-brain barrier

The blood-brain barrier (BBB) is the structure which separates circulating blood from the brain parenchyma. It is formed by endothelial cells (ECs), astrocyte endfeet,

pericytes and basement membranes of ECs and glia. This barrier regulates the transport of ions and proteins in and out of the brain and keeps macromolecules out of the brain parenchyma, maintaining a stable composition of cerebrospinal fluid (CSF), even when alterations happen in the peripheral circulation (Abbott *et al.*, 2010). The BBB is damaged after stroke, and an increase in its permeability has been observed both in experimental and clinical settings (Abbott *et al.*, 2010; Israeli *et al.*, 2010).

1.1.1.1.3 Endothelial cells

ECs are immediately affected as stroke happens, since the occlusion itself triggers shear stress and local platelet aggregation, which immediately activates the vessels and alters the function of the BBB (Iadecola & Anrather, 2011). ECs quickly produce oxidative substances such as reactive oxygen species (ROS) and express cell adhesion molecules (Dole *et al.*, 2005; Iadecola & Anrather, 2011). ROS can diffuse into the perivascular space and can damage neurones and activate glial cells (Love, 1999). Adhesion molecules contribute to the aggregation of platelets and leukocytes which further obstruct and activate the vessels. Adhesion molecules expressed on the luminal side of ECs include selectins, immunoglobulin gene superfamily (IgSF) (including intercellular cell adhesion molecule-1 (ICAM-1), vascular cell adhesion molecule-1 (VCAM-1) and platelet endothelial cell adhesion molecule-1 (PECAM-1)) and integrins (Zaremba & Losy, 2002).

In addition to alterations in adhesion molecules, levels of tight junction (TJ) proteins also vary. TJ are proteins that seal the intercellular space between ECs. For instance, claudin and occludin from adjacent ECs bind to each other and are anchored to intracellular zonula occludens (ZO) proteins which link to the actin cytoskeleton (Abbott *et al.*, 2010). After ischaemic stroke the levels of TJ proteins in the EC

membrane decrease, loosening the boundary between the vessel lumen and the brain parenchyma and allowing macromolecules and even peripheral cells to infiltrate (Jiao *et al.*, 2011).

Cytokines, which are potent soluble mediators of the inflammatory response, are also produced during the acute phase and, as it will be explained in section 1.1.1.1.10, cytokines reinforce this initial EC activation (Zaremba & Losy, 2002).

1.1.1.1.4 Pericytes

Pericytes are found mostly around the microvasculature, embedded in the basement membrane, generally located over TJ complexes (Balabanov & Dore-Duffy, 1998). They express α -smooth muscle actin (α -SMA), which contributes to the contractile action of pericytes, regulating blood flow (Dalkara *et al.*, 2011). After stroke, pericytes retract in response to oxidative stress, and they maintain constriction of the vessels for extended periods of time, even after reperfusion, hindering the restoration of normal cerebral blood flow (CBF) and thus contributing to neuronal death (Yemisci *et al.*, 2009).

1.1.1.1.5 Astrocytes

Astrocytes account for approximately half of the brain volume and they are generally identified by their characteristic expression of glial fibrillary acidic protein (GFAP), an intermediate cytoskeleton filament. Astrocytes are involved in the regulation of neuronal metabolism and synaptic function, as well as having an essential role as structural and extracellular matrix (ECM)-secreting components of the BBB (Chen & Swanson, 2003). Astrocytes have processes which sprout from their soma and whose ends surround the abluminal vessel wall. These structures are called astrocyte endfeet,

and they cover the vast majority of brain vessels, with the exception of scarce gaps where some microglia and neurones contact the basement membrane (Mathiisen *et al.*, 2010).

In areas with low oxygen availability but still partial glucose delivery such as the penumbra (Obrenovitch, 1995), astrocytes are capable of maintaining their energy production through anaerobic metabolism of glucose; however, this process is impaired in acidic conditions, in which energy production is limited (Swanson *et al.*, 1997). Astrocytes express high levels of ROS-scavenging enzymes and glutathione (Wilson, 1997), which dampen oxidative stress and can reduce neuronal death (Tanaka *et al.*, 1999). Astrocytes can also modulate glutamate-mediated excitotoxicity. On the one hand, healthy astrocytes can uptake large quantities of glutamate, reducing excitotoxicity. However, when energy production decreases (for instance, in anoxic and acidic conditions), glutamate intake decreases and even reverses, so that glutamate is released, worsening neuronal damage (Bonde *et al.*, 2003).

1.1.1.1.6 Basement membrane

The basement membrane is a net of ECM proteins. It is divided into the endothelial basement membrane (secreted by ECs), and the parenchymal basement membrane (secreted by astrocytes and other glial elements). It contains laminins (which account for most of the parenchymal basement membrane), fibronectin, collagen IV and heparan sulphate proteoglycans amongst other ECM molecules. The basement membrane serves as cell anchoring point, since cells from the BBB express ECM receptors (e.g., integrins) which bind to basement membrane components (e.g., collagen IV and laminin) (for a detailed review of basement membrane components and its receptors see (Baeten & Akassoglou, 2011)). In addition to providing structural

support, the basement membrane contributes to BBB functions through the bioactive properties of its components. For instance, cell-matrix interactions signal for processes like cell survival or proliferation, and mediate transmigration of peripheral cells into the brain (Hynes, 2002).

After stroke, cytokines such as IL-1 β and tumour necrosis factor (TNF)- α and hypoxia-induced factors such as hypoxia-inducible factor (HIF)-1 α , induce production of matrix metalloproteinases (MMPs) (Hosomi *et al.*, 2005; McMahon *et al.*, 2005; Ruhul-Amin *et al.*, 2003). MMPs degrade ECM components including collagen and laminin (Fukuda *et al.*, 2004). Some ECM receptors, including some integrins, are downregulated after stroke; therefore, cells from the BBB detach from the basement membrane after stroke and BBB structural integrity gets compromised, increasing permeability (del Zoppo & Milner, 2006). In addition, cell-matrix detachment can signal for cell death (Grossmann, 2002).

1.1.1.1.7 Oedema

As mentioned before, ischaemia induces an influx of cations into the cells which is followed by cell swelling. This event is called cytotoxic oedema, and happens independently of BBB disruption (Kahle *et al.*, 2009). As the amount of positive charges in the extracellular space decreases, cations from the peripheral circulation are mobilised into the brain parenchyma in a process called ionic oedema, which does not involve movement of fluid but only of ions (Kahle *et al.*, 2009). As the ischaemic cascade acts upon the ECs and the permeability of the BBB increases, an influx of fluid from the vascular lumen into the brain parenchyma occurs in order to stabilise the ionic differences caused by the previous ionic oedema. Once TJ complexes are disrupted, blood stream components leak into the site of injury, increasing protein

concentration in the brain parenchyma and promoting a further influx of water. The influx of fluid into the brain parenchyma that happens once BBB permeability is altered is known as vasogenic oedema (Kahle *et al.*, 2009). Apart from ionic transporters, water channels are also key players in oedema formation. Aquaporin-4 (AQP-4) is the main water transport channel, which acts as a passive pore in ECs and astrocytes and whose expression increases after stroke (Ribeiro *et al.*, 2006; Zelenina, 2010). Brain swelling due to oedema increases intracranial pressure, and it is one of the main factors that contributes to poor outcome in stroke patients, especially in those with large infarcts (Gupta *et al.*, 2004).

1.1.1.1.8 Neutrophils

Peripheral cells are also involved in the inflammatory response. Neutrophils are a type of granular leukocyte found in the blood stream which, upon activation, can infiltrate into damaged tissues and display phagocytic and cytotoxic activity. After stroke, neutrophils move towards the highest concentration of chemo-attracting molecules (chemokines), which are mostly produced in the site of injury (Minami & Satoh, 2003). Through interactions between adhesion molecules expressed by neutrophils and ECs, neutrophils enter the brain parenchyma by a multi-step mechanism. First, selectins make transient interactions with neutrophils (tethering), which facilitates the rolling of neutrophils over the endothelial lumen (Zaremba & Losy, 2002). One of the key interactions for tethering occurs between P-selectin glycoprotein 1 (PSGL-1) (which is translocated to the membrane of neutrophils) and P-selectin expressed by ECs (Dole *et al.*, 2005). Chemokines signal for the arrest of neutrophil rolling (Cinamon *et al.*, 2001) and ICAM-1, VCAM-1 and PECAM-1 form stronger contacts with EC integrins, which slow down the rolling (Zaremba & Losy, 2002). MMPs

released by neutrophils partially digest basement membrane and TJ components, facilitating transmigration (Rosenberg, 2002). Neutrophils acquire a neurotoxic phenotype when they transmigrate through the activated endothelium. Transmigration promotes the release of neutrophil extracellular traps (NETs), which are composed of decondensed DNA and proteases which are toxic to neurones (Allen *et al.*, 2012). Neutrophils also release oxidative molecules, cytokines and chemokines that exacerbate the damage and further amplify the inflammatory response (Jin *et al.*, 2010). The peak of neutrophil infiltration occurs around 48 h after the onset of stroke (Jin *et al.*, 2010), and the extent of neutrophil infiltration correlates with the severity of brain damage in clinical studies (Buck *et al.*, 2008; Price *et al.*, 2004).

1.1.1.1.9 Microglia and macrophages

Microglia are the resident macrophages of the brain. They constantly survey the environment and quickly change their phenotype after injury. Microglia become activated even before cell death happens, as soon as ROS or damage-associated molecular patterns (DAMPs, including intracellular proteins, nucleic acid fragments, ATP or uric acid) are released (Iadecola & Anrather, 2011; Piccinini & Midwood, 2010). When neurones die, the loss of neurone-microglia interactions, which contribute to the resting state of microglia, can trigger microglial activation (Iadecola & Anrather, 2011; Piccinini & Midwood, 2010). Activated microglia start producing pro-inflammatory cytokines within minutes, and this increases tissue damage (Jin *et al.*, 2010).

Macrophages from the peripheral circulation are recruited to the site of injury in a similar way to that of neutrophils (Ley *et al.*, 2007), and they become activated displaying similar activity and expressing identical cellular markers to those expressed

by activated microglia. Recent studies using chimeric mice have shown that by the time peripheral macrophages are recruited there is already a significant amount of activated microglia (Schilling *et al.*, 2003) and that phagocytic activity is displayed mostly by resident microglia rather than infiltrated macrophages (Jin *et al.*, 2010; Schilling *et al.*, 2005). In fact, phagocytosis of neutrophils seems to be one of the key features of resident microglia (Denes *et al.*, 2007).

1.1.1.1.10 Cytokines: interleukin-1

As a consequence of the phenotypic changes in the cells of the CNS that occur after ischaemia, several soluble factors are secreted, including cytokines. TNF- α , IL-6 and IL-1 are well characterised as pro-inflammatory cytokines, whose expression highly increases (up to 60 fold) after experimental stroke (Lambertsen *et al.*, 2012). In particular, IL-1 is considered one of the most potent pro-inflammatory cytokines. The IL-1 family is composed of two ligands: IL-1 α and IL-1 β , which bind IL-1 receptor type 1 (IL-1R1) with similar affinity (Sims *et al.*, 1988). Activation of IL-1R1 activates the mitogen-activated protein kinase (MAPK) and nuclear factor kappa B (NF- κ B) pathways, leading to expression of several downstream inflammatory mediators and thus amplifying the inflammatory response (O'Neill & Greene, 1998). IL-1 expression is low in basal conditions but it rapidly increases after brain injury (Lambertsen *et al.*, 2012). All cell types in the CNS are able to produce IL-1, but microglia are the main producers (Pinteaux *et al.*, 2009). Passive diffusion of IL-1 activates surrounding cells and quickly spreads the inflammatory response.

High concentrations of IL-1 increase neuronal depolarisation and activate pathways of cytokine production. However, it is thought that neurotoxic actions of IL-1 are primarily mediated by glial-secreted substances including free radicals, cytokines and

proteases (Pinteaux *et al.*, 2009). Astrocytes proliferate in response to IL-1, and they produce proteases (including MMP-9), nitric oxide (NO), growth factors such as vascular endothelial growth factor (VEGF), and more cytokines and chemokines. Isolated microglia are much less responsive to IL-1 than other cell types but, in the presence of other cells, IL-1 indirectly induces microglial proliferation and secretion of pro-inflammatory molecules (Pinteaux *et al.*, 2002; Pinteaux *et al.*, 2009). In ECs, IL-1 induces ICAM-1 and VCAM-1 expression (Zaremba & Losy, 2002), promoting leukocyte recruitment (Ley *et al.*, 2007). IL-1 also induces the production of vasodilating agents such as NO (Juttler *et al.*, 2007) and vasoconstrictor agents such as endothelin (Skopal *et al.*, 1998). The combined effects of IL-1 during the acute phase of brain injury worsen the initial ischaemic damage. Indeed, addition of IL-1 increases infarct size after MCAo (Loddick & Rothwell, 1996) and genetic deletion of IL-1 (Boutin *et al.*, 2001) or blockade of IL-1 by administration of IL-1 receptor antagonist (IL-1RA) (Loddick & Rothwell, 1996) decrease infarct size.

1.1.1.2 Interplay between central and peripheral inflammatory responses

1.1.1.2.1 Central inflammation

In summary, during the acute phase after stroke, ischaemia induces quick neuronal death; and the shear stress of the occlusion activates ECs, which produce ROS and express adhesion molecules. DAMPs from cell debris and oxidative stress are recognised by microglia, astrocytes and ECs, which start producing soluble mediators (e.g. cytokines and chemokines) that propagate the inflammatory response. Microglia, in particular, are one the main producers of IL-1. Effector cells and molecules are then

activated: microglia proliferate and acquire a phagocytic phenotype; ECs facilitate recruitment of macrophages and neutrophils from the circulation; neutrophils release oxidative molecules and proteases which degrade basement membrane components; astrocytes proliferate around the infarct core and increase expression of water channels (e.g. AQP-4) in their end-feet. These effects, amongst others, occur in the CNS; however, soluble mediators of inflammation diffuse into the blood stream and activate a peripheral inflammatory response.

1.1.1.2.2 Peripheral inflammation

Circulating pro-inflammatory cytokines and chemokines activate peripheral targets leading to activation of the autonomic nervous system, fever, metabolic changes and expression of acute phase proteins (APPs). APPs are proteins whose expression varies by at least 25 % after an acute insult (Ceciliani *et al.*, 2002). APPs include coagulation factors, pro- and anti-inflammatory molecules, components of the complement system and some pentraxin proteins, which will be described in detail in section 1.2. The systemic acute phase provides a fast non-specific defence response during the first days after the acute insult (Ceciliani *et al.*, 2002).

Since cytokines are key inducers of the acute phase response, pre-existing peripheral inflammation can facilitate this systemic reaction. In fact, pre-existing inflammation is associated with worse stroke outcome (Denes *et al.*, 2010). Moreover, risk factors for stroke such as ageing and comorbidities are associated with inflammatory changes, which reinforces the relevance of inflammation (both central and peripheral) in stroke incidence and outcome (Smith *et al.*, 2013).

1.1.1.3 Pro-/anti-inflammatory balance

Increased expression of pro-inflammatory signals is characteristic of the acute phase. Following the acute phase, the pathways of production of pro-inflammatory molecules are inhibited, expression of anti-inflammatory cytokines such as IL-10, IL-4 and transforming growth factor (TGF)- β becomes more prominent, and resolution of inflammation starts (Nathan & Ding, 2010). In addition, the same pro-inflammatory cytokines can possibly exert different effects at later stages. For instance, it has been shown that the inflammatory actions of IL-1 upon neurones and glial cells are concentration and time dependent (Pinteaux *et al.*, 2009).

The change in the pro/anti-inflammatory balance alters the phenotype of surrounding cells, which start signalling to promote resolution of inflammation and brain repair.

1.1.1.3.1 Microglia and macrophage polarisation

As mentioned above, early oxidative stress and neuronal death, amongst others, can trigger microglial activation. This early activation is characterised by a pro-inflammatory expression profile which is generally associated with increased brain damage (Banati *et al.*, 1993). When surrounding signals change (DAMPs from cell debris get cleared, pro-/anti-inflammatory cytokine balance changes), the phenotype of microglial activation is also altered. The switch in phenotype has been mostly studied in macrophages. Pro-inflammatory signals induce an M1-type activation characterised by NO and pro-inflammatory cytokine expression which worsens CNS damage (Kigerl *et al.*, 2009). In the presence of anti-inflammatory signals, however, macrophages acquire a M2-type phenotype which induces resolution of inflammation in the CNS (Kigerl *et al.*, 2009).

Microglial cells are also able to acquire M1 and M2 phenotypes in response to pro-/anti-inflammatory signals *in vitro*. After cerebral ischaemia, however, microglial cells do not express the characteristic M1 or M2 markers (Girard *et al.*, 2013), although they are still thought to contribute to resolution of brain damage. For instance, reduced microglial proliferation correlates with increased brain damage after experimental stroke (Denes *et al.*, 2007), and there is increasing evidence that microglia can be neuroprotective. Activated microglia phagocytose neuronal debris (Schilling *et al.*, 2005) and neutrophils (Denes *et al.*, 2007) after focal ischaemia, and they can increase neuronal survival (Butovsky *et al.*, 2005).

1.1.1.3.2 Glial scar

Astrocytes change their behaviour and anatomical distribution after acute injury. They rapidly proliferate around the core of the infarct forming part of a structure called the glial scar. The glial scar is formed not only by astrocytes, but also by microglia, macrophages and deposited ECM. The glial scar is essential for limiting brain injury by limiting the spread of toxic substances and contributing to restoration of homeostasis. Activated astrocytes help detoxifying the environment by buffering ROS and excitotoxic molecules. In addition, microglia and macrophages clean off debris and secrete anti-inflammatory mediators. At later stages, astrocytes and ECM components also provide structural support for angiogenesis. Unfortunately, the composition of the ECM within the glial scar inhibits axonal growth, which limits the formation of new synaptic contacts (Rolls *et al.*, 2009).

1.1.1.4 Repair mechanisms

The pro-/anti-inflammatory switch and the clearance of debris are the first steps to initiate brain repair and formation of new neurones (neurogenesis) and vessels (angiogenesis), two closely linked phenomena (Figure 2).

1.1.1.4.1 Angiogenesis

Angiogenesis is the process by which new vessels sprout from the existing vasculature. Angiogenesis critically determines the evolution of core into penumbral tissue since availability of blood flow is essential for the survival of neurones in the penumbra (Moskowitz *et al.*, 2010). Indeed, survival after stroke correlates with the formation of new blood vessels in the penumbra (Krupinski *et al.*, 1994). Astrocytic support is essential for angiogenesis, not only as scaffolding, but also for the secretion of the required ECM (Zhao & Rempe, 2010). In addition to *de novo* secretion of ECM, there is also strong remodelling of the pre-existing ECM, in which MMPs play a pivotal role.

ECM remodelling is accompanied by production of factors that induce EC proliferation and migration. These factors include VEGF, fibroblast growth factor (FGF) and TGF- β , which are naturally produced in the brain in response to injury (Slevin *et al.*, 2006). VEGF is thought to be one of the most potent angiogenic stimuli, acting through the activation of VEGF receptor 2 (VEGFR2), present in ECs (Beck & Plate, 2009). VEGF also signals for astrocytic proliferation and motility (Wuestefeld *et al.*, 2012). The expression of VEGFR2 increases after ischaemia, primarily in the penumbra, followed by the core (Marti *et al.*, 2000). In addition to its angiogenic effect, VEGF increases vascular permeability, which can induce oedema and brain damage, especially during the acute phase when BBB permeability is already above

physiological levels (Slevin *et al.*, 2006). Therefore, whilst delayed VEGF actions are thought to be beneficial, early VEGF administration does not seem to help recovery (Zhang *et al.*, 2000). In addition, VEGF is implicated in pathological angiogenesis (Hicklin & Ellis, 2005).

A peak of vascular proliferation, occurs three days after stroke, although variations in angiogenesis-related genes occur as early as 1 h after the ischaemic event (Hayashi *et al.*, 2003).

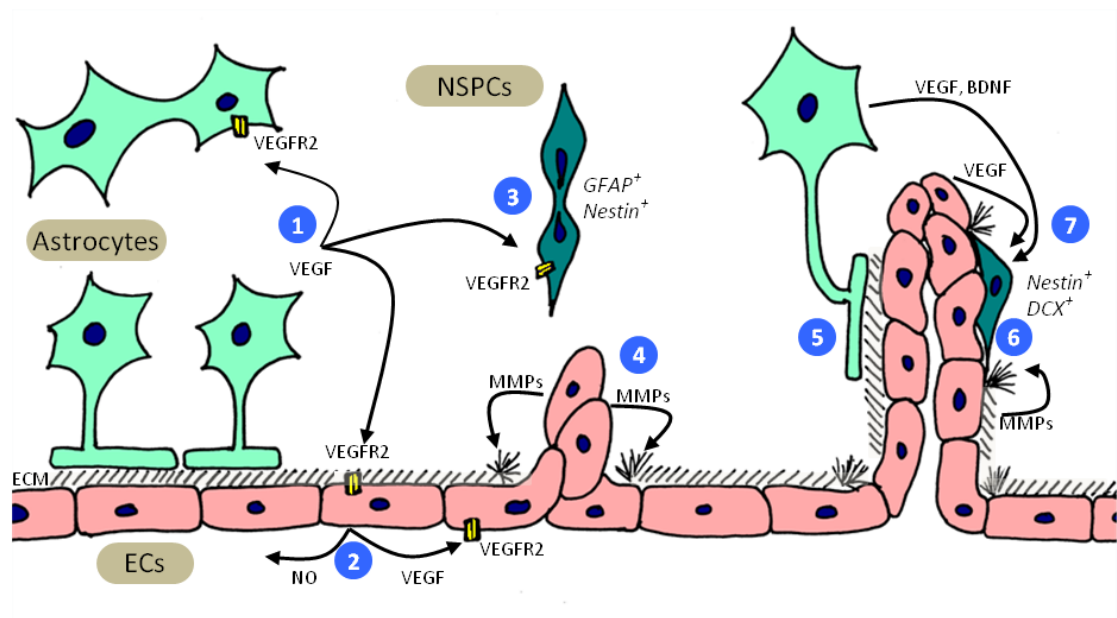


Figure 2. Common elements of angiogenesis and neurogenesis. Astrocytes release VEGF which activates astrocytic proliferation and migration (1), EC proliferation and NO release (2) and neural progenitor stem cell (NSPC) proliferation and migration (3). NSPCs express general glial markers (GFAP) and specific NSPC markers (nestin). ECs produce MMPs which degrade ECM components and allow EC sprouting from the main vessel (4). Astrocytes secrete ECM components to support the new vessels (5). MMPs allow NSPCs to migrate over ECs (6). VEGF and brain-derived neurotrophic factor (BDNF) secreted by ECs and astrocytes induce NSPC migration and differentiation (7). In the neuroblast stage, NSPCs lose GFAP expression and start expressing doublecortin (DCX).

1.1.1.4.2 Neurogenesis

Unlike other cell types, mature neurones do not have the ability to proliferate, and regeneration of neuronal tissue is restricted to differentiation of neural stem progenitor cells (NSPCs) into neurones. Neurogenesis happens in very low amounts, and only in few areas of the brain including the subventricular zone (SVZ) and the dentate gyrus (DG) located within the hippocampus (Conover & Notti, 2008). NSPCs migrate following different routes depending on the location of the damage. In the case of striatal ischaemia, cells from the SVZ migrate perpendicularly to the ventricle, and they mature and integrate within the striatum (Ohab & Carmichael, 2008). Hippocampal NSPCs of the subgranular zone of the DG differentiate and integrate in the granular layer of the DG (Abrous *et al.*, 2005).

Specific environmental conditions are necessary for the proliferation, migration and maturation of NSPCs, and many of these conditions are coupled to inflammatory mediators and the angiogenic process (Figure 2). Vascular growth factors such as VEGF promote neurogenesis through VEGFR2, also present in NSPCs (Ara *et al.*, 2010). NSPCs require the action of proteases (e.g. MMP-9, which is also involved in angiogenesis) to migrate through the ECM, keeping contact with ECs for their migration (Ohab & Carmichael, 2008). Cytokines and chemokines also contribute to neurogenesis. TGF- β promotes proliferation, chemokines induce migration and trophic factors such as brain-derived neurotrophic factor (BDNF) promote differentiation (Ziv & Schwartz, 2008). There are contradictory results regarding the role of IL-1 in neurogenesis, with some studies showing that IL-1 promotes neurogenesis whilst others showing the opposite effect (Whitney *et al.*, 2009). Microglial cells, depending on their phenotype (and thus the mediators they secrete) can also alter the pattern of

migration and the fate of NPSC differentiation (Butovsky *et al.*, 2006; Ziv & Schwartz, 2008).

NSPCs are of glial origin and as such they express the glial marker GFAP, in addition to characteristic markers of neural progenitor cells such as nestin. After brain injury, progenitor cells start proliferating and, depending on the signals they receive, they can differentiate into neurones or glial cells. As they start differentiating, progenitor cells lose GFAP expression, but nestin expression remains until the cell differentiates into a neuroblast. In the neuroblast stage doublecortin (DCX) expression starts (Abrous *et al.*, 2005). Soluble factors such as VEGF and BDNF contribute to NSPC differentiation (Jin *et al.*, 2002; Schabitz *et al.*, 2007). Finally, once the neuroblast matures into a neurone, characteristic neuronal markers such as NeuN are expressed, and nestin and DCX are not expressed anymore (Abrous *et al.*, 2005). Even though the amount of newborn neurones is not even close to match the vast amount of neurones lost after stroke, discrete amounts of neurogenesis have been shown to make an impact on functional recovery (Zhang *et al.*, 2005).

1.1.2 Remote damage

Section 1.1.1 dealt with local damage, i.e. damage seen in the core of the infarct. Whilst inflammation can increase local damage, the primary cause of local cell death is ischaemia itself. However, post-stroke neurodegeneration also happens in non-ischaemic areas of the brain. Neuronal death and inflammation have been observed in brain structures which are far from the ischaemic core, but are innervated by neurones sprouting from that core. This type of injury is called remote damage (Block *et al.*, 2005).

1.1.2.5 The substantia nigra

When the MCA is occluded, the striatum is the core of the damage, i.e., the area primarily affected by the ischaemia. The striatum innervates several regions of the basal ganglia such as the globus pallidus and the substantia nigra (SN); the sub-striatal components of the basal ganglia signal back to the striatum through direct and indirect connexions involving the thalamus and the cortex. Figure 3 depicts some of the key feedback loops between these structures. These pathways are known to be involved in motor control and addictive behaviours (Kreitzer & Malenka, 2008).

The SN receives its name from the dark pigmentation of neuromelanin produced by dopaminergic neurones in that area. The SN is divided into two sub-areas, the SN reticulata (SNr) and the SN compacta (SNc). Amongst other connexions, there is a striato-nigral feedback loop (shadowed in blue in Figure 3): striatal projections innervate the SNr, and the SNr innervates the SNc, which signals back releasing dopamine into the striatum. This circuit is essential for motor control. In Parkinson's disease (PD), whose early symptoms include motor impairments, there is a characteristic degeneration of the SN. It is estimated that motor impairments appear when there is already a severe (80 %) death of dopaminergic neurones of the SN, which accounts for the insufficiency of dopamine release in the striatum (Ma *et al.*, 1996).

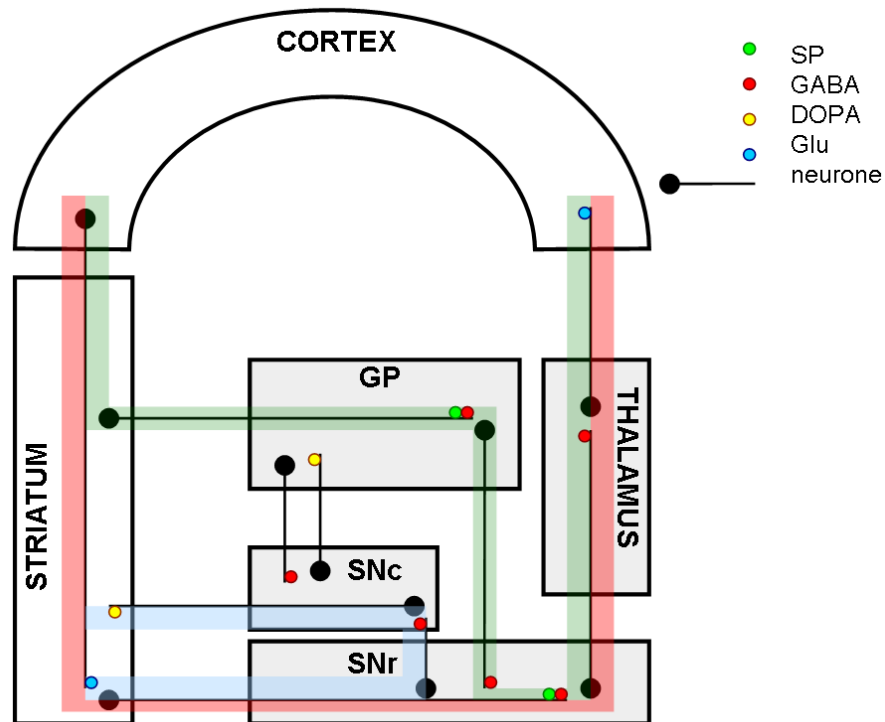


Figure 3. Striato-nigral circuitry. Cortical neurones stimulate striatal activity through the release of glutamate (Glu, blue dots). The striatum innervates the globus pallidus (GP) and SN, which release gamma aminobutyric acid (GABA) in the thalamus, inhibiting its activity. This reduces thalamic activation of the cortex. This feedback loop happens through several pathways implicated. In the direct pathway (shaded in red), striatal neurones release GABA (red dots) and substance P (SP, green dots) in the SNr. The SNr then releases GABA in the thalamus. In the indirect pathway (shaded in green), striatal signalling goes through the GP before reaching the SNr. Importantly, dopaminergic (yellow dots) neurones from the SNc innervate the striatum, providing a direct negative feedback loop to the striatum (shaded in blue). Apart from these pathways, other connections are present within these structures, some of which are depicted in the figure.

1.1.2.6 Neurotransmitters in the SN

Striatal neurones modulate the activity of the SN through the release of gamma aminobutyric acid (GABA) and substance P (SP), which are inhibitory and excitatory neurotransmitters respectively. After experimental stroke the GABAergic system is

impaired, and this has been related to motor deficits (Lin *et al.*, 2010). SP-ergic changes in the SN after stroke have not been studied, despite the fact that the SN is the area of the brain where SP and its receptor neurokinin-1 (NK1) tachykinin receptor (NK1R) are found at the highest levels (Bolam & Smith, 1990; Whitty *et al.*, 1997). Apart from being an excitatory neurotransmitter, SP is known as an inducer of neurogenic inflammation, a process by which certain neuropeptides promote inflammation through the increase of vascular permeability (O'Connor *et al.*, 2004). In fact, alterations in SP levels in the core of the infarct promote local neurogenic inflammation after an ischaemic event (Turner *et al.*, 2006). Loss of SP in the SN is reported in PD patients (Mauborgne *et al.*, 1983), however, how striatal damage alters remote SP levels in the SN had not been studied.

1.1.2.7 Remote inflammation and remote neurodegeneration

When striatal neurones die after an ischaemic stroke, signalling into the SN is altered. Furthermore, neuronal death is observed in the SN weeks to months after striatal ischaemia (Nakane *et al.*, 1992; Ogawa *et al.*, 1997). Experimental models show that remote neuronal death, including death of dopaminergic neurones, is accompanied by an inflammatory response (Arlicot *et al.*, 2010; Nagasawa & Kogure, 1990; Uchida *et al.*, 2010). Microglial and astrocytic activation has been observed from 3 days to 20 weeks after the ischaemic event (Uchida *et al.*, 2010). It is known that the initial trigger of neuronal death in the striatum is ischaemia itself, and that inflammation is a secondary contributor that extends neuronal damage. In the SN, both inflammation and neurodegeneration occur after stroke, but it is not known whether remote neurodegeneration happens first, triggering an inflammatory response; or if

inflammation occurs first, followed by neurodegeneration. The order of these events could have important implications for choosing therapeutic approaches.

Whilst it is not clear to what extent remote neurodegeneration affects delayed motor deficits, the risk of developing PD is double in post-stroke survivors (Becker *et al.*, 2010), suggesting a link between stroke and PD.

1.1.3 The search for new targets for stroke treatment

Given that acute inflammation worsens stroke outcome, diverse anti-inflammatory approaches have been considered to reduce stroke damage, and many have shown efficacy in animal models of stroke. Most of them however, have failed in clinical trials and the thrombolytic tPA is the only treatment available to date, which can only be administered within the first few hours after stroke, leaving many patients without the possibility of any treatment (Iadecola & Anrather, 2011).

To date, most emphasis has been put on targeting the acute phase of stroke and assessing the impact of early interventions, but the increasing knowledge about the plasticity of the brain and the possibility that brain repair could be enhanced has opened a new therapeutic window. A better understanding of the time dependent effects of the cellular and soluble mediators of brain damage and repair is a crucial step for the design of more effective treatments. Therapeutic targets should ideally limit acute damage but also enhance recovery at later stages. In addition, taking remote damage into consideration may improve long-term functional outcome.

The acute phase protein pentraxin 3 (PTX3) can modulate several inflammatory and immune responses in several peripheral disease models and it has been suggested to be neuroprotective. Moreover, PTX3 can act as a nodal point of assembly of the ECM which, as mentioned above, is critical for repair. In addition, as PTX3 is produced in

inflammatory environments such as the one found in the ischaemic brain, we hypothesised that PTX3 would be expressed in the brain after stroke. We considered therefore necessary to explore the potential of PTX3 in neuroprotection and modulation of the inflammatory response after stroke.

1.2 Pentraxin 3

1.2.1 Pentraxins

Pentraxins are proteins which contain a 200-long amino acid sequence including the “pentraxin signature”, 8 amino acids (aa) highly conserved through evolution: HxCxS/TWxS, with x being any aa (Garlanda *et al.*, 2005). The pentraxin superfamily is divided into short and long pentraxins. There are only two short pentraxins: C-reactive protein (CRP) and serum amyloid P component (SAP), which are mostly produced by the liver as part of the acute phase response. Long pentraxins have a longer N-terminal domain than short pentraxins, which generally contains extra binding domains that account for new functions. Long pentraxins include several neuronal pentraxins, PTX3 and the recently discovered PTX4 (Garlanda *et al.*, 2005; Martinez de la Torre *et al.*, 2010).

CRP is possibly the best known pentraxin and it is widely used in clinical settings as a marker of severity of infection or injury (Windgassen *et al.*, 2011; Joshi *et al.*, 2013; Salazar *et al.*, 2024); however, as described in section 1.2.2, PTX3 has recently awoken the interest of researchers and clinicians, since it is a more accurate biomarker than CRP in certain diseases (Latini *et al.*, 2004). Despite the increasing interest in PTX3, very few studies (Ravizza *et al.*, 2010; Zanier *et al.*, 2010) have addressed the role of PTX3 in the brain.

1.2.2 PTX3 as a biomarker

PTX3 is emerging as a very accurate marker of disease, especially of vascular disease. After acute myocardial infarction, PTX3 is a better predictor of 3-month mortality than CRP (Latini *et al.*, 2004) and circulating PTX3 levels correlate with heart failure incidence (Kaess & Vasan, 2011) and left ventricular diastolic dysfunction (Matsubara *et al.*, 2011). Plasma levels of PTX3 also correlate with mortality after ischaemic stroke (Ryu *et al.*, 2012), and PTX3 is elevated in CSF of patients suffering subarachnoid haemorrhage (Zanier *et al.*, 2010). PTX3 is found in atherosclerotic plaques (Rolph *et al.*, 2002), and its levels correlate with the vulnerability of the plaques to be ruptured (Soeki *et al.*, 2011).

PTX3 plasma levels also correlate with the severity of infection in meningococcal disease, tuberculosis and dengue (Deban *et al.*, 2010a), with lung cancer severity (Diamandis *et al.*, 2011) and even with all-cause death (Jenny *et al.*, 2009). In addition, animal models of chronic neurodegeneration express more PTX3 than wild type (WT) mice when challenged with lipopolysaccharides (LPS) (Cunningham *et al.*, 2005).

1.2.3 PTX3 expression

As most APPs, basal levels of plasma PTX3 are very low (<2 ng/ml in humans, <25 ng/ml in mice), with the exception of PTX3 expression in the ovary during the preovulatory period and in pregnancy, when PTX3 levels increase (Garlanda *et al.*, 2005). Aside from the ovaries, other organs express only very low levels of PTX3 in healthy conditions. Under inflammatory conditions, however, PTX3 expression rapidly increases and, contrary to other APPs, the heart rather than the liver seems to be the organ where this increase is more pronounced (Polentarutti *et al.*, 2000). Neutrophils and dendritic cells are thought to be the main source of PTX3, and they quickly release

the protein into the site of injury (Maina et al., 2009). Several other cell types such as macrophages, adipocytes, hepatocytes, microglia and astrocytes produce PTX3 upon exposure to inflammatory mediators (Garlanda *et al.*, 2009; Jeon et al., 2010; Maina et al., 2009). PTX3 is also named TNF stimulated gene (TSG)-14, since it was first characterised as a TNF-induced protein (Lee *et al.*, 1990) which was then identified as the same IL-1-induced pentraxin cloned by Breviario and colleagues (Breviario *et al.*, 1992). Glial cells lacking IL-1R1 fail to produce PTX3 in response to IL-1 (Andre *et al.*, 2006). Brain PTX3 production in response to injected inflammatory (IL-1), infectious (LPS) and seizure-inducing (kainate) stimuli has also been reported (Polentarutti *et al.*, 2000; Ravizza *et al.*, 2001). Several microbial moieties can induce PTX3 production (Bottazzi *et al.*, 2010). Degraded low density lipoprotein (LDL), which is found in atherogenic plaques, can induce local production of PTX3 in vascular smooth muscle cells (Klouche et al., 2004). Glucocorticoids increase PTX3 expression in ECs cells but inhibit it in macrophages. This difference is due to the different mechanism of action of the glucocorticoid receptor in ECs compared to macrophages. This cell-dependent effect may account for differences in PTX3 production in different tissues (Doni *et al.*, 2008).

1.2.4 PTX3 from gene to protein

NF- κ B (which, as mentioned in section 1.1.1.1.10, is downstream of IL-1R1) activates *ptx3* gene transcription. Toll-like receptor (TLR) ligands can also drive *ptx3* transcription. TLR activation leads to MAPK and I κ B kinase (IKK) activation, and both MAPK and IKK can lead to NF- κ B translocation into the nucleus (Okun *et al.*, 2009). *Ptx3* gene promoter also contains binding sites for Pu1, SP1, AP-1 and NF-IL-6 (Basile *et al.*, 1997). AP-1 regulates PTX3 production in basal conditions, whereas

NF- κ B is required for PTX3 production in response to TNF- α and IL-1, and SP1 modulates this cytokine-induced production. The single site of NF-IL-6 binding does not seem to be enough to activate gene transcription by itself, since IL-6 does not induce PTX3 expression (Basile *et al.*, 1997). *Ptx3* gene contains a leader sequence and two introns (Figure 4, upper panel). Once transcribed and translated, the tertiary structure of PTX3 is held together by the formation of intramolecular disulphide bonds (Inforzato *et al.*, 2008). The protein is then glycosylated; differences in glycosylations may happen depending on the microenvironment where the protein is produced, and this can affect the affinity of PTX3 for certain ligands such as components of the complement system (Inforzato *et al.*, 2006). PTX3 oligomerises through the formation of disulphide bonds between molecules. Octamers seem to be the most likely form of PTX3 oligomers (Inforzato *et al.*, 2010) (Figure 4, lower panel). The oligomerisation state of CRP seems to be important for its function (Eisenhardt *et al.*, 2009). Similarly, the oligomeric status of PTX3 determines its properties (e.g. tetramers are the minimum oligomers that allow PTX3 to bind to FGF2 (Inforzato *et al.*, 2010) and to expand cumulus matrix (Ievoli *et al.*, 2011)).

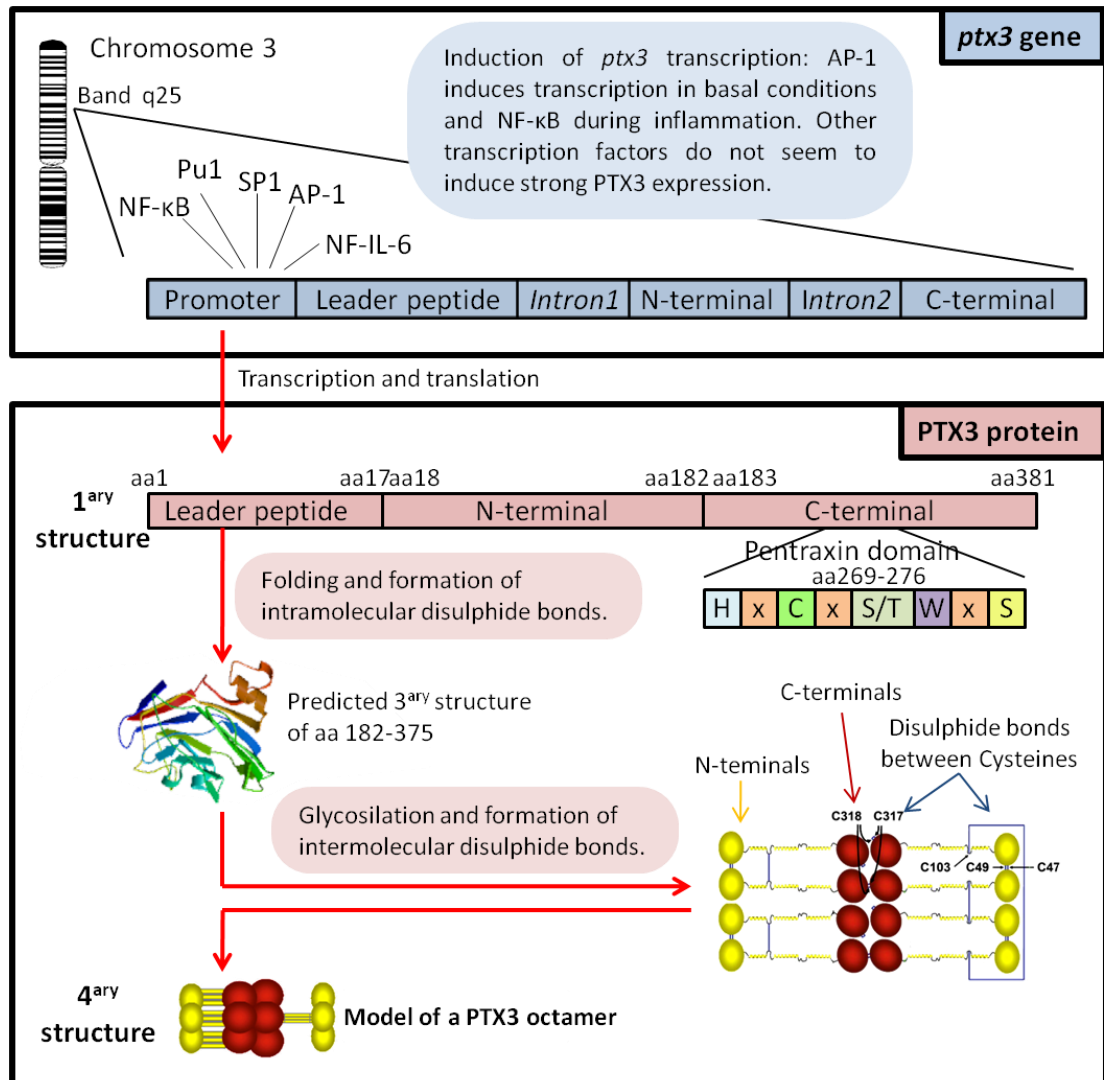


Figure 4. Structure of PTX3 gene and protein. H=Histidine, C=Cysteine, S=Serine, T=Threonine, W=Tryptophan, x=any aminoacid (aa). PTX3 3^{ary} structure model of aa 182-375 of PTX3 taken from Swiss-Model (swissmodel.expasy.org). Model of PTX3 4^{ary} structure based on biophysical analyses, taken from (Inforzato *et al.*, 2010) .

PTX3 has orthologues in species ranging from amphibians (*Xenopus laevis*) to fish (*Takifugu rubripres*) and mammals, which indicates PTX3 is highly conserved through evolution. Human and murine *ptx3* genes share the same organisation in terms of introns and exons, and both proteins have 92 % of conserved aa, from which 82 % are

identical. In addition, PTX3 protein has the exact same length in both species (Garlanda *et al.*, 2005).

1.2.5 PTX3 ligands and functions

PTX3 has several ligands although a specific PTX3 receptor has not been identified. Amongst the described ligands are several pathogens (Garlanda *et al.*, 2009), components of the complement system (Ma *et al.*, 2009; Nauta *et al.*, 2003; Deban *et al.*, 2008; Gout *et al.*, 2011), the ECM molecules TSG-6 (Salustri *et al.*, 2004) and inter- α trypsin inhibitor (I α I) (Scarchilli *et al.*, 2007), P-selectin (Deban *et al.*, 2010b), apoptotic cells (Rovere *et al.*, 2000), FGF-2 (Rusnati *et al.*, 2004) and certain fragment crystallisable (FC) γ receptors (FC γ R) (Lu *et al.*, 2008). Since PTX3 is an oligomer, it can bind several ligands at the same time, and it has been proposed that PTX3 mediates some of its actions by facilitating interactions between its ligands. Apart from the molecular studies regarding the binding properties of PTX3, the development of genetically modified mice overexpressing or lacking PTX3 protein has revealed more information about the role of PTX3 in physiological and pathological conditions, although the exact mechanisms of action are not known in many cases.

1.2.5.8 Peripheral functions

1.2.5.8.1 Pathogen recognition

PTX3 is best known by its anti-infectious properties, which occur through the facilitation of pathogen phagocytosis once PTX3 has bound to the pathogen. This has been observed in virus (i.e. influenza (Reading *et al.*, 2008)), bacteria (i.e. *Klebsiella pneumoniae* and *Salmonella typhimurium* (Garlanda *et al.*, 2009)) and fungal (i.e. *Aspergillus fumigatus* (D'Angelo *et al.*, 2009) infections. Additionally, macrophages

overexpressing PTX3 have more phagocytic activity (Diniz *et al.*, 2004). It has also been shown that mutations in PTX3 correlate with rates of tuberculosis infection (Olesen *et al.*, 2007).

1.2.5.8.2 ECM stability and fertility

PTX3 is also essential for ECM stability. As mentioned above, PTX3 can bind TSG-6, which is necessary to incorporate PTX3 to matrices of the polysaccharide hyaluronan (HA) (Salustri *et al.*, 2004). PTX3 does not directly bind HA, but it binds heavy chains (HC) of IαI (Scarchilli *et al.*, 2007), which is a ligand for HA. PTX3, TSG-6 and IαI are essential for the assembly of the HA-rich matrix which stability is required for the correct organisation of cumulus cells around the oocyte and thus is required for fertility (Salustri *et al.*, 2004). Furthermore, PTX3 helps entrapment and migration of spermatozoa, which helps the fertilisation process (Garlanda *et al.*, 2005).

The process of assembly occurs in a stepwise manner, in which PTX3 needs to interact with IαI or IαI-TSG6 before it is incorporated to the matrix (Baranova *et al.*, 2014), where PTX3 would be the point of linkage of several HA-bound HC (Scarchilli *et al.*, 2007; Baranova *et al.*, 2014). PTX3 expression in the amniotic membrane leads to HA-HC-PTX3 matrix formation, which exerts anti-inflammatory actions (He *et al.*, 2013, Zhang *et al.*, 2014).

1.2.5.8.3 Neutrophil infiltration

PTX3 is produced by different types of leukocytes recruited to the site of injury and, once released, PTX3 inhibits their infiltration, acting as negative feedback regulator. The interaction between PTX3 and the vascular adhesion molecule P-selectin reduces neutrophil infiltration, since it impedes the interaction between neutrophil adhesion

molecules and vascular P-selectin (Deban *et al.*, 2010b). In this way PTX3 prevents excessive neutrophil infiltration in several models of peripheral inflammation (Deban *et al.*, 2010b; Lo Giudice *et al.*, 2010; Salio *et al.*, 2008). PTX3 is contained in neutrophil granules, ready to be released quickly at the site of injury, where it is found associated with NETs (Jaillon *et al.*, 2007; Savchenko *et al.*, 2011). Since PTX3 is found in neutrophil granules in basal conditions, neutrophils provide an almost immediate source of PTX3, as opposed to other cells in which *ptx3* transcription and translation are required. It is believed that fast release of PTX3 by recruited leukocytes and production of PTX3 by local cells provide a very fast innate defence mechanism in the site of the injury, whereas CRP provides a more widespread but slower response (Deban *et al.*, 2010a; Garlanda *et al.*, 2009).

1.2.5.8.4 Vascular events

PTX3 is involved in thrombosis and coagulation. Like ECs, platelets also express P-selectin and thus, leukocytes bind to platelets too, forming aggregates. Binding of PTX3 to P-selectin of platelets impedes adhesion of platelets to each other and to neutrophils. In this way, PTX3 exerts anti-thrombotic actions (Maugeri *et al.*, 2011). On the other hand, PTX3 induces the production of the pro-coagulation factor tissue factor in LPS or IL-1 β stimulated ECs (Napoleone *et al.*, 2002) and in LPS-stimulated monocytes (Napoleone *et al.*, 2004). Whether the anti-thrombotic or the pro-coagulating action of PTX3 is more potent *in vivo* is not known. PTX3 knockout (KO) mice have reduced reperfusion after acute myocardial infarction; this, together with higher infiltration of neutrophils, increased apoptosis of cardiomyocytes and decreased amount of blood vessels, causes increased damage after acute myocardial infarction in PTX3 KO mice (Salio *et al.*, 2008), suggesting a protective role of PTX3 in ischaemia-

reperfusion models. On the other hand, it has been suggested that PTX3 could be noxious through inhibition of angiogenesis. The angiogenic factor FGF2 binds to the N-terminal domain of PTX3 (Camozzi *et al.*, 2006; Leali *et al.*, 2010; Rusnati *et al.*, 2004). Each PTX3 octamer can bind 2 molecules of FGF2 (Inforzato *et al.*, 2010), and this prevents the angiogenic actions of FGF2 (Camozzi *et al.*, 2006; Leali *et al.*, 2010; Leali *et al.*, 2012; Rusnati *et al.*, 2004). Moreover, overexpression of PTX3 inhibits angiogenesis whereas PTX3 silencing promotes it *in vitro* or in Matrigel (Margheri *et al.*, 2010). Interestingly, TSG-6 competes with FGF2 for the binding of PTX3, inhibiting PTX3 anti-angiogenic properties (Leali *et al.*, 2012).

1.2.5.8.5 Other peripheral functions

PTX3 helps preventing the autoimmune response. Although PTX3-pathogen interaction facilitates pathogen phagocytosis, binding of PTX3 to apoptotic cells impedes their phagocytosis by dendritic cells, which prevents autoantigen presentation (Baruah *et al.*, 2006). Another way through which PTX3 modulates pathogen and apoptotic cell clearance is through interactions with the complement system, although PTX3 can both activate and inhibit the complement. PTX3 can bind ficolins, activating the complement (Ma *et al.*, 2009; Gout *et al.*, 2011). When bound to a solid surface or a cell surface, PTX3 also activates the complement through its binding to C1q (Nauta *et al.*, 2003). However, when PTX3 binds C1q in the fluid phase, it prevents complement activation (Nauta *et al.*, 2003). PTX3 also prevents complement activation through the complement-blocking agent FH: apoptotic cells bind more FH after being preincubated with PTX3 (Deban *et al.*, 2008).

1.2.5.9 Central functions

As mentioned above, PTX3 can be produced by cells of the CNS, and plasma PTX3 levels correlate with post-ischaemic stroke mortality. However, little is known about the functions of PTX3 in the CNS. The only *in vivo* study investigating PTX3 function in the brain was carried out using an animal model of epilepsy. Kainate-induced seizures caused neurodegeneration and expression of PTX3 in the brain of WT mice. PTX3 KO mice had more widespread neurodegeneration in the brain after a kainate injection despite having the same amount of seizures (Ravizza *et al.*, 2001), suggesting that PTX3 could have neuroprotective properties. An *in vitro* study showed that PTX3 can reduce the neurotoxic effect of LPS-stimulated microglia, supporting the neuroprotective function of PTX3 (Jeon *et al.*, 2010). That same study revealed that PTX3 can modulate microglial phagocytic activity, promoting non-self phagocytosis but inhibiting self phagocytosis (Jeon *et al.*, 2010), which implies that PTX3 can be involved in regulation of autoimmunity and pathogen clearance in the CNS as well.

1.3 Rationale for studying PTX3 in stroke

Following the initial neuronal and vascular damage triggered by ischaemia, activation of central and peripheral cells facilitates the development of the inflammatory response. Inflammatory cells and soluble mediators contribute to the exacerbation of neuronal damage. After the acute phase, however, the balance of pro- versus anti-inflammatory signals changes and the actions of those same soluble mediators and inflammatory cells, which acquire a different phenotype, may contribute to repair processes. In remote areas of the brain, inflammation and neurodegeneration occur with a marked delay compared to the core of the damage, and the initial triggers of remote damage remain unclear.

The only available treatment for stroke can only be administered to a subset of patients, and only targets the acute phase of the damage. Anti-inflammatory interventions seem to improve stroke outcome, but a better understanding of time- and concentration-dependent effects of the molecules involved in ischaemic damage is required to find new targets and optimise new interventions. Ideally, therapeutic targets should acutely prevent neuronal death and limit the early inflammatory response, but also enhance the beneficial actions of inflammatory mediators during the repair process.

To this end, PTX3 emerged as an interesting target, since it had been suggested to be neuroprotective and could limit infiltration of neutrophils. Furthermore, given its ability to modulate macrophage responses and stabilise the ECM, we hypothesised PTX3 may mediate repair mechanisms. As PTX3 expression can be induced by inflammatory molecules in different cell types, including glia, and injection of inflammatory molecules in the brain promotes central PTX3 expression, we also hypothesised that PTX3 is expressed in the brain after cerebral ischaemia.

1.4 Aims and objectives

Aim 1

To explore the role of PTX3 in brain inflammation and repair after ischaemic stroke.

Objectives to aim 1

A. To elucidate whether PTX3 is expressed in the brain after experimental stroke and, if so, to investigate brain structures and cell types that express PTX3.

B. To analyse the involvement of PTX3 in neurodegeneration and inflammation after experimental stroke by measuring:

B.1. Infarct size and neuronal survival.

B.2. Neutrophil recruitment and vascular and glial activation.

B.3. Oedema formation and BBB integrity.

B.4. Glial scar formation.

C. To analyse the involvement of PTX3 in recovery after experimental stroke by measuring neurogenesis and angiogenesis.

Aim 2

To elucidate whether remote inflammation precedes neurodegeneration in the SN after experimental stroke and whether PTX3 contributes to this process.

Objectives to aim 2

A. To investigate when remote inflammatory and neurodegenerative responses take place in the SN early after experimental stroke.

B. To analyse the involvement of PTX3 in those responses.

Chapter 2: Supplementary Materials and Methods

Due to space constraints in peer-reviewed journals, the materials and methods within each of the results chapters may not contain the level of detail required for a doctoral thesis. This chapter complements the materials and methods of each chapter, completing the missing details about the materials and the methodology used when necessary. It also contains the materials and methods used in the sections which are not written in journal article format (Additional supplementary information to Chapter 3 and Chapter 4). To avoid unnecessary repetitions, the materials and methods that were addressed in depth in the journal articles have not been included in this chapter.

2.1 Materials

Tables in Appendix 1 contain the brands and providers from all reagents, commercial kits and equipments, and the composition of all buffers and cell media used.

2.2 Methods

2.2.1 PTX3 genotyping

Earsnips and embryo samples were digested in lysis buffer (see buffer composition in Appendix 1) overnight at 55 °C, then centrifuged at 21382 g for 5 min and the supernatant was collected and kept at 4 °C until use. 1 µl of DNA was added to 49 µl of PCR master mix (see buffer composition appendix). Settings for the polymerase chain reaction (PCR) in the TC-312 Techne machine were as follows: 1 cycle at 94 °C for 5 min; followed by 30 cycles at 94 °C for 30 sec, 56 °C for 30 sec and 72 °C for 30 sec; followed by 1 cycle at 72 °C for 7 min. 16 µl of DNA sample was mixed with 4 µl of sample buffer, loaded into an 2,5% w/v agarose gel containing ethidium bromide and run at 110 V for 1 h or until the bands were defined. Information about the primers, the fragments amplified by PCR and interpretation of band sizes are detailed in Chapter 3 and Supplementary information of chapter 3.

2.2.2 Middle cerebral artery occlusion

Experimental stroke was induced by transient middle cerebral artery (MCA) occlusion (MCAo). Mouse littermates weighing 25-30 g (16 weeks average age) were used for the experiments. Anaesthesia was induced by 4% isoflurane, and maintained using 2% isoflurane in 0.2% O₂ and 0.5% NO₂ mixture (v/v in all cases). The common carotid artery was exposed and, after cauterisation of the occipital artery, the external carotid

artery (ECA) was cauterised and cut. An incision was made in the distal ECA trunk and a silicone coated 6-0 nylon monofilament (0.21 mm tip diameter) was introduced and advanced along the internal carotid artery (ICA) until it blocked the blood flow in the MCA. During the occlusion, isoflurane levels were lowered to 1.7% v/v. Cessation in blood flow was monitored by the use of a laser Doppler with a probe fixed on the surface of the skull, between the eye and the ear to constantly monitor the blood flow. After the required occlusion time (30 min or 45 min) the filament was withdrawn, the distal ECA trunk was cauterised and the wound was closed. During recovery (4 h – 14 days post-ischaemia) mice were constantly monitored for signs of pain or distress. Saline was injected subcutaneously twice a day to avoid dehydration. Analgesia (EMLA cream and 0.05 mg/kg buprenorphine subcutaneously injected) was provided at the end of the surgery.

2.2.3 Bromodeoxyuridine (BrdU) injections

To monitor post-stroke cellular proliferation, mice that were allowed to recover for 48 h or 6 days were intraperitoneally injected with 50 mg/kg BrdU dissolved in sterile phosphate buffer saline (PBS) once a day from the day after the surgery and until perfusion. Mice that were allowed to recover for 14 days were injected with 50 mg/kg BrdU once a day on days 4 and 8, and twice a day on days 5-7.

2.2.4 Behavioural tests

Y maze test was performed the evening before the mice were euthanized, and assessment of motor scores and open field test were performed on the day of sacrifice.

2.2.4.1 Motor scores

To measure basic motor deficits we used a 15-point system adapted from (Hunter *et al.*, 2000) (1 point for torso flexion to right in the air; 2 points for deficit in gripping with a paw; 3 points for circling with the front paws when suspended from the tail; 4 points for spontaneous circling on the floor; 5 points for non responsive animals). Points were added and the total was used as the score of motor deficit.

2.2.4.2 Y maze test

The mouse was placed in the middle of a Y-shaped chamber made of Perspex, containing different visual stimuli at the end of each arm (arm A: line; arm B: cross; arm C: square). The mouse was initially placed facing arm A and, during 8 min, the order of the entries in the arms was annotated and the total amount of entries and the percentage of alternations over the total amount of triads were calculated. A triad consisted of three consecutive entries regardless of whether the arms were repeated or not (i.e. ACC, CBA, etc.), while an alternation consisted of three consecutive entries only when the arms were all different to each other (i.e. ABC, CBA, BAC, etc.). Exploration of an arm was counted as an entry only when the four extremities were in the arm. Spontaneous alternations reflect short-term memory, according to the natural preference of mice to explore new environments (a new arm of the maze in this case), rather than the previously explored ones (Hughes, 2004).

2.2.4.3 Open field

The mouse was put in the centre of a square Perspex chamber (45x45 cm contour and 30 cm height) and recorded for 5 min with a camera placed above the chamber. The recording was analysed using 2020 PLUS tracking software. This software divides the

area of the chamber in a 16-squares grid and tracks the mouse movement providing several parameters that reflect general motor activity and motivation to explore (time mobile, number of line crossings, number of rearings) and also the degree of rotational bias (asymmetric rotation that occurs as a consequence of unilateral MCAo).

2.2.5 Tissue collection

Mice were anaesthetised with 3.5% isoflurane in 0.2% O₂ and 0.5% NO₂ mixture (v/v in all cases), and anaesthesia was sustained throughout the entire procedure described hereafter. An incision was made around the rib cage to expose the internal organs. Cardiac blood was collected from the right ventricle and plasma was separated from blood cells by centrifugation at 1700 g, 4 °C for 10 min. Plasma samples and blood cell pellets were stored at -20 °C until use. Mice were transcardially perfused with 0.9% saline (NaCl in H₂O, w/v) to clear blood contamination. Peripheral organs (liver, spleen) were quickly removed, snap frozen in dry ice and stored at -80 °C. This was followed by perfusion with 4% (w/v) paraformaldehyde (PFA), after which the brain was removed and post-fixed in 20% sucrose-4 % PFA overnight (w/v in both cases). Brains were cryoprotected by incubation in 20% (w/v) sucrose for 5 h. Serial 20-25 µm-thick coronal brain sections were cut using a sledge microtome and kept at -20 °C in cryoprotectant.

2.2.6 Cell or tissue processing

Cell cultures were washed with PBS and cells were incubated in ice cold cell lysis buffer (see buffer composition in appendix 1, table 5) for 3 min before collecting cell lysates and freezing the samples at -20 °C until use.

Liver or spleen samples were homogenised in tissue homogenisation buffer (5 µl/mg) using a mechanical homogeniser. Samples were incubated on ice for 30 min and then centrifuged at 21382 g for 30 min at 4 °C in a benchtop centrifuge. Supernatants were processed for protein assay determination by bicinchoninic acid (BCA) assay and enzyme-linked immunosorbent assay (ELISA) or frozen at -20 °C until use.

2.2.7 Enzyme-linked immunosorbent assay

Capture antibody was diluted in PBS and used to coat 96-well plates (50 µl/well) overnight at room temperature (RT). Plates were then washed 5 times with wash buffer and blocked with reagent diluent (300 µl/well) for 1 h at RT (See all buffers in appendix 1, table 5). Samples and standards were then loaded (50 µl/well) and incubated for 2 h at RT. After washing 5 times detection antibody was diluted in reagent diluent incubated (50 µl/well) for 2 h at RT. Plates were then washed 5 times and incubated in the dark for 20 min with streptavidin horseradish peroxidase diluted in reagent diluent (1:200, 50 µl). Substrate reagent was added (50 µl/well) and incubated for 10-20 min. 25 µl of 1 M H₂SO₄ was added to stop the reaction and optical densities were measured in a plate reader at 490 nm corrected at 570 nm. Since the standard curve did not generally fit an exponential or a linear function with sufficient accuracy, one linear function ($y=a_i+b_i.x$) was fitted to the data corresponding to the lower concentrations of the standard curve and a different linear function ($y=a_{ii}+b_{ii}.x$) was fitted to the data corresponding to the higher concentrations of the standard curve. Optical density corresponded to the ordinate axis (y) and concentration to the coordinate axis (x). Concentrations of the samples were extrapolated from those linear regression equations using the optical densities from the samples.

2.2.8 Bicinchoninic acid assay

20 µl of cell or tissue lysates and BSA standards were incubated with 200 µl of BCA protein assay reagent from a commercial kit for 30 min at 60 °C. Plates were then read at 570 nm. The linear regression from the standard curve was calculated and the protein concentration of the samples was extrapolated using that linear regression.

2.2.9 Immunofluorescence

Free floating brain sections were washed with PBS and incubated in 2% (v/v) normal donkey serum in primary diluent for 50 min at RT to block unspecific staining. Brain sections were then incubated with suitable dilutions of primary antibodies in primary diluent (see primary antibodies in Appendix 1, Table 2; and buffers in Appendix 1, Table 5) overnight at 4 °C. After three 10 min washes with PBS, brain sections were incubated in the appropriate mixture of fluorescent secondary antibodies diluted in primary diluent (see secondary antibodies in Appendix 1, Table 3) for 2 h at RT in the dark. Brain sections were washed twice with PBS for 10 min and once for 20 min before being mounted onto gelatine coated slides. Once dried, slides were coverslipped using Prolong Gold Antifade with or without a nuclear stain (DAPI).

For BrdU immunostaining, brain sections were pretreated with HCl 1M, first on ice for 2 min, and then at 37 °C for 30 min. For Nestin immunostaining, antigen retrieval was performed by pretreating the slides with 10 mM sodium citrate at 70 °C for 30 min. After each pretreatment, sections were washed several times with PBS to restore the original pH before starting the standard immunohistochemistry protocol.

2.2.10 Brain damage assessment

2.2.10.1 *Cresyl violet staining*

Brain sections were washed with PBS and mounted onto gelatine coated slides and left to dry overnight at RT. Sections were delipidized by treating them with 99% (v/v) ethanol (EtOH) (for 5 min) and xylene (for 10 min) and then rehydrated with 99% (v/v) EtOH (for 5min), 95% (v/v) EtOH (for 2 min) and running H₂O (for 2 min) followed by staining in 1.5% (w/v) cresyl violet for 3 min. Sections were then contrasted and dehydrated by submerging them in running H₂O (until it ran clear), then in 95% (v/v) EtOH for 30 min, 99% (v/v) EtOH for 20 min and 10 min in xylene. Slides were coverslipped using Depex mounting medium.

2.2.10.2 *IgG staining*

Free floating brain sections were washed with PBS and incubated with primary diluent for 2 min before 30 min incubation with 1% (v/v) H₂O₂ in distilled H₂O. Sections were then washed three times with PBS and incubated for 1 h with 10% (v/v) normal horse serum diluted in primary diluent. After removing the blocking solution, biotinylated anti-mouse IgG (raised in horse) was added and incubated overnight. Samples were washed three times and incubated for 30 min in equal amounts of solution A and B (1:500 of each, in PBS, from ABC kit) in the dark. After three washes, 3,3'-diaminobenzidine (DAB, 1 mg/ml) was added and incubated in the dark until the desired contrast was reached. Sections were washed in PBS and mounted onto gelatine-coated slides and dried overnight. Slides were then dehydrated in 70% (v/v) EtOH (for 3 min), 90% EtOH (v/v) (for 3 min) 100% EtOH (5 min) and xylene (10 min) and were coverslipped using DEPEX mounting medium.

2.2.10.3 *Calculation of brain damage*

To calculate infarct size, 8 cresyl violet-stained coronal sections covering the infarct rostro-caudally were measured using Image J. The increase in infarct size due to oedema was calculated as follows: $(A_{\text{ipsi}} - A_{\text{contra}}) * 100 / A_{\text{ipsi}}$ and was subtracted to obtain oedema-corrected infarct values. Percentage of oedema was expressed as the increase in hemispheric volume ipsilaterally compared to the contralateral hemisphere $((V_{\text{ipsi}} - V_{\text{contra}}) * 100 / V_{\text{contra}})$. The same procedure was used to assess BBB injury following IgG staining.

2.2.11 Cell cultures

For experiments involving PTX3 KO and WT mice, the tails of the embryos/pups were kept for genotyping, and cell cultures were prepared separately from the brain of each embryo.

2.2.11.1 *Primary neuronal cultures*

Primary neuronal cultures were prepared using brains from embryos of mice at day 15-16 of gestation. Brains were dissected out and placed in starve medium (DMEM supplemented with 1% (w/v) penicillin/streptomycin) preheated at 37 °C. Starve medium was replaced with dissociation medium (starve medium containing 562.5 U/ml trypsin and 417 U/ml DNase), and brains were placed in a shaking incubator at 50 rpm and 37 °C for 30 min. Ice-cold foetal calf serum (FCS) was added until brains were fully covered. After 2 min, FCS was aspirated and brains were washed three times with DMEM containing 10% (v/v) FCS and 1% (w/v) penicillin/streptomycin. Tissue was then homogenised in neuronal seeding medium using a 5 ml stripette. Homogenates were then filtered through an 80 µm nylon mesh. 5,-fluoro-2-

deoxyuridine (FUDR) was added to a final concentration of 20 μM to inhibit glial proliferation. Cells were counted and seeded at 600,000 cells/cm². Neurons were seeded in plates coated with poly-D-lysine. Media was replaced with neuronal change medium on day *in vitro* (DIV) 5. Half the total volume of medium was then changed with change medium every 2-3 days until confluency was reached (DIV 11-14).

2.2.11.2 *Mixed glial cultures*

2-3 day old pups were decapitated and the brains were immediately removed from the skulls and kept in DMEM. Brains were then rolled over sterile filter paper to remove the meninges, and then they were then placed in glial medium (3 ml per brain). Brains were dissociated into cells by several passages through pipettes of decreasing diameters (from a 10 ml pipette to a glass pipette). Cell suspension was then centrifuged at 155 g for 10 min in a Sigma 2-16PK centrifuge, the supernatant was discarded and the pellet was resuspended in glial media to the required concentration (10 ml per brain used). Medium was fully changed at DIV 5, and half of the total volume of medium changed every three days from then on. Glial cultures were used when cells reached confluency (DIV 15-20).

2.2.11.3 *Mouse brain endothelial cell (MBEC) cultures*

MBECs were seeded on transwells for neutrophil transmigration studies. Polycarbonate transwell inserts with 3 μm pore diameter (2×10^6 pores/cm²) were coated with collagen IV. Transwell surface was covered with a collagen solution (50 $\mu\text{g}/\text{ml}$), kept at 4 °C overnight and washed twice with PBS before use. Adult (4-8 week old) mice were decapitated and the brains were removed and kept in ice-cold DMEM. The meninges, cerebellum and white matter were removed and the remaining tissue

was minced into pieces using a scalpel blade and then homogenised with a dounce homogeniser using 4 ml of starve media (loose pestle: 0.04 mm clearance; tight pestle: 0.07 mm clearance; 20-30 strokes with each pestle). The homogenate was centrifuged for 5 min at 200 g in a Sigma 2-16PK centrifuge and the pellet was resuspended in a dextrane solution of 18% (w/v) and centrifuged for 10 min at 3893 g. The microvessel pellet was resuspended in 1 ml of Ca²⁺ and Mg²⁺ free Hank's balanced salt solution (HBSS) and filtered through a 75 µm nylon mesh. The microvessels remaining in the mesh were collected in 4.5 µl of HBSS and a combination of enzymes (750 U/ml DNase, 0.5 U/ml collagenase, 4 U/ml dispase and 50 µg/ml of the protease inhibitor tosyllysine chloromethyl ketone) was added to partially digest the ECM in between ECs. Digestion went on for 20 min in a shaker within an incubator at 37 °C. Microvessels were then centrifuged for 7 min at 800 g and the pellet was resuspended in 700 µl of maintenance media per brain, supplemented with 3 µg/ml puromycin. Media was changed to maintenance media on DIV 2 and every 4 days until confluency was reached (DIV 14 approx).

2.2.11.4 Neutrophil isolation

Naive neutrophils were collected in neutrophil buffer by flushing femurs and tibia of adult mice using a 25 G needle. The suspension was aspirated through a 19 G needle and centrifuged for 5 min at 400 g. 3 ml of 0.2% (w/v) NaCl was added to lyse red blood cells and then 7 ml of 1.2% (w/v) NaCl to restore osmolarity. Neutrophils were passed through a 30 µm filter and then centrifuged for 5 min at 400 g. The pellet was resuspended in 200 µl of neutrophil buffer (see Appendix 1, table 5 for buffer composition) and then anti-Lymphocyte antigen 6G (Ly6G) biotinylated antibody (50 µl) was added and incubated for 10 min at 4 °C. 100 µl of anti-biotin microbeads

dissolved in 150 μ l of neutrophil buffer were added to the preparation and incubated for 15 min. 5 ml of neutrophil buffer was then added and neutrophils were centrifuged for 5 min at 400 g. The pellet was resuspended in 500 μ l of neutrophil buffer and passed through a magnetic MACS® LS column. Ly6G-labelled cells retained by the LS column were eluted by passing 5 ml of neutrophil buffer through the column. Neutrophil yield was counted with an hemocytometer and the preparation was diluted in neurobasal medium with 1% (w/v) penicillin/streptomycin and 1% (w/v) glutamine to a concentration of 4×10^6 cells/ml.

2.2.12 Cell treatments

To induce excitotoxicity, oxidative stress, stimulate hypoxic cascades or deprive cells from glucose we used N-methyl-D-aspartate (NMDA) 100 μ M or 500 μ M, H₂O₂ 50 μ M, CoCl₂ 500 μ M and 2-deoxyglucose (2DG) 15 mM respectively. To induce PTX3 expression, IL-1 β (0.03–30 IU/ml diluted in vehicle) was added to the cultures. When indicated, IL-1RA (100 ng/ml) was added 30 min prior to IL-1 β treatment.

2.2.13 Neutrophil transmigration and neurotoxicity assays

2×10^5 naive neutrophils were collected and allowed to transmigrate through IL-1 β (100 ng/ml)-treated MBECs. The inserts were then removed from the transwells and the medium in the abluminal compartment was centrifuged 10 min at 400 g. Pellet was resuspended in 40 μ l of DMEM and the amount of neutrophils was quantified using an haemocytometer. Transmigration was expressed as fold increase in the number of transmigrated neutrophils compared to transmigration through untreated endothelium.

For neutrophil neurotoxicity experiments, primary neuronal cultures were incubated with naïve or transmigrated neutrophil-conditioned medium, which was obtained as

described previously (Allen *et al.*, 2012). Primary neuronal cultures were incubated with neutrophil-conditioned medium (1:4 dilution) for 24 h. Lactate dehydrogenase (LDH) release was used to quantify cell death.

2.2.14 Lactate dehydrogenase assay

Cell death was quantified by measuring the amount of LDH released into the media. LDH is a cytosolic enzyme released only when the cell membrane is disrupted. A tetrazolium salt is used as a substrate for LDH, which catalyses its conversion into a red formazan product. 50 µl of culture supernatant or cell lysate were mixed with 50 µl of substrate and left for 20 min in the dark. 50 µl of 0.1 M acetic acid was added to stop the reaction and absorbance at 490 nm was measured in a plate reader. LDH assay values from cell lysates of control wells were used to establish the 100% of cell death, and levels of LDH released into the supernatants were used to establish the degree of cell death in the cultures. The required reagents for the assay were from a CytoTox-96 kit.

2.2.15 MTT assay

MTT (4,5-Dimethylthiazol-2-yl)-2,5-diphenyltetrazolium bromide) is a salt which can be incorporated into living cells, where it is reduced into a purple product. The amount of incorporation of MTT to the culture correlates to the amount of living cells. Cultures were treated with 0.5 mg/ml of MTT for 2 h, supernatants were then removed and cultures were washed once with PBS. Cells were lysed and MTT product dissolved by addition of propanol (200 µl per well in a 96-well plate) and absorbance at 570 nm was measured in a plate reader.

2.2.16 Microscopy/Image acquisition and image analysis

Image acquisition and analysis were conducted in a blinded manner. Images within corresponding regions of the ipsi- and contralateral hemispheres were randomly selected. Olympus BX51 upright microscope with 4x/ 0.13 Plan fln, 10x/ 0.3 Plan fln and 20x/0.5 Plan fln objectives was used. Images were acquired with a Coolsnap EZ camera and MetaVue Software. Specific band pass filter sets were used for DAPI (31000v2, BP350/50nm), Alexa 488 (41001, BP480/40nm) and Alexa 594 (41004, BP 560/55 nm). A bright field microscope attached to a Q-Image camera was used to take images of Nissl and IgG stained sections.

Microscope and camera settings were optimised for each experiment, and the chosen settings were used for the acquisition of images from all samples within the experiment.

2.2.17 Statistical analysis

Animals were randomized and *in vivo* measurements were done in a blinded manner. Data was analysed in a blinded manner. Due to the small size of certain samples, normality tests were not advised as a reliable tool to determine sample distribution. Observation of the general sample distribution of the variables under consideration in previous publications with bigger sample size (Boutin *et al.*, 2001; Denes *et al.*, 2007; Li *et al.*, 2010; Allen *et al.*, 2012) was recommended. Based on this, data was analysed with a parametric approach and Graphpad Prism software was used to perform the following statistical tests. Unpaired student t-test was used to compare the means between two groups. One-way ANOVA with Bonferroni post-hoc test was used to compare the means of more than 2 groups with each other, and One-way ANOVA with Dunnett's post-hoc test was used to compare the means of more than two groups to the mean of the control group. One sample t-test was

used to compare the mean of one group to a given number (e.g. compare the percentage of cell survival to 100%). Two-way ANOVA with Bonferroni post-hoc test was used to compare the means of two groups across different conditions (e.g. in different areas). For non-continuous data, median values were used instead of mean values (e.g. for motor scores), and Mann-Whitney test was used to compare medians of several groups. Wilcoxon Signed Rank test was used to compare the medians of several groups against a given value. In all cases statistical significance was set for $p \leq 0.05$.

Chapter 3: The role of PTX3 in brain damage and inflammation after cerebral ischaemia

This chapter corresponds to the article titled “The acute-phase protein PTX3 is an essential mediator of glial scar formation and resolution of brain edema after ischemic injury” (Rodriguez-Grande *et al.*, 2014). The article was written in American English due to journal requirements, and the language has not been modified. Supplementary information is provided following the main article.

The acute phase protein PTX3 is an essential mediator of glial scar formation and resolution of brain edema after ischemic injury

Running title: *IL-1-induced PTX3 mediates post-stroke recovery*

Beatriz Rodriguez-Grande, MRes¹, Matimba Swana, MRes¹, Loan Nguyen, PhD¹,
Pavlos Englezou, MRes¹, Samaneh Maysami, PhD¹, Stuart M. Allan, PhD¹, Nancy J.
Rothwell, PhD¹, Cecilia Garlanda, PhD², Adam Denes, PhD^{1,3,*} and Emmanuel
Pinteaux, PhD^{1,*}

¹Faculty of Life Sciences, A.V. Hill Building, University of Manchester, Oxford Road,
Manchester, M13 9PT, UK; ²Department of Immunology and Inflammation,
Humanitas Clinical and Research Center, 20089 Rozzano (MI), Italy; ³Laboratory of
Molecular Neuroendocrinology, Institute of Experimental Medicine, Budapest H-1450,
Hungary

*Share senior authorship

Address for Correspondence: Emmanuel Pinteaux, PhD, Faculty of Life Sciences,
A.V. Hill Building, University of Manchester, Oxford Road, Manchester, M13 9PT,
UK. Tel: +44 161 275 1825, Fax: +44 161 275 5948, E-mail:
emmanuel.pinteaux@manchester.ac.uk

Funding was provided by the Medical Research Council (Grant G0801296) the
European Union's Seventh Framework Programme (FP7/2008-2013) under Grant
agreements Nos. 201024 and 202213 (European Stroke Network) and the Simon and
Simone Collins studentship.

Abstract

Acute phase proteins (APPs) are key effectors of the immune response and are routinely used as biomarkers in cerebrovascular diseases, but their role during brain inflammation remains largely unknown. Elevated circulating levels of the APP pentraxin-3 (PTX3) are associated with worse outcome in stroke patients. Here we show that PTX3 is expressed in neurons and glia in response to cerebral ischemia, and that the pro-inflammatory cytokine interleukin-1 (IL-1) is a key driver of PTX3 expression in the brain after experimental stroke. Gene deletion of PTX3 had no significant effects on acute ischemic brain injury. In contrast, the absence of PTX3 strongly compromised blood-brain barrier integrity and resolution of brain edema during recovery after ischemic injury. Compromised resolution of brain edema in PTX3-deficient mice was associated with impaired glial scar formation and alterations in scar-associated extracellular matrix production. Our results suggest that PTX3 expression induced by pro-inflammatory signals after ischemic brain injury is a critical effector of edema resolution and glial scar formation. This highlights the potential role for inflammatory molecules in brain recovery after injury and identifies APPs, in particular PTX3, as important targets in ischemic stroke and possibly other brain inflammatory disorders.

Keywords: brain inflammation; cerebral ischemia; edema; glial scar; IL-1; pentraxin-3

Introduction

Inflammation is critically implicated in the pathogenesis of ischemic and haemorrhagic stroke, and is generally associated with poor clinical outcome (Denes *et al.*, 2010b; Iadecola & Anrather, 2011; Lee *et al.*, 2009; McNaull *et al.*, 2010). A new mediator of inflammation is the acute phase protein pentraxin 3 (PTX3), which has an emerging role in cardiovascular and cerebrovascular disorders. PTX3 plays an important role in innate immunity (Manfredi *et al.*, 2008), vascular inflammation (Mantovani *et al.*, 2006) and extracellular matrix (ECM) functionality (Salustri *et al.*, 2004; Scarchilli *et al.*, 2007; Tranguch *et al.*, 2007) in the periphery. Importantly, elevated PTX3 plasma levels are recognised as an independent predictor of mortality at three months after acute myocardial infarction (Latini *et al.*, 2004), and is associated with the incidence of heart disease (Jenny *et al.*, 2009; Kaess & Vasani, 2011; Matsubara *et al.*, 2011) and hypoxic respiratory failure (Sciacca *et al.*, 2010). Furthermore, PTX3 has been recently identified as a novel and independent prognostic marker in ischemic stroke (Ryu *et al.*, 2012). Despite the strong clinical association between plasma PTX3 levels and vascular disease, no studies have addressed whether PTX3 is expressed in the brain after stroke and whether PTX3 contributes to stroke pathology.

Inflammation in the brain after stroke is critically regulated by the cytokine interleukin-1 (IL-1); IL-1 expression increased early after ischemic injury contributing to neurotoxicity (Allan *et al.*, 2005), and early inhibition of IL-1 actions by the naturally occurring IL-1 receptor antagonist (IL-1Ra) markedly reduces brain damage induced by experimental ischemia (Relton & Rothwell, 1992). We and others have shown that PTX3 expression can be induced by treatment with IL-1 (Andre *et al.*, 2006; Polentarutti *et al.*, 2000) but whether this occurs during cerebral ischemia is

unknown. Whilst detrimental actions mediated by IL-1 in the early phase of the central inflammatory response are well characterized, the role of IL-1 during the later stages of inflammation in recovery and brain repair is completely unknown. Recent research suggests however that inflammation could have some beneficial effects when repair mechanisms are initiated (Schwartz, 2003), although mechanisms by which inflammation mediates repair are not well understood.

We demonstrate here that IL-1 induces PTX3 expression in the brain after cerebral ischemia and that in addition to its well recognized role in the periphery, PTX3 has unique actions in the brain mediating the formation of the glial scar and resolution of brain edema. Thus, we identify a link between pro-inflammatory factors and brain repair after cerebral ischemia and show that PTX3 is a key mediator of this process.

Materials and Methods

Animals

C57BL/6 wild type (WT) mice were supplied by Harlan Olac (UK), IL-1 α/β double knockout (KO) and IL-1 β KO mice were provided by Prof. Yoichiro Iwakura (University of Tokyo, Japan) and PTX3 KO mice were provided by Dr. Cecilia Garlanda (Humanitas Clinical and Research Center, Rozzano, Italy). All mice were on C57BL/6 background and were bred in-house. Age (12 to 20-week-old) and weight-matched male littermates were used for all experiments. Pentraxin 3 KO mice were bred as heterozygous and litter genotyping was performed as described previously (Rolph *et al.*, 2002). (A sample of genotyping is included in Supplementary figure 1). Levels of plasma PTX3 measured in a representative group of WT and PTX3 KO mice

confirmed that PTX3 was not expressed in PTX3 KO mice (see Supplementary figure 2).

Animals were maintained at 21 °C ± 1 °C, 55 % ± 10% humidity, in a 12 hour light-dark cycle with free access to food and water. All animal procedures were performed under the Home Office (UK) project license number (40/3076) and were carried out in accordance with STAIR and ARRIVE guidelines, the European Council directives (86/609/EEC) and the Animal Scientific Procedures Act (UK) 1986.

Cerebral Ischemia Induced by Transient Middle Cerebral Artery

Occlusion

Transient middle cerebral artery occlusion (MCAo) was performed using the intraluminal filament method as described previously (Wheeler *et al.*, 2003). To investigate PTX3 expression in the brain and periphery after MCAo the occlusion time was 45 min, as this length of occlusion in our hands ensures the development of a severe striatal and cortical infarct. To study the role of PTX3 in brain injury and repair over time (48 h and 6 days post MCAo), 30 minutes occlusion was used, since this duration of MCAo increases long term animal survival and is suitable to study either neuroprotection or increased brain injury in this animal model. Monitoring of cerebral blood flow within the middle cerebral artery territory was performed during the entire surgical procedure by using a laser Doppler (Moor Instruments, Devon, UK). Doppler signal showed no significant difference between WT and PTX3 KO mice prior to MCAo, after occlusion ($77 \pm 7\%$ and $76 \pm 5\%$ drop in WT and PTX3 KO mice, respectively) and during reperfusion. Mice that did not show at least a 70% drop, or a Doppler signal that did not recover fully within 5 min after reperfusion were excluded from the study (n=1). We also confirmed that absence of PTX3 is not associated with

altered vascular density after 48 h reperfusion (assessed by PECAM-1 and ICAM-1 quantification; see Supplementary Figure 3). After surgery, mice were subjected to reperfusion and allowed to recover for 24 hours, 48 hours or 6 days. Mice were injected subcutaneously with 0.5 mL of sterile saline daily for rehydration and continuously monitored for neurologic symptoms. To assess cell proliferation, mice euthanized at 48 hours and 6 days reperfusion were intraperitoneally injected twice daily with bromodeoxyuridine (BrdU) (50 mg/kg, Sigma-Aldrich, Dorset, UK), dissolved in sterile phosphate buffer saline (PBS).

IL-1 β Administration

Mice were randomized and were injected intraperitoneally with 4 μ g/kg of recombinant human IL-1 β (National Institute for Biological Standards and Control, NIBSC, Potters Bar, UK) dissolved in sterile phosphate-buffer saline containing 0.1% low endotoxin bovine serum albumin. Four hours or 24 hours after injection, animals were transcardially perfused with 0.9% saline to remove blood contamination.

Tissue Processing

For immunohistochemistry, mice were perfused transcardially with 0.9% saline followed by 4% paraformaldehyde. Brains were removed, post-fixed overnight in 20% sucrose/ paraformaldehyde and sectioned on a sledge microtome (Bright, Cambridgeshire, UK). Typically, 20 parallel series of 20 μ m (for mice undergoing 24 hour or 48 hour reperfusion) or 25 μ m (for mice undergoing 6 days reperfusion) coronal brain sections were cut and stored in antifreeze solution at -20°C. Cardiac blood was collected from the right ventricle before perfusion. Plasma was separated from blood cells by centrifugation at 1,700 g, 4°C for 10 minutes. For enzyme-linked

immunosorbent assay measurements, organs were collected and tissues were homogenized as previously described (Chapman *et al.*, 2009). Protein concentrations were measured with bicinchoninic acid assay (Pierce, Thermo-Fisher Scientific, Hemel Hempstead, UK).

Enzyme-linked immunosorbent assay

Pentraxin 3 levels were measured by enzyme-linked immunosorbent assay (R&D Systems, Abingdon, UK). Absorbance was read at 450 nm and corrected at 570 nm with a plate reader (Synergy HT, BioTek, UK). The limit of detection for PTX3 was 1.35 ng/mL in plasma samples and 110 pg/mL in other samples.

Measurement of Infarct Size, Brain Edema and Blood-Brain Barrier (BBB) Breakdown

Infarct size was measured using Nissl staining as described previously (McColl *et al.*, 2007) and IgG infiltration in the brain was used to assess blood-brain barrier (BBB) breakdown as reported earlier (Denes *et al.*, 2010a). Eight defined coronal levels according to Bregma were measured, and integrated to obtain the infarct and BBB damage volume. Edema was calculated as the percentage of ipsilateral hemisphere volume increase compared to the contralateral hemisphere. Infarct and BBB damage volumes were corrected for edema to avoid possible masking effects of edema as described previously (Denes *et al.*, 2010a).

Immunofluorescence

Free floating brain sections were incubated in 2% normal donkey serum (Jackson laboratories, Bar Harbor, ME, USA) in primary diluent (0.3 % Triton X-100 in

phosphate-buffer saline) for 1 hour. Suitable combinations of primary antibodies were added and left overnight. The primary antibodies used were rat anti-PECAM-1 (1:250, BD Biosciences, Oxford, UK), goat anti-ICAM-1 (1:250, R&D Systems), goat anti-MAP-2 (1:500, Santa Cruz Biotechnology, Dallas, USA), rat anti-CD45 (1:250, Serotec, Kidlington, UK), rat anti-myelin basic protein (1:1000, Abcam, Cambridge, UK), goat anti-IL-1 β (1:100, R&D Systems), chicken anti-PGP9.5 (1:500, Santa Cruz Biotechnology), chicken anti-glia fibrillary acidic protein (GFAP) (1:1000, Abcam), goat anti-laminin- α 4 (1:100, Santa Cruz Biotechnology), rabbit anti-PTX3 (1:500, Abcam). A second PTX3 antibody (rabbit anti-PTX3, 1:500, kindly donated by Prof. A. Mantovani) was used to ensure specificity of PTX3 staining. Staining was abolished by 5 min preincubation with 45 ng/mL recombinant PTX3 (R&D Systems). Secondary antibodies were conjugated with Alexa 488 or 594 fluorochromes (Invitrogen, Paisley, UK) to visualize the antigens. Sections were mounted onto gelatin-coated slides and coverslipped with Prolong Gold antifade with or without 4',6-diamidino-2-phenylindole (Invitrogen). Images were acquired using Olympus BX51 upright microscope and captured using a Coolsnap ES camera (Photometrics, Tucson, AZ, USA) through MetaVue Software (Molecular Devices, Sunnyvale, CA, USA). A similar protocol was used for immunocytochemical staining on cell cultures.

Image Analysis

All measurements were conducted in a masked manner in randomly selected images within corresponding regions of the ipsi- and contralateral hemispheres. Total hemispheric counts were calculated from overlapping images covering all regions of interest within the hemisphere. Glial scar integrity was estimated on GFAP-immunostained brain sections by measuring the perimeters of the damaged area and of

the surrounding glial scar. The percentage of infarct area surrounded by GFAP-positive scar was calculated. Image J software (National Institutes of Health, USA) was used for image analysis and quantification.

Cell Cultures

Primary neuronal cell cultures were prepared from the brains of mice embryos at 14 to 16 days of gestation as described previously (Nguyen *et al.*, 2011). Cultures were used for experiments at day *in vitro* 12. Primary mixed glial cultures were prepared from the brains of 1 to 3-day-old mice as described previously (Pinteaux *et al.*, 2002b) and grown until confluency (day *in vitro* 14 to day *in vitro* 20).

Cell Treatments for Pentraxin 3 Expression Experiments

To study PTX3 expression, neuronal and glial cultures were treated with vehicle (0.1% low-endotoxins bovine serum albumin diluted in 0.9% NaCl), recombinant rat IL-1 α or IL-1 β (National Institute for Biological Standards and Control, NIBSC, UK) (0.03–30 IU/mL diluted in vehicle) in the presence or absence of IL-1Ra (NIBSC) (10 μ g/mL for glia and 1 μ g/mL for neurons) for 24 hour. Cultures were also treated with IL-1 α or IL-1 β (0.3 or 3 IU/mL) heated at 95°C for 30 minutes, N-methyl-D-aspartate (100 μ mol/L and 500 μ mol/L, Tocris Bioscience), CoCl₂ (500 μ mol/L), 2-deoxyglucose (2DG, 15 mmol/L) and H₂O₂ (50 μ mol/L or 500 μ mol/L) for 24 hour.

Glial Proliferation Assays

To study the effect of PTX3 on glial proliferation *in vitro*, cells were trypsinized, centrifuged, resuspended and counted, and 10,000 cells were seeded per well (in 96-well plates). Cells were kept in serum-free media for 2 hours before being treated for

48 hours with one single dose of PTX3 (0.3 ng/mL, R&D Systems), FGF2 (100 ng/mL, Invitrogen) or cytosine arabinoside (10 μ mol/L, Sigma-Aldrich). Cell proliferation was assessed using a commercial BrdU cell proliferation kit (Calbiochem/Merk, Nottingham, UK). Briefly, cells were incubated with BrdU for 48 hours before 1-hour incubation with anti-BrdU antibody. Horseradish peroxidase-conjugated secondary antibody was added, and a colorimetric assay was performed. Percentage of proliferation was calculated in comparison with the control well.

Statistical Analysis

Animals were randomized for *in vivo* experiments and all quantitative measurements were performed in a masked manner. Data were analyzed with GraphPad Prism 5.0 (GraphPad Software, San Diego, CA, USA). Comparisons between two groups were made using Student's *t*-tests. For multiple groups comparisons, one-way analysis of variance followed by Bonferroni's (to evaluate differences between all groups) or Dunnett's (to compare other groups to a control/vehicle group) post hoc tests were used. For multiple groups, two-way analysis of variance was used.

Results

Cerebral ischemia induces Pentraxin 3 expression in the brain.

Pentraxin 3 protein levels increased significantly by 26-fold ($P<0.01$) in the ipsilateral hemisphere compared to the ipsilateral hemisphere of sham-operated animals, and were higher by fourfold ($P<0.05$) in the ipsilateral hemisphere compared to the contralateral side, 24 hours after cerebral ischemia (Figure 1A). PTX3 expression

strongly declined in the ipsilateral hemisphere (by fivefold, $P < 0.05$) but remained higher than the contralateral side, 48 hours after cerebral ischemia (Figure 1A). Immunofluorescent staining revealed expression of PTX3 in the ipsilateral, but not in the contralateral hemisphere (Figure 1B). Pentraxin 3 immunostaining was particularly intense in white matter bundles of the striatum, in fine nerve fibers surrounded by myelin basic protein-positive structures (Figure 1C). We detected PTX3 expression in MAP-2-positive neurons in the ipsilateral cortex (Figure 1D) and in GFAP-positive astrocytes within the ipsilateral corpus callosum (Figure 1E). We did not find any recruited CD45-positive leukocytes and macrophages/microglia containing PTX3 24 hours (Figure 1F and G respectively), 48 hours or 6 days (Supplementary Figure 4) after MCAo. In WT mice, immunoneutralization of PTX3 antibodies with recombinant PTX3 protein fully eliminated immunostaining (Figure 1H, i and iii). However, some PTX3 KO mice still showed a pale staining (Figure 1H, ii). Residual PTX3 immunostaining detected in PTX3 KO mice might be due to a low level of cross-reactivity with other pentraxins known to be expressed in the brain (Garlanda *et al.*, 2005).

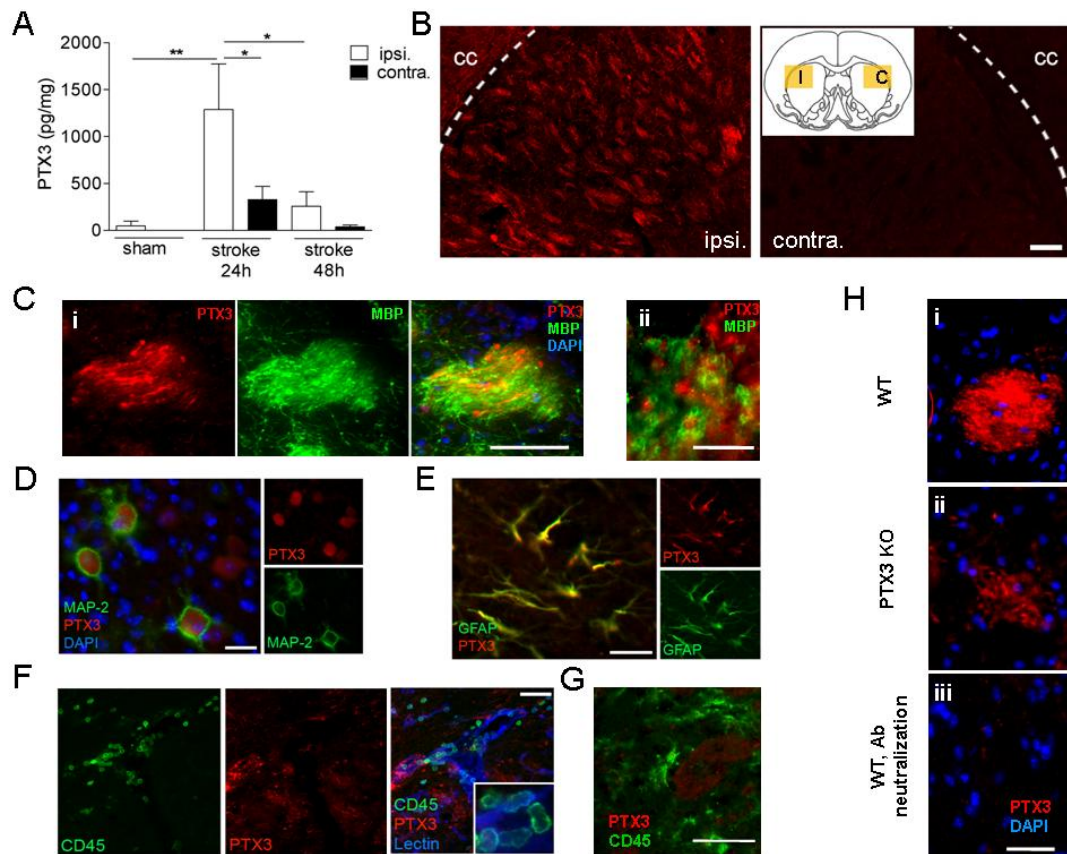


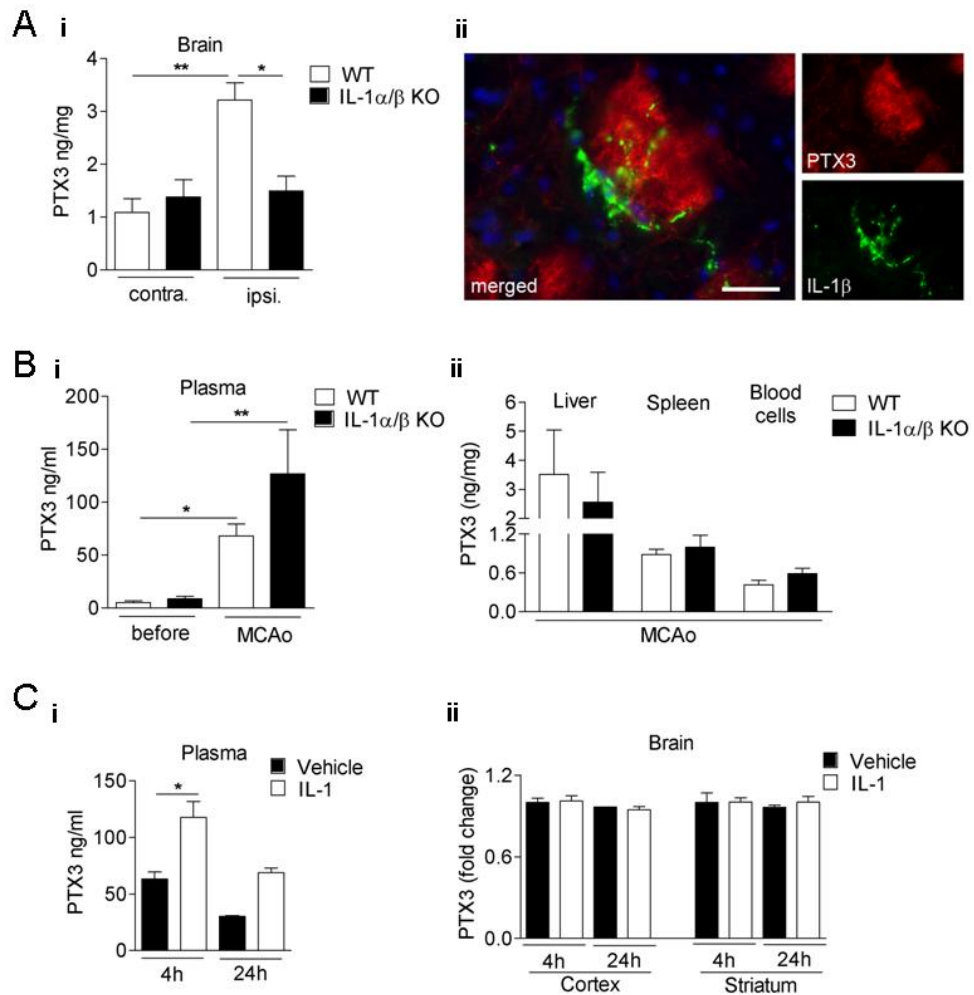
Figure 1. Cerebral ischemia drives pentraxin-3 (PTX3) expression in the brain. **A**, Cerebral ischemia results in PTX3 production in the ipsilateral (ipsi.) hemisphere 24 hours after experimental stroke compared to the contralateral (contra.) hemisphere and sham surgery as measured by ELISA. **B**, Immunohistochemistry reveals PTX3 staining in the ischemic (I, ipsi.) but not on the contralateral (C, contra.) striatum. cc- corpus callosum. Yellow rectangles in the insert show the place of the fluorescent micrographs. **C**, PTX3 and myelin basic protein (MBP) staining in white matter tracts of the ipsilateral striatum (i). High magnification shows the proximity of myelin and PTX3 profiles (ii). **D**, **E**, MAP-2-positive neurons (D) and GFAP-positive astrocytes (E) (in the ipsilateral cortex and cc respectively) show PTX3 staining. **F**, **G**, CD45-positive neutrophils recruited to the ischemic striatum (F) and macrophages (G) do not show PTX3 staining 24 hours after middle cerebral artery occlusion. **H**, Striatal PTX3 staining along with 4',6-diamidino-2-phenylindole (DAPI) in wild-type (WT) (i) and PTX3 knockout (KO) (ii) animals. Pentraxin 3 staining is abolished by PTX3 antibody neutralization (preincubation with recombinant PTX3 peptide, iii). Scale bars: 100 mm (B), 40 μ m (C i) 10 μ m (C ii), 20 μ m (D-E), 50 μ m (F), 50 μ m (G), 100 μ m (H).

* $P < 0.05$, ** $P < 0.01$, one-way analysis of variance, followed by Bonferroni's *post hoc* test (n=3-6). Error bars show s.e.m.

Central, but not Peripheral Expression of Pentraxin-3 is Dependent on Interleukin-1 after Cerebral Ischemia.

To investigate whether endogenous IL-1 drives PTX3 expression after cerebral ischemia, we measured PTX3 levels in the brain of WT or IL-1 α/β KO mice after MCAo. IL-1 α/β KO mice showed no increase in brain PTX3 levels after MCAo compared to WT mice (Figure 2A, i), suggesting that IL-1 is essential for central PTX3 production. In WT mice, IL-1 β immunostaining was observed in close proximity to PTX3-positive bundles (Figure 2A, ii). In marked contrast with the brain, plasma PTX3 levels were increased in both WT and IL-1 α/β KO mice (Figure 2B, i), and similar levels of PTX3 were found in liver, spleen and circulating blood cells in both genotypes (Figure 2B, ii). These data indicate that central, but not systemic, expression of PTX3 is dependent on IL-1 after acute brain injury. The fact that IL-1 α/β KO mice have high plasma-derived but not brain-derived PTX3 after MCAo suggests that peripheral PTX3 does not substantially contribute to central PTX3 levels even after stroke.

Peripheral IL-1 injection nearly doubled plasma PTX3 levels (Figure 2C, i), with no effect on PTX3 expression in the cortex or striatum (Figure 2C, ii). These results suggest that peripheral PTX3 does not cross the BBB in the absence of brain injury.



[§]**Figure 2. Central, but not peripheral pentraxin-3 (PTX3) expression is interleukin-1 (IL-1)-dependent after cerebral ischemia.** **A**, Enzyme-linked immunosorbent assay (ELISA) analyses of brain from wild type (WT) and IL-1 α/β knockout (KO) mice 24 hours after middle cerebral artery occlusion (MCAo) indicates that brain PTX3 protein levels are elevated in the ipsilateral hemisphere of WT, but not of IL-1 α/β KO mice (i). IL-1 β -positive (green) cells are found in close vicinity of PTX3-positive structures (red) within the ipsilateral striatum (ii). **B**, Plasma PTX3 increases 24 hours after MCAo in both WT and IL-1 α/β KO mice (i), and PTX3 levels in liver, spleen and blood cells do not vary between genotypes (ii), as measured by ELISA. **C**, Peripheral IL-1 β injection (i.p.) results in an upregulation of PTX3 in plasma (i), but not in cerebral cortex or striatum (ii). Scale bar, 25 μ m. * P <0.05, ** P <0.01, one-way analysis of variance followed by Bonferroni's *post hoc* test (**A,B**), $n=3$; (**C**) i $n=3$, ii $n=2$ to 3. Error bars show s.e.m. [§]See errata at the end of the chapter.

Interleukin-1, but not Injury-Driven Stimuli, Induces Pentraxin-3 Expression in Brain Cells

To confirm the role of IL-1 as key driver of PTX3 expression in the brain, we treated neuronal (Figure 3A, i and ii) and mixed glial (Figure 3A, iii and iv) cultures with IL-1 α or IL-1 β , and we measured PTX3 release. Low basal levels of PTX3 protein were detected in untreated or vehicle-treated cultures. In contrast, both IL-1 isoforms induced a marked increase in PTX3 synthesis and release, which was abrogated by heat inactivation of IL-1, or in the presence of the naturally occurring IL-1Ra, whilst IL-1Ra alone had no effect on PTX3 expression (Figure 3A). These findings were also confirmed by immunocytochemistry. Neurons (Figure 3B, i) and astrocytes (Figure 3C, i) showed a marked increase in PTX3 staining after treatment with IL-1 compared to basal conditions (Figure 3C, ii). Interleukin-1-induced PTX3 immunostaining was absent when the PTX3 antibody was immune-neutralized with recombinant PTX3 (Figures 3B and 3C, ii and iii).

We next investigated whether PTX3 expression is induced primarily by inflammatory (IL-1 dependent) mechanisms, or can be induced by other (injury dependent) stimuli present *in vivo* after cerebral ischemia such as excitotoxicity, hypoxia, glucose depletion or oxidative stress (Moskowitz *et al.*, 2010). Pentraxin-3 (PTX3) production was not induced by treatment of neuronal cultures with excitotoxic (N-methyl-D-aspartate), hypoxic (activation of HIF-1 by CoCl₂) (Moroz *et al.*, 2009) stimuli, after glucose depletion with 2-deoxyglucose (2DG) or after oxidative stress (H₂O₂) (Figure 3D), suggesting that the main inducer of PTX3 in ischemic injury is IL-1.

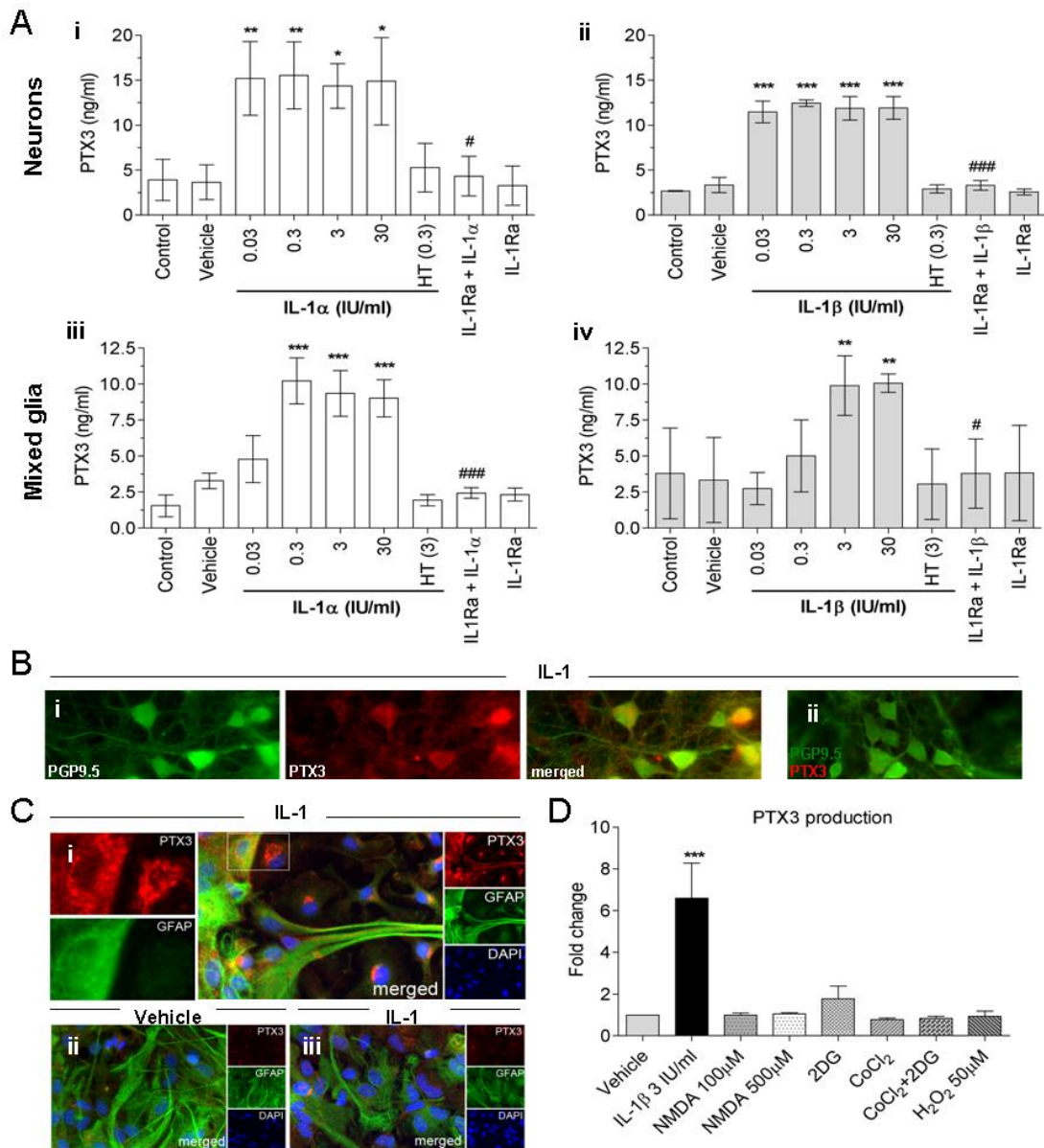


Figure 3. Interleukin-1 (IL-1) but not ischemic, excitotoxic or oxidative stimuli induce PTX3 release *in vitro*. **A**, Primary neuronal (i and ii) and mixed glial (iii and iv) cultures were treated with IL-1 α or IL-1 β (0.03 IU/mL - 30 IU/mL), heat-treated (HT) IL-1 α /IL-1 β (0.3 or 3 IU/mL respectively), IL-1Ra (10 μ g/mL) plus IL-1 α /IL-1 β (0.3 or 3 IU/mL respectively) or IL-1Ra alone for 24 hours, and PTX3 release was measured in the culture supernatants by enzyme-linked immunosorbent assay (ELISA). Both IL-1 α (i and iii) and IL-1 β (ii and iv) significantly induced release of PTX3 from neurons and mixed glial cells, which was completely inhibited by heat-treatment of IL-1 or co-incubation with IL-1Ra. **B**, Pentraxin-3 is expressed by cultured neurons (PGP9.5-positive) treated with IL-1 (i). Pentraxin-3 staining is

abolished by PTX3 antibody neutralization (preincubation with recombinant PTX3 peptide, ii). **C**, Astrocytes (glial fibrillary acidic protein (GFAP)-positive) treated with IL-1 (i) express PTX3, whereas vehicle-treated astrocytes do not express PTX3 (ii). Pentraxin-3 staining is abolished by PTX3 antibody neutralization (iii). **D**, Pentraxin-3 ELISA of supernatants of neuronal cultures treated with IL-1 β (3 IU/mL), N-methyl-D-aspartate (NMDA) (100 or 500 μ mol/L), CoCl₂ (500 μ mol/L) with or without 2-deoxyglucose (2DG) (1500 μ mol/L) or H₂O₂ (50 μ mol/L) for 24 hours. Only IL-1 β induced PTX3 production *in vitro*. * $P < 0.05$, ** $P < 0.01$, *** $P < 0.001$ IL-1 treated vs. vehicle. # $P < 0.05$, ### $P < 0.001$ IL-1+IL-1Ra vs. IL-1 alone, using one-way analysis of variance and Bonferroni's (A) $n=3-5$ or Dunnett's (D) $n=3$ *post hoc* tests. Error bars show s.e.m. DAPI, 4',6-diamidino-2-phenylindole.

Pentraxin-3 Deficiency Affects Delayed but not Acute Brain Damage after Middle Cerebral Artery Occlusion

To explore whether PTX3 influences neuronal death, brain damage was assessed in WT and PTX3 KO mice early (48 hours) and late (6 days) after acute ischemic brain injury. No significant differences were found in infarct volume, BBB damage (Figure 4A), or brain edema (Figure 4B) between WT and PTX3 KO mice 48 hours after MCAo, although a trend for reduced edema ($2 \pm 2\%$ in PTX3 KO vs $5 \pm 3\%$ in WT; mean \pm s.e.m.) in PTX3 KO mice was observed (Figure 4B). The absence of a significant effect may be due to the high variation. In contrast, 6 days after MCAo, BBB damage was significantly higher (Figure 5A) and resolution of edema did not occur (Figure 5B) in PTX3 KO mice. Infarct volume was not significantly different between WT and PTX3 KO mice 6 days after MCAo. To understand the reason for differences in resolution of brain edema between WT and PTX3 KO mice after cerebral ischemia, we measured expression of the tight junction proteins occludin and zonula occludens-1, the matrix metalloproteinase-9 and the water channel aquaporin-4.

Zonula occludens-1 expression was higher in PTX3 KO compared to WT mice, but we did not find differences in expression of other markers assessed (Supplementary Figure 5).

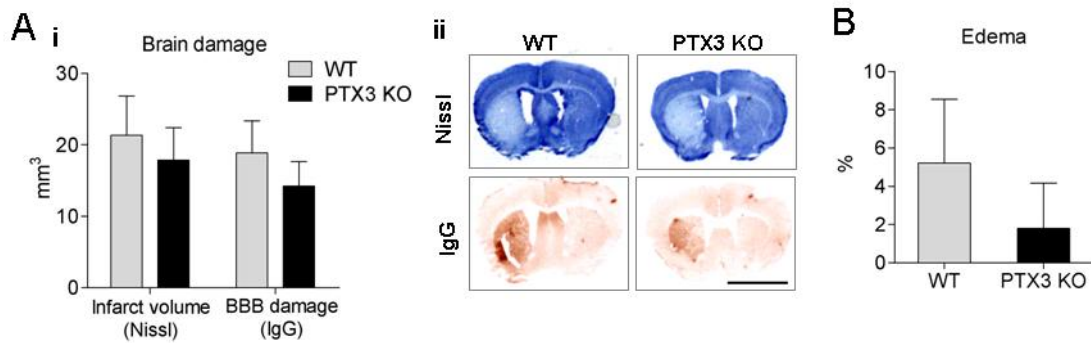


Figure 4. Lack of pentraxin-3 (PTX3) does not affect brain damage acutely after middle cerebral artery occlusion (MCAo). **A**, Forty-eight hours after MCAo, no significant difference is observed in infarct size or blood-brain barrier (BBB) damage between wild type (WT) and PTX3 knockout (KO) mice (i), as measured by Nissl (cresyl violet) staining and immunoglobulin G (IgG) infiltration (ii). **B**, No significant difference is observed in edema between WT and PTX3 KO mice, 48 hours after MCAo. Scale bar, 3 mm. Students *t*-test (A, B) *n*=6-7. Error bars show s.e.m.

Pentraxin-3 Deficiency Compromises Glial Scar Formation after Cerebral Ischemia

We then investigated the role of PTX3 in glial responses that are involved in brain repair after injury. Astrocytic scar formation (GFAP-positive cells surrounding the infarct) was markedly impaired in mice lacking PTX3 (Figure 5C): only 52% of the perimeter of the infarct was covered by astrocytic scar in PTX3 KO mice, vs. almost complete coverage (87%) in WT mice (Figure 5C, v). Although scar formation was profoundly affected, the overall number of astrocytes was similar between both

genotypes in the ipsilateral hemisphere (Figure 5C, vi). Astrocytic proliferation was quantified to explore whether it could account for deficient scar formation, but no significant difference was observed (data not shown). As PTX3 is involved in the stabilization of the extracellular matrix in peripheral tissues, we assessed the levels of laminin- α 4 in the astrocytic scar and in the gaps of the scar. Both genotypes had a similar amount of laminin- α 4 within the scar, however, over 50% of laminin- α 4 staining was lost in the gaps (seen in PTX3 KO mice) compared to the scar of WT mice (Figure 5D), indicating that the absence of PTX3 compromises glial responses and extracellular matrix deposition after brain injury. Microglial proliferation, which is also important for glial scar formation, was profoundly reduced in PTX3 KO compared to WT mice both in the scar surrounding the infarct and in the core of the infarct in the striatum (Figure 5E). We have shown earlier that proliferation of microglia in the striatum after MCAo is not affected significantly by the size of infarct or amount of neuronal injury, unlike in the cerebral cortex (Denes *et al.*, 2007); therefore, our data indicate that PTX3 is involved in glial proliferative responses in response to brain injury. To study if PTX3 could directly affect glial proliferation, BrdU incorporation was quantified in WT mixed glial cultures treated with PTX3. Low concentration of PTX3 (0.3 ng/mL) was effective at inducing glial proliferation although a higher concentration of PTX3 (30 ng/mL) was not effective (Figure 5F). As expected, FGF2 (used as a positive control) strongly induced proliferation, whereas cytosine arabinoside (used as a negative control) inhibited it (Figure 5F).

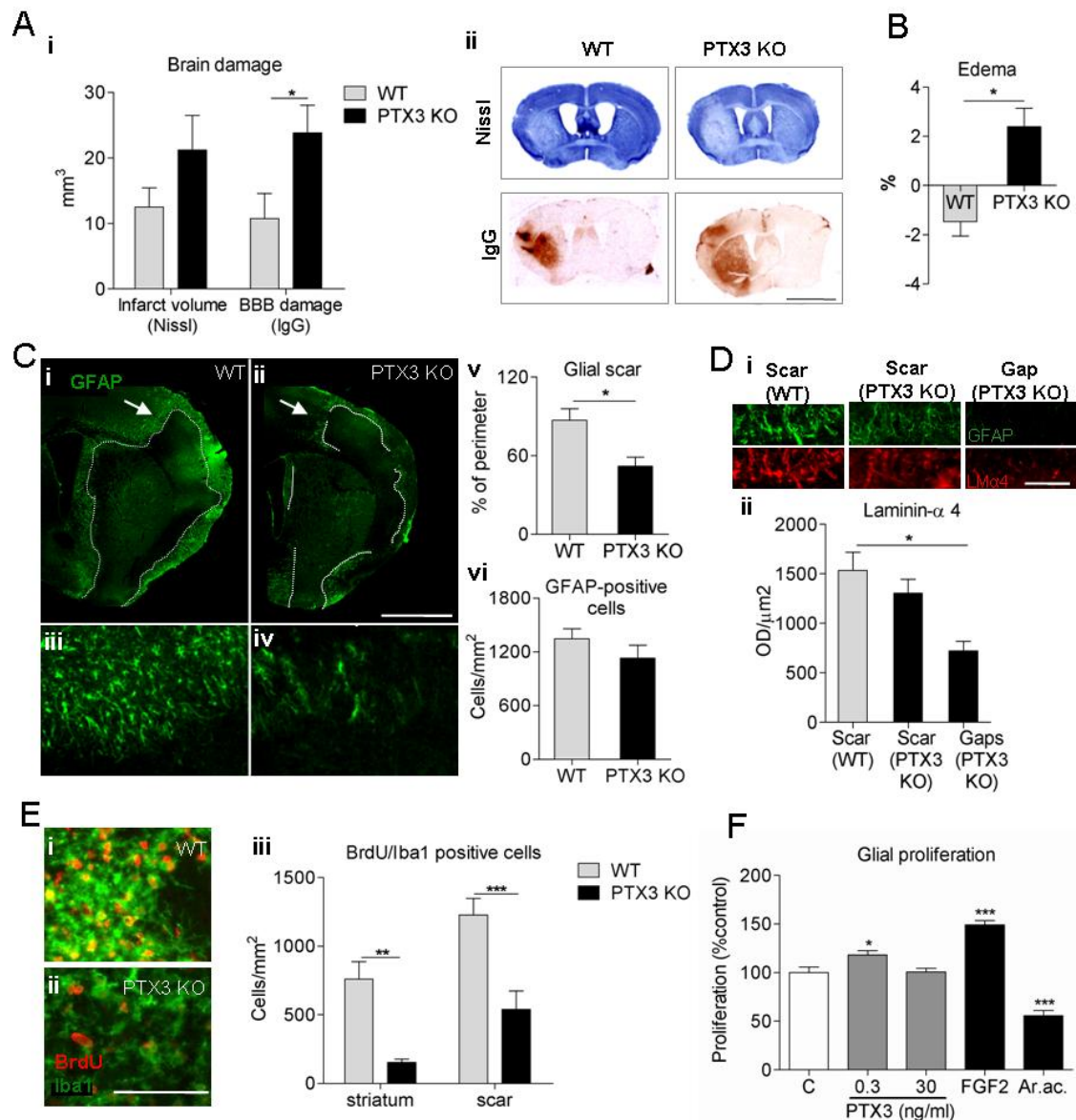


Figure 5. Pentraxin-3 (PTX3) knockout (KO) mice show increased blood-brain barrier (BBB) damage and edema, and impaired glial responses compared to wild type (WT) mice, 6 days after middle cerebral artery occlusion (MCAo). **A**, Blood-brain barrier breakdown, but not overall infarct size is significantly increased in PTX3 KO mice compared to WT mice, as measured on Nissl (cresyl violet) and immunoglobulin G (IgG) infiltration. **B**, Edema is not resolved in PTX3 KO mice whereas it is reversed in WT mice. **C**, Lack of PTX3 disrupts astrocytic scar formation as observed by glial fibrillary acidic (GFAP) staining in the ipsilateral hemisphere of PTX3 KO mice. Arrows in “i” and “ii” correspond to the inserts shown in “iii” and “iv”. The length of injured area surrounded by astrocytic scar is delineated with a dotted line. In average, GFAP-positive scar covers only 52% of the perimeter of the

injured area in PTX3 KO mice, whereas in WT mice it covers 87% (v). The total amount of astrocytic cells is not different between genotypes (vi). **D**, The gaps in the glial scar of PTX3 KO mice (areas where GFAP-positive astrocytes are absent surrounding the infarct) showed significantly less extracellular matrix production identified by laminin- α 4 staining compared to that of WT mice where astrocytic scar formation was not impaired around the infarct. **E**, Immunohistochemical staining reveals a profound decrease in proliferating (bromodeoxyuridine (BrdU)-positive) microglia (Iba1-positive) in the striatum and around the glial scar of PTX3 KO mice compared to WT mice. **F**, Addition of low (0.3 ng/mL) but not high (30 ng/mL) concentration of PTX3 to WT mixed glial cultures induces significant proliferation within 48 hours. LM α 4-Laminin- α 4, AraC-cytosine arabinoside. Scale bar, 3 mm (A), 1 mm (C), 50 μ m (D), 100 μ m (E) Students *t*-test (A-C, E) *n*=5 to 6) or one-way analysis of variance followed by Bonferroni's (D) *n*=3 to 4 or Dunnett's *post hoc* tests (F) *n*=9) were used. **P*<0.05, ***P*<0.01, ****P*<0.001. Error bars show s.e.m.

Discussion

The present study is the first to show that the acute-phase protein PTX3, lately associated with severity of vascular diseases (Jenny *et al.*, 2009; Kaess & Vasan, 2011; Latini *et al.*, 2004; Matsubara *et al.*, 2011; Ryu *et al.*, 2012), is expressed in the brain after acute ischemic brain injury. Our data demonstrate that IL-1, which has acute detrimental effects in brain injury (Allan *et al.*, 2005), induces PTX3 after cerebral ischemia, and that PTX3 contributes to brain recovery by promoting repair mechanisms such as glial scar formation and resolution of edema.

Here we show that not only circulating (as shown by Ryu et colleagues) (Ryu *et al.*, 2012) but also local PTX3 expression takes place in the brain in response to ischemic damage. Pentraxin-3 is reportedly expressed by macrophages, but we found no PTX3-positive leukocytes or microglia/macrophages in the brain. We cannot exclude the

possibility that PTX3 is released very quickly by macrophages, and could also contribute to elevated PTX3 levels in the brain after cerebral ischemia. Since PTX3 levels correlate positively with worse outcome in stroke patients (Ryu *et al.*, 2012), further investigation is needed to reveal how brain-derived PTX3 contributes to circulating PTX3 levels in experimental models. We demonstrate that IL-1 produced locally after cerebral ischemia (Allan & Pinteaux, 2003) is the key driver of brain PTX3 expression after MCAo. It has been shown that IL-1 injection into the brain can induce PTX3 expression (Polentarutti *et al.*, 2000), but we show that the increase in endogenous IL-1 after MCAo induces PTX3 expression in the brain after MCAo. Also *in vitro*, IL-1 (but not other ischemia-associated stimuli) greatly enhances PTX3 expression. Pentraxin-3 levels are thus likely to be increased in many CNS inflammatory disorders, since most of them present high levels of IL-1 (Allan & Pinteaux, 2003).

Although IL-1 also enhances circulating PTX3 levels, peripheral PTX3 expression can occur in an IL-1-independent manner (as observed in IL-1 α/β KO mice), highlighting a different regulation of PTX3 expression in the CNS. Pentraxin-3 can be induced by other pro-inflammatory cytokines such as TNF- α (Polentarutti *et al.*, 2000) which could account for the increase in peripheral PTX3 after MCAo. Furthermore, circulating IL-1 did not drive central PTX3 expression in our model, demonstrating the specific role for centrally expressed IL-1 in brain PTX3 production. Other cytokines may contribute to brain PTX3 production although to a lower extent than IL-1, since even IL-1 α/β KO mice show an increase in PTX3 levels after MCAo compared to sham.

Interestingly, PTX3 depletion did not affect brain damage early after the ischemic event (48 hours after MCAo), but we found that PTX3 is a critical mediator of brain

responses 6 days after ischemic brain injury. In particular, lack of PTX3 impaired glial scar formation, and low levels of PTX3 promoted glial proliferation. The glial scar is fundamental to limit the spread of the damage and may also help the recovery of vascular functions (Kawano *et al.*, 2012; Rolls *et al.*, 2009). Indeed, we found that PTX3 KO mice had higher level of BBB damage and delayed resolution of brain edema. Surprisingly, PTX3 KO mice had higher expression of zonula occludens-1, which could suggest more endothelial tight junctions and hence a less damaged BBB. However, our data indicate increased BBB permeability and edema, implying that tight junctions in PTX3 KO mice were less functionally intact than in WT animals at 6 days reperfusion. Therefore, it is possible that zonula occludens-1 upregulation is a compensatory response in PTX3 KO mice to counterbalance the increased BBB damage. Extracellular matrix instability in the areas of the scar that were depleted of astrocytes was suggested by the decrease in levels of laminin- α 4, which is essential for stability of the basal lamina and for the formation of new blood vessels (Thyboll *et al.*, 2002). Furthermore, we also found impaired microglial proliferation in PTX3 KO mice. There is increasing evidence that microglial activation and proliferation can promote repair (Denes *et al.*, 2007; Polazzi & Monti, 2010). Further research is needed to reveal the molecular mechanisms whereby PTX3 exerts its actions on glial responses and extracellular matrix deposition. We observed a non-significant trend for smaller infarct size ($41\% \pm 28\%$) in WT mice compared to PTX3 KO mice at 6 days reperfusion, but the robust reduction of glial proliferation (which was also confirmed *in vitro*), reduced scar formation and increased edema in PTX3 KO mice cannot be explained by variable differences in infarct size. We demonstrated earlier that microglial proliferation after cerebral ischemia in the striatum is largely independent from infarct size (Denes *et al.*, 2011). In addition, PTX3 KO mice showed no

significant difference in infarct volume from WT mice at 48-hour reperfusion, arguing against the contribution of the primary ischemic injury to later inflammatory actions in these experiments.

In summary, our results demonstrate for the first time that IL-1 induces PTX3 expression in the brain after cerebral ischemia, and that PTX3 modulates glial responses and resolution of edema. Understanding the effects of IL-1 at different stages after brain injury could allow selective blockade of the detrimental acute effects of IL-1 actions while allowing its potential role in repair during the recovery phase. The exact mechanisms by which IL-1-induced PTX3 contributes to brain recovery need further investigation, but the current results highlight PTX3 as a new possible target for CNS inflammatory disorders.

Disclosure/conflict of interests

The authors declare no conflict of interest.

Acknowledgements

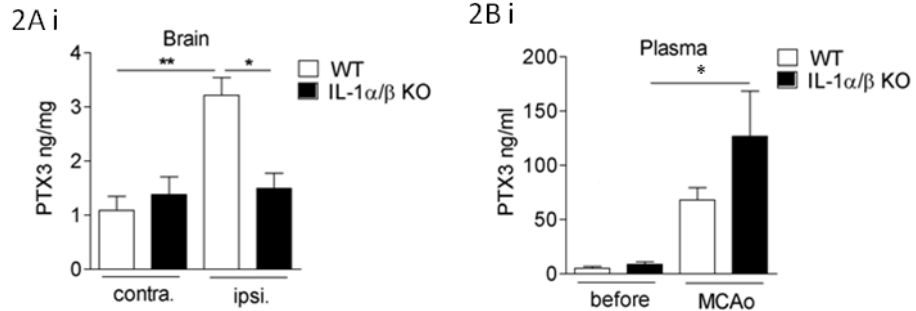
We would like to thank Professor Alberto Mantovani and Professor Richard Grencis for critically reviewing the manuscript, and Ms Catherine Smedley for genotyping.

Supplementary information is available at the Journal of Cerebral Blood Flow & Metabolism website –www.nature.com/jcbfm

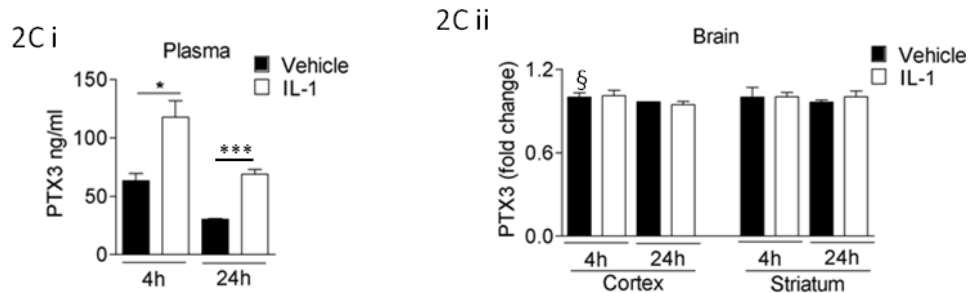
§Errata

Errata were found in Figure 2. See corrected statistical analyses and graphs below.

- Figure 2A i and 2B i: in order to evaluate the difference between areas or time points in addition to inter-group differences, two-way ANOVA should have been used as follows:



- Information missing in the original article: Figure 2B ii and 2C ii were analysed with t-tests.
- Figure 2C i: t-tests should have been used since the objective was to compare vehicle vs IL-1 treatment, but not to compare differences across time points.
- Figure 2C ii contains a group with an n=2 (cortex, 4h, vehicle group), which should have been indicated in the graph (§). Cortex 4h groups should have not been included in the statistical analysis.



The following sentences should be amended in the original article as a consequence of the loss/gain of significance in graphs 2B i and 2C i:

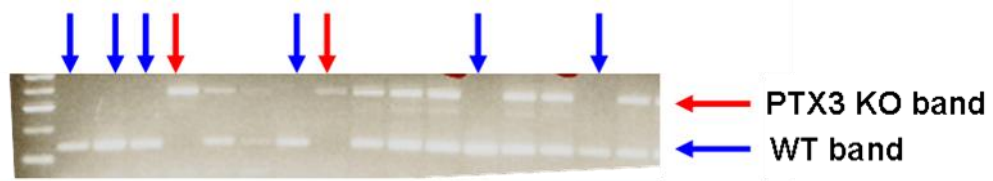
- The significant difference between WT groups before and after MCAo is lost (2B i), and thus figure legend 2B i should read “*Plasma PTX3 increases 24 hours after MCAo in IL-1 α/β KO mice (i)*” and line 11 in article page 14 should read “*In marked contrast with the brain, plasma PTX3 levels were increased in IL-1 α/β KO mice*”. This changes do not compromise interpretation of the results, since the main finding was the increase in PTX3 levels in plasma (Figure 2B i) but not in

brain (Figure 2A i) of IL-1 α/β KO mice as a consequence of MCAo. These results are conserved with the corrected statistical tests.

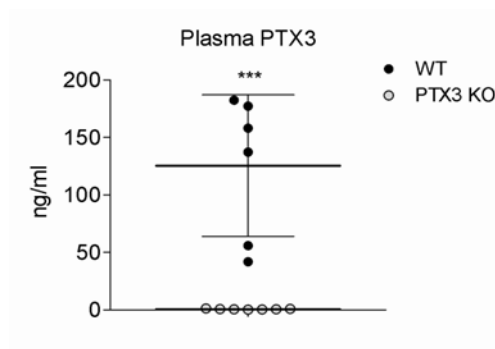
- Significance between groups at 24h in figure 2C i only reinforces the point made in the article and no modification in the article text is required.
- The last sentence of the figure legend should read “* $P < 0.05$, ** $P < 0.01$, *** $P < 0.001$. Two-way analysis of variance followed by Bonferroni's post hoc test (**A, B i**), $n=3$; and unpaired t -test (**B ii, C**) $n=3$ were used. § indicates $n=2$ and exclusion from statistical analysis. Error bars show s.e.m.”

Supplementary information to Chapter 3

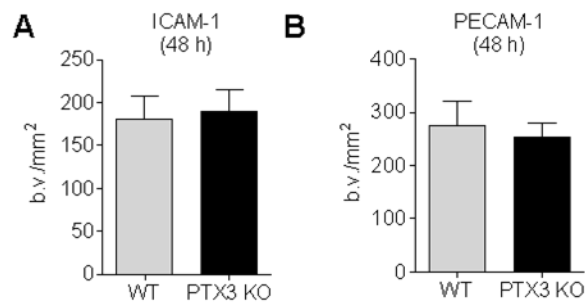
The following data was published as Supplementary information of the previous article (Rodriguez-Grande *et al.*, 2014).



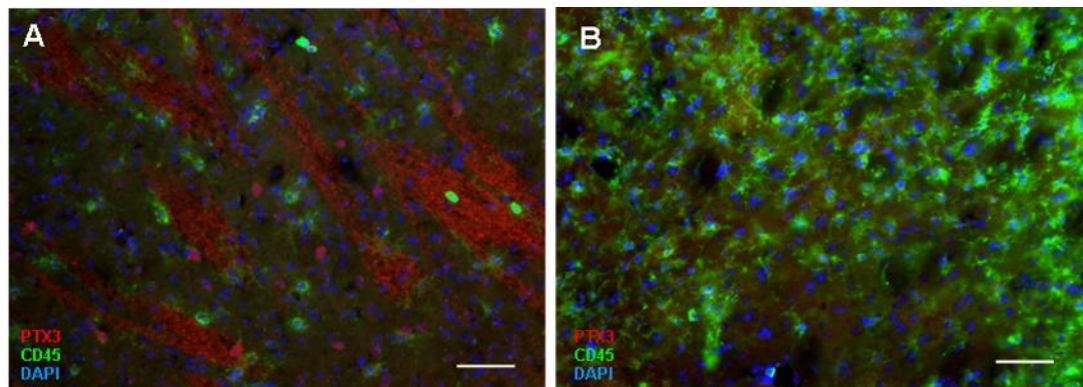
Supplementary figure 1. Representative example showing a PCR gel used for genotyping of littermates. PCR was performed using 3 oligonucleotides: 1 and 2 recognize WT *ptx3*; 3 and 2 recognize the mutation site. As a result, WT animals have one band of 124 bp, PTX3 KO animals have one band of 300 bp and heterozygous animals have two bands: one of 124 bp and one of 300 bp. PTX3 KO animals are indicated with a red arrow and WT animals with a blue arrow. The remaining animals shown are heterozygous. For details about PTX3 KO generation see supplementary data of the article (Garlanda *et al.*, 2002).



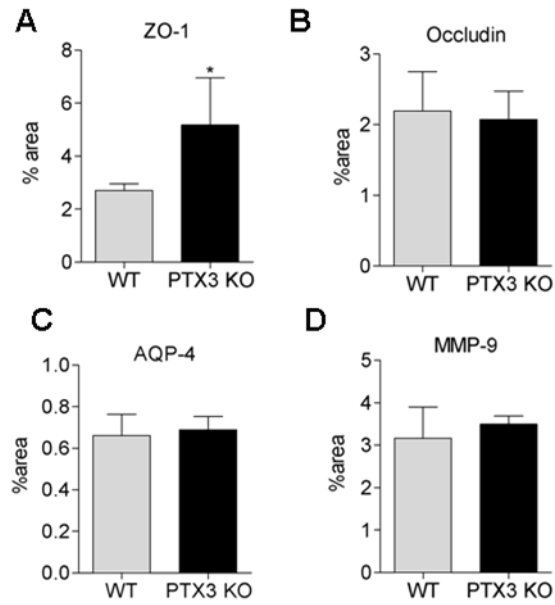
Supplementary figure 2. PTX3 ELISA on plasma samples from mice after 30 min MCAo and 48 h reperfusion. Plasma PTX3 concentrations ranged from 41.9 to 182.5 ng/ml in WT mice whereas were lower than 1.35 ng/ml in all PTX3 KO mice (limit of detection was 1.2 ng/ml). Error bars show s.e.m.



Supplementary figure 3. Vascular density in WT and PTX3 KO mice. A, B, Quantification of ICAM-1 (**A**) or PECAM-1 (**B**) positive blood vessels (b.v.) in the striatum of WT and PTX3 KO mice 48 h after MCAo reveal no significant difference between genotypes. Students t-test (A, n=6-7; B, n=4) was performed. Error bars show s.e.m.



Supplementary figure 4. CD45-PTX3 immunostaining. A, B, CD45-positive neutrophils and macrophages do not colocalize with PTX3 staining in the ipsilateral striatum 48 h (**A**) or 6 days (**B**) after MCAo. Scale bar 50 µm.



Supplementary figure 5. Quantification of vascular and BBB proteins. **A, B**, ZO-1 (A), but not occludin (B) is upregulated in PTX3 KO mice compared to WT mice. **C, D**, Levels of AQP-4 and MMP-9 are similar in both genotypes. Students t-test (A, n=4-6; B, C, n=5-6; D, n=3-5) was used. *P<0.05. Error bars show s.e.m.

Additional supplementary information to Chapter 3

This section contains additional data that complements the previous article (Rodríguez-Grande *et al.*, 2014) but that could not be published due to space constraints in the main article and its Supplementary information.

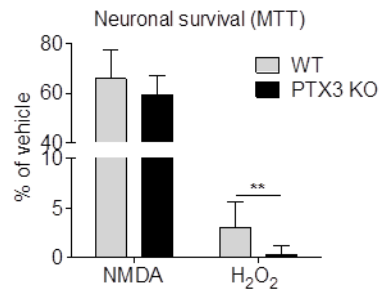


Figure 1. Neuroprotection by endogenous PTX3. Endogenous PTX3 protects from neurotoxicity mediated by oxidative stress but not excitotoxicity, as reflected by neuronal survival of primary neuronal culture measured by MTT assay 24 h after treatment with H₂O₂ or NMDA. One-way ANOVA followed by Bonferroni's post-hoc test (n=3) was used. **P<0.01. Error bars show s.e.m.

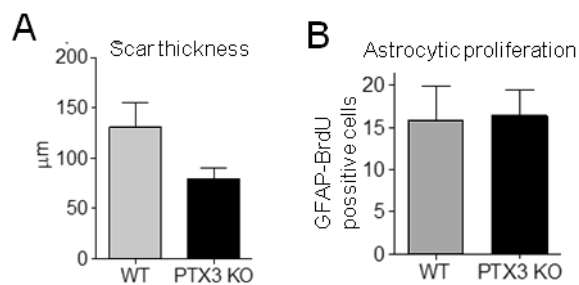


Figure 2. Scar thickness and astrocytic proliferation in the scar are not altered by PTX3 6 days after MCAo. **A**, There is a non significant trend for a reduced scar thickness in PTX3 KO compared to WT mice. **B**, Astrocytic proliferation is similar in both genotypes. Students t-test (n=3-4) was used.

Chapter 4: PTX3 in angiogenesis and neurogenesis

This chapter is written in a research paper format waiting to be sent for peer review.

Pentraxin 3 mediates angiogenesis and neurogenesis after cerebral ischaemia.

Beatriz Rodriguez-Grande, MRes¹, Lidiya Varghese, MRes¹, Francisco Molina-Holgado², Adam Denes, PhD^{1,3} and Emmanuel Pinteaux, PhD¹

¹Faculty of Life Sciences, A.V. Hill Building, University of Manchester, Oxford Road, Manchester, M13 9PT, UK; ²Health Sciences Research Centre, Roehampton University, Whitelands College, Holybourne Avenue, London SW15 4SD, UK; ³Laboratory of Molecular Neuroendocrinology, Institute of Experimental Medicine, Budapest H-1450, Hungary

Abstract

The acute phase protein pentraxin 3 (PTX3) is a biomarker of stroke severity, and is a key regulator of oedema resolution and glial responses after cerebral ischaemia, emerging as a possible target for brain repair after stroke. Neurogenesis and angiogenesis are essential events in post-stroke recovery. Here we investigated for the first time the role of PTX3 in angiogenesis and neurogenesis after experimental stroke in mice. We used the middle cerebral artery occlusion (MCAo) model of cerebral ischaemia in PTX3 knock out (KO) mice, and quantified proliferating blood vessels in brain sections 6 and 14 days after MCAo. This revealed that 14 days but not 6 days after MCAo PTX3 KO mice had less vasculature, and that vasculature was less proliferative. Expression of vascular endothelial growth factor receptor (VEGFR)2 was reduced in PTX3 KO mice at both times. Neurogenesis, measured as the amount of nestin-positive neural progenitor cells, was reduced in the hippocampus of PTX3 KO mice 6 days after MCAo, but not after 14 days recovery. In addition, recombinant PTX3 was neurogenic when added to neurospheres, which was mediated by the pro-inflammatory cytokine interleukin 1 (IL-1). Lack of PTX3 potentiated contralateral motor deficits after 14 days of recovery. These results indicate that PTX3 enhances angiogenesis and facilitates neurogenesis after stroke. This strengthens the relevance of PTX3 as a mediator of brain repair, and highlights it as a possible target for stroke treatment.

Introduction

The acute phase protein pentraxin-3 (PTX3) is known for its role in immune regulation in the periphery, where it also has anti-inflammatory actions (Deban *et al.*, 2010a). PTX3 levels rapidly increase after stroke, and plasma levels of PTX3 correlate with stroke mortality after ischaemic stroke (Ryu *et al.*, 2012). However, the exact role of PTX3 in the brain is not well characterised. Our recent work showed that PTX3 is important for blood brain barrier (BBB) integrity, resolution of oedema and glial scar formation during the early stages of repair after stroke (Rodriguez-Grande *et al.*, 2014); however, the role of PTX3 in delayed repair processes such as angiogenesis and neurogenesis has not been studied to date. We have previously reported no significant changes in the vasculature or the cerebral blood flow (CBF) of PTX3 KO mice up to 48 h after experimental cerebral ischaemia, suggesting that PTX3 does not have a main role in early vascular remodelling (Rodriguez-Grande *et al.*, 2014). Whilst PTX3 can exert anti-angiogenic actions in peripheral vascular beds (Leali *et al.*, 2012), its role in post-stroke angiogenesis remains unknown. Angiogenesis takes place primarily in the penumbra surrounding the ischaemic core, correlates with survival after stroke (Krupinski *et al.*, 1994) and is tightly linked with neurogenesis, since neural progenitor cells differentiate and migrate along the angiogenic niche (Ohab & Carmichael, 2008). The role of PTX3 in neurogenesis has never been explored and therefore the aim of this study was to characterize the role of PTX3 in post-stroke angiogenesis and neurogenesis, and to explore whether PTX3 has an impact on functional recovery.

Materials and Methods

Animals

PTX3 knockout (KO) mice, kindly provided by Dr. Cecilia Garlanda (Humanitas Clinical and Research Center, Rozzano, Italy), were bred as heterozygous and litter genotyping was performed as described previously (Garlanda *et al.*, 2002). Age- and weight-matched wild-type (WT) and PTX3 KO littermates were used for all experiments. IL-1 β KO mice were provided by Prof. Yoichiro Iwakura (University of Tokyo, Japan). All mice were bred on a C57BL/6 background. Mice had free access to food and water and were kept at 21 °C \pm 1 °C, 55 % \pm 10 % (v/v) humidity, in a 12 h light-dark cycle. All animal procedures were carried out in accordance with the European Council directives (86/609/EEC) the Animal Scientific Procedures Act (UK) 1986 and the ARRIVE guidelines.

Middle cerebral artery occlusion and BrdU administration

Transient middle cerebral artery occlusion (MCAo) was used as a model of transient ischaemic stroke, and performed as described previously (Denes *et al.*, 2007). Briefly, a filament was introduced through the left common carotid and advanced up to the middle cerebral artery (MCA). Drop in blood flow in the MCA territory was confirmed by laser Doppler monitoring (Moor Instruments, UK). After 30 min of occlusion, the filament was removed and mice recovered for 48 h, 6 days or 14 days. Mice were daily injected subcutaneously with 0.5 ml of sterile saline during the first week and continuously monitored for neurologic symptoms. Bromodeoxyuridine (BrdU) (50 mg/kg, Sigma, UK) was intraperitoneally injected twice daily in mice that recovered for 6 days. For mice recovering for 14 days, BrdU was injected once a day on days 4 and 8, and twice a day on days 5-7.

Behavioural tests

Mice recovering for 14 days were tested for behavioural deficits. Basic motor deficits were measured with a points system adapted from (Hunter *et al.*, 2000) as follows: 1 point for torso flexion to right in the air; 2 points for deficit in gripping with a paw; 3 points for circling with the front paws when suspended from the tail; 4 points for spontaneous circling on the floor; 5 points for irresponsiveness to stimuli. The sum of all points was used as the score of motor deficit. General motivation to explore and motor function were measured in an open field: mouse movement within a square chamber was tracked for 5 min and analysed by overlapping the recording to a 16-squares grid with 2020 PLUS tracking software (HVS Image, UK). Time mobile, number of line crossings, number of rearings and rotational bias (asymmetric rotation that occurs as a consequence of unilateral MCAo) were measured. Short-term memory was measured in a Y-maze as described in (Hughes, 2004). Briefly, mouse entries in each arm of a Y-shaped chamber containing a different visual stimulus at the end of each arm were measured during 8 min. The percentage of alternations (i.e. ABC, CBA, BAC, etc.) was calculated. Y-maze test was performed on the evening of day 13 after MCAo, and assessment of motor scores and open field test were performed on the morning of day 14 after MCAo, when mice were euthanized.

Tissue collection and immunohistochemistry

Brains were collected and immunostained as explained in (Rodriguez-Grande *et al.*, 2014). Briefly, mice were transcardially perfused with 0.9 % (w/v) saline followed by 4 % (w/v) paraformaldehyde (PFA) and brains were removed and sectioned in coronal brain sections using a sledge microtome (Bright, UK). For BrdU visualization, sections were pretreated with 1 M HCl first for 2 min on ice, and then for 30 min at 37 °C. For

NeuN, doublecortin and nestin immunohistochemistry, sections were pretreated for 30 min with 10 mM sodium citrate at 50 °C. Non-specific staining was blocked with 2 % (v/v) normal donkey serum (Jackson laboratories, USA) in primary diluent (0.3 % (v/v) Triton X-100 in PBS). Overnight incubation in primary antibodies was followed by three washes and 2 h incubation in secondary fluorescent antibodies. Primary antibodies used were sheep anti-BrdU (1:500, Abcam, UK), rat anti-BrdU (1:500, AbD Serotec, UK), rat anti-PECAM-1 (1:200, BD Pharmingen, UK), rabbit anti-VEGFR2 (1:300, Cell Signalling, UK), mouse anti-NeuN (1, Millipore, UK), mouse anti-nestin (1:500, Millipore, UK) and goat anti-doublecortin (1:750, Santa Cruz Biotechnologies, USA). Secondary antibodies were conjugated to Alexa 488 or 594 fluorochromes (Invitrogen, UK). Sections were coverslipped with Prolong Gold antifade with or without DAPI (Invitrogen, UK). An Olympus BX51 upright microscope coupled to a Coolsnap ES camera (Photometrics, UK) and MetaVue Software (Molecular Devices, USA) were used to capture the images.

Image analysis

Counts of BrdU positive nuclei, PECAM-1 positive vessels and nestin positive profiles were done manually. Areas and mean optical density (OD) were measured using Image J (National Institutes of Health, USA). Percentages of area stained were measured manually using the threshold tool of Image J.

Neural stem progenitor cell cultures and proliferation

Neural stem progenitor cell (NSPC) cultures were prepared from the cerebral cortex of WT and IL-1 β KO mice embryos at 16 days of gestation as previously described (Reynolds & Weiss, 1992). Cells were then cultured as free-floating neurospheres in 75 cm² flasks (Nunc, Denmark) at a density of 20 cells/ μ l (Seaberg & van der Kooy,

2002) in DMEM/F12 supplemented with B27, 3 µg/ml heparin and 20 ng/ml fibroblast growth factor (FGF) and epidermal growth factor (EGF) (PeproTech, London, UK). Primary neurospheres were grown for 7-10 days before secondary cultures were established with mechanically dissociated cells. Thereafter, the spheres were passaged every 5–7 days and experiments were performed after three to seven passages.

NSPCs proliferation was assessed using a well accepted measure of neurosphere proliferation (Kokuzawa *et al.*, 2003; Schwindt *et al.*, 2009). NSPCs were progressively diluted from 4000 to 125 cells in 96-well plates. Dissociated cells were exposed for 7 days to a single optimal concentration of PTX3 (100 ng/ml), after which the number of neurospheres formed was counted. The number of new neurospheres was plotted against the initial number of cells plated, from which the behaviour of the neural stem cells was evaluated (Campos *et al.*, 2004; Tropepe *et al.*, 1999).

Measurement of neurogenesis *in vitro*

After 6 days in culture, the effect of PTX3 on neurosphere proliferation was quantified by treating the cells with PTX3 (100 ng/ml) for 24 h. BrdU (10 µM) was added in the last 18 h. Neurospheres were then dissociated, plated onto poly-L-ornithine coated (15 µg/ml) 24-well plates for 1 h, fixed for 20 min in 4 % (w/v) PFA and immunostained. For BrdU immunostaining, cells were treated with 2 M HCl for 10 min, which was neutralized with 0.1 M borate buffer, pH 9.5. BrdU was visualized with a BrdU monoclonal antibody (clone MoBU-1) Alexa Fluor conjugate 594 (Invitrogen, UK). BrdU incorporation was defined by the cells labeled by HOE 33342 (10 µM) and with the BrdU antibody. For neurosphere proliferation assays, images were acquired using a fluorescence microscope (Olympus BX51) and analyzed using the image analysis software ViewFinder 3.0.1 (Pixera Corporation, USA). Six microscope fields were

counted in each well at a 10× magnification, and two to four wells were used per treatment in each experiment.

Statistical analysis

Unpaired Student's t-test was used to compare two groups. For the comparison of more than two groups over serial dilutions (for NSPC *in vitro* proliferation) two-way ANOVA followed by Bonferroni's post-hoc test was used. For the comparison of means to a given value, one sample t-test was used. For motor scores, Mann-Whitney test was used. All graphs show mean ± SEM, except for motor deficit scores, in which medians and interquartile ranges have been used. Statistical significance was set at $P < 0.05$. All analysis were made using GraphPad Prism 5.0 (GraphPad Software Inc., USA).

Results

Lack of PTX3 impairs angiogenesis after MCAo

PTX3 KO mice had significantly less vascular staining (quantified as a percentage of the total area which was stained by PECAM-1) 14 days after MCAo (Fig.1 B), and the same trend, although not significant, was already observed 6 days after MCAo (Fig.1 A).

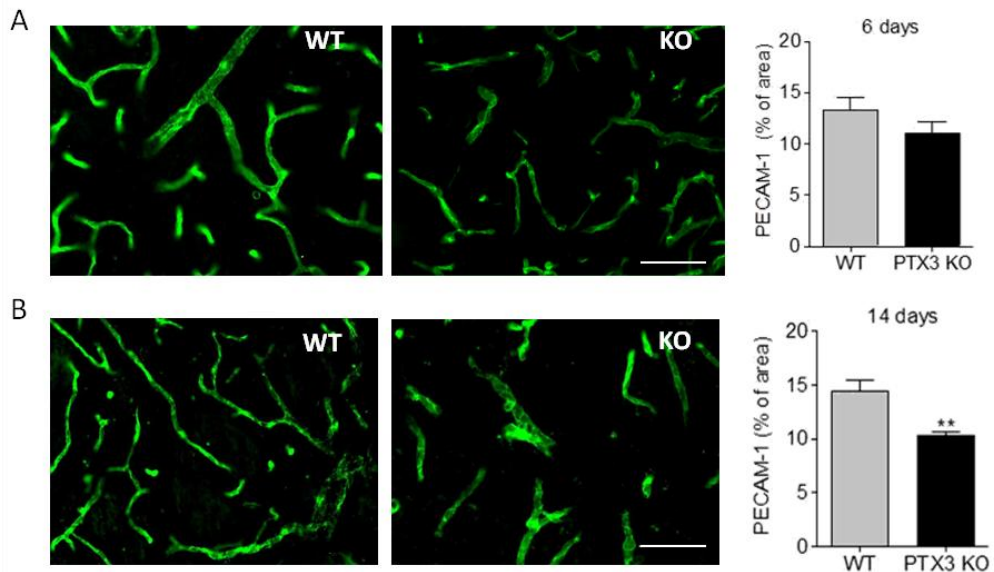


Figure 1. PTX3 KO mice have less vasculature in the striatum than WT mice during the recovery phase. A, B, PECAM-1 staining in the striatum of WT (A i and B i) and PTX3 KO (A ii and B ii) mice was quantified, showing that PTX3 KO mice have significantly less vasculature 14 days after MCAo (B iii). A similar trend, although not significant, is seen 6 days after MCAo (A iii). Scale bars = 50 μ m. Students t-test (n=4) was used. **P<0.01. Error bars show SEM.

To confirm that this variation in the vasculature was due to angiogenesis, we quantified the amount of BrdU incorporated by the vasculature. We did not find any proliferating vessels (PECAM-1 positive vessels containing BrdU) 48 h after MCAo (Fig. 2A). However, 6 days (Fig. 2B) and 14 days (Fig. 2C) after MCAo, we found several vessels that had incorporated BrdU. Lack of PTX3 significantly affected the amount of proliferating vessels 14 days (Fig. 2C iii) but not 6 days (Fig. 2B iii) after MCAo. To determine if the reduced amount of vascular BrdU was only due to the fact that PTX3 KO mice had less vessels, we normalised the amount of BrdU to the amount of vascular staining (Fig. 2B iv and 2C iv). This also indicated a significant deficit in angiogenesis in PTX3 KO mice 14 days after MCAo.

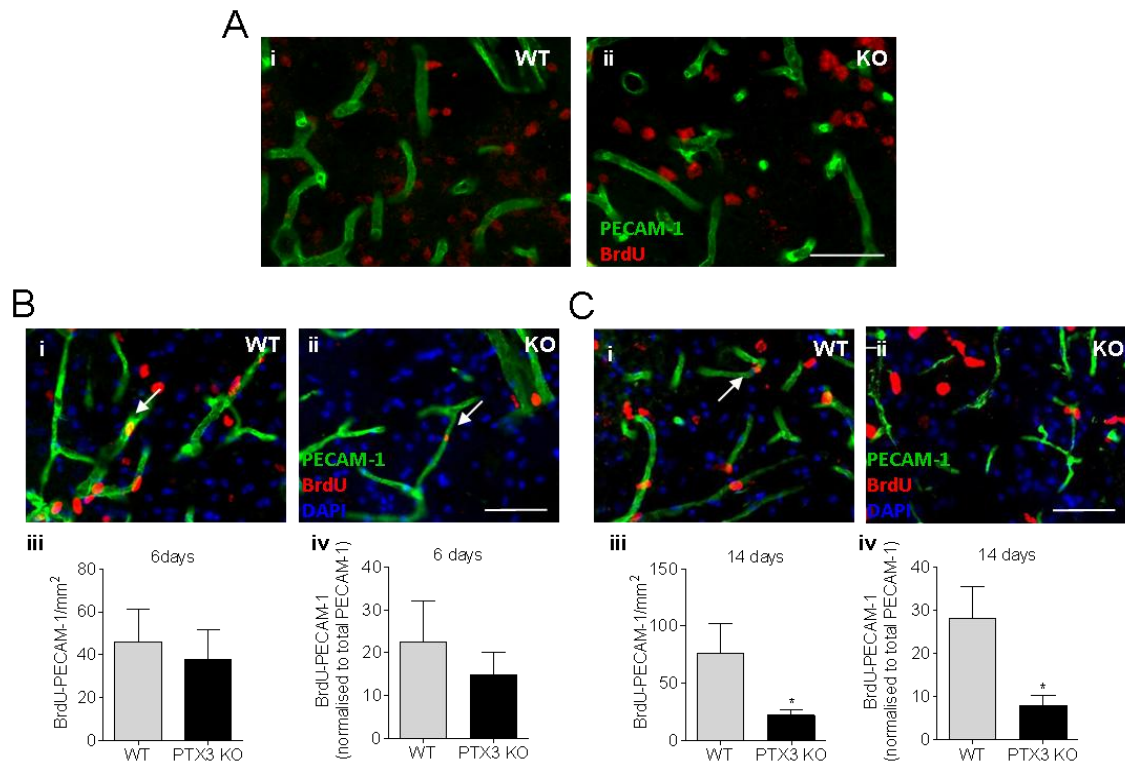


Figure 2. Lack of PTX3 impairs angiogenesis 14 days after MCAo. **A**, No angiogenesis (PECAM-1-BrdU positive blood vessels) is observed in the striatum 48 h after MCAo. **B**, **C**, Proliferating vessels (indicated by white arrows) are seen in the striatum 6 days (**B**) and 14 days (**C**) after MCAo. Angiogenesis is similar for both genotypes 6 days after MCAo (**B**), but PTX3 KO have less striatal proliferating vessels than WT mice 14 days after MCAo (**C** iii), even after normalisation with the total amount of PECAM-1 (**C** iv). Scale bars = 50 μ m. Students t-test (n=4) was used. *P<0.05. Error bars show SEM.

In addition to less proliferating vessels, PTX3 KO mice had less vascular VEGFR2 14 days after MCAo (Fig. 3), both as percentage of the total area (Fig. 3B, i) and when normalised and expressed as percentage of PECAM-1-positive area (Fig. 3B, ii). VEGF exerts a potent pro-angiogenic effect through activation of VEGFR2 (Beck & Plate, 2009), which levels increase after ischaemia (Marti *et al.*, 2000).

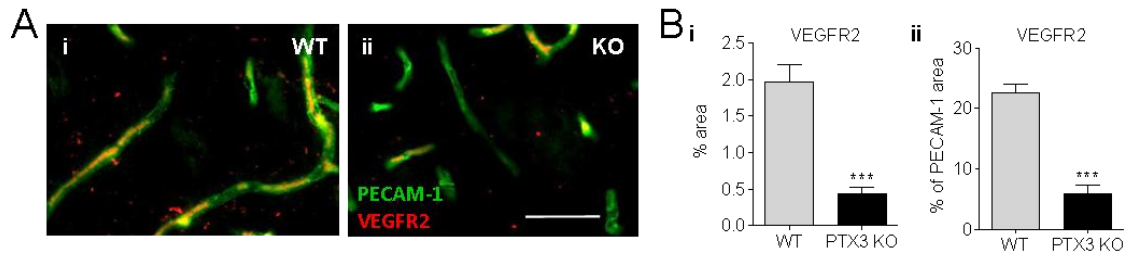


Figure 3. VEGFR2 is reduced in PTX3 KO mice 14 days after MCAo. A, B, Quantification of VEGFR2 immunostaining (red in A) indicate that PTX3 KO mice have a significantly reduced amount of VEGFR2 (B i), even when normalised with the levels of PECAM-1 (green in A) (B ii). Scale bars = 50 μ m. Students t-test (n=4) was used. ***P<0.001. Error bars show SEM.

PTX3 promotes neurogenesis

As neurogenesis is coupled to angiogenesis (Ohab & Carmichael, 2008) we tested whether PTX3 deletion affects newly formed NSPCs. Due to the dense immunofluorescent staining, it was difficult to identify double positive (BrdU-nestin or BrdU-doublecortin) cells 6 days after MCAo, and thus the intensity of each single staining was quantified. PTX3 KO mice had significantly less BrdU staining in the subventricular zone (SVZ) (Figure 4A i), and a similar trend was observed for nestin and doublecortin staining (Figure 4A ii and iii respectively). Importantly, nestin-positive NSPCs in the dentate gyrus (DG) of PTX3 KO mice were less abundant than in WT mice (Figure 4B i). Some of these nestin-positive NSPCs were proliferating as shown by BrdU incorporation (Figure 4B ii).

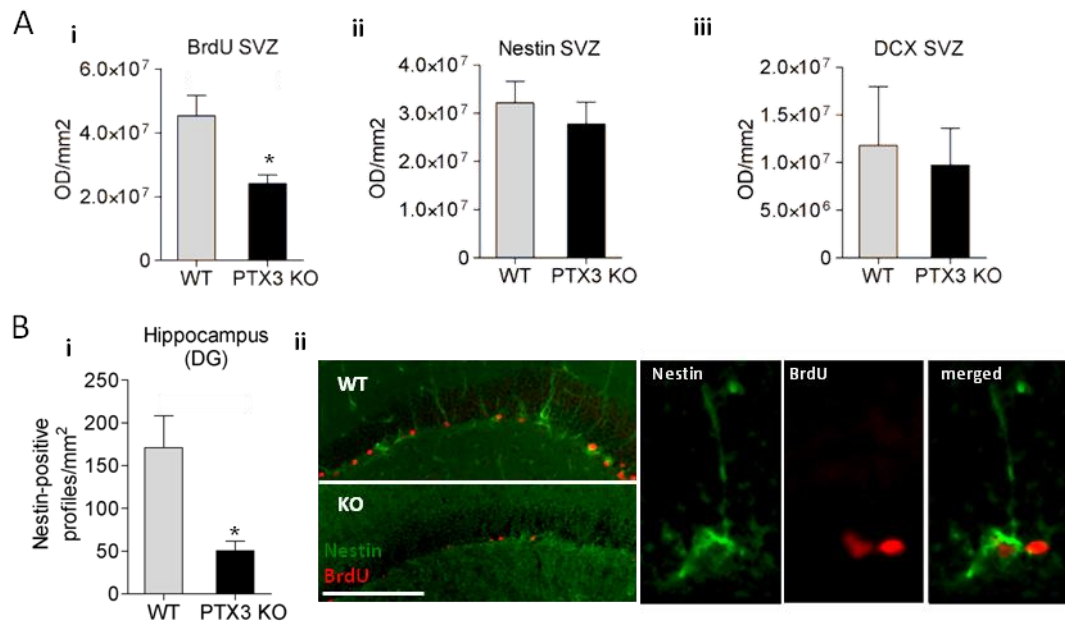


Figure 4. PTX3 deficiency impairs neurogenesis in the ischaemic brain 6 days after MCAo. **A**, PTX3 KO mice have significantly less BrdU staining than WT mice in the subventricular zone (SVZ) 6 days after MCAo (i), and the same trend, although not significant, is observed for nestin (ii) and doublecortin (DCX) (iii) staining. **B**, Less nestin-positive profiles are found in the dentate gyrus (DG) of PTX3 KO mice compared to WT mice 6 days after MCAo (i). BrdU-nestin double immunofluorescence reveals some proliferating nestin-positive cells (ii). Scale bar: 200 μm. Students t-test (A, n=5; B, n=4-6) was used. *P<0.05. Error bars show SEM.

Given that one week after MCAo NSPCs are still starting to divide, we decided to look at a later time point (14 days after MCAo) and explore whether they had migrated to the striatum and whether they had already integrated as mature (NeuN-expressing) neurones. Lack of PTX3 did not significantly alter the amount of nestin-BrdU positive cells in the SVZ (Fig. 5A iii), although colocalisation between the two markers was difficult to establish due to the low intensity of nestin staining in some samples (Fig. 5A i and ii).

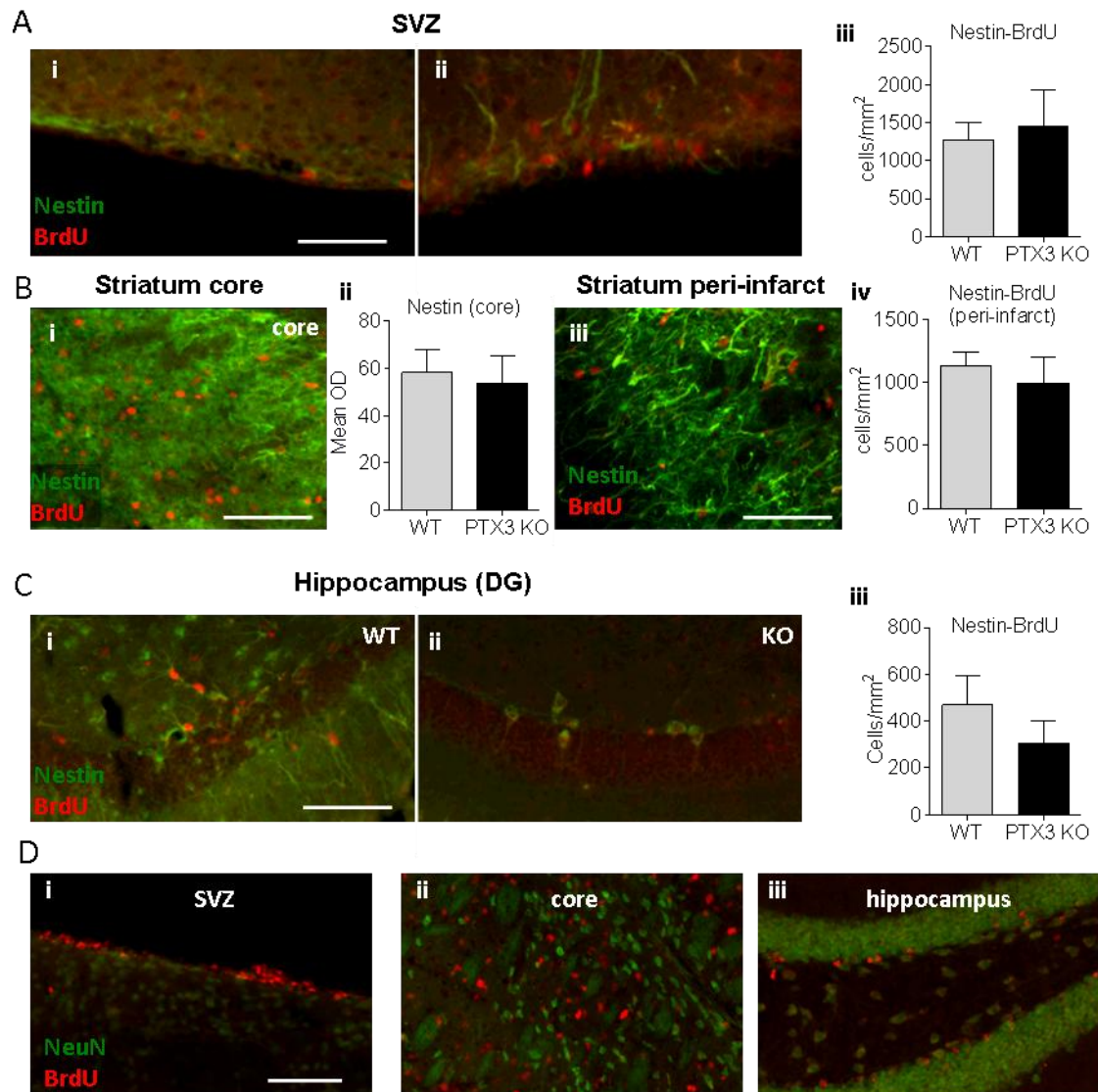


Figure 5. NSPC proliferation is not altered by PTX3 deficiency 14 days after MCAo. **A, B,** Lack of PTX3 does not affect the amount of proliferating NSPCs in the SVZ (**A**) or in the peri-infarct area (**B iii** and **iv**). Nestin-BrdU positive cells could not be counted within the core of the infarct due to high nestin staining (**B i**), but the intensity of nestin staining in the core is similar in both genotypes (**B ii**). **C,** Within the DG, PTX3 KO has a non-significant trend towards a reduced amount of proliferating NSPCs. **D,** No mature newborn neurones (BrdU-NeuN positive cells) are found in the SVZ, core or hippocampus of either genotype. Scale bars: 50 μ m (**A-C**); 100 μ m (**D**). Students t-test (**A**, $n=2-6$; **B,C** $n=3-6$) was used. Error bars show SEM.

Nestin staining within the core of the damage was extremely high in some cases (Fig. 5B i), making quantification of nestin-positive cells impossible. Mean intensity of the

staining in that area showed no difference between genotypes (Fig. 5B ii). Quantification of BrdU-nestin positive cells in the peri-infarct area (Fig. 5B iii) revealed no difference between genotypes (Fig. 5B iv). In the hippocampus, there was a non significant trend for a reduced number of Nestin-BrdU positive cells in PTX3 KO mice (Fig. 5C). It is worth mentioning that the reduced number of PTX3 KO mice (n=2-3) compared to WT mice (n=6) may account for the lack of significance in this set of data. New mature (NeuN-BrdU positive) neurones were not found in any of the areas in either genotype (Fig. 5D).

To confirm that PTX3 drives neurogenesis, we next investigated the effect of recombinant PTX3 on NSPC proliferation using neurospheres *in vitro*. Treatment of WT neurosphere cultures with recombinant mouse PTX3 resulted in an increase in proliferation indicated by an increase in BrdU incorporation (Fig. 6A). The number of neurospheres was also significantly increased after PTX3 treatment of WT cells, and this effect was absent in IL-1 β KO cultures (Fig. 6B), suggesting that endogenous IL-1 is necessary for the neurogenic effect of PTX3.

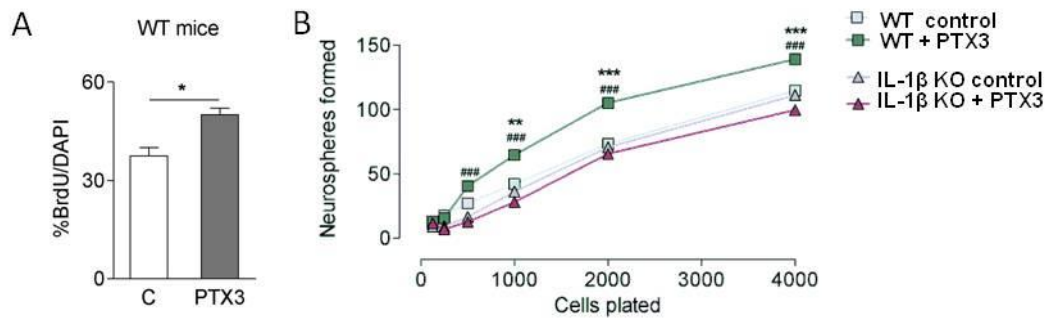


Figure 6. PTX3 deficiency impairs *in vitro* neurogenesis. **A**, PTX3 (100 ng/ml) induces neural stem progenitor cell (NSPC) proliferation, as shown by BrdU/DAPI ratio after 24 h treatment. **B**, PTX3 (100 ng/ml) treatment of NSPCs for one week increases neurosphere formation in WT, but not in IL-1 β KO cultures. Students t-test (A, n=4) or two-way ANOVA followed by Bonferroni's post-hoc test (B, n=4) were used. *P<0.05, **P<0.01, ***P<0.001, ####P<0.001. In B, *WT control vs. other experimental groups, #WT + PTX3 vs. IL-1 β KO + PTX3. Error bars show SEM.

Lack of PTX3 reinforces rotational bias after MCAo

Increased neurogenesis has been linked with improved function after stroke (Zhang *et al.*, 2005). To determine whether the lack of PTX3 had an effect on behavioural outcome, several tests were carried out analyzing basic parameters of activity, exploratory behaviour, motor function and memory 14 days after MCAo. The amount of time mobile, the number of lines crossed and the number of rearings within an open field test (Fig. 7A) were used to study alterations in general activity and exploratory behaviour, but no significant differences between genotypes were identified (Fig. 7B). The proportion of anti-clockwise rotations was over 50 % (50% would correspond to a healthy mouse) in both genotypes, indicating a motor deficit. This rotational bias, however, was only significant in PTX3 KO mice (93 % of anti-clockwise rotations on average) (Fig. 7C). Inter-genotype difference, however, was not significant (Fig. 7C). The score reflecting general motor activity did not vary between genotypes (Fig. 7D).

Short term memory, measured in a Y maze, was not significantly affected by the lack of PTX3, although a trend indicated that PTX3 KO mice could have a slight memory deficit compared to WT mice (Fig. 7E).

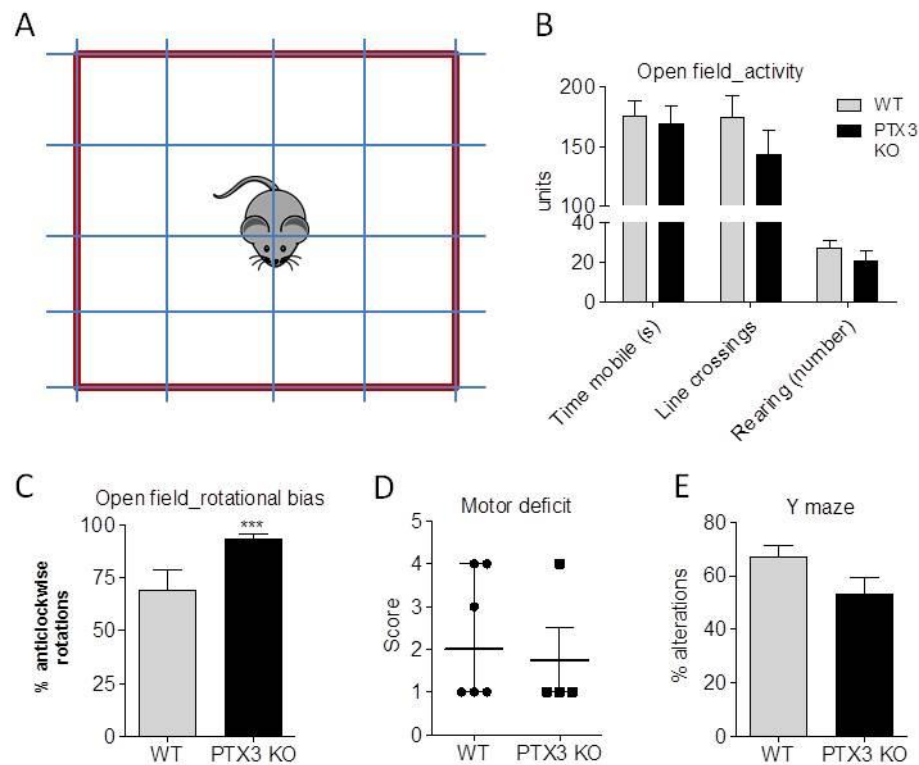


Figure 7. PTX3 KO mice have increased rotational bias 14 days after MCAo. **A**, Scheme of the open field display. **B** Open field test reveals no difference in parameters reflecting general anxiety and activity such as time mobile, number of line crossings and number of rearings. **C**, Rotational bias is significant in PTX3 KO but not in WT mice. **D**, General motor activity is not affected by the lack of PTX3. **E**, Short term memory, measured as the percentage of alternations made on a Y-maze, is not affected either. Student's t-test (B, C, E, n=4-6), one-sample t-test vs. 50 % (C, n=4-6) and Mann-Whitney tests (D, n=4-6) were used. ***P<0.05 were performed. In C, *** corresponds to the result of the one-sample t-test vs 50 %. Error bars show SEM (B, C, E) or interquartile range (D).

Discussion

Here we show for the first time that the acute phase protein PTX3, a biomarker of stroke severity (Ryu *et al.*, 2012), is a key regulator of angiogenesis and neurogenesis during the recovery phase after cerebral ischaemia. The relevance of PTX3 in oedema resolution and post-stroke glial responses days after stroke had already been highlighted (Rodriguez-Grande *et al.*, 2014); here we observe that weeks after the ischaemic event other recovery responses such as angiogenesis and neurogenesis are also affected by the lack of PTX3.

In contrast to our observations, PTX3 has been described as an anti-angiogenic factor *in vitro* and in matrigel or alginate bead implants *in vivo* (Leali *et al.*, 2012; Margheri *et al.*, 2010). However, it is possible that the concentration of PTX3 used in those experiments is higher than the concentration of PTX3 found in the brain once the acute phase is over. Low concentrations of PTX3 may not have the same effect on angiogenesis than high concentrations. Interestingly, in a study of cardiac ischaemia, lack of PTX3 reduced the amount of capillaries in the reperfused area, as well as inducing a worse outcome after the ischaemic event (Salio *et al.*, 2008), which supports our results showing a beneficial role of PTX3 in angiogenesis. The effect of PTX3 in other mechanisms of repair (Rodriguez-Grande *et al.*, 2014) may benefit the overall recovery and indirectly facilitate angiogenesis, overruling the anti-angiogenic actions of PTX3. VEGF is thought to be produced by astrocytes after cerebral ischaemia (Lee *et al.*, 1999; Sinor *et al.*, 1998) and it then binds to VEGFR2 in endothelial cells, promoting angiogenesis (Marti & Risau, 1998). Baldini and colleagues found elevated levels of both PTX3 and VEGF in samples of patients suffering from arterial inflammation (Baldini *et al.*, 2011) and we observed a lower amount of VEGFR2 in blood vessels of PTX3 KO mice. Lower VEGFR2 levels may

relate to lower levels of VEGF. Since VEGF promotes microglial proliferation (Forstreuter *et al.*, 2002) and astrocytic proliferation and migration (Wuestefeld *et al.*, 2012), low VEGF production could partly account for the deficit in microglial proliferation and differences in astrocytic scar integrity observed in PTX3 KO mice (Rodriguez-Grande *et al.*, 2014). Further research is required to explore the role of PTX3 in VEGF production. Since microglial-derived factors can also promote angiogenesis (Rymo *et al.*, 2011), reduced microglial proliferation, such as that induced by the lack of PTX3 (Rodriguez-Grande *et al.*, 2014), could be an additional mechanism by which lack of PTX3 impairs angiogenesis.

Decreased angiogenesis in PTX3 KO mice could partly account for a decreased amount of neurogenesis, since it is well known that both processes are linked (Ohab & Carmichael, 2008). Furthermore, our *in vitro* data indicates that PTX3 is a key endogenous neurogenic mediator by itself, independently of the presence of vascular factors. PTX3 induced NSPC proliferation *in vitro*, which was abrogated in IL-1 β KO cultures. IL-1, induced by acute brain injury drives PTX3 expression (Rodriguez-Grande *et al.*, 2014), which in turn, facilitates neurogenesis via IL-1 during the repair phase. Supporting this, IL-1 β has been shown to promote NSPC differentiation (Molina-Holgado & Molina-Holgado, 2010). These observations highlight the importance of IL-1 and PTX3 in brain repair. High levels of IL-1 during the acute phase are known to worsen ischaemic damage (Loddick & Rothwell, 1996), and anti-inflammatory stroke treatments based on IL-1 receptor antagonist have been tested in clinical settings (Emsley *et al.*, 2005). Discriminating between early IL-1 noxious actions and late IL-1 repair-promoting actions is necessary to choose the appropriate time of administration of anti-inflammatory treatments.

In vivo, we observed PTX3 neurogenic effect in the number of nestin-positive progenitor cells 6 days, but not 14 days after MCAo; however, nestin only marks an early stage of differentiation (Abrous *et al.*, 2005). We did not observe newborn mature neurones, but it is possible that doublecortin-positive migrating neuroblasts were present 14 days after MCAo. However, due to technical difficulties and limitations in the amount of tissue, we were not able to explore markers of this middle stage of differentiation. Further research is required to validate whether PTX3 has an effect in final stages of progenitor cell differentiation and integration.

In terms of behaviour, lack of PTX3 caused a significant increase in rotational bias, which occurs as a consequence of the unilateral brain damage and reflects asymmetric motor function (Modo *et al.*, 2000) and may indicate the slower recovery of contralateral motor function in PTX3 KO mice. Since there were no new mature functional neurones at the time when behavioural tests were performed (14 days after MCAO), differences in behaviour cannot be attributed to differences in neurogenesis. However, reduced angiogenesis could affect the functioning of the surviving neurones, maintaining a compromised metabolic status for longer, and thus delaying recovery. Other motor tests were not altered and lack of PTX3 did not seem to affect short term memory. Due to the high plasticity and fast recovery of brain damage in mice, it is difficult to assess neurological deficits and behavioural differences at advanced stages of recovery with broad spectrum tests (Durukan & Tatlisumak, 2007). Finer tests have been recently developed, which may be able to reveal more subtle deficits, even in mice (Balkaya *et al.*, 2013). It is worth pointing out that in this study behaviour was only measured at endpoint (14 days after MCAo). Normalization of the behaviour of each individual animal with his own basal pre-surgery score could provide a more accurate insight of how post-stroke behaviour is affected by the lack of PTX3.

In conclusion, we have shown here that PTX3, known as a biomarker of stroke, is involved in angiogenesis and neurogenesis after cerebral ischaemia, and can have a beneficial impact on functional recovery. This strengthens the relevance of PTX3 as a potential target for stroke recovery. In the long term this could have important clinical implications given the increasing incidence of stroke, and the lack of treatments targeting the recovery phase.

Chapter 5: The role of PTX3 in post-stroke inflammation

This chapter extends the study of PTX3 in brain inflammation, complementing the publications corresponding to Chapters 3 and 4. Due to space constraints in publications, the content of this chapter could not be included in the previous two chapters. This chapter is not written in paper format.

5.1 Introduction

As mentioned in sections 1.2.3 to 1.2.5 of the Introduction, PTX3 is an APP induced by inflammatory mediators (Garlanda *et al.*, 2005) which can exert anti-inflammatory actions. For instance, PTX3 limits neutrophil infiltration (Deban *et al.*, 2010b) as well as autoimmune responses (Baruah *et al.*, 2006). Neutrophils are thought to mediate post-stroke brain damage (Buck *et al.*, 2008; Price *et al.*, 2004) and PTX3 has been found to be part of neutrophil extracellular traps (NETs) (Savchenko *et al.*, 2011), which mediate neutrophil neurotoxicity (Allen *et al.*, 2012). We therefore decided to study the role of PTX3 in neutrophil migration and toxicity after stroke. Since vascular activation is key to neutrophil recruitment (Zaremba & Losy, 2002), here we also investigate vascular activation in order to complete the study of the inflammatory response in the context of PTX3 and stroke. Since we have previously seen alterations in the astrocytic scar and microglial proliferation 6 days after MCAo, we extended astrocytic and microglial activation studies to 48 h and 14 days post-MCAo.

5.2 Materials and Methods

A brief summary of the materials and methods used in this chapter is provided hereafter. Detailed information is found in Chapter 2.

5.2.1 MCAo and brain sample processing

Cerebral ischaemia was induced by occluding the left MCA for 30 min and animals were left to recover 48 h, 6 days or 14 days, after which they were perfused with PFA. Coronal brain sections were cut with a microtome and used for immunohistochemical analysis. Cressyl violet staining was used to determine infarct size, and antigen-

specific antibodies with their corresponding fluorescent secondary antibodies were used to visualise neutrophils, activated blood vessels, microglia/macrophages and astrocytes.

5.2.2 Neutrophil infiltration

To evaluate neutrophil infiltration *in vivo*, CD45-positive bright cells (excluding microglia) were counted in the ischaemic site of WT and PTX3 KO mice 48 h, 6 days or 14 days after MCAo. Anti-granulocyte serum kindly donated by Sandra J. Campbell (SJC) was used to further confirm neutrophil infiltration. To study transmigration *in vitro*, WT and PTX3 KO neutrophils were isolated, and transmigration through WT brain endothelium upon IL-1 β treatment was evaluated.

5.2.3 Neutrophil neurotoxicity

Neurotoxicity of WT and PTX3 KO neutrophils was assessed by measuring neuronal death after incubating WT primary neuronal cultures with neutrophil-conditioned media for 24 h. LDH assay was used to evaluate neurotoxicity, which was expressed as the percentage of cell death compared to controls.

5.2.4 Glial and vascular activation

Astrocytic (GFAP), microglia/macrophage (Iba1) and vascular (ICAM-1) staining was quantified in WT and PTX3 KO mice 48 h, 6 days and 14 days after MCAo. Laminin- α 4 staining within the glial scar was also quantified.

5.3 Results

5.3.1 The role of PTX3 in neutrophil migration and toxicity

To study whether PTX3 inhibits neutrophil recruitment in the CNS as it does in the periphery (Deban *et al.*, 2010b), we quantified the amount of infiltrated neutrophils in the striatum of WT and PTX3 KO mice 48 h, 6 days and 14 days after MCAo. Surprisingly, recruitment of neutrophils in the brain was higher in WT mice compared to PTX3 KO mice (3-fold) and this was also indicated by higher number of recruited CD45-positive leukocytes (CD45-positive bright cells, excluding microglia) 48 h after MCAo (Fig. 1A). No significant difference was observed at 6 days reperfusion (Fig. 1B) and, given the high intensity of the staining 14 days after MCAo, it was not possible to count cells within the striatum at that time point (Fig. 1C i). Only the intensity of the staining could be quantified in that area, and it was similar in both genotypes (Fig. 1C ii). However, lack of PTX3 induced an increase in the amount of neutrophils infiltrated in the peri-infarct area 14 days after MCAo (Fig. 1C iii and iv). To explore whether differences in peri-infarct neutrophil recruitment were due to differences in infarct size, we used Cresyl violet stained sections (Fig. 1D i). No differences were seen in infarct size between genotypes 14 days after MCAo (Fig. 1D ii), and both genotypes had the same proportion of cortical infarcts (Fig. 1D iii).

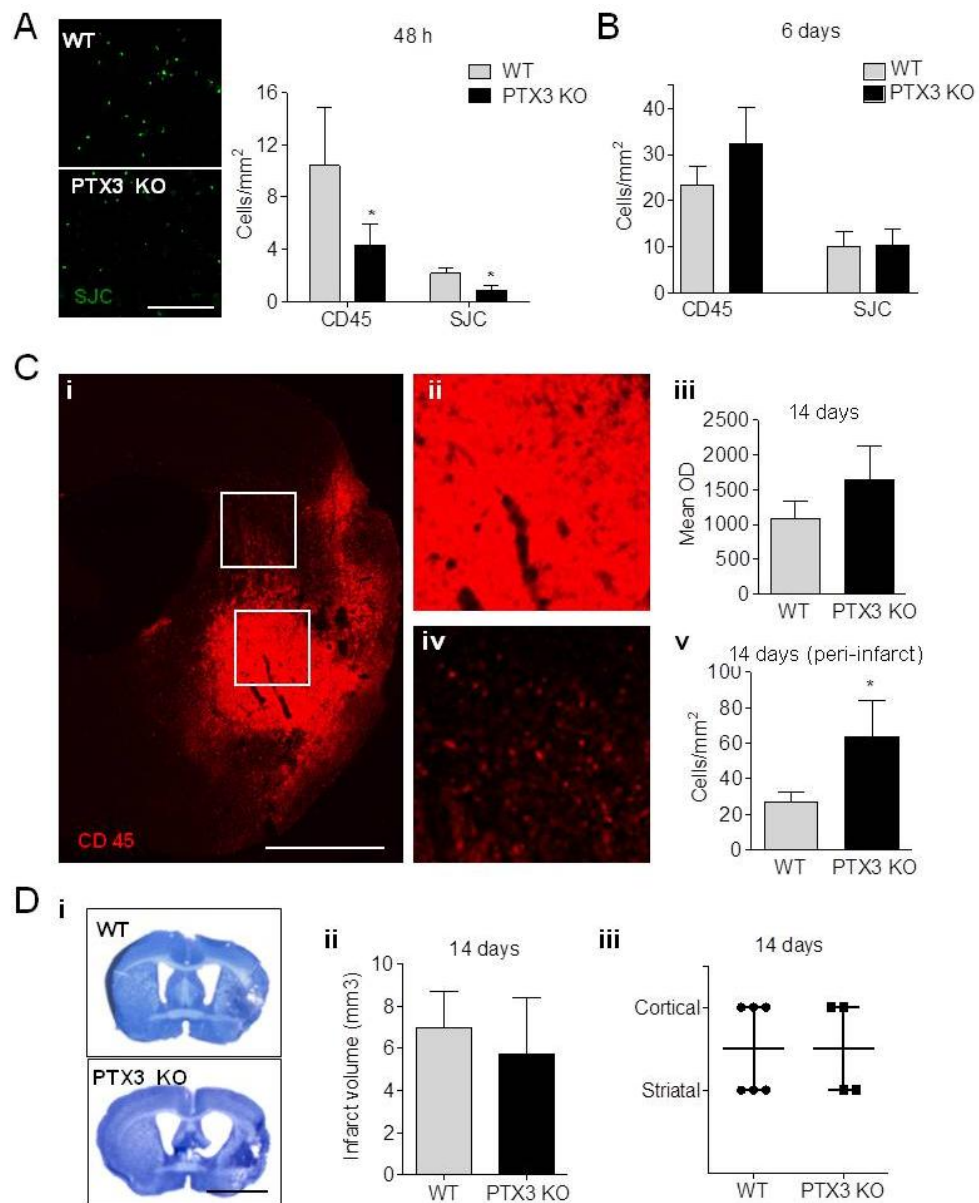


Figure 1. PTX3 depletion promotes neutrophil recruitment 48 h after MCAo but prevents neutrophil recruitment 14 days after MCAo. **A**, Fluorescent image of infiltrated neutrophils (SJC) in WT and PTX3 KO mice 48 h post-MCAo (i). Significantly less infiltrated neutrophils (SJC) and CD45-positive bright round cells, (leukocytes, excluding microglia) are found in PTX3 KO mice compared to WT mice 48 h post-MCAo (ii). **B**, There is no significant difference in the number of recruited neutrophils between genotypes 6 days after MCAo. **C**, After 14 days, the high intensity of CD45 staining in the infarct core (i and ii) did not allow quantification of number of neutrophils. The intensity of the staining in the core of the infarct is not significantly different between genotypes, but the amount of CD45-positive neutrophils in the peri-

infarct area is significantly higher in PTX3 KO mice. **D**, Both genotypes have similar infarct size (ii) and proportion of cortical infarcts (iii), as measured in Cressyl violet stained sections (i). Scale bar: 200 μ m (A), 1mm (C), 3mm (D). Students t-test (A-B, n=5-6; C, n=4-5; D, n=4-6) was used. *P<0.05 Error bars show SEM.

We further addressed the role of PTX3 in neutrophil migration using an *in vitro* model of BBB. *In vitro* transmigration assays showed that lack of endogenous PTX3 in neutrophils is sufficient to decrease neutrophil transmigration through WT brain endothelium (Fig. 2A). Interestingly, when we analysed the neurotoxic potential of neutrophils, we found that conditioned medium from transmigrated PTX3 KO neutrophils was more toxic to neuronal cultures than that of WT neutrophils (Fig. 2B), suggesting that neutrophil-associated PTX3 inhibits neutrophil-induced neurotoxicity.

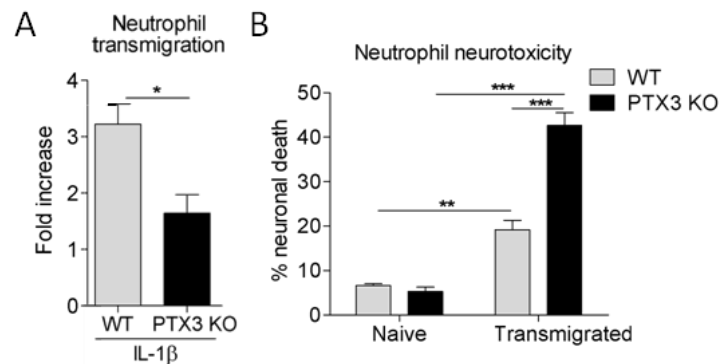


Figure 2. Lack of PTX3 leads to decreased neutrophil transmigration but increased neutrophil toxicity in a cell-autonomous manner *in vitro*. **A**, Neutrophils lacking PTX3 are less transmigrative, as quantified after *in vitro* transmigration of WT and PTX3 KO neutrophils (through WT endothelium). **B**, LDH measurements reveal that PTX3 KO transmigrated neutrophils are significantly more toxic to primary neurons than WT transmigrated neutrophils. T-test (A, n=3) or two-way ANOVA followed by Bonferroni's post-hoc test (B, n=3) were used. *P<0.05, **P<0.01, ***P<0.001. Error bars show SEM.

5.3.2 The role of PTX3 in vascular activation after MCAo

Expression of adhesion molecules increases after cerebral ischaemia, facilitating neutrophil recruitment. We had previously observed that ICAM-1 expression was not altered 48 h after MCAo (chapter 3). Here we explore levels of ICAM-1 6 days and 14 days after MCAo. Counts of activated blood vessels (ICAM-1 positive) and measurements of intensity of the staining in the core of the infarct showed that lack of PTX3 did not affect vascular activation 6 days (Fig. 3A) after MCAo.

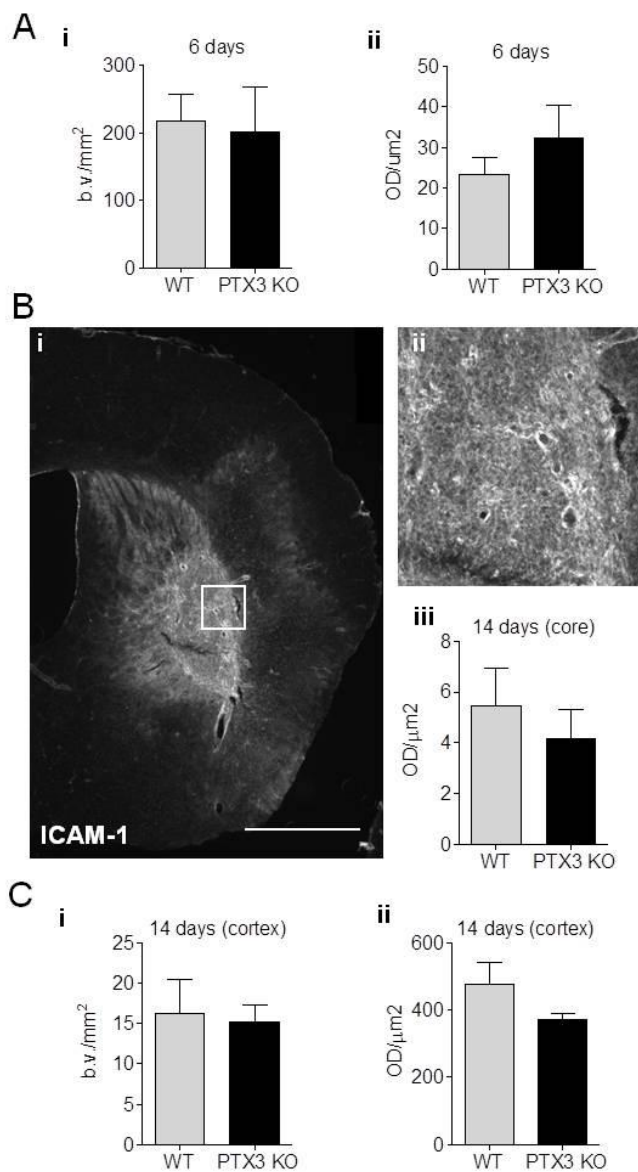


Figure 3. PTX3 does not affect blood vessel activation after MCAo. **A**, Both genotypes have a similar amount of ICAM-1 positive blood vessels (i) and intensity of ICAM-1 staining (ii) within the striatum 6 days after MCAo. **B**, High ICAM-1 staining is displayed in the core of the infarct 14 days after MCAo (i and ii), with similar intensity in both genotypes (iii). **C**, No significant difference in the number of blood vessels (i) or intensity of staining (ii) is observed in the cortex. Scale bar: 1 mm. Students t-test (A, n=4-6; B, C, n=4-5) was used. Error bars show SEM.

Blood vessel count within the core of the infarct 14 days after MCAo was not possible due to the intensity of the staining (Fig. 3B i and ii), and both genotypes had similar intensity of staining in that area (Fig. 3B iii). Within the cortex, blood vessel counts (Fig. 3C i) and intensity of the staining (Fig. 3C ii) 14 days after MCAo were also similar.

5.3.3 PTX3 in astrocytic activation after MCAo

Astrocytes are essential in buffering excitotoxicity and oxidative stress in the early stages of inflammation (Tanaka *et al.*, 1999), and are essential for angiogenesis and neurogenesis during the repair phase after stroke (Zhao & Rempe, 2010). We had observed that the glial scar of PTX3 KO did not fully seal the injury 6 days after MCAo (Rodriguez-Grande *et al.*, 2014) and thus we explored astrocytic activation at the other time points. Lack of PTX3 did not have a significant effect on the number of activated astrocytes within the striatum (Fig. 4A i) or the corpus callosum (CC) (Fig. 4A ii) 48 h after MCAo, although the overall amount of astrocytes was very low in both areas (Fig. 4A iii). After 14 days, we found less astrocytic activation than 6 days after MCAo in both genotypes, but the ring of astrocytes around the infarct core was still observable, and some activated astrocytes were also found in the cortex (Fig. 4B i). The number of astrocytes (Fig. 4C ii) or the intensity of the staining (Fig. 4C iii) were not affected by the lack of PTX3 in the core, scar or cortex 14 days after MCAo.

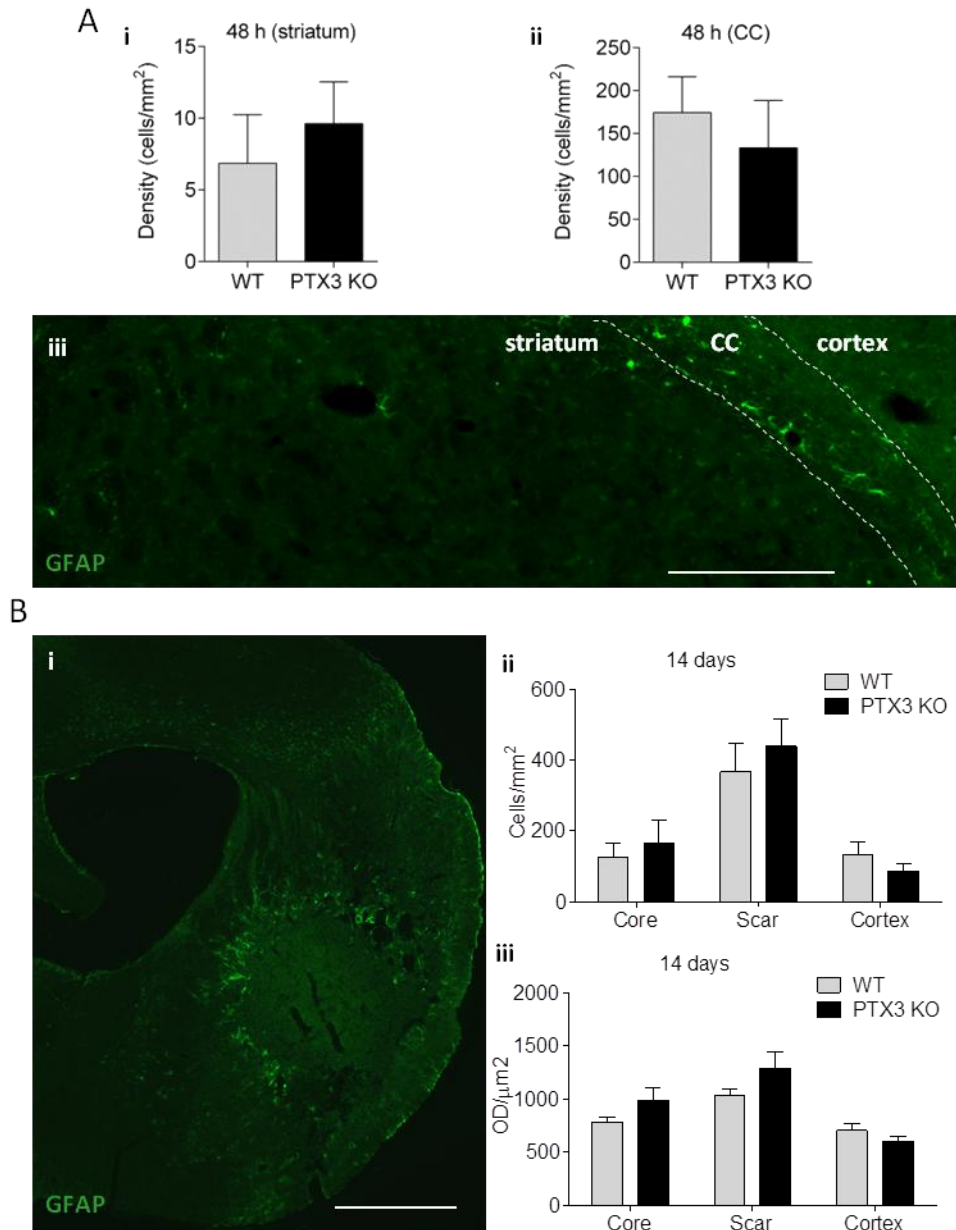


Figure 4. Level of astrogliosis is not affected by lack of PTX3 48 h and 14 days after MCAo. **A**, Quantification of astrocyte density in the striatum (i) and corpus callosum (ii) reveals no difference in astrogliosis between PTX3 KO and WT mice 48 h after MCAo. Few astrocytes are found at that time (iii). **B**, After 14 days of reperfusion the glial scar is still recognisable, and some astrogliosis is also found in the cortex (i). Lack of PTX3 does not significantly affect astrocyte density (ii) or intensity of GFAP staining (iii) in the core, scar or cortex. Scale bars: 50 μ m (A); 1 mm (B). Student's t-test was used (A, n=6-7; B, n=4-5). Error bars show SEM.

5.3.4 The role of PTX3 in microglial/macrophage activation after MCAo

Microglial cells can acutely increase neuronal damage but are thought to be neuroprotective at later stages due to a change in their phenotype. We had observed differences in glial proliferation 6 days after MCAo (Rodriguez-Grande *et al.*, 2014), but lack of PTX3 did not significantly affect the amount of activated microglia/macrophages 48 h (Fig. 5A) or 14 days (Fig. 5B, preliminary data) after MCAo in the core (Fig. 5A i and B i) or the peri-infarct area (Fig. 5A ii and B ii). Despite not being significant, there seemed to be a trend indicating that PTX3 KO mice had more microglia/macrophages than WT 48 h after MCAo (Fig. 5A), and the opposite was seen at 14 days reperfusion (Fig. 5B). In the case of the 14 days reperfusion sample, the low number of animals per group (n=2-3) impedes making statistical analyses.

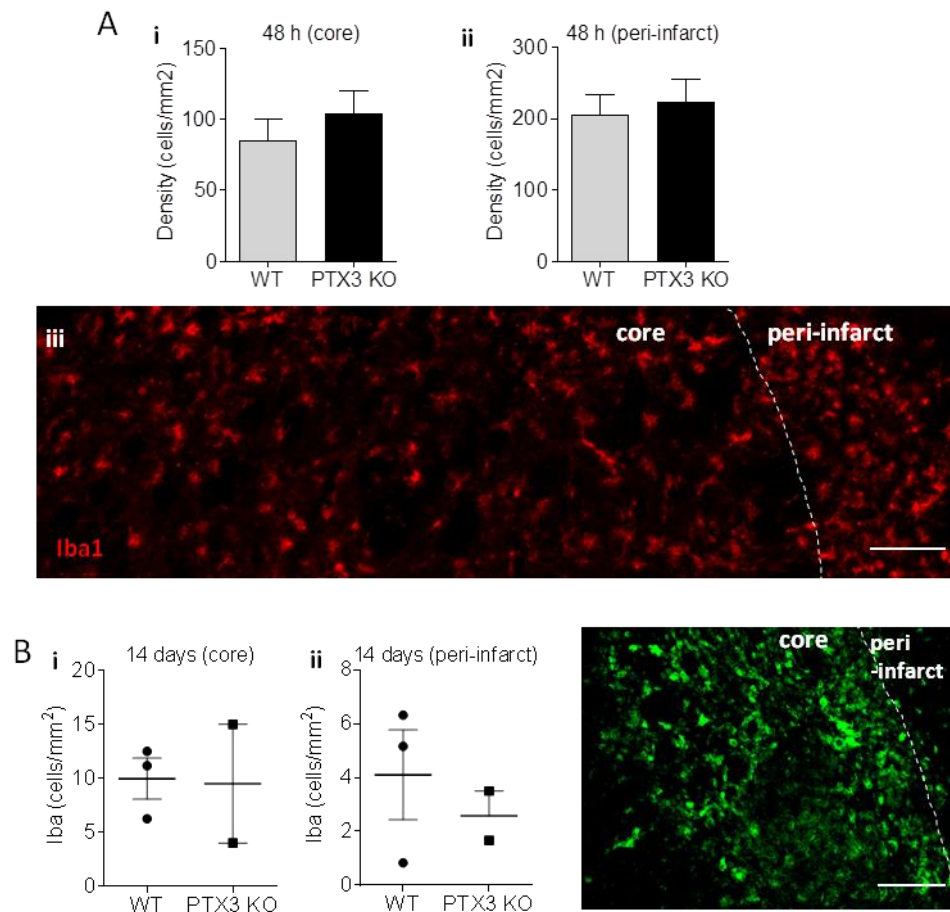


Figure 5. Lack of PTX3 does not affect the amount of activated microglia 48 h or 14 days after MCAo. A, Quantification of Iba1-positive cell density within the core (A i, B i) and peri-infarct area (A ii, B ii) reveals no significant difference between genotypes 48 h after MCAo (A), and preliminary data suggests a similar trend 14 days after MCAo, although small group size impedes making statistical analyses (B). Scale bars: 100 μ m (A), 150 μ m (B). Student's t-test was used (A, n=6-7) Error bars show SEM.

5.4 Discussion

Here we show for the first time that PTX3 affects neutrophil transmigration and neurotoxicity in the CNS, but does not seem to have a main role in vascular activation, or in the number of activated astrocytes. Microglia/macrophage activation does not seem affected by the lack of PTX3 either, but in this case the small sample size makes

it difficult to reach a valid conclusion about the effect of PTX3 in microglia/macrophage proliferation.

Several models of peripheral inflammation have shown that PTX3 can reduce neutrophil infiltration through binding to P-selectin; this reduces neutrophil rolling and adhesion, and thus reduces neutrophil infiltration (Deban *et al.*, 2010b; McEver, 2010; Salio *et al.*, 2008). In accordance with this, we observed an increase in neutrophil load in the cortex of PTX3 KO late (14 days) after the ischaemic event. We did not find any effect 6 days after MCAo and, surprisingly, we observed that PTX3 facilitated neutrophil infiltration into the CNS early (48 h) after cerebral ischaemia. Interestingly, our *in vitro* experiments supported that PTX3 enhances transmigration through brain endothelium, as we observed 48 h after MCAo. Over time variations in PTX3 actions may indicate that PTX3 has concentration-dependent actions. As an APP, PTX3 levels are expected to decrease after the acute insult, and we had observed a steep drop in brain PTX3 levels from 24 h to 48 h (Rodriguez-Grande *et al.*, 2014), however, how concentration varies at later times is yet to be determined.

Changes in vascular activation could also account for different neutrophil infiltration. We did not observe any effect of the lack of PTX3 on vascular activation in terms of the adhesion molecule ICAM-1. On the contrary, Norata and colleagues (Norata *et al.*, 2009) had found that PTX3 KO atherosclerotic mice had increased expression of ICAM-1 and other adhesion molecules (Norata *et al.*, 2009). Their findings support an anti-transmigratory role for PTX3, however, this was done in atherosclerotic mice, and examining peripheral tissue (Norata *et al.*, 2009). Differences between observations in brain and periphery may be due to structural differences between BBB and peripheral endothelium. PTX3 is known to bind some ECM molecules and keep ECM integrity (Salustri *et al.*, 2004; Scarchilli *et al.*, 2007) and its depletion has been reported to alter

ECM expression in atherosclerosis (Norata *et al.*, 2009). Differences between the ECM of BBB and peripheral blood vessels may account for central vs. peripheral actions of PTX3. Further investigation about the mechanisms of action of PTX3 is required to clarify the cause of these varying effects.

In addition to alterations in transmigration, here we show that PTX3 reduces neutrophil toxicity. It has been recently shown that IL-1 regulates neutrophil neurotoxicity via NETs (Allen *et al.*, 2012), with which PTX3 is associated (Savchenko *et al.*, 2011). Our study shows that neutrophil PTX3 is neuroprotective, since it dampens the toxicity of transmigrated neutrophils in WT neuronal cultures. Furthermore, as shown in Figure 1 of the Additional supplementary information to Chapter 3, endogenous neuronal PTX3 seems to play a role in neuronal survival as well. These data suggest that PTX3 could exert neuroprotective actions, which is in agreement with earlier findings in which PTX3 KO mice had more neuronal damage after limbic seizures compared to WT mice (Ravizza *et al.*, 2001), and in which PTX3 decreased microglial-mediated neurotoxicity (Jeon *et al.*, 2010).

PTX3 did not affect astrogliosis, or microglia/macrophage activation, at least in terms of the amount of cells. We had previously observed that PTX3 can induce mixed glial proliferation *in vitro* (Rodriguez-Grande *et al.*, 2014) but it is worth pointing out that only low concentrations induced proliferation *in vitro*. Maybe higher concentrations are found *in vivo* and thus PTX3 is not regulating glial activation *in vivo* at this time. It is important to consider that a small sample size, especially in the study of microglia/macrophages 14 days after MCAo, does not allow drawing definite conclusions from the results obtained. It has been reported that PTX3 can induce phagocytic activity (Diniz *et al.*, 2004; Jeon *et al.*, 2010), and that it can reduce LPS-induced microglial neurotoxicity (Jeon *et al.*, 2010). Therefore, apart from differences

in cell numbers, in the future it would be interesting to address the effect of PTX3 in glial phenotype. In addition, if PTX3 induces microglial proliferation but reduces leukocyte recruitment (as Deban suggests (Deban *et al.*, 2010b)), PTX3 KO mice would have less microglia but more recruited macrophages, and here we would have missed those effects since Iba1 marks both microglia and macrophages. Microglia seems to be more abundant (Schilling *et al.*, 2003) and more proliferative (Denes *et al.*, 2007) than recruited macrophages after MCAo, and thus it is likely that most Iba1-positive cells are indeed microglia. Therefore, what we have observed probably reflects the effect of PTX3 on microglia rather than in macrophages, but further studies are required to verify this.

In brief, we found that PTX3 could be neuroprotective through dampening neutrophil toxicity. For the first time we observed that PTX3 favours neutrophil transmigration *in vitro* and *in vivo* at early stages after MCAo, but has the opposite effect during the delayed phase, despite not affecting vascular activation. As PTX3 concentration is expected to drop over time after the stroke, the different actions of PTX3 over time could be concentration-dependent. Further work is needed to understand the different mechanisms of action of PTX3 at different stages of recovery, in the brain vs. the periphery, and in glial responses. Besides the pending questions about PTX3 mechanisms of action, it is increasingly clear that PTX3 is not a passive element of the CNS inflammatory response, but has a crucial role in regulating several responses not only during the acute phase, but also during the repair phase after brain injury.

Chapter 6: Loss of substance P and inflammation precede delayed neurodegeneration in the substantia nigra after cerebral ischaemia.

This chapter corresponds to the characterisation of the evolution of remote inflammation and neurodegeneration, which was published as an article (Rodriguez-Grande *et al.*, 2014), whereas the role of PTX3 in this context will be addressed in Chapter 7.

Loss of Substance P and inflammation precede delayed neurodegeneration in the substantia nigra after cerebral ischemia.

Beatriz Rodriguez-Grande, Victoria Blackabey, Beatrice Gittens, Emmanuel Pinteaux[§],
Adam Denes

Faculty of Life Sciences, A.V. Hill Building, University of Manchester, Oxford Road,
Manchester, M13 9PT, UK.

Conflict of interest statement: All authors declare that there are no conflicts of interest.

[§]Corresponding author: Faculty of Life Sciences, 2.002 A.V. Hill Building, University
of Manchester, Oxford Road, Manchester, M13 9PT, UK. E-mail address:
emmanuel.pinteaux@manchester.ac.uk, Tel: +44 161 275 1825, Fax: +44 161 275

3938

Abstract

Focal cerebral ischemia leads to delayed neurodegeneration in remote brain regions. The substantia nigra (SN) does not normally show primary neuronal death after ischemic events affecting the striatum, but can exhibit delayed neuronal loss after the ischemic injury through mechanisms that are unknown. No data are available in mice showing acute post-stroke inflammation and remote injury in the SN. Substance P (SP), a mediator of neurogenic inflammation, is a key element of the striato-nigral circuitry, but alterations of SP in the SN have not been studied after acute striatal injury. Inflammation, a key contributor to neuronal death, is found in the SN after striatal ischemia, but it is unknown whether it precedes or occurs concomitantly with neuronal death. We hypothesized that focal striatal ischemia induces changes in SP levels in the SN and that inflammation precedes neuronal death in the SN. Using the middle cerebral artery occlusion model, we found a significant loss of SP in the ipsilateral SN 24 h after striatal ischemia in mice. In the same area where SP loss occurs, significant glial and vascular activation, but no neuronal death, were observed. In contrast, a marked neuronal loss was observed within 6 days in the area of SP loss and inflammation. Our data suggest that focal loss of SP and early inflammatory changes in the SN precede remote neuronal injury after striatal ischemic damage. These observations may have important implications for motor impairment in stroke patients and indicate that striatal ischemia might facilitate Parkinson's disease development.

Introduction

Cerebral ischemia that occurs in stroke induces rapid neuronal death in the core of the infarct, followed by secondary neuronal injury triggered by inflammation that evolves in the surrounding hypoperfused region. In addition to this neuronal injury, cerebral ischemia also triggers changes in remote areas which are connected to the ischemic core. Indeed, clinical and experimental data from rat models indicate that neuronal death and inflammation also occur in remote areas such as the substantia nigra (SN) (Block *et al.*, 2005). The SN is a key structure involved in motor control, and is strongly affected in Parkinson's disease (PD). The SN has bi-directional neuronal connections with the striatum, which becomes ischemic after occlusion of the middle cerebral artery (MCA). Striatal neurons innervate the SN pars reticulata (SNr), where they release both substance P (SP) and GABA (Kopell *et al.*, 2006). The SNr partially innervates the SN pars compacta (SNc) (Hajos & Greenfield, 1994), and the SNc projects dopaminergic neurons to the dorsal striatum, regulating voluntary motor activity (Kopell *et al.*, 2006; Saklayen *et al.*, 2004). Stroke patients with striatal, but not cortical, damage display SN degeneration (Nakane *et al.*, 1992; Ogawa *et al.*, 1997) and middle cerebral artery occlusion (MCAo) in rat induces extensive delayed neurodegeneration and inflammation in the SN from 1 to 20 weeks after the onset of ischemia (Dihné & Block, 2001; Loos *et al.*, 2003; Nagasawa & Kogure, 1990; Uchida *et al.*, 2010).

Although the mechanisms underlying remote injury are largely unclear, it has been suggested that changes in neurotransmitter signalling can contribute to remote injury. Indeed, post-ischemic alterations of the striato-nigral GABAergic system are associated with neuronal death in the SN and later motor deficits (Lin *et al.*, 2010). Another key striato-nigral neurotransmitter is SP. SP belongs to the tachykinin family

and binds to the neurokinin-1 (NK1) tachykinin receptor (NK1R), both of which are expressed at highest levels in the SN (Bolam & Smith, 1990; Whitty *et al.*, 1997) and play a crucial role in the modulation of motor functions. In addition, SP is a well known mediator of neurogenic inflammation (O'Connor *et al.*, 2004), a process through which released neuropeptides increase vascular permeability, facilitating the development of an inflammatory response. SP alterations have been observed in the core of the damage in the brain (Turner *et al.*, 2006). However, no reports have studied remote alterations of SP after striatal ischemia and its effects in remote inflammation and neuronal injury.

Neuronal cell death in the ischemic striatum is profoundly influenced by inflammation (Hossmann, 2006; Jin *et al.*, 2010), which is an important therapeutic target after stroke (Denes *et al.*, 2010b). Activation of glial cells (Stoll *et al.*, 1998), upregulation of vascular adhesion molecules and disruption of the blood-brain barrier, which allow circulating leukocytes to infiltrate the cerebral tissue (Ley *et al.*, 2007), are hallmarks of the inflammatory response, some of which are observed in the SN weeks after MCAo (Block *et al.*, 2005; Uchida *et al.*, 2010). However, whether early inflammatory changes precede and contribute to neuronal death in the SN after MCAo is completely unknown.

Therefore, we hypothesized that cerebral ischemia affecting the striatum might alter SP-ergic innervation or SP levels in the SN, and induces early inflammatory changes that may contribute to delayed neuronal death. Our results show that focal loss of SP and inflammation occur in anatomically corresponding areas of the SN early after MCAo preceding significant neuronal death.

Methods

Animals

This study used 10-18 week-old male C57/BL6 mice, weighing 25-30 g. All animal procedures were performed under Home Office license (UK) and adhered to regulations specified in the Animals (Scientific Procedures) Act (1986). Mice were kept at $21^{\circ}\text{C} \pm 1^{\circ}\text{C}$ and 65% humidity) with a 12 h light-dark cycle with free access to food and water.

Middle cerebral artery occlusion and motor assessment.

Mice were anaesthetised by inhalation of 4% isoflurane, and anaesthesia was maintained with 1.5% isoflurane during surgery. Core body temperature was maintained at $37.0 \pm 0.5^{\circ}\text{C}$. In order to induce focal cerebral ischemia, a silicone coated 6-0 nylon monofilament (0.21 mm tip diameter, Doccol, US) was inserted into the left external carotid artery and advanced around 10 mm along the internal carotid artery to occlude the MCA. Successful occlusion of the MCA was observed by laser Doppler monitoring (Moor Instruments, Devon, UK) during the procedure, and cresyl violet immunostaining was performed on brain sections to confirm the development of ischemic injury. The duration of occlusion was 45 or 30 min, after which the filament was removed to allow reperfusion. After 4 h, 24 h or 6 days of reperfusion, motor function was assessed according to a neurological grading score of increasing severity of deficit (0, no observable deficit; 1, torso flexion to right; 2, spontaneous circling to right; 3, leaning/falling to right; 4, no spontaneous movement). Mice were then transcardially perfused with saline, followed by 4% paraformaldehyde (PFA) (Sigma, Dorset, England). Brains were removed, post fixed in 4% PFA and cryoprotected in phosphate-buffered saline (PBS) containing 20% sucrose for 24 h.

Tissue processing

Brain sections were cut with a sledge microtome (Bright Instruments, Huntingdon, UK) at a thickness of 20-25 µm. Coronal sections were stored at -20°C in an antifreeze solution (30% ethylene glycol (Sigma, UK) and 20% glycerol (Fisher Scientific, Loughborough, UK) in PBS) until histological staining.

Cresyl violet staining

Brain sections were stained with 1.5% cresyl violet solution, contrasted and dehydrated in 95% and 99% ethanol for 30 min, followed by incubation in xylene for 20 min and coverslipped with Depex mounting medium. Parallel series of brain section were assessed by immunohistochemistry for morphological changes and inflammation.

Immunohistochemistry

Brain sections were washed in PBS and incubated for 1 h at room temperature with 2% normal donkey serum in PBS containing 0.3% Triton X-100 to block non-specific binding. Sections were then incubated overnight at 4 °C with primary antibodies as follows: chicken anti-glial fibrillary acidic protein (GFAP) (1:1000, Abcam, UK), rat anti-myelin basic protein (MBP) (1:1000, Abcam, UK), rat (1:200, AbDSerotec, UK) or mouse (1:100, R&D Systems, UK) anti-substance P (SP), rabbit anti-NK1R (1:500, Millipore, UK), rat anti-CD45 (1:250, AbDSerotec, UK), rabbit anti-Iba1 (1:1000, Wako, Germany), goat anti-ICAM-1 (1:250, R&D Systems, UK), goat anti-VCAM-1 (1:250, R&D Systems, UK), rabbit anti-TH (1:2000, Abcam, UK) and mouse anti-NeuN (1:250, Millipore, UK). Sections were then incubated with secondary antibodies conjugated to Alexa 488 or Alexa 594 fluorochrome (1:500, Invitrogen, UK) for 2 h at room temperature. Sections were washed, mounted onto microscope slides and covered with glass coverslips using Prolong Gold antifade reagent with or without

DAPI (Invitrogen, UK). Images were taken using an Olympus BX51 upright microscope equipped with 4x/ 0.13 Plan fln, 10x/ 0.3 Plan fln and 20x/0.5 Plan fln objectives, and captured using a Coolsnap EZ camera (Photometrics, UK) and MetaVue Software (Molecular devices, USA). Specific band pass filter sets were used for DAPI (31000v2, BP350/50nm), Alexa 488 (41001, BP480/40nm) and Alexa 594 (41004, BP560/55nm). Settings were kept constant, and randomly selected areas of the same magnification were used across groups for each particular marker.

Quantification of damage and neuroinflammation

The infarct volume was calculated by integrating the infarct area (assessed in cresyl violet-stained sections) of 8 sections per brain, of corresponding coronal levels. To avoid possible masking effects due to edema, infarct areas were corrected before integration. The percentage increase in the volume of the ipsilateral hemisphere due to edema was calculated $((A_{\text{ipsi}} - A_{\text{contra}}) * 100 / A_{\text{ipsi}})$ and subtracted from the measured infarct area. Edema was calculated as the increase in the volume of the ipsilateral hemisphere compared to the contralateral hemisphere, and expressed as a percentage of the contralateral side $(\% \text{edema} = (V_{\text{ipsi}} - V_{\text{contra}}) * 100 / V_{\text{contra}})$. Image J software (National Institutes of Health, USA) was used to measure the area of the infarct, the area of SP loss and the integrated optical density (OD) of SP staining within the SN. Cell and blood vessels counts were done manually. For blood vessel counts, each branch was counted as a separate blood vessel.

Statistical Analysis

Animals were randomized for experiments and all quantitative analyses were performed in a blinded manner. A total of 27 animals were used (5 to 8 in each group).

Unpaired student's t-test (two tailed) was used to compare two means and Mann Whitney test to compare two medians. One sample t-test (for means) or Wilcoxon Signed Rank test (for medians) was performed to compare two or more groups to a given value. Two-way ANOVA was used to compare TH-positive neuronal populations at different time points and areas. All data are expressed as mean \pm standard error of the mean (SEM) except for neurological scores, in which medians and interquartile ranges have been used. Statistical significance was set at * $p < 0.05$, ** $p < 0.01$ and *** $p < 0.001$.

Results

Focal ischemic damage results in profound morphological alterations of NK1R-positive nerves in the striatum.

Within the healthy striatum, we detected NK1R immunoreactive (ir) neurons co-localised with SP-positive nerve terminals (Fig. 1A). 45 min MCAo induced marked morphological changes in the NK1R-ir neuronal processes within 24 h in the ipsilateral striatum including swelling of boutons, and an increase in NK1R expression (Fig. 1B). Cresyl violet staining revealed a marked reduction of viable neurons in the ipsilateral striatum and cortex (Fig. 1B), confirming the presence of focal ischemic damage. These results showed that morphological changes of NK1R -ir neurons are indicative of focal ischemic injury.

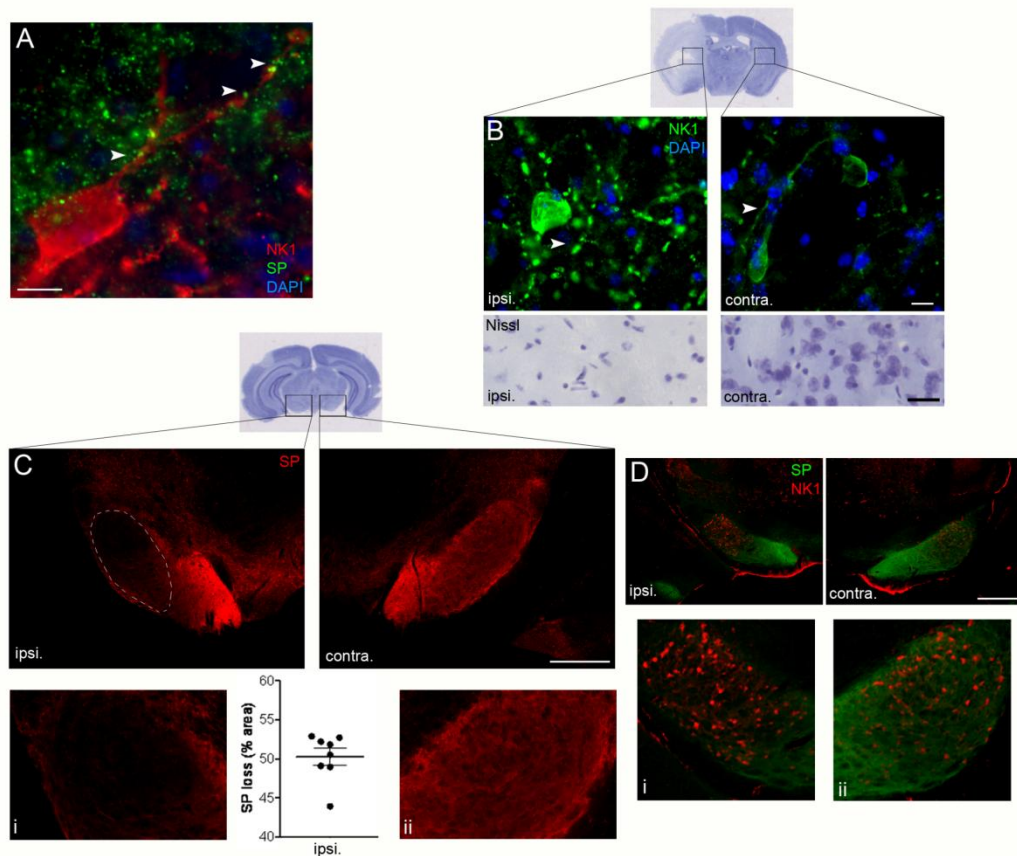


Figure 1. MCAo leads to ischemic damage in the striatum and focal loss of SP in the SN. **A.** NK1R -positive neurons were detected in the striatum co-localising with SP-ir nerve terminals (arrowheads). **B.** 45 min MCAo followed by 24 h reperfusion resulted in ischemic injury in the ipsilateral striatum and cerebral cortex (Nissl), which was associated with swelling of NK1R -positive profiles (green, arrowhead) and a large increase in NK1R on the neuronal membranes compared to the contralateral side. **C.** MCAo leads to the loss of SP in the ipsilateral SN (ipsi., see “i” for higher magnification compared to “ii”). Graph showing the average loss of SP-ir area. No focal ischemic injury was observed in the ipsilateral SN on cresyl violet (Nissl)-stained brain sections. **D.** In line with SP loss, NK1R -ir increases in the ipsilateral SN (ipsi. and “i”) compared to the contralateral side (contra. and “ii”) but no swelling of NK1R -positive structures observed. Scale bars: A-10 μ m; B-25 μ m; C, D-500 μ m. ipsi., ipsilateral; contra., contralateral.

SP immunoreactivity (ir) in the ipsilateral SN is lost within 24 h after MCAo, in the absence of focal ischemic damage.

In the ipsilateral SN, a pronounced loss of SP was observed, mostly in the SNr. On average, 50% of the area of the SN lost SP-ir in the ipsilateral side compared to the contralateral SN (Fig. 1C). A slight increase of NK1R -ir was observed in the ipsilateral SN (Fig. 1D), but no signs of focal ischemic injury were detected, and NK1R-ir boutons displayed intact morphology, similar to the contralateral SN.

Inflammation is induced in the ipsilateral SN within 24 h after MCAo.

We next investigated whether inflammatory changes take place in the ipsilateral SN early after cerebral ischemia. We found a significantly increased number of GFAP-positive astrocytes ($p < 0.01$) which overlapped the area of SP loss 24 h after MCAo (Fig. 2A). The number of CD45-positive cells was also markedly increased in this area. CD45-ir structures were mostly elongated, with microglial morphology and only very few CD45-ir profiles had monocyte/neutrophil morphology (round shape, high levels of CD45) (Fig. 2B). CD45 levels are very low on unactivated microglia, and an increase of CD45 levels is a hallmark of microglial activation (Campanella *et al.*, 2002). In line with this, elongated, CD45-positive and Iba1-positive microglia/macrophages were more abundant in the ipsilateral SN, and displayed an increased expression of ICAM-1 (Fig. 2C). ICAM-1 was significantly upregulated (Fig. 2C) and VCAM-1 also showed a trend to increase (Fig. 2D) on local blood vessels in the SNr, indicating the presence of neuroinflammation in the area corresponding to the loss of SP-ir.

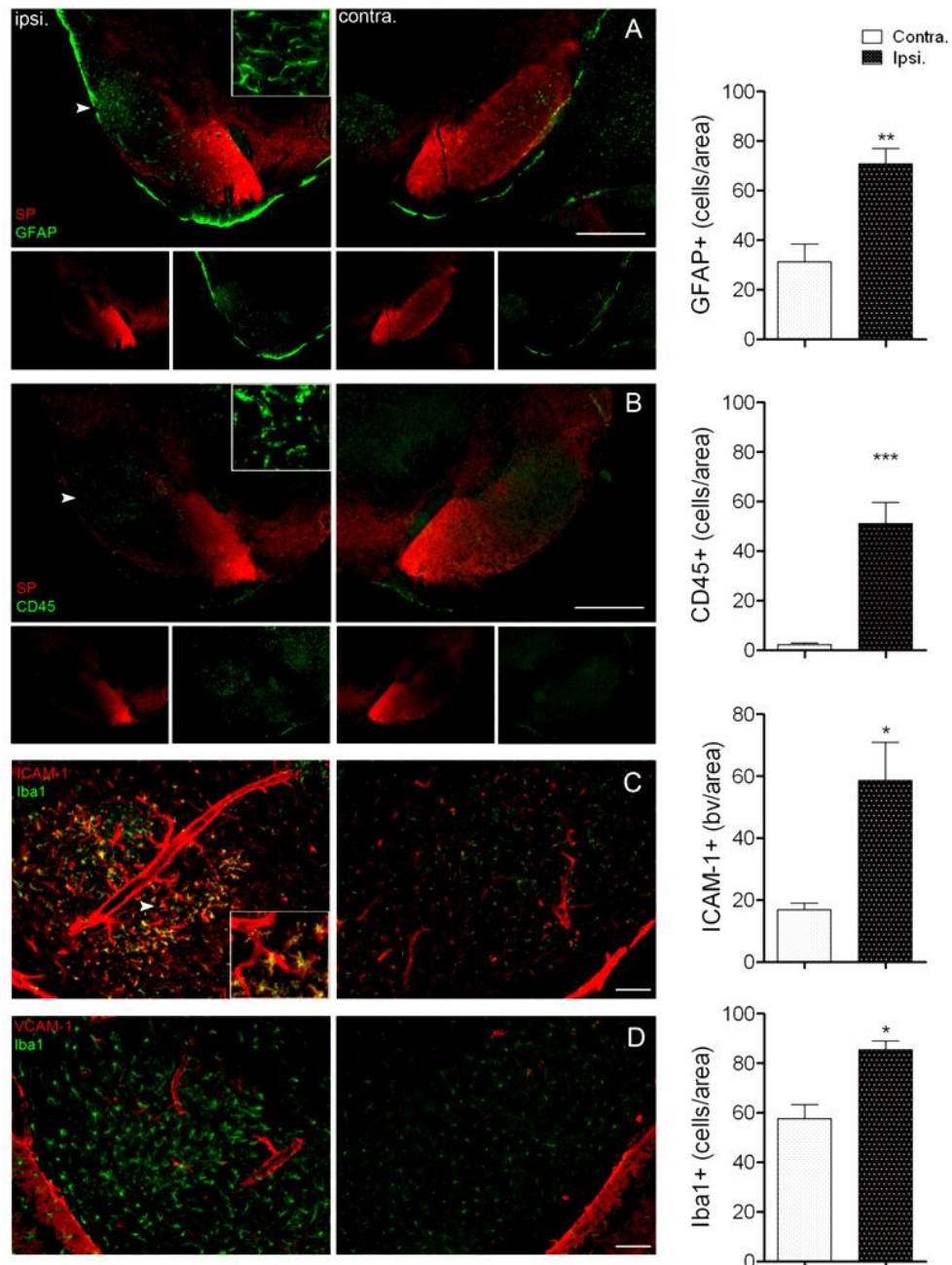


Figure 2. Neuroinflammation is induced in the SN within 24 h reperfusion after MCAo. **A.** Immunohistochemistry identified an increase in GFAP-ir (arrowhead) in the ipsilateral SN after 45 min MCAo followed by 24 h reperfusion. Note that the activation of astrocytes corresponds to the area of SP loss in the ipsilateral SN. **B.** CD45-positive cells increase in the ipsilateral SN. CD45-positive cells with microglial morphology (insert) are abundant in the area where SP loss is observed. ICAM-1 (**C**) and VCAM-1 (**D**) are upregulated in the ipsilateral SN on blood vessels. ICAM-1-ir is also increased on Iba1-positive microglial cells (**C**, insert). * $p < 0.05$, ** $p < 0.01$, *** $p < 0.001$, unpaired t -test (GFAP, $n = 6$; CD45, $n = 7$; ICAM, $n = 5$; Iba1, $n = 3$). Scale bars: A, B-500 μm ; C, D-100 μm . ipsi., ipsilateral; contra., contralateral.

No significant neuronal loss occurs in the SN after MCAo within 24 h.

We then investigated whether striatal ischemia induced remote neuronal death in the SN as early as 24 h after MCAo. Cresyl violet staining showed no neuronal loss in the SN, although some animals showed morphological alterations in a small number of neurons in the SNr (Fig. 3A). The number of cresyl violet-stained neurons was not significantly reduced in any area of the SN (Fig. 3B). Quantification of NeuN-positive cells did not reveal any significant difference in the number of neurons between the ipsilateral and the contralateral SN (Fig. 3B). Neurons undergoing acute injury lose NeuN immunopositivity within 6-24 h after MCAo in the infarct and the penumbra, which has been found to correlate with other markers of neurodegeneration (Liu *et al.*, 2009). CD45-ir cells with glial morphology surrounded viable (NeuN-positive) neurons in the ipsilateral SNr (Fig. 3C), whilst no microglial-shaped CD45-positive cells were seen in the corresponding area on the contralateral side.

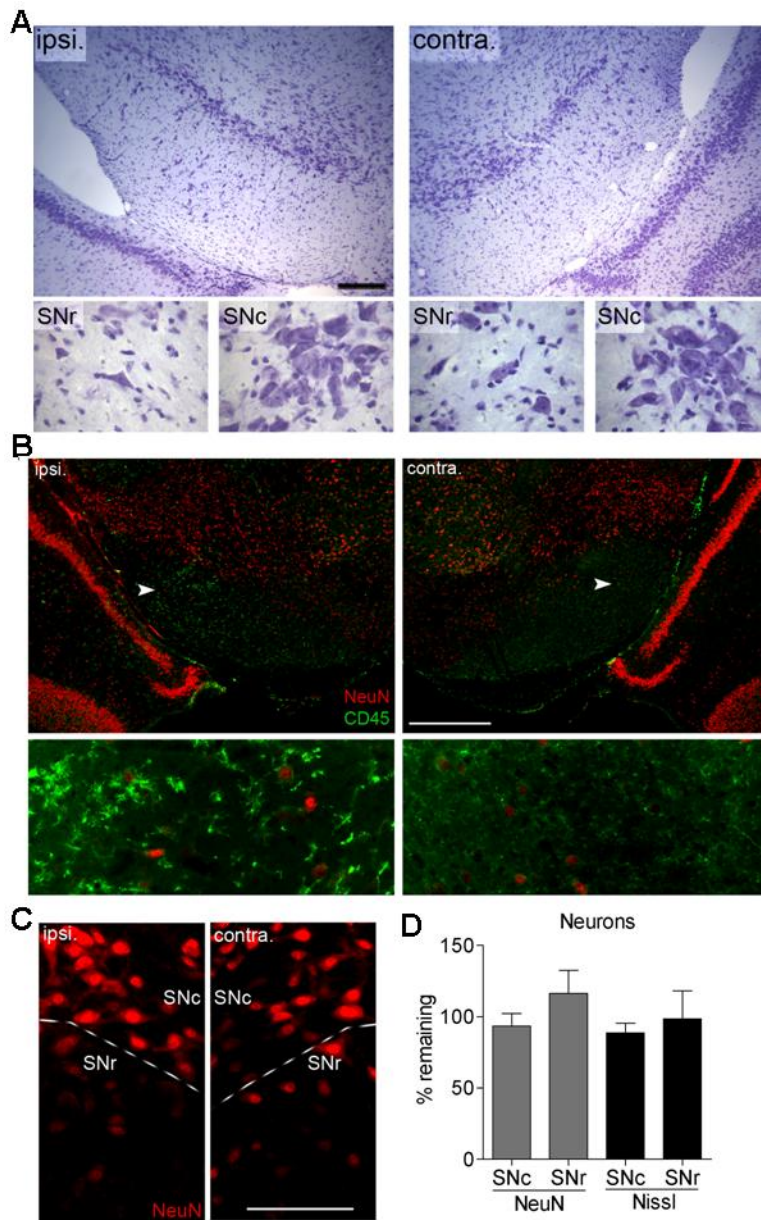


Figure 3. No significant cell loss occurs in the SN after 45min MCAo during 24 h reperfusion. **A.** Cresyl violet staining indicates no sign of focal ischemia in the ipsilateral SN. **B.** CD45-ir cells with microglial morphology are found in the ipsilateral SN around NeuN-positive cells (inserts below), which are not observed in the contralateral hemisphere. **C.** No loss of NeuN-ir cells is observed in the SNr and SNc (inserts, right). **D.** Quantification of cresyl violet (Nissl)-positive neurons and NeuN-positive cells show no significant level of cell death in the ipsilateral pars reticulata (SNr) and pars compacta (SNc) of the SN. One sample *t*-test (NeuN, n=6; Nissl, n=8). Scale bars: A-200 μ m; B-500 μ m; C-100 μ m. ipsi., ipsilateral; contra., contralateral.

Mild MCAo results in inflammation and early loss of SP in the SN in the absence of focal neuronal injury.

To confirm that changes in the SN are not the result of collateral injury triggered by the surrounding ischemic area in response to a major ischemic challenge, a mild ischemia was induced. 30 min MCAo followed by 24 h reperfusion induced ischemic brain injury exclusively in the striatum (Fig. 4A), but resulted in a significant (30%) reduction in the SP-ir area in the SN (Fig. 4B). CD45-positive cells were significantly increased around the area of SP loss in the ipsilateral SN compared to the contralateral SN (Fig. 4C and D). This may indicate that local microglial cells become activated, which was supported by the elongated microglia-like morphology of the CD45-positive cells and the fact that, after 24 h of reperfusion, very little infiltration of monocytes/macrophages is observed in this model in the ipsilateral hemisphere (Jin *et al.*, 2010). No changes were observed in other inflammatory markers (Iba1, GFAP, ICAM-1 and VCAM-1, Fig. 4C and D). No significant variation in the amount of neurons was found between the ipsilateral and the contralateral sides (Fig. 4E).

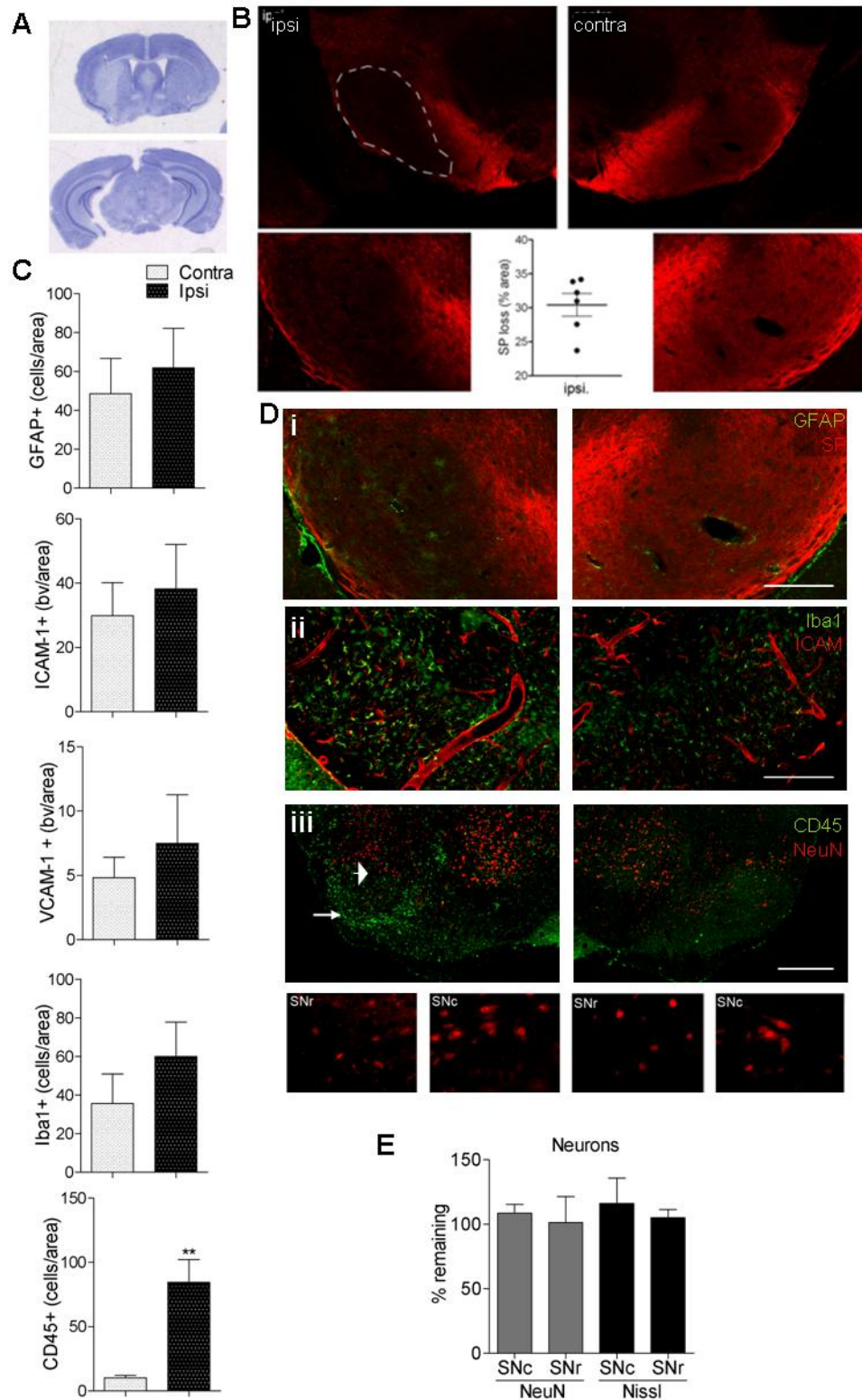


Figure 4. Mild focal cerebral ischemia results in loss of SP and inflammation in the SN without inducing significant neuronal damage. **A**, 30 min MCAo followed by 24 h reperfusion results in mild focal ischemia, which is restricted to the striatum (cresyl violet staining). **B**, 30 min MCAo leads to an average of 30% loss of SP-ir area in the ipsilateral SN. **C**, Quantification of inflammatory markers indicates a significant

increase in CD45-positive cells in the ipsilateral SN. **D**, GFAP (i), ICAM-1 (ii), Iba1 (ii) and CD45 (iii) levels are higher in the ipsilateral SN. CD45-positive cells with microglial morphology are surrounding the area of SP loss in the ipsilateral SN (iii, arrow). No neuronal loss is observed in the ipsilateral SN (iii, arrowhead and arrow indicate the place of the inserts in SNc and SNr respectively). **E**, Quantitative analysis shows no significant reduction in cresyl violet (Nissl) or NeuN-positive cell numbers in the ipsilateral SN. $**p < 0.01$, C-unpaired *t*-test (ICAM, n=3; GFAP, n=6; CD45 and Iba1, n=5) D- one sample *t*-test (NeuN, n=4; Nissl, n=5). Scale bars: D-200 μ m (i-ii), 500 μ m (iii). ipsi., ipsilateral; contra., contralateral.

No alteration in SP expression, inflammation or neurodegeneration is observed 4 h after mild MCAo.

To clarify how early SP changes and inflammation start we analysed the SN 4 h after mild MCAo. Even as early as 4 h post MCAo, striatal (but not SN) neurodegeneration was observed (Fig. 5A). In the SN there was no apparent loss of SP, therefore an area of loss could not be quantified. Intensity of SP immunoreactivity was quantified, but no differences were detected (Fig. 5B). Inflammation (Fig. 5C) and neurodegeneration (Fig. 5D) were not significantly altered in the SN at 4 h reperfusion.

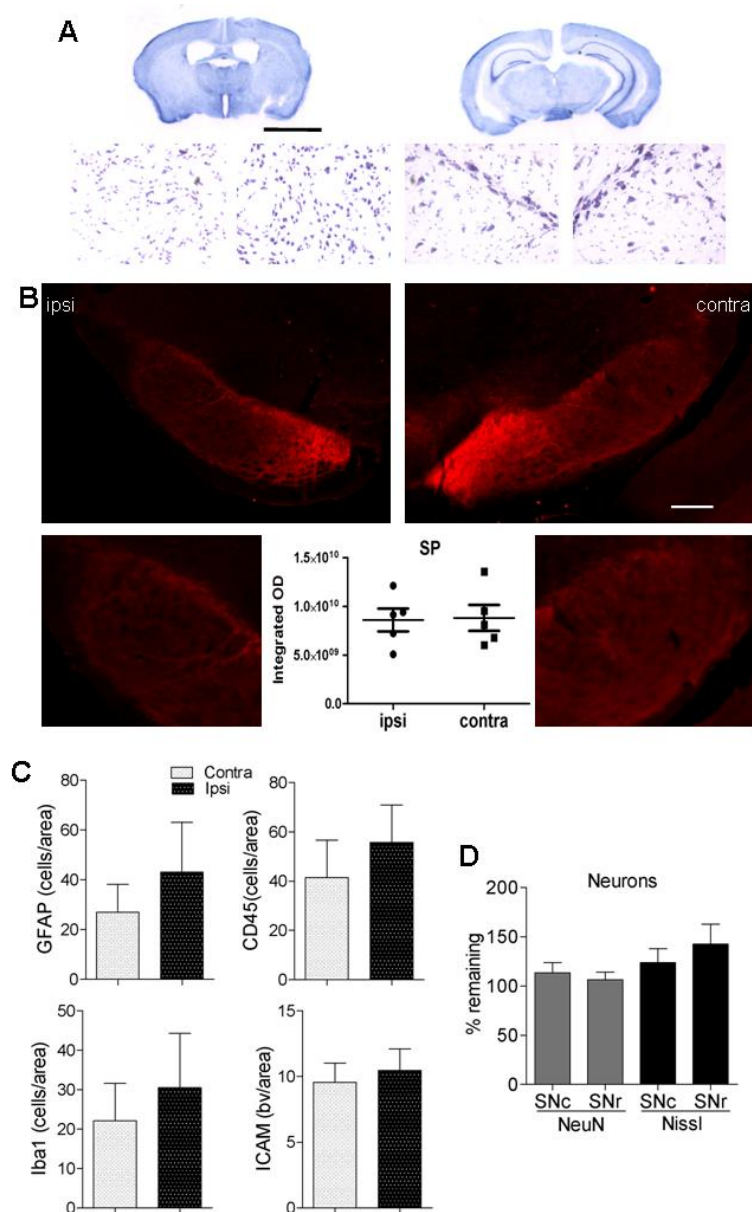


Figure 5. No changes in SP levels, inflammation or neuronal death are observed in the SN 4 h after mild (30 min) MCAo. **A.** Neuronal death is observed in the striatum but not in the SN 4 h after mild ischemia. **B.** No changes in SP levels are observed in the SN. **C.** Inflammation levels are similar in the SN in both hemispheres. **D.** No significant difference in cresyl violet (Nissl) or NeuN-positive cell numbers is found between ipsilateral and contralateral SN. B,C-unpaired *t*-test (all n=5); D- one sample *t*-test (all n=5). Scale bars: A-3 mm; B-200 μ m. ipsi., ipsilateral; contra., contralateral.

Inflammation and SP loss precede neurodegeneration in the SN

We next examined the effect of early inflammation on delayed changes. Delayed neuronal death in the SN occurs after striatal ischemia in patients and in rats (Nakane *et al.*, 1992; Uchida *et al.*, 2010). To corroborate that this response also occurs in our mouse model, we assessed neuronal death in the SN 6 days after mild MCAo. A significant decrease in neuronal numbers was observed in the SN, particularly in the SNr, as quantified by Nissl staining (Fig. 6A i) and NeuN immunofluorescence (Fig 6A ii). This is in line with the fact that the SNr is directly innervated by striatal neurons, whereas the SNc receives only indirect striatal input. We also examined whether SP loss was sustained over time, since a recent study found sprouting of striato-nigral axons after stroke (Sun *et al.*, 2011), which could have an effect on SP levels in the SN. At 6 days, SP loss was apparent in nearly 50% of the area of the SN (Fig. 6B). We investigated whether inflammatory changes also occurred at this time. We found a significant increase in the amount of microglial shaped CD45-positive and Iba1-positive cells in the ipsilateral SN (Fig. 6C). Microglial/macrophage cells also displayed ICAM-1-ir (Fig. 6C). Interestingly, ICAM-1-positive blood vessels were more numerous in the contralateral SN (Fig. 6C) at this time point.

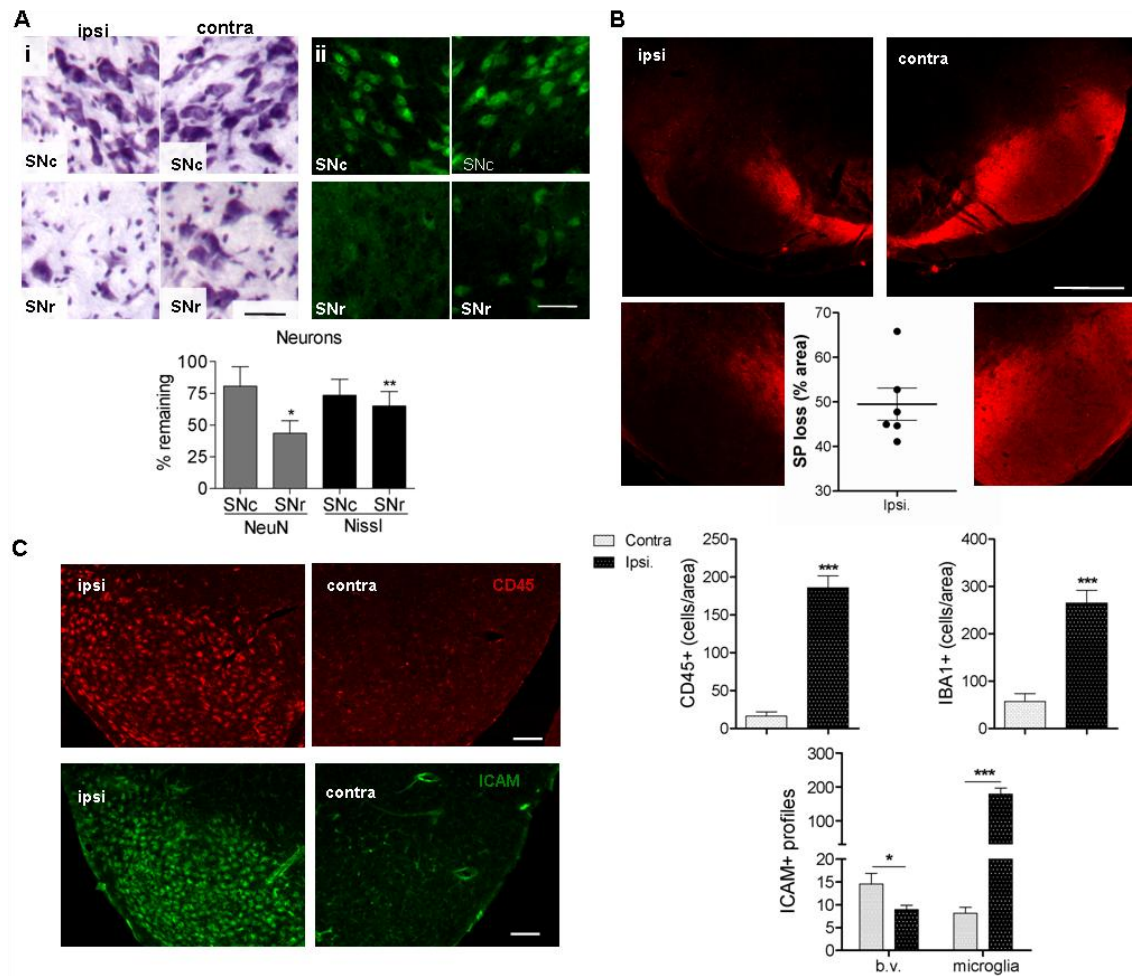


Figure 6. Neuronal death is accompanied by sustained SP loss and inflammatory changes in the SN 6 days after mild MCAo. **A**, Quantification of “i” cresyl violet (Nissl)- and “ii” NeuN- positive cells in the SN reveals a significant decrease in the amount of neurons in the SN, particularly in the SNr. **B**, SP loss affects an average of 49.5% of the area of the SN 6 days after 30 min MCAo. **C**, Significantly higher amounts of CD45-positive, Iba1- positive or ICAM- positive cells with microglial morphology are found in the ipsilateral SN, as compared to the contralateral SN. ICAM-positive blood vessels (b.v.) are more numerous in the contralateral SN. * $p < 0.05$, ** $p < 0.01$, *** $p < 0.001$, A- one sample t -test (all $n = 6$); C-unpaired t -test (all $n = 6$). Scale bars: A-50 μm ; B-500 μm ; C-100 μm . ipsi., ipsilateral; contra., contralateral.

Dopaminergic neuronal loss follows inflammation and SP loss.

As dopaminergic neurons are essential for motor control, we explored whether this particular subtype of neurons was affected in the SN after MCAo. A significant reduction of TH-positive neurons occurred in the SNr from 4 h to 6 days after mild MCAo (Fig. 7A), and there was a significant overall loss of SN neurons (percentage remaining from the contralateral side) 6 days after mild MCAo (Fig. 7A). There was a trend for loss of TH-positive neurons in the SNc even 24 h after 45 min MCAo, but two-way ANOVA or one sample t-test did not detect an overall loss of these cells in the SN. Neurological deficits were significant 24 h after MCAo (Fig. 7B). As expected, smaller infarct size correlated with better neurological scores (Fig. 7C, red, $p < 0.001$). Although not statistically different, there was a trend suggesting that fewer TH-positive neurons in the SN were associated with worse neurological outcome (Fig. 7C).

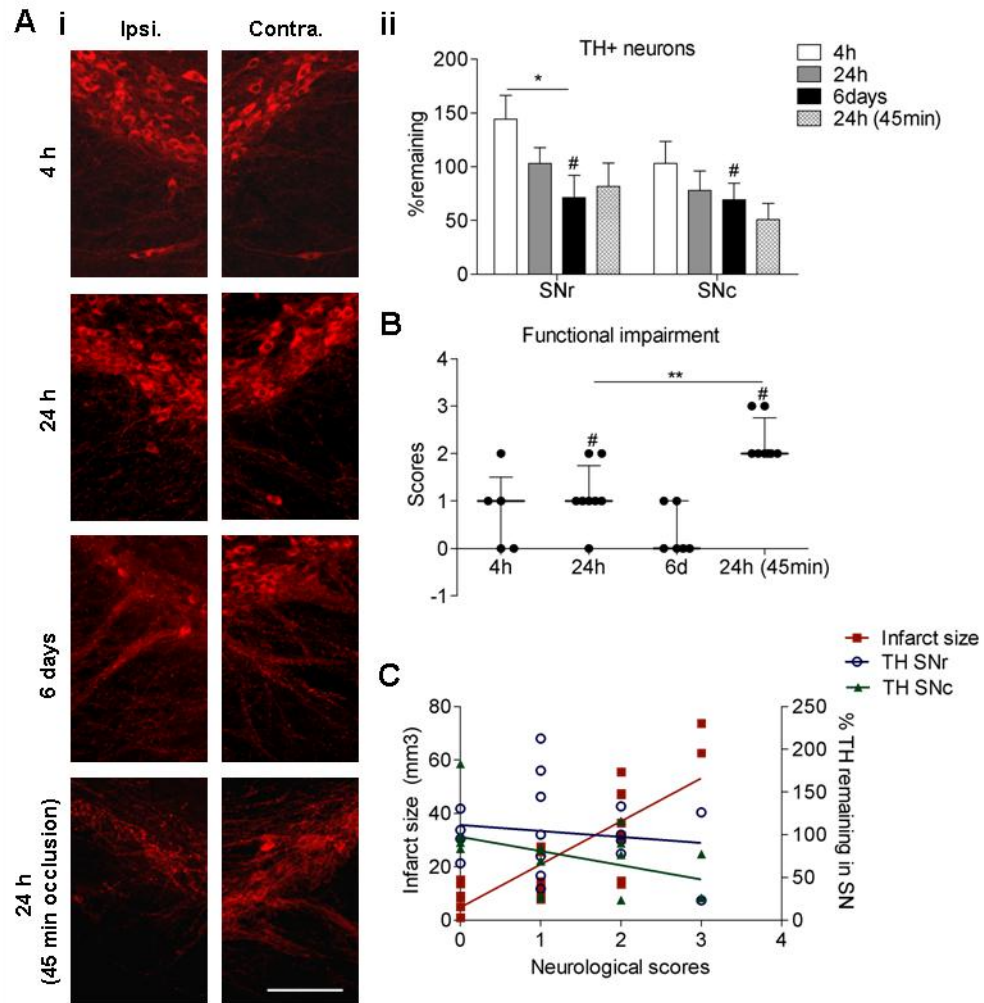


Figure 7. Dopaminergic neuronal loss follows inflammation and SP loss without worsening general motor function. **A**, TH staining over time in the SN (**i**). TH+(dopaminergic)-neuronal loss is observed at 6 days in the SN and a significant drop of remaining neurons occurs in the SNr from 4 h to 6 days (**ii**). **B**, Neurological deficits are significant 24 h after MCAo with both occlusion times, being higher in the 45 min occlusion model. **C**, Neurological deficits correlate with infarct size ($r^2=0.6505$, $p<0.001$), but not with dopaminergic loss in the SN. * $p<0.05$, ** $p<0.01$, # $p<0.05$, A- two-way ANOVA (*) and one sample *t*-test (#) (4 h, $n=5$; 24 h, 6 days and 24 h(45 min), $n=4$); B- Wilcoxon Signed Rank test (#) or Mann Whitney test (*) (4 h, $n=5$; 24 h and 24 h (45 min), $n=8$; 6 days, $n=6$). C- linear regression (infarct size, $n=17$; TH SNc and SNr, $n=13$) Scale bar: 100 μ m. ipsi., ipsilateral; contra., contralateral.

Discussion

In order to better understand mechanisms of remote injury in the SN following transient focal ischemia, we investigated whether changes in SP levels and inflammation occur in the SN preceding neuronal injury. To date, no studies investigated early changes in remote neuronal injury and inflammation in the SN after focal cerebral ischemia in mice, and no studies addressed local variations of SP levels in the SN after stroke. We report here for the first time a loss of SP in the SN after transient MCAo, which takes place in precise anatomical overlap with the development of an inflammatory response 24 h after cerebral ischemia, but without apparent neuronal cell death. In contrast, remote neuronal injury occurs in the SN 6 days after MCAo in the same area where SP loss and inflammation were detected.

No previous reports provided a direct correlation of anatomical changes in the SN with neurotransmitter alterations after acute brain injury. In contrast, our study clearly demonstrates that early inflammatory changes occur in the SN prior to neuronal injury and that they take place in a precisely overlapping area with the loss of SP. It is unknown whether SP loss merely parallels inflammation and is indicative of loss of afferent striato-nigral terminals, or whether it also contributes to the development of the inflammatory response. SP variations had also been observed in a PD model, finding increased SP at early time points (Thornton & Vink, 2012) and decreased SP later on (Lindfors *et al.*, 1989). It has been reported that changes in SP levels could modulate focal inflammatory responses (O'Connor *et al.*, 2004). Overproduction of SP can indeed trigger vasodilation and facilitate inflammation, whereas inhibition of SP proved to be beneficial in experimental models of cerebral ischemia (Turner *et al.*, 2011). However SP loss, together with the loss of GABA in the SN (Yamada *et al.*, 1996) may affect other properties of dopaminergic neurons or glial cells, alter the

expression of NK1 receptors, or change the excitability of local neurons leading to excitotoxic processes and/or an inflammatory response.

Inflammation in the SN was observed at 24 h and sustained at 6 days. Earlier reports in rats showed delayed inflammatory changes in the SN, which can evolve up to 20 weeks after MCAo (Arlicot *et al.*, 2010; Uchida *et al.*, 2010), suggesting that the early inflammatory response we observed could be sustained for a long time. How inflammation contributes to delayed neuronal injury in remote brain regions after cerebral ischemia is currently not well understood. We show that inflammation precedes neurodegeneration in the SN after MCAo, even after mild striatal ischemia. Studies done in rats support that glial activation in could take place before neurodegeneration in the SN (Dihné & Block, 2001; Loos *et al.*, 2003), although no studies observed activation of microglia and astrocytes as early as 24 h post-stroke. Neurodegeneration in the SN of PD patients (Mauborgne *et al.*, 1983) has also been linked to inflammation (McGeer & McGeer, 2004; Tansey *et al.*, 2007), and it is well known that microglia respond rapidly to subtle neuronal changes such as synaptic stripping or synapse degeneration, however it is debated whether these cells are actively involved in chronic neurodegeneration (Perry & O'Connor, 2010). Similarly, the role of microglial function in stroke is under intense debate (Denes *et al.*, 2010b). The current study does not provide any functional evidence for a possible detrimental effect of microglia in remote injury, but it shows that microglial and astrocytic activation occurs in area of delayed neuronal loss, and is therefore an early harbinger of pathology in the SN. Neuronal death in the SN has been associated with changes in other inflammatory markers too, such as altered tumour necrosis factor-alpha (TNF- α) and interleukin-6 (IL-6) levels, or more delayed activation of microglia and astrocytes (Dihné & Block, 2001; Loos *et al.*, 2003; Uchida *et al.*, 2010).

Neurodegeneration in the SN has also been observed in post-stroke patients (Nakajima *et al.*, 2010; Nakane *et al.*, 1992; Ogawa *et al.*, 1997), and a recent large population-based study showed a 2-fold increase in the relative risk of developing PD in those with a history of ischemic stroke (Becker *et al.*, 2010). Since dopamine is essential for motor control, the integrity and functionality of dopaminergic neurons is particularly important to prevent PD symptoms arising. We observed a significant loss of dopaminergic neurons 6 days after mild ischemia, although it did not correlate with neurological outcome. Neurodegeneration happens in a progressive manner in PD and dopaminergic loss in PD is much more profound than what we observe 6 days after MCAo, with symptoms appearing only when approximately 80 percent of cells are lost (Ma *et al.*, 1996). Nevertheless, single or repeated ischemic episodes might contribute to inflammation or neurodegeneration in the SN augmenting overall cell loss and/or accelerating the progression of the disease. Silent strokes, transient ischemic events or hypoxic episodes affecting the MCA territory might also affect neurotransmitter levels and facilitate inflammatory responses remote to the ischemic injury and therefore could be relevant in the very early stages of the development of chronic neurodegenerative diseases, such as PD.

In conclusion, we show for the first time the early development of remote injury in a mouse focal cerebral ischemia model in the SN and identify early loss of striatal-derived SP and inflammation in the SN that precede neuronal death, including dopaminergic neurons which may have implications to delayed loss of motor function after stroke, and to the development of chronic neurodegenerative diseases.

Acknowledgements

We are grateful for funding provided by the European Union's Seventh Framework Programme (FP7/2008-2013) under Grant agreements Nos. 201024 and 202213 (European Stroke Network) and the Simon and Simone Collins studentship. We would like to thank Professor Nancy Rothwell for critically reviewing the manuscript.

Chapter 7: The role of PTX3 in remote inflammation and neurodegeneration after cerebral ischaemia.

This chapter is written in a scientific paper format, waiting to be sent for peer-review.

**The role of PTX3 in remote inflammation and neurodegeneration
after cerebral ischaemia**

Beatriz Rodriguez-Grande¹, Adam Denes^{1,2} and Emmanuel Pinteaux¹

¹Faculty of Life Sciences, A.V. Hill Building, University of Manchester, Oxford Road,
Manchester, M13 9PT, UK; ²Laboratory of Molecular Neuroendocrinology, Institute
of Experimental Medicine, Budapest H-1450, Hungary

Abstract

The substantia nigra (SN) is a brain structure involved in motor control and addiction. The SN is severely affected in Parkinson's disease, but also presents neurodegeneration after acute brain injury induced by focal striatal ischaemia. We showed that inflammatory changes in the SN after an ischaemic event affecting the striatum precede delayed remote neurodegeneration. We also demonstrated that the acute phase protein pentraxin-3 (PTX3) influences glial inflammatory responses and formation of the glial scar in the brain after ischaemic stroke. Using transgenic mice which lack PTX3 we explored the effects of PTX3 on remote inflammation and neurodegeneration in the SN following middle cerebral artery occlusion. Lack of PTX3 had no effect on vascular inflammation or neutrophil recruitment, however, PTX3 KO mice had less microglia and astrocytes in the SN 6 days after the ischaemic event. Despite having less glia overall, the relative increase compared to the contralateral side (percentage of increase in the ipsilateral amount of glia compared to the contralateral amount of glia) in the SN was higher in PTX3 KO than WT mice. This supports the emerging role of PTX3 in regulating glial responses, and highlights its possible role in remote brain injury.

Introduction

After acute brain injury, remote damage can occur in areas connected to the core of the primary damage. After cerebral ischaemia affecting the striatum, the substantia nigra (SN) suffers remote injury, which has been observed both in experimental (Nagasawa & Kogure, 1990) and clinical settings (Nakane *et al.*, 1992; Ogawa *et al.*, 1997). The striato-nigral circuitry is essential for motor control and a severe loss of dopaminergic neurones is observed in the SN of Parkinson's disease (PD) patients (Bartels & Leenders, 2009; Ma *et al.*, 1996). In addition, the incidence of PD increases 2-fold in patients which had suffered a stroke (Becker *et al.*, 2010). Understanding the chain of events which take place in the SN after stroke could help the prevention of remote damage and long term motor complications. We showed recently that remote inflammation precedes neurodegeneration in the SN (Rodriguez-Grande *et al.*, 2013). It is thus possible that inflammation has an impact in the neurodegenerative process in the SN. Alterations in gliosis (Arlicot *et al.*, 2010; Block *et al.*, 2005) have been suggested as potential contributing factors to remote neurodegeneration. Our recent data indicate that an acute phase protein, pentraxin-3 (PTX3), is induced in the brain by the pro-inflammatory cytokine interleukin (IL)-1 in response to brain injury, and it alters the inflammatory response after ischaemic stroke, in part by inducing glial proliferation (Rodriguez-Grande *et al.*, 2014). PTX3 also regulates neutrophil infiltration in peripheral organs (Deban *et al.*, 2010b) and coats apoptotic cells preventing their phagocytosis and subsequent presentation of autoantigens (Rovere *et al.*, 2000), modulating inflammatory and immune responses. Besides, PTX3 has been suggested to be neuroprotective after brain seizures (Ravizza *et al.*, 2001). The fast and elevated increase of PTX3 expression in inflammation-related disorders makes it a good biomarker of disease severity, indeed, PTX3 is an independent predictor of

mortality after ischaemic stroke (Ryu *et al.*, 2012). The role of PTX3 in remote damage after focal cerebral injury however, had never been addressed. We hypothesised that after striatal ischaemia PTX3 could have a neuroprotective effect in the SN through modulation of inflammatory responses.

Materials and Methods

Animals

PTX3 knockout (KO) mice (on C57BL/6 background) were provided by Dr. Cecilia Garlanda (Humanitas Clinical and Research Center, Rozzano, Italy), and were bred in-house as heterozygous. Litters were genotyped as described earlier (Rolph *et al.*, 2002). Age and weight matched littermates were used for all experiments. Mice were kept at $21^{\circ}\text{C} \pm 1^{\circ}\text{C}$ and 65% (v/v) humidity with a 12 h light-dark cycle with free access to food and water. Animal procedures followed the European Council directives (86/609/EEC) and the Animal Scientific Procedures Act (UK) 1986.

Middle cerebral artery occlusion and sample obtention

Anaesthesia was induced with 4% (w/v) isoflurane, and maintained during surgery with 1.5% (w/v) isoflurane. A thermal blanket and a rectal probe were used to maintain core body temperature at $37.0 \pm 0.5^{\circ}\text{C}$. Cerebral ischaemia was induced by introducing a silicone coated 6-0 nylon monofilament (0.21 mm tip diameter, Doccol, US) through the left external carotid artery and advanced into the internal carotid artery to occlude the MCA. Occlusion of the MCA was monitored by laser Doppler (Moor Instruments, Devon, UK). After 30 min of occlusion, the filament was removed to allow reperfusion. 48 h or 6 days after reperfusion, mice were transcardially perfused using 9

g/ml saline, followed by 4% (w/v) paraformaldehyde (PFA) (Sigma, Dorset, England). Brains were post fixed overnight in 20% (w/v) sucrose in 4% (w/v) PFA, and then incubated in 20% (w/v) sucrose in phosphate-buffered saline (PBS) for 5-10 h before being cut in coronal sections with a sledge microtome (Bright Instruments, Huntingdon, UK). Samples were stored at -20°C in cryoprotective solution (30% (v/v) ethylene glycol (Sigma, UK) and 20% (v/v) glycerol (Fisher Scientific, Loughborough, UK) in PBS).

Immunohistochemistry and image acquisition

Immunofluorescent staining was performed as described before (Rodriguez-Grande *et al.*, 2013). Briefly, brain sections were incubated for 1 h with 2% (v/v) normal donkey serum before overnight incubation with the corresponding primary antibodies: rat (1:200, AbDSerotec, UK) or mouse (1:100, R&D Systems, UK), rat anti-CD45 (1:250, AbDSerotec, UK), goat anti-ICAM-1 (1:250, R&D Systems, UK), chicken anti-gial fibrillary acidic protein (GFAP) (1:1000, Abcam, UK), rabbit anti-Iba1 (1:1000, Wako, Germany), mouse anti-NeuN (1:250, Millipore, UK) and rabbit anti-TH (1:2000, Abcam, UK) or sheep anti-TH (1:500, Millipore, UK). Sections were incubated with Alexa 488- or Alexa 594-conjugated secondary antibodies (1:500, Invitrogen, UK) for 2 h and then mounted onto microscope slides using Prolong Gold antifade reagent (Invitrogen, UK). Cressyl violet (Nissl staining) was carried out as explained in (Rodriguez-Grande *et al.*, 2013).

Images from fluorescent immunohistochemistry were taken with an Olympus BX51 upright microscope attached to a Coolsnap EZ camera (Photometrics, UK) with MetaVue Software (Molecular devices, USA). Images from Nissl staining were acquired using a Leica (Germany) bright field microscope attached to a Q-Image

(Canada) camera. Acquisition settings were established for each immunological staining and then kept constant during the acquisition of the images from all samples.

Quantification and statistical analysis

Areas and number of cells/blood vessels were quantified manually using Image J software (National Institutes of Health, USA), and density of cells/blood vessels per mm^2 was calculated. Due to the low number of neutrophils found in the SN, neutrophil infiltration was quantified by counting the total number of neutrophils in the SN rather than the density. To assess activation in response to remote damage, the density of cells/blood vessels in the ipsilateral SN was expressed as a percentage of the cells/blood vessels in the contralateral SN.

Two-way ANOVA with Bonferroni post-hoc test was used to compare cell/blood vessels densities in WT vs. PTX3 KO across different areas (SNc and SNr, ipsi and contra) and overall significant difference between WT and PTX3 KO (yielded by Two-way ANOVA) was indicated by # whereas difference between WT and PTX3 KO within each area (yielded by Bonferroni post-hoc test) was indicated by *.

Unpaired t-test was used to compare cell/blood vessel activation due to remote damage (increase in ipsilateral cell/blood vessel density as a percentage of contralateral cell/blood vessel density) in WT vs. PTX3 KO (statistical significance indicated by *).

One-sample t-test was used for the comparison of the percentage of remaining neurones vs. 100% (which was calculated from the neuronal density values from the contralateral side) and statistical significance indicated by *.

In all cases statistical significance was set at $P < 0.05$.

Results

Lack of PTX3 reduces astrocytic activation in the SN 48 h after MCAo, with no effect on other inflammatory cells or neurodegeneration.

Astrocytic activation due to remote damage was observed both in WT and PTX3 KO mice (Fig. 1A i). The increase (expressed as a percentage) in the density of astrocytes (GFAP positive cells/mm²) in the ipsilateral SN compared to the contralateral SN was significantly lower in PTX3 KO than in WT mice (Fig. 1A ii). In addition, there was a trend for less activated astrocytes in the SN of PTX3 KO mice compared to the SN of WT mice, both in the ipsilateral and the contralateral hemisphere, although the difference was not significant (Fig. 1A iii). On the other hand, the amount of microglial activation due to remote damage, which is the most prominent response observed in the SN in previous studies (Rodriguez-Grande *et al.*, 2013), was similar in both genotypes (Fig. 1B i), and the density of microglial cells within each hemisphere was not different either (Fig. 1B ii). Levels of vascular activation (Fig. 1C) and neutrophil infiltration (Fig. 1D) were not significantly affected by the lack of PTX3 48 h after the ischaemic event, although there was a trend towards higher vascular activation (Fig. 1C) and lower neutrophil infiltration (Fig. 1D) in PTX3 KO mice.

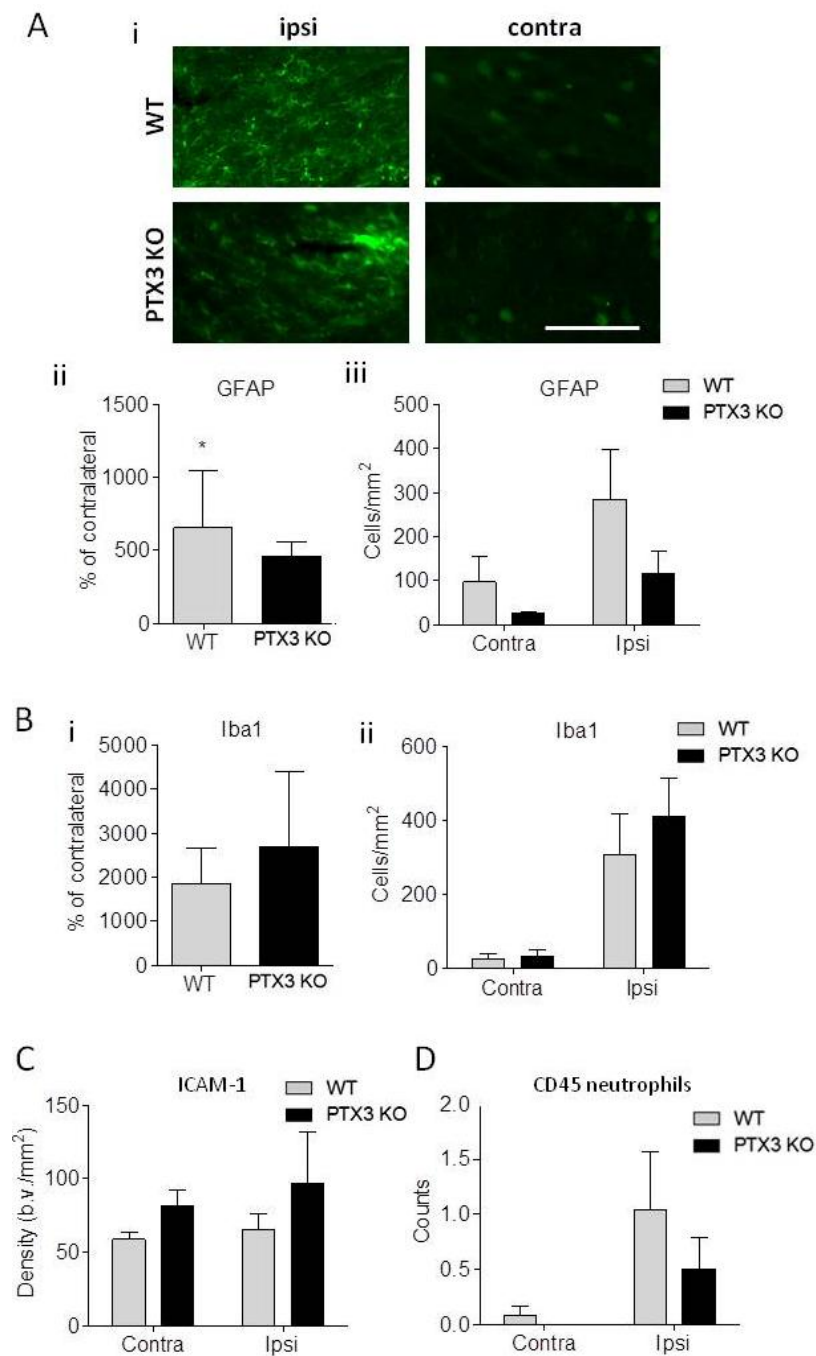


Figure 1. Inflammatory response in the SN 48 h after MCAo. **A**, Astrocytic activation in the SN due to remote damage (increase in ipsilateral vs. contralateral density of astrocytes) occurs in both genotypes (i), but it is significantly lower in PTX3 KO mice than in WT mice (ii). There is a non-significant trend towards less density of astrocytes (GFAP positive cells/mm²) in both the contralateral and ipsilateral SN in PTX3 KO mice compared to WT

mice (iii). **B**, **C**, **D**, No significant difference is observed in the density of microglia (Iba1 positive cells/mm²) (B ii) or in the increase in activation in the ipsilateral SN (B i), activated blood vessels (ICAM-1 positive blood vessels) (C) or infiltrated neutrophils (bright round CD45 positive cells in the whole SN) (D). A iii, B ii, C, D were analysed by two-way ANOVA with Boferroni post-hoc test. b.v. blood vessel. Aii, Bi were analysed by unpaired Students t-test (*P<0.05). Error bars show SEM (n=4).

Neuronal death, quantified as the remaining neuronal density (NeuN positive neurones/mm²) in the ipsilateral compared to the contralateral SN, indicated that WT mice suffered significant neurodegeneration in the SNr whereas PTX3 KO mice did not (Fig. 2A). However, no neurodegeneration was found in the SNc of any genotype (Fig. 2A). Survival of dopaminergic neurones (identified by TH staining, Fig. 2B) was not affected by the lack of PTX3.

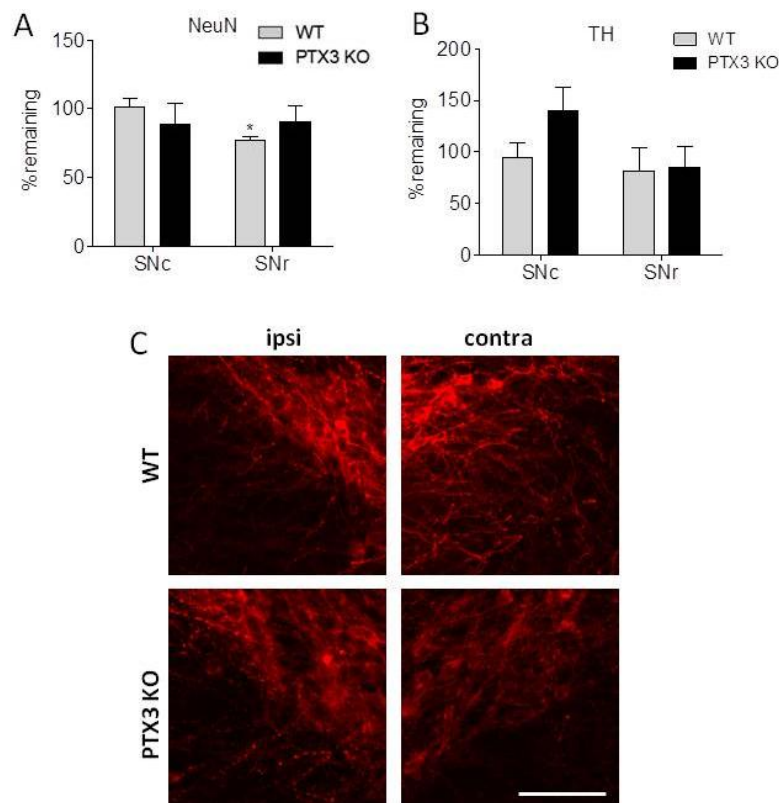


Figure 2. Neuronal death in the SN 48 h after MCAo. **A**, There is a significant decrease in the percentage of remaining NeuN positive neurones in the SNr of WT mice (vs. 100%) which is not observed in PTX3 KO mice or in the SNc of either genotype. **B**, PTX3 KO mice show a trend for increased number of dopaminergic (TH positive) neurones in the SNc compared to WT mice, but it is not significant. **C**, Immunofluorescent TH staining of the SN shows no observable difference between genotypes. One-sample t-test vs 100% (* $P < 0.05$) and two-way ANOVA with Bonferroni post-hoc test were performed. Error bars show SEM (WT $n=4$, PTX3 KO $n=3$).

Lack of PTX3 alters astrocytic and microglial responses in the SN 6 days after MCAo

Astrocytic activation due to remote damage (percentage of increase in cell density in the ipsilateral compared to the contralateral hemisphere) was observed in the SN of both genotypes (Fig. 3A i), but a trend suggested it was higher in PTX3 KO mice (Fig. 3A iii). Despite this increase in activation in the ipsilateral compared to the contralateral side, a trend pointed towards a lower amount of activated astrocytes overall in PTX3 KO mice compared to WT mice, both within the ipsilateral and the contralateral SN (Fig. 3A ii). The same effect was observed for microglia: despite the fact that PTX3 KO mice showed a trend for higher increase in microglial density in the ipsilateral compared to the contralateral SN (Fig. 3B iii), PTX3 KO mice had less microglial cells in both the ipsilateral and contralateral SN (Fig. 3B ii). This suggests that, despite having less activated glial cells, PTX3 KO mice have a more sensitive response to remote damage, which is reflected by the higher increase in glial activation in their ipsilateral compared to their contralateral SN. Similarly to the earlier time point, 6 days after MCAo there was no difference in remote vascular activation (Fig. 3C) or neutrophil infiltration (Fig. 3D) between genotypes, although there was a trend towards a decrease in the number of neutrophils in the SN of PTX3 KO mice compared to that of WT mice (Fig. 3D).

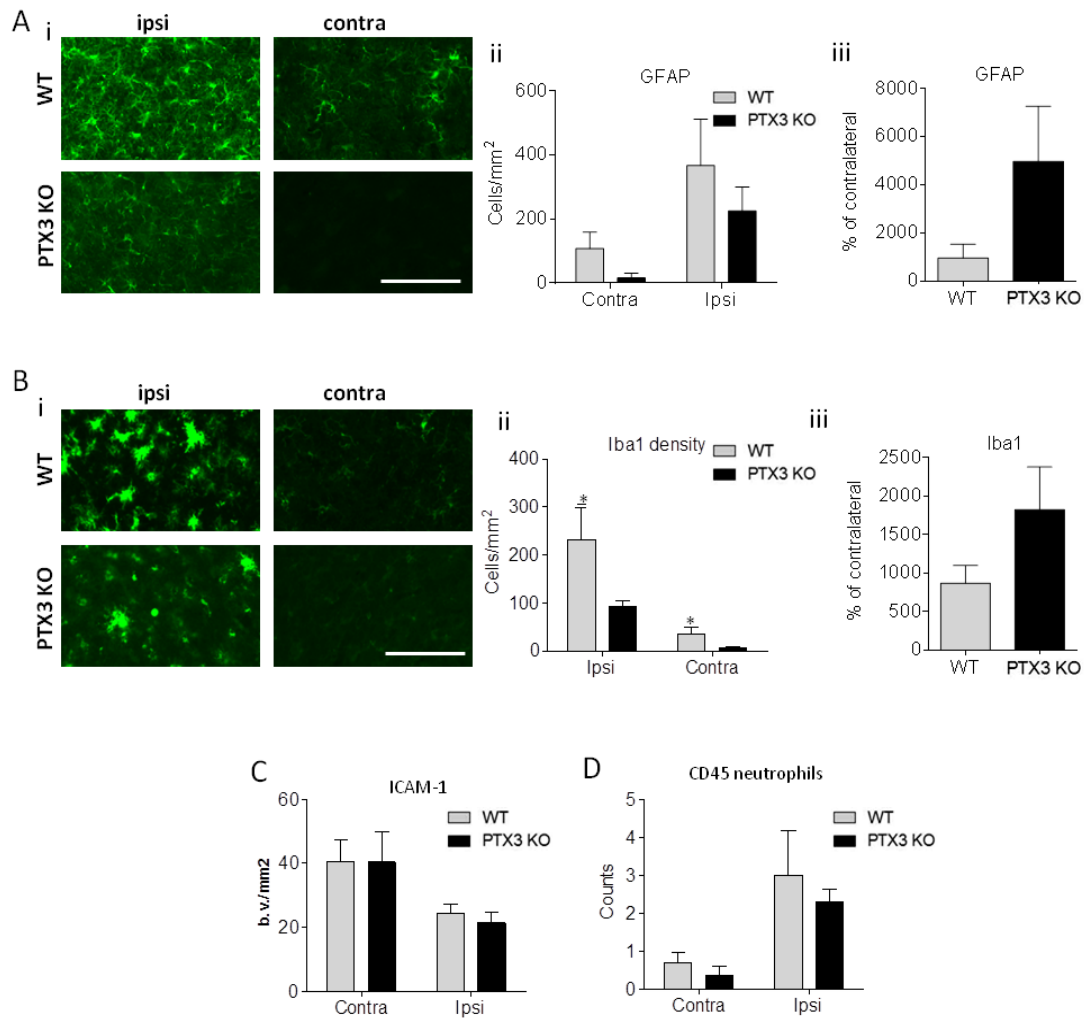


Figure 3. Inflammatory response in the SN 6 days after MCAo. A, B. A trend suggests that the increase in ipsilateral astrocytic (A i) and microglial (B i) activation in response to remote damage is higher in PTX3 KO mice compared to WT mice (A iii, B iii). No significant difference is observed in the density of astrocytes (GFAP positive cells/mm²) in the SN between genotypes, although there is a trend towards a decreased astrocytic density in PTX3 KO mice compared to WT mice in both the ipsilateral and contralateral SN (A ii). The same effect is observed in microglia (Iba1 positive cells), but in this case the difference between WT and PTX3 KO mice is significant (B ii). **C, D.** No significant difference is observed in the amount of recruited neutrophils (C) or vascular activation (D) between genotypes. A ii, B ii, C, D were analysed by two-way ANOVA (*P<0.05) with Boferroni post-hoc test. Aiii, Biii were analysed by unpaired students t-test. b.v. blood vessel. Error bars show SEM (A, B, D. WT n=5, PTX3 KO n=4; C. n=5).

Lack of PTX3 alters neuronal death in the SN 6 days after MCAo

Remote neuronal death in the SNr has previously been reported 6 days after MCAo (Rodriguez-Grande *et al.*, 2013). At this time point, we observed a significant amount of neuronal death (quantified as a reduced percentage of remaining NeuN positive neurones vs. 100%) in the SNr of both WT and PTX3 KO mice (Fig. 4A). Degeneration of dopaminergic neurones (compared to 100%) was observed in the SNr of WT but not of PTX3 KO mice, although the difference between genotypes was not significant when analyzed by two-way ANOVA (Fig. 4B). Regarding the SNc, only PTX3 KO mice showed significant neurodegeneration when quantified using NeuN staining, although two-way ANOVA did not detect a significant difference between genotypes (Fig. 4A), and loss of dopaminergic neurones was not significant in either genotype in this area (Fig. 4B).

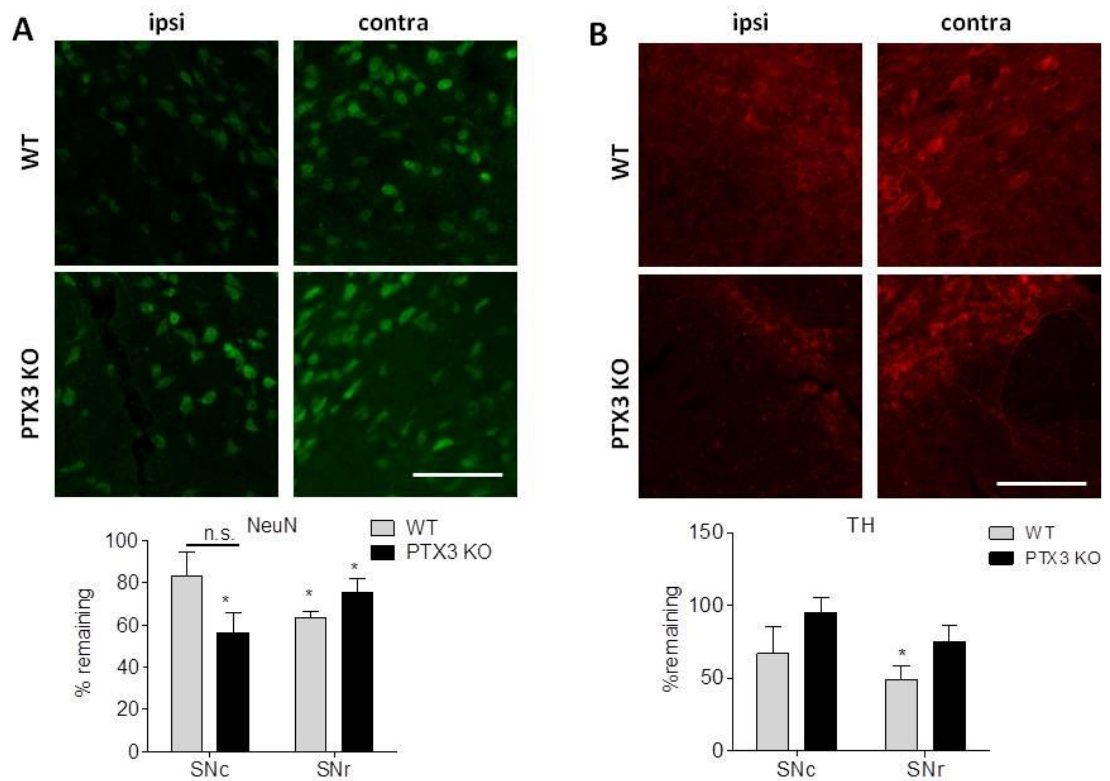


Figure 4. Neuronal death in the SN 6 days after MCAo. **A.** Except for the SNc of WT mice, there is a significant decrease in percentage of remaining NeuN positive neurones (compared to 100%) in all areas of both genotypes. **B.** Although not significant, there is a trend towards an increased survival of dopaminergic (TH positive) neurones in the SN of PTX3 mice compared to WT mice, and dopaminergic loss (compared to 100%) is only significant in the SNr of WT mice. One-sample t-test vs. 100% (* $P < 0.05$) and two-way ANOVA were performed. Error bars show SEM (n=4).

Discussion

We had hypothesised that PTX3 could be involved in neuroprotection through the modulation of glial responses. Indeed, we found that lack of PTX3 modulated remote glial responses; however, it did not have a consistent neuroprotective effect. Importantly, this is the first study of the function of PTX3 in non-focal brain damage, and it suggests that PTX3 may be involved in the modulation of the inflammatory

response in chronic CNS disease which, as remote damage, involves slower neurodegeneration.

We had previously found that PTX3 induces glial proliferation *in vitro*, and that lack of PTX3 decreases the amount of microglial proliferation in the core and peri-infarct area days after the ischaemic insult (Rodriguez-Grande *et al.*, 2014). In agreement with that, 6 days after MCAo mice lacking PTX3 had less activated microglia and astrocytes. Interestingly, despite the overall lower number of activated glial cells, a trend indicated that the glial activation due to remote damage (ipsilateral compared to contralateral) was stronger in PTX3 KO mice than in WT mice. This increase in remote cellular activation was not observed 48 h after MCAo; in fact, remote astrocytic activation in the SN was lower in PTX3 KO mice than WT mice at that time. We had previously seen that the effect of PTX3 on several inflammatory responses in the CNS changes over time (Rodriguez-Grande *et al.*, 2014). Further work needs to be done to clarify how these time-dependent changes happen. Moreover, it would also be important to determine the phenotype of microglia in this context. Much has been discussed about the role of microglia in neurodegeneration (Perry & O'Connor, 2010; Polazzi & Monti, 2010), in particular in the SN in PD (Bartels & Leenders, 2007; McGeer & McGeer, 2004; Tansey *et al.*, 2007), and it is known that PTX3 can modulate microglial phagocytic activity in certain conditions, decreasing phagocytosis of apoptotic cells (Jeon *et al.*, 2010). Characterising the phenotype of PTX3 KO microglia would bring valuable information about the physiological effect of PTX3 depletion.

There is some controversy about the role of PTX3 in neutrophil recruitment. It is well established that PTX3 inhibits neutrophil infiltration in the periphery (Deban *et al.*, 2010b), however we observed both *in vivo* (in the infarct core 48 h after MCAo) and *in*

vitro that the lack of PTX3 decreases neutrophil infiltration in the brain (unpublished data). In agreement with our previous findings in the brain, the trends observed in the current study indicate that lack of PTX3 could reduce the neutrophil load in the brain. Regarding neurodegeneration, the current results suggest that PTX3 has only a moderate effect in remote neuronal damage. PTX3 seems to facilitate neurodegeneration in the SNr 48 h after the ischaemic event, since WT but not PTX3 KO mice had a significant decrease in neurones in the SNr. However, 6 days after MCAo both genotypes show significant neurodegeneration in that area. On the other hand, PTX3 seems to prevent neurodegeneration in the SNc 6 days after MCAo. It is worthy of mention that the difference between genotypes was not very strong, since the appropriate statistical tests did not yield a significant difference between genotypes. Something similar is observed for dopaminergic neurones: although mice lacking PTX3 did not suffer significant remote dopaminergic neurodegeneration in the SNr 6 days after MCAo and WT mice did, the inter-genotype difference was not statistically significant. This suggests that the effect of PTX3 on neuronal survival is not very potent, which agrees with our previous studies in stroke, where PTX3 depletion did not significantly affect neuronal survival (in the form of infarct size, (Rodriguez-Grande *et al.*, 2014)). Our *in vitro* studies show that only under oxidative stress conditions PTX3 can be protective (data not published). On the other hand, Ravizza and colleagues (Ravizza *et al.*, 2001) found that, after kainate-induced seizures, PTX3 KO mice had a higher degree of neurodegeneration; however, the mechanisms of seizure-induced neuronal death are likely to differ from the ones in ischaemia or remote damage.

In summary, we found that PTX3 mouse had generally less activated glial cells in the SN of both hemispheres after striatal ischaemia, although lack of PTX3 lowered the

increase in activation observed in the ipsilateral SN due to remote damage 6 days (but not 48 h) after the infarct. Our findings support the previously described role of PTX3 in modulation of astrocytic and microglial responses and the time-dependent effect of PTX3, and reveal that PTX3 has a role not just in acute brain damage, but also in less severe damage such as remote damage, which encourages the study of PTX3 in chronic and other CNS diseases which display milder inflammation and neurodegeneration.

Chapter 8: Discussion

8.1 Introduction

We have shown for the first time that the APP PTX3 is highly expressed in the brain after cerebral ischaemia, induced by IL-1, and that PTX3 is involved in several post-stroke repair processes. PTX3 did not have a major role in post-stroke remote damage, but we found that remote inflammation precedes neurodegeneration in the SN after striatal ischaemia.

We first observed high PTX3 expression in the ipsilateral hemisphere after MCAo, and elucidated that, whilst central IL-1 is the main inducer of brain PTX3 expression, peripheral PTX3 expression is not dependent on IL-1. We then used PTX3 KO mice to study the role of PTX3 in several aspects of inflammation and repair 48 h, 6 days and 14 days after MCAo. Lack of PTX3 caused a reduction in neutrophil infiltration 48 h post-MCAo, and PTX3 reduced neutrophil neurotoxicity *in vitro*. Lack of PTX3 altered resolution of oedema and BBB damage, modulation of glial responses, angiogenesis and neurogenesis 6 and 14 days after MCAo. The mechanisms by which PTX3 orchestrates the above mentioned repair processes remains to be determined, but the general trend in our results is that PTX3 has a beneficial effect in post-stroke recovery. This highlights the relevance of PTX3 as a possible target for stroke treatment, and supports the idea that APPs are not only anti-infectious elements, but also part of the response of our body to sterile inflammation, with functions that impact on recovery days to weeks after the initial insult.

I will discuss the implications and limitations of this study, the potential mechanisms of action of PTX3, and some future directions to refine our knowledge about the role of PTX3 after stroke.

8.2 Interpretation of results

8.2.1 PTX3 expression

In vivo and *in vitro*, IL-1 was a very potent inducer of PTX3 expression by neurones and glia. We have shown for the first time that endogenous IL-1 is enough to induce PTX3 expression in the brain after stroke; moreover, IL-1 is the main contributor to central PTX3 production after stroke, whilst it is not essential for peripheral PTX3 expression induced by experimental stroke (Chapter 3). TNF α can also induce PTX3 production (Lee *et al.*, 1990), and thus may contribute to peripheral PTX3 production in the absence of IL-1 (Chapter 3). These cytokines activate pathways leading to NF κ B activation (Allan & Rothwell, 2001) that leads to PTX3 expression during inflammation (Basile *et al.*, 1997), which we have observed also in our stroke model. Importantly, inflammation is a hallmark of several forms of acute and chronic brain disease such as meningitis, PD, Alzheimer's disease or multiple sclerosis (Aktas *et al.*, 2007; Glass *et al.*, 2010). It is worthy of mention that in brain cells cultured *in vitro*, even low concentrations of IL-1 induced PTX3 expression (Chapter 3), and thus understanding the actions of PTX3 in the brain is potentially useful to gain a better insight into brain diseases in general, even those with lower degrees of inflammation.

8.2.2 Neuroprotection and inflammation

One of the early observations leading to the study of PTX3 in stroke was the possibility that PTX3 was neuroprotective, as Ravizza and colleagues had proposed based on their observations that PTX3 KO mice had increased neurodegeneration in an epilepsy model (Ravizza *et al.*, 2001). Our results suggest that, whilst PTX3 does not have a major neuroprotective effect in our *in vivo* model of cerebral ischaemia, PTX3

can be neuroprotective, as we observed *in vitro* in neuronal cultures (Additional supplementary information to Chapter 3). The most appropriate time point to evaluate direct neuroprotection *in vivo* is the earlier one (48 h). Impaired recovery can also account for variations in infarct size and thus the later the time point, the more additional factors that can account for variations in brain damage. The early time point (48 h) is thus more likely to reflect the direct action of PTX3 on neuronal injury. The fact that 48 h after MCAo there were no significant differences in infarct size between genotypes, suggests that PTX3 does not have a strong neuroprotective effect in cerebral ischaemia. However, MCAo is an *in vivo* model where several factors affect infarct size. Even if PTX3 can be neuroprotective, as we observed *in vitro*, PTX3 could act upon other cell types and molecules and indirectly contribute to neuronal damage. Lack of PTX3 did not cause any alterations in CBF, vascular activation (Chapter 3) or glial responses (Chapter 5) 48 h after MCAo, but it reduced the number of infiltrated neutrophils (Chapter 5). Neutrophils can worsen brain injury, especially when there is preceding systemic inflammation (McColl *et al.*, 2007) and a reduction in the number of neutrophils would generally be associated with smaller infarct size but, interestingly, we found that PTX3 KO neutrophils had increased neurotoxicity (Chapter 5). PTX3 KO mice would then have fewer infiltrated neutrophils (which would reduce the damage) with higher neurotoxicity (which would increase the damage). It is possible that the lack of difference in infarct size is in part due to those two factors (PTX3 facilitation of neutrophil infiltration and PTX3-mediated neuroprotection) balancing out. The direct neuroprotective potential of endogenous PTX3 is supported by the fact that PTX3 KO neurones are more sensitive to oxidative stress, as shown in Figure 1 of the Additional supplementary information to Chapter 3. The APP ceruloplasmin has antioxidant and neuroprotective effects (Hineno *et al.*,

2011), but whether it shares any mechanism of action with PTX3 remains to be determined.

The complement system has emerged as a regulator of neurodegeneration in the CNS (Bonifati *et al.*, 2007). Inhibition of complement activity in ischaemia-reperfusion models generally improves stroke outcome (Banz *et al.*, 2011; Elvington *et al.*, 2012). PTX3 could be neuroprotective through inhibition of complement activity. Soluble PTX3 inhibits C1q-mediated complement activation (Nauta *et al.*, 2003), and inhibition of C1q, which is expressed by ischaemic neurones, is neuroprotective (Huang *et al.*, 1999). PTX3 also binds to FH, enhancing the ability of FH to block alternative complement pathway activation (Deban *et al.*, 2009). Inhibition of this pathway reduces inflammation and enhances outcome after stroke (Elvington *et al.*, 2012). An increase in FH is neuroprotective in experimental autoimmune encephalomyelitis (Griffiths *et al.*, 2009), but it is unknown whether the same happens in ischaemic stroke, in which case PTX3 could also be contributing to neuronal survival through binding to FH (Deban *et al.*, 2009). However, complement inhibition in stroke was not neuroprotective in pre-clinical trials in primates (Mocco *et al.*, 2006; Ducruet *et al.*, 2007). Further research is required to understand interspecies differences and to explore PTX3-complement interactions in the brain.

To the best of our knowledge, it is the first time that the role of an APP in neutrophil neurotoxicity has been examined. We demonstrate that endogenous PTX3 from transmigrated neutrophils dampens their neurotoxicity. Neutrophil neurotoxicity is partly due to release of oxidative molecules and thus, it is possible that the reduction of neurotoxicity in WT compared to PTX3 KO mice is due to PTX3 dampening oxidative stress-mediated death (Additional supplementary information to Chapter 3).

Apart from the direct role of PTX3 in neurotoxicity, one of our initial aims was to investigate whether PTX3 inhibited neutrophil recruitment in the CNS as it does in the periphery (Deban *et al.*, 2010b). Surprisingly, lack of PTX3 reduced neutrophil transmigration through brain endothelium *in vitro* and *in vivo* 48 h after MCAo (Chapter 5). However, lack of PTX3 promoted neutrophil infiltration 14 days after MCAo (Chapter 5), supporting findings by Deban and colleagues (Deban *et al.*, 2010b); whereas no significant difference was observed 6 days after MCAo (Chapter 5).

Several factors have to be considered to interpret this set of results. First, PTX3 KO mice could have an altered amount of systemic neutrophils, which could be the cause of the different amount of recruited neutrophils, regardless of any alteration in the mechanism of transmigration itself. However, the same amount of WT and PTX3 KO neutrophils was used for the study of transmigration *in vitro*, and yet less PTX3 KO neutrophils transmigrated through the WT brain endothelium (Chapter 5), suggesting that regardless of the amount of systemic neutrophils, endogenous PTX3 from neutrophils can increase transmigration through brain endothelium. This is in agreement with our findings 48 h but not 14 days after MCAo. It is worthy of mention that the amount of neutrophils infiltrated 48 h after MCAo was smaller than at later time points (< 12 cells/mm² at 48 h, > 20 cells/mm² at 6 or 14 days), and thus the impact of PTX3 in early neutrophil recruitment may not be as physiologically relevant as later on.

A second element to consider is the expression of adhesion molecules, which could partly account for differences in neutrophil recruitment. In fact, in peripheral blood vessels PTX3 reduces neutrophil recruitment by blocking the adhesive action of P-selectin (Deban *et al.*, 2010b). The adhesion molecule PECAM-1 was reduced in

PTX3 KO mice 14 days after MCAo (Chapter 4), which could account for reduced recruitment of neutrophils; however, we observed increased rather than reduced recruitment of neutrophils in PTX3 KO at this time. In addition, we did not see differences in the amount of ICAM-1 between genotypes at any time point (Chapter 5). These findings prompt us to discard the expression of adhesion molecules as a major cause of differences in neutrophil recruitment between genotypes.

Differences between the effects of PTX3 in the CNS and periphery may also be due to differences between the BBB and peripheral vasculature: the presence of TJs impeding paracellular infiltration, the different composition of the basal membrane and the presence of pericytes and astrocyte end-feet could alter the mechanisms of action of PTX3. Besides from the study of CNS vs. periphery differences, time-dependent differences also need further clarification. It is possible that time-dependent effects of PTX3 are related to concentration-dependent actions, which will be discussed in more detail in section 8.3.2 dealing with possible mechanisms of action.

PTX3 is a biomarker of vascular disease, it is highly produced by the heart (Polentarutti *et al.*, 2000) and can be produced by ECs (Breviario *et al.*, 1992). How PTX3 affects vascular function, however, is less clear, and one of our aims was to determine if PTX3 mediates BBB function after stroke. We examined CBF, BBB permeability, oedema and expression of adhesion molecules. As previously mentioned, no difference in CBF between genotypes was observed before or after reperfusion (Chapter 3), and no difference in density of activated (ICAM-1 or PECAM-1 positive) vasculature was found 48 h or 6 days after MCAo (Chapters 3 and 4), suggesting that vascular density and vascular activation are not strongly affected by the lack of PTX3 before or during the early stages of stroke. A decrease in the amount of PECAM-1 in PTX3 KO mice 14 days after MCAo could indicate lower vascular activation;

however, that sample also had less angiogenesis than its WT counterpart (Chapter 4). Therefore, it is likely that the decrease in PECAM-1 reflects a decrease in the amount of vasculature, but not a decrease in the activation of that vasculature.

On the other hand, lack of PTX3 increased BBB permeability 6 days after MCAo, when unresolved oedema was observed in PTX3 KO mice (Chapter 3). We did not find the mechanism by which PTX3 mediates permeability. Levels of the TJ occludin, the water channel AQP-4 and the protease MMP-9 were not altered by the lack of PTX3. PTX3 KO mice had more TJ ZO-1 (Chapter 3), which would correlate with lower but not higher permeability, opposite to our observations. It is worthy of consideration that if the assembly of the TJ was defective, the levels of protein expression would not make a difference in TJ functionality.

Regarding AQP-4, Ribeiro and colleagues showed that AQP-4 increase was more pronounced in astrocytes around the damaged area (Ribeiro *et al.*, 2006). We quantified overall levels of AQP-4 in the core, but not astrocytic expression of AQP-4; therefore, the possibility that increased oedema in PTX3 KO mice is partly due to astrocytic AQP-4 cannot be excluded. In addition, AQP-4 expression has one peak of expression 1 h after MCAo and another peak of expression 48 h after MCAo (Ribeiro *et al.*, 2006). It is possible that PTX3 affects transient alterations in AQP-4 at those times, but not 6 days after MCAo.

Differences in oedema were no longer present 14 days after MCAo, which implies that lack of PTX3 does not permanently impair oedema resolution, but only delays it. Since the exact mechanism by which lack of PTX3 impeded oedema resolution at 6 days reperfusion is not clear, theories about how that unknown defective mechanism is restored 14 days after MCAo would be too speculative and have therefore not been included here.

One remarkable effect of PTX3 deletion is the loss of integrity of the astrocytic scar 6 days after MCAo, demonstrated by the increased number of gaps in the astrocytic scar in PTX3 KO mice (Chapter 3), and the trend towards a thinner scar in that genotype (Figure 2 of the Additional supplementary information to Chapter 3). However, considering the results gathered from different time points and areas, the direct effect of PTX3 in astrocytic proliferation is not clear. In the core of the infarct we did not observe differences in the total number of astrocytes, intensity of GFAP staining or astrocytic proliferation (Additional supplementary information to Chapter 3 and Chapter 5). In the study of remote inflammation, we found that PTX3 KO had less astrocytes in both the ipsilateral and the contralateral SN, and the relative activation (the percentage of astrocytes in the ipsilateral compared to the contralateral side) was lower 48 h post-MCAo (Chapter 7). There is no characterised PTX3 receptor or ligand in astrocytes, and it is possible that the observed deficits in the glial scar are due to PTX3 being involved in activation or spatial distribution of astrocytes rather than their proliferation. Alterations in astrocytic behaviour could also be due to variations in ECM structure. HA is found in the brain after ischaemic damage (Lindwall *et al.*, 2013), and I α I has been found in brain (Spasova *et al.*, 2014). If TSG6 was found at the lesion site, it would be possible that a HA-HC-PTX3 matrix was formed after ischaemic stroke. HA can inhibit glial scar formation (Lin *et al.*, 2009) and HA degradation promotes astrocytic proliferation (Struve *et al.*, 2005). Lack of PTX3 could alter HA assembly and/degradation and thus alter scar formation.

Microglia proliferate more than macrophages after MCAo in the brain (Denes *et al.*, 2007). In addition, more resident microglia than recruited macrophages are found in the brain after MCAo (Schilling *et al.*, 2003). Therefore, it is likely that microglia rather than macrophages account for most Iba1-positive cells and thus the following

discussion will deal with Iba1-based results obtained through the chapters as results regarding microglia, which inherently include a certain level of infiltrated macrophages.

The general trend in our results, with some exceptions, is that PTX3 promotes microglial activation. We observed that lack of PTX3 impairs microglial proliferation in the ischaemic brain 6 days after MCAo (Chapter 3), but 48 h or 14 days after MCAo microglial density in the ischaemic area was similar in both genotypes (Chapter 5). It is worth mentioning that 14 days after MCAo microglial density was quite high, and cell bodies were found in such proximity that quantification was difficult. This and the small size of the sample used for quantification of Iba1 14 days after MCAo makes it difficult to discard a false negative result in that analysis. PTX3 has been reported to promote phagocytosis (Diniz *et al.*, 2004; Jeon *et al.*, 2010) which, like proliferation, is characteristic of activated microglia. In addition, low concentration of PTX3 promoted *in vitro* mixed glial proliferation (Chapter 3). Considering the fact that astrocytic proliferation was not altered at any time *in vivo*, it is possible that those *in vitro* changes in mixed glial cultures are mostly due to microglial proliferation rather than astrocytic proliferation. Supporting a role of PTX3 in microglial activation, we found that PTX3 KO mice had less microglial density than WT mice in the SN (Chapter 7). However, although PTX3 KO mice had reduced microglial density in the SN, they had a trend towards higher relative increase in the ipsilateral compared to the contralateral SN. This last observation would indicate that PTX3 KO microglia are more rather than less reactive. PTX3 could be acting in different ways in the core and the SN. Since we saw a concentration-dependent effect of PTX3 *in vitro* (where only the lowest PTX3 concentration induced proliferation (Chapter 3)), differences in PTX3 concentration as

well as differences in the composition of the microenvironment could account for the different actions of PTX3 between the core and the SN.

The interaction between microglial receptors and PTX3 has not been specifically studied, but microglia express FC γ Rs (Lunnon *et al.*, 2011; Shafer LL, 2002) and recombinant FC γ RIII is known to bind PTX3 (Lu *et al.*, 2008). Activation of microglial FC γ R has been linked to increased brain damage after cerebral ischaemia (Komine-Kobayashi *et al.*, 2004) and with increased neurodegeneration in a model of neurodegenerative disease (Lunnon *et al.*, 2011). It is possible that the effect of PTX3 in microglia after stroke is mediated through FC γ Rs. Another mechanism through which PTX3 could be regulating microglial activation is matrix formation. HA-HC-PTX3 matrix has been shown to polarise macrophages towards an M2 phenotype (He *et al.*, 2013; Zhang *et al.*, 2014). Testing whether this happens in the brain would provide information potentially useful not only for the field of cerebral ischaemia, but also for neurodegenerative diseases where microglial activation seems to play a key role (Glass *et al.*, 2010).

8.2.3 Angiogenesis and neurogenesis

We have seen that lack of PTX3 impairs angiogenesis in the post-ischaemic brain. PTX3 can be promoting angiogenesis through several factors. For instance, we have seen that lack of PTX3 alters BBB integrity (Chapter 3), astrocytic distribution (Chapter 3) and microglial activation (Chapters 3 and 5). All these factors have an impact on angiogenesis. A certain degree of BBB plasticity is required to remodel the existing vessels and allow the sprouting of new ones (Slevin *et al.*, 2006); astrocytes secrete part of the basement membrane and provide support for new vessels (Zhao & Rempe, 2010); and microglia can also secrete pro-angiogenic factors (Rymo *et al.*,

2011). Lower levels of VEGFR2, which mediates the angiogenic effects of VEGF (Beck & Plate, 2009), were observed in PTX3 KO mice, which also displayed less EC proliferation than WT mice 14 days after MCAo (Chapter 4). As discussed in Chapter 4, more research is needed to clarify how PTX3 contributes to VEGFR2 expression and if it modifies VEGF production. Altered VEGF production could alter microglial proliferation (Forstreuter *et al.*, 2002), which we have observed. Although we have seen an overall pro-angiogenic effect of PTX3 *in vivo* after MCAo, PTX3 can have an anti-angiogenic effect in some *in vitro* models, or in matrigel and bead implants *in vivo* (Leali *et al.*, 2012; Margheri *et al.*, 2010). PTX3 anti-angiogenic effect is mediated through its binding to the angiogenic factor FGF2, which can be reversed by TSG6-PTX3 interaction (Leali *et al.*, 2012). It is possible that a certain concentration of PTX3 is required for its anti-angiogenic potential, and that that concentration is not reached in the ischaemic site at the time when angiogenesis starts. Another possibility is that the affinity of PTX3 for other ligands is higher than the affinity of PTX3 for FGF2, and thus other actions of PTX3 (changes to the BBB, astrocytic distribution or microglial activation) have a stronger effect and indirectly promote angiogenesis. As we mentioned in Chapter 4, this seems to be the case in cardiac ischaemia, where WT mice had a better capillary growth in the reperfused area than PTX3 KO mice (Salio *et al.*, 2008), also supporting a pro-angiogenic role for PTX3 *in vivo*.

In agreement with the angiogenic action of PTX3, we also observed a neurogenic effect (Chapter 4). Angiogenesis and neurogenesis share common pathways, for instance, NSPCs migrate and differentiate along angiogenic niches (Ohab & Carmichael, 2008) and VEGFR2 mediates NSPC proliferation (Ara *et al.*, 2010). Although PTX3 KO mice had less VEGFR2 than WT mice, most of that staining was

vascular, and further experiments would be required to examine if PTX3 KO NSPCs also have less VEGFR2 than WT NSPCs.

NSPCs are of glial origin and can differentiate into astrocytes (Abrous *et al.*, 2005), but most nestin-positive cells after MCAo are phenotypically different from astrocytes (Kronenberg *et al.*, 2005). Therefore, the decrease in nestin-positive cells observed 6 days after MCAo in the hippocampus of PTX3 KO mice is likely to reflect a deficit in early stage NSPCs. Small sample size and difference in size between genotypes (WT, n=6; PTX3 KO, n=2-3) 14 days after MCAo highly limit the power of the analysis of nestin-positive cells at that time, and thus lack of differences between genotypes cannot be interpreted as a lack of effect of PTX3 with total certainty. PTX3 could be regulating neurogenesis through the complement system. The complement component C3 is required for post-MCAo neurogenesis (Rahpeymai *et al.*, 2006) and PTX3 can bind complement components which are upstream of C3, enhancing complement activation (Nauta *et al.*, 2003; Ma *et al.*, 2009; Gout *et al.*, 2011).

The study of later stages of NSPC differentiation was not possible since we could not quantify doublecortin-positive cells (migrating NSPCs) due to technical difficulties and we did not find any BrdU-NeuN-positive cells (differentiated neurones) 14 days after MCAo. *In vitro*, PTX3 induced NSPC proliferation and, interestingly, IL-1 was required for that neurogenic effect (Chapter 4). How IL-1 mediates PTX3 actions is still unknown. One possibility is that IL-1 alters the phenotype of NSPCs making them responsive to PTX3 (for example, expressing or activating a hypothetical PTX3 receptor in NSPCs), or inducing secretion of mediators that cooperate with PTX3 in promoting NSPC proliferation. The ability of IL-1 to induce NSPC proliferation and differentiation has already been shown (Molina-Holgado & Molina-Holgado, 2010), but there are no precedents in the study of the role of PTX3 in neurogenesis *in vitro* or

in vivo, and more complete analysis are required to understand how PTX3 acts upon NSPCs, and how NSPCs change in response to IL-1. Interestingly, ECM in neurogenic niches is important for NSPC proliferation and migration (Preston & Sherman, 2011; Lindwall *et al.*, 2013) and variations in HA-matrix structures could mediate stem cell differentiation into neurones or glia (Her *et al.*, 2013). PTX3 neurogenic effect could therefore be occurring through stabilisation of HA matrices.

8.2.4 Functional outcome

One of the major criticisms from stroke animal research is that drug candidates do not always have an impact on functional outcome, despite providing neuroprotection (Green *et al.*, 2003). We carried out several behavioural tests to determine whether the above mentioned changes in post-stroke pathophysiology (transient unresolved oedema and altered BBB integrity, alterations in neutrophil recruitment and glial responses, impaired angiogenesis and neurogenesis) had an impact in functional recovery after MCAo. Lack of PTX3 increased rotational bias, which reflect asymmetry in motor function (Modo *et al.*, 2000), but the rest of parameters analysed were not significantly different. Since no newborn mature neurones were found at the time of the behavioural tests (14 days after MCAo), neurogenesis cannot be the cause of differences in motor function. Reduced angiogenesis however, may partially affect the function of the pre-existing neurones, since angiogenesis has been linked to functional recovery (Krupinski *et al.*, 1994).

The rest of behavioural tests were similar in both genotypes. It is worthy saying that the behavioural tests we used can only detect major changes but not subtle differences. The degree of recovery after cerebral ischaemia in mice is very high; although there are obvious neurological deficits straight after MCAo, the extent of the impairments is

highly reduced after the first few days (Durukan & Tatlisumak, 2007), and improved methods may be required to detect further differences in behaviour. In addition, whilst the alterations in pathophysiology associated with lack of PTX3 did not affect most aspects of mouse behaviour 14 days after MCAo, we cannot discard that they could affect human recovery. It is possible that reinforcement of recovery mechanisms has a bigger impact in old age when plasticity is more limited (Oberman & Pascual-Leone, 2013; Todd *et al.*, 2010), than in young subjects who have higher plasticity.

8.2.5 Remote damage

With regards to the role of PTX3 in remote responses in the SN after striatal ischaemia, we have observed some alterations in gliosis and neuronal survival. Gliosis has previously been discussed in section 8.2.2. In the SNr, survival of NeuN-positive neurones 48 h after MCAo and TH-positive neurones 6 days after MCAo was significantly reduced (compared to 100%) in PTX3 KO mice but not in WT mice. The opposite was found in NeuN-positive neurones in the SNc 6 days after MCAo. However those reductions in neuronal survival (vs. 100%) were not statistically different between genotypes in any case, and therefore we cannot conclude that PTX3 is neuroprotective or neurotoxic in remote areas. Interestingly, recent research showed that newborn neurones can form striato-nigral connexions after stroke (Sun *et al.*, 2011). Since PTX3 seems to disrupt glial scar integrity, and the glial scar limits axonal growth (Kawano *et al.*, 2012) it is possible that PTX3 deletion helps restoring striato-nigral connexions. However, ablation of the glial scar has been shown to hinder BBB repair (Bush *et al.*, 1999), and thus the overall effect may not be beneficial. In addition, since PTX3 seems to promote NSPC proliferation, PTX3 deletion could hinder neurogenesis and thus hinder the formation of these new connexions. Further research

is required to clarify the long-term behavioural effects of remote neuronal death, and the role of PTX3 in it.

The most relevant finding related to remote inflammation and neurodegeneration is however, not related to the role of PTX3, but to the sequence of events that happen in the SN after striatal ischaemia. We found that loss of SP and inflammation occur in the SN before neurodegeneration starts, which opens the possibility that SP loss and/or inflammation contribute to delayed remote neurodegeneration. The causality of SP loss and/or inflammation in neurodegeneration in the SN however, still needs to be proved. As we discussed in Chapter 6, this could have important implications for prevention of remote neurodegeneration and perhaps delayed post-stroke motor deficits and appearance of PD symptoms.

8.3 Hypothesis about the mechanisms of action of PTX3

We have observed that certain effects of PTX3 seem to disappear over time, or even oppose the effects observed at previous time points. For instance, in the case of neutrophil infiltration, lack of PTX3 has opposite effects 48 h and 14 days after MCAo; increased oedema and BBB breakdown in PTX3 KO mice are transient; and some changes in the amount of microglia and astrocytes due to lack of PTX3 in the SN vary over time. Two possible hypotheses that could partially explain time-dependent actions of PTX3 are discussed.

8.3.1 Aggregation hypothesis

Monomeric PTX3 in plasma is associated to survival in patients with sepsis (Cuello *et al.*, 2014). PTX3 monomers, tetramers and octamers were found in plasma and peripheral organs of LPS-treated mice, but tetrameric and monomeric PTX3 were not

found in the brain in that mouse model (Cuello *et al.*, 2014). Jaillon and colleagues suggested that PTX3 is stored as a monomer in neutrophil granules and it assembles after being released (Jaillon *et al.*, 2007); however, their results regarding oligomerisation of PTX3 are based on western blots made under reducing conditions, which are not suitable for the study of multimers. It is unknown whether changes in PTX3 oligomerisation occur in the brain after stroke, and how those changes could affect the functions of PTX3. The short pentraxin CRP has different aggregation status which have different functions: monomeric CRP is pro-inflammatory whereas pentameric CRP has been reported to exert both pro- and anti-inflammatory actions (Eisenhardt *et al.*, 2009). Once CRP is in its monomeric form, it can be reduced and acquire higher pro-inflammatory activity (Wang *et al.*, 2011). Since the oligomeric status of PTX3 determines its binding to some ligands (as seen in section 1.2.4 of Chapter 1) variations in oligomerisation would alter PTX3 functions.

8.3.2 Concentration hypothesis

If PTX3 concentration changes over time, the different effects of PTX3 observed at different times may reflect the different effects of PTX3 at different concentrations. We observed a steep drop in PTX3 concentration from 24 h to 48 h after MCAo in the brain (Chapter 3) and, since PTX3 is an APP induced by IL-1 (Chapter 3), it is likely that its levels keep on decreasing beyond the acute phase when inflammation remits (and levels of IL-1 decrease). Low concentrations of PTX3 induced microglial proliferation *in vitro*, but when a higher concentration of PTX3 was added, the effect disappeared (Chapter 3). When PTX3 is less abundant it may only bind to the ligands for which it has more affinity, whilst when PTX3 is more abundant, it could also bind to other ligands and thus mediate other actions. However, we do not currently have

enough data to show variations of PTX3 concentration beyond 48 h post-stroke, or of the affinity of PTX3 for different ligands to further support this theory.

8.4 Limitations of the study

A careful interpretation of our results is required to understand to which extent we can relate our results in mice recovering from MCAo to what occurs in the brain of a human patient who has suffered a stroke. We performed our studies in mice, since the mouse brain is well characterised and mouse models of stroke have provided a solid background about cytokine expression, oedema, inflammatory cell activation, neurogenesis, etc (Jin *et al.*, 2010; Kahle *et al.*, 2009; Lambertsen *et al.*, 2012; Ohab & Carmichael, 2008). In addition, there is a high degree of conservation between murine and human PTX3 (described in Chapter 1), and PTX3 functions as an APP in both species, increasing sharply after injury, which does not happen for other pentraxins such as SAP, whose levels highly increase in rodents but not in humans in response to acute stimuli (Inforzato *et al.*, 2012). Furthermore, the availability of PTX3 KO mice facilitated the study of PTX3 functions. However, mice are likely to recover better than stroke patients. Mice have more plasticity than humans (Durukan & Tatlisumak, 2007) and young mice such as the ones we used are healthier than stroke patients, who often suffer comorbidities, i.e. additional conditions that are known to interact with stroke pathology, generally worsening stroke outcome (Smith *et al.*, 2013). However, the pathology of comorbidities that accompany stroke is not always well characterised and, given that this is the first study about PTX3 in the ischaemic brain, we required a homogenous and well characterised system to distinguish the effects of PTX3 deletion from possible confounding factors. Nevertheless, basic mechanisms of ischaemic injury are very similar across all mammals; therefore evolutionarily conserved proteins

such as PTX3 are expected to have similar effects on brain injury and recovery in both mouse and man.

The experimental model, transient MCAo, is one of the most used models of stroke, therefore it allows comparisons with studies carried out by other research groups (Durukan & Tatlisumak, 2007). Since it is a model of transient ischaemia it allows the study of reperfusion-induced damage (Aronowski *et al.*, 1997), and human cerebral ischaemia is generally transient rather than permanent and frequently occurs in areas supplied by the MCA (Durukan & Tatlisumak, 2007). The surgical protocol within our research group had been optimised so that shorter occlusion times always induced a smaller infarct size in a reproducible manner, followed by a proportional inflammatory response. Homogeneity in the surgical procedure is required to be able to compare experimental groups and to be able to attribute the observed differences to the inter-group difference (PTX3 deletion, in our case); however, the cohort of stroke patients is not homogenous, and thus it is possible that our results apply only to a subset of patients with a certain infarct size or stroke type.

Despite the aim to have an homogeneous sample, there are unavoidable differences between animals (despite all being from the same background and matched weight and age) and between surgeries (slight differences in duration of the procedure or complications such as small bleeds may arise in some surgeries but not in others), which translate into a certain degree of variability in infarct size which is unavoidable. This variability in initial infarct size largely accounts for the variability in the responses that follow the ischaemic event. To identify a given difference between groups, the higher the variability within an experimental group, the bigger the groups should be for that difference to be identified (i.e. to be significant). Given the limited availability of samples in certain groups and their variability, the statistical analysis

used would only be able to identify major differences and therefore type 2 errors (failure to identify a difference) may be present.

A final consideration is that statistical differences may not always have a physiological impact. For instance, 48 h after MCAo we observed a significant difference in the amount of leukocytes between genotypes (from 4 cells/mm² to 10 cells/mm²). However, even 10 cells/mm² is a relatively low density of leukocytes (compared to the other time points) and thus the statistically significant difference may not have a big repercussion physiologically.

8.5 Future work

Lack of PTX3 caused a plethora of alterations in the ischaemic brain. Detailed studies of the mechanisms by which PTX3 alters the pathways involved in each of the aspects of brain damage and repair that we have explored would be highly time-consuming. A possible starting point to identify which are the most relevant direct targets of PTX3 would be, first, to identify which cell types have receptors or domains that bind to PTX3 and, second, to determine the affinity of PTX3 for each of those receptors and for other soluble ligands that PTX3 can bind. Affinity studies could provide some indications about which are the dominating targets of PTX3, and this would also help prioritise some of the following future work above other.

One of our first observations was that PTX3 reduced neutrophil neurotoxicity, and lack of PTX3 increased neuronal death in oxidative stress conditions. It would be interesting to determine if PTX3 decreases oxidative stress and if that is how it protects neurones in this context. We also observed differences in the effect of PTX3 on neutrophil infiltration to the brain compared to the periphery. Studying the binding of PTX3 to components of the BBB which are not present in peripheral vessels may

indicate how PTX3 differently regulates leukocyte trafficking in the brain compared to the periphery.

The study of interactions between PTX3 and brain ECM components may provide further information about how PTX3 mediates glial scar integrity (since the ECM is an essential component of the glial scar) and angiogenesis (since ECM deposition and stabilisation is part of the BBB formation (Baeten & Akassoglou, 2011)). It would also be of great interest to analyse the effect of PTX3 in VEGF production. Differences in VEGF production could partially explain the differences seen in angiogenesis and neurogenesis, although the definite measurement to confirm the role of PTX3 in neurogenesis would be the quantification of BrdU-NeuN positive cells *in vivo* after MCAo. Since we did not observe BrdU-NeuN-positive cells 14 days post-MCAo, this analysis would have to be performed at later time points.

We previously discussed the possibility that PTX3 interacts with microglia through FC γ Rs. *In vitro* studies confirming this interaction and whether it affects the phenotype of microglia would be of great interest. Interestingly, brain-derived factors increase levels of FC γ Rs in BV2 microglial cells and alters their immune function (Shafer LL, 2002). Phenotypic characterisation of microglia would also be relevant for the study of remote damage. We observed that microglial activation preceded neurodegeneration, and microglial profiles were found surrounding neurones in the SN, but we did not prove the causality of microglial activation in delayed neuronal death. If those microglial cells showed a pro-inflammatory damaging phenotype (M1) at the times studied that would suggest that microglia are actually contributing to neurodegeneration and an anti-inflammatory therapeutic approach could be of use; on the other hand, if microglia had a protective phenotype (M2) from the early stages of the inflammatory response, we would not want to inhibit microglial activation. As seen

in section 8.2.2, HA-HC-PTX3 matrix can polarise macrophages towards a M2 phenotype (Zhang *et al.*, 2014; He *et al.*, 2013), supporting a beneficial role of PTX3 in resolution of inflammation.

More generally, evaluation of remote neurodegeneration after MCAo in subjects which have received an anti-inflammatory treatment could determine the causality of inflammation in neurodegeneration. Causality of SP loss in remote inflammation and/or neurodegeneration could be tested by blocking SP receptors in the SN (e.g. by stereotactic injection of anti-NK1R1 antibody in the SN). In terms of the consequences of remote neurodegeneration, behavioural and histological analysis would have to be made later after MCAo. Uchida and colleagues showed that neurodegeneration progresses up to 20 weeks after MCAo (Uchida *et al.*, 2010), but whether that affected motility, or how it would affect behaviour in combination with a PD model is not known. Evaluation of these outcomes in subjects treated with anti-inflammatory drugs after MCAo would also be of great interest.

Finally, the method of evaluation of behaviour should be refined. Balkaya and colleagues have recently validated a set of behavioural tests which can be used to detect functional deficits induced by MCAo in mice (Balkaya *et al.*, 2013). The study of the evolution of behaviour over different time points (baseline behaviour before surgery, after 48 h, after 1 week and at end point) may provide further information about the speed of recovery of each function, and whether PTX3 is involved in it. In the long term, the study of the effects of adding exogenous PTX3 after MCAo and the use of higher species with less plasticity and slower recovery could provide more accurate outcome measures.

8.6 Conclusions and implications

Our main aims were: first, to analyse the role of PTX3 in brain inflammation and repair after stroke and, second, to elucidate if inflammation precedes neurodegeneration in the SN after stroke and if PTX3 is involved in this.

Regarding the first aim, we have demonstrated that PTX3 is indeed involved in several aspects of brain inflammation and repair after stroke. PTX3 produced in the ipsilateral side in response to IL-1 mediates brain repair. Contrary to our expectations, PTX3 KO mice had similar infarct size, and lack of PTX3 decreased early neutrophil infiltration, but increased delayed neutrophil infiltration. Lack of PTX3 impaired glial scar integrity but did not affect overall astrocytic or vascular activation. PTX3 was transiently involved in oedema resolution and BBB integrity and also mediated angiogenesis and early stages of neurogenesis.

These results have several implications. Importantly, they show that APPs are not only important biomarkers, but are functional elements of the brain response to injury. Thus PTX3 has important functions in sterile injury in addition to its role in defence against infection. Despite the correlations between PTX3 levels and stroke mortality, PTX3 does not worsen but improves stroke outcome, mediating recovery processes that occur days to weeks after the ischaemic event. The fact that local IL-1 is such a potent inducer of PTX3 production raises the possibility that PTX3 expression is also increased in several other diseases where brain inflammation is also a key feature.

PTX3 emerges as a target for brain inflammatory diseases, but there are several steps to be taken towards a therapeutic approach targeting PTX3. A better understanding of time-dependent actions of PTX3 and how those changes are mediated would be crucial to choose a therapeutic window when PTX3 could have the desired effect. Unraveling

the mechanisms of action of PTX3 could also provide the necessary information to synthesise a PTX3-like molecule which could be active through time. Intervention studies evaluating the role of exogenous PTX3 in the brain, and studies in higher species with more accurate behavioural outcomes would also be essential for translation into the clinic.

Regarding the second aim, we have shown that remote inflammation precedes remote neurodegeneration in the SN after stroke and that PTX3 does not have a consistent effect in remote inflammation and neurodegeneration.

These results have important implications, since they open the possibility that remote inflammation has a causal role in remote neurodegeneration, and thus that early anti-inflammatory treatments may be neuroprotective. Maintenance of neurones in the SN is especially relevant in PD, but other areas such as the globus pallidus also undergo remote damage after striatal ischaemia and thus, neuroprotection would theoretically benefit the integrity of several parts of the circuit that regulates motility (shown in Figure 4 of Chapter 1). In clinical studies testing the efficacy of anti-inflammatory treatments in stroke, it would be of great interest to also evaluate remote neurodegeneration. Given that imaging of the whole brain is widely used in those clinical trials, images of the SN are already available, but generally not taken into account when evaluating brain damage. Long-term follow up of patients and correlations with incidence of PD would be of great clinical value.

In summary, we have shown that brain PTX3, induced by central inflammation, orchestrates several inflammatory and reparative processes after ischaemic stroke, generally having a beneficial effect. This highlights PTX3 as a target for stroke treatment and for other inflammatory brain diseases. In addition, we found that remote

inflammation precedes remote neurodegeneration after stroke, supporting a possible beneficial role of early anti-inflammatory approaches in long term stroke recovery.

Appendix 1

Materials

Reagent	Company
2DG	Sigma Aldrich, UK
Anti-biotin microbeads	Miltenyi Biotec, UK
B27 with/without antioxidants	Invitrogen, UK
BCA protein assay reagent	Thermo Scientific, UK
BrdU	Sigma Aldrich, UK
BSA	Sigma Aldrich, UK
Buprenorphine	Vetegesic, Alstoe Ltd, UK
CoCl ₂	Sigma Aldrich, UK
Collagen IV	VWR International, UK
Collagenase-dispase	Roche, UK
DAB	Sigma Aldrich, UK
DMEM	Sigma Aldrich, UK
DMSO	Sigma Aldrich, UK
DNase	Invitrogen, UK
dNTPs (for PCR)	Bioline, UK
Doccol filaments	Doccol, USA
DMEM	Sigma Aldrich, UK
Endothelial cell growth supplement	VWR International, UK
Ethylene glycol	Sigma Aldrich, UK
FCS	PAA Laboratories, UK
FUDR	Sigma Aldrich, UK
Glutamine	Sigma Aldrich, UK
Glycerol	Sigma Aldrich, UK
H ₂ O (for PCR)	Gibco, Life Technologies, UK
H ₂ O ₂	Sigma Aldrich, UK
H ₂ SO ₄	Fluka, UK
HCl	Sigma Aldrich, UK
Heparin	Sigma Aldrich, UK

IL-1RA	NIBSC, UK
IL-1 β	R&D Systems, UK
Isoflurane	Abbott, UK
KCl (for PCR)	Bioline, UK
LDH CytoTox-96 kit	Promega, USA
Lubrithal eye gel	Vetxx, UK
MgCl ₂ (for PCR)	Bioline, UK
NaCl (for PCR)	Bioline, UK
Neurobasal medium	Invitrogen, UK
NH ₄ (for PCR)	Bioline, UK
NMDA	Tocris Bioscience, UK
NP-40 (for PCR)	Bioline, UK
Nylon mesh	Plastoc Associates, UK
PBS	Sigma Aldrich, UK
Penicillin-streptomycin	Sigma Aldrich, UK
PFA (Paraformaldehyde)	Sigma Aldrich, UK
Plasma-derived horse serum	First Link Ltd. UK
Poly-D lysine	Sigma Aldrich, UK
Prolong Gold antifade with/without DAPI	Invitrogen, UK
Protease and phosphatase inhibitor cocktail	Calbiochem, Merk, Germany
Proteinase K	Sigma Aldrich, UK
PTX3 (recombinant protein)	R&D Systems, UK
PTX3 ELISA kit	R&D Systems, UK
Puromycin	R&D Systems, UK
Sample buffer (for DNA samples)	Bioline, UK
Sodium azide	Sigma Aldrich, UK
Sodium citrate	Sigma Aldrich, UK
SDS	Sigma Aldrich, UK
Streptavidin-HRP	R&D Systems, UK
Substrate solution	R&D Systems, UK
Taq Polymerase	Bioline, UK

Tosyllysine chloromethyl ketone	Sigma Aldrich, UK
Trypsin	Invitrogen, UK
Tween-20	Sigma Aldrich, UK

Table 1. Reagents.

Primary antibodies (anti-mouse)	Raised in	Dilution	Company
AQP-4	rabbit	1/200	Millipore, USA
BrdU	rat	1/500	AbD Serotec, UK
BrdU	sheep	1/500	Abcam, UK
CD206	rat	1/100	R&D Systems, UK
CD45	rat	1/250	AbD Serotec, UK
Collagen IV	rabbit	1/500	Abcam, UK
DCX	goat	1/750	Santa Cruz Biotechnology, USA
GFAP	chicken	1/1000	Abcam, UK
Iba1	rabbit	1/1000	Wako, Germany
ICAM-1	goat	1/250	R&D Systems, UK
IL-1 β	goat	1/100	R&D Systems, UK
Laminin α -4	goat	1/100	Santa Cruz Biotechnology, USA
Lectin	biotinylated	1/100	Sigma Aldrich, UK
Ly6G	Rat, biotinylated	1/5	Miltenyi Biotec, UK
MAP-2	goat	1/500	Santa Cruz Biotechnology, USA
MBP	rat	1/1000	Abcam, UK
MMP-9	goat	1/300	R&D Systems, UK
Nestin	mouse	1/500	Millipore, USA
NeuN	mouse	1/300	Millipore, USA
PECAM-1	rat	1/200	BDPharmingen
PTX3	rabbit	1/100	Santa Cruz Biotechnology, USA

PTX3 Mantovani	rabbit	1/500	Not commercial, provided by Prof. Mantovani, Humanitas Clinical and Research Center, Italy
SJC	rabbit	1/10000	Not commercial, provided by Dr. Daniel Anthony, University of Oxford, UK
SP	mouse	1/100	R&D Systems, UK
SP	rat	1/200	AbD Serotec, UK
TH	rabbit	1/2000	Abcam, UK
TH	sheep	1/500	Millipore, USA
VCAM	goat	1/250	R&D Systems, UK
VEGFR2	rabbit	1/300	Cell Signalling, USA
ZO-1	rabbit	1/250	Invitrogen, UK
α -SMA	mouse	1/500	Sigma Aldrich, UK

Table 2. Primary antibodies.

Secondary antibodies	Species	Dilution	Company
Alexa 488 or 594	Donkey anti-mouse	1/500	Invitrogen, UK
Alexa 488 or 594	Donkey anti-goat	1/500	Invitrogen, UK
Alexa 488 or 594	Donkey anti-rabbit	1/500	Invitrogen, UK
Alexa 488 or 594	Donkey anti-rat	1/500	Invitrogen, UK
Alexa 350	Streptavidin	1/300	Invitrogen, UK
Biotin	Horse anti-mouse	1/500	Vector, UK

Table 3. Secondary antibodies.

Equipment and software	Company
2020 PLUS tracking software	HVS Image, UK
24-well plates	Corning, UK
Bright field microscope	Leica, Germany

Coagulator	AESCU LAP, Germany
Coolsnap EZ camera	Photometrics, UK
ELISA 96-well plates	Nunc-immunoplate, maxisorp plates, Sigma Aldrich, USA
Hettich Mikro 200R centrifuge	Hettich, Germany
Laser Doppler	Moor instruments, UK
Magnetic MACS® LS column	Miltenyi Biotec, UK
MetaVue Software	Molecular devices, USA
Motic software	Motic, China
Moticam 2300 camera	Motic, China
Olympus CKX31 microscope	Olympus, Japan
Polycarbonate Transwell inserts	Corning, UK
Q-Image camera	QImaging, Canada
Sigma 2-16PK centrifuge	Sigma Laborzentrifugen, Germany
Sledge microtome	Bright, UK
Spectrophotometer-plate reader	Synergy HT, NorthStar Scientific Ltd., UK
Termic blanket	Harvard apparatus Ltd., UK

Table 4. Equipment and software.

Cell culture media	MBECs maintenance medium	DMEM/F12 with 10 % v/v plasma-derived horse serum (PDS), 10 % v/v foetal calf serum (FCS,) 1 % w/v penicillin-streptomycin (P/S), 1 % w/v glutamine, 100 µg/ml heparin and 100 µg/mL endothelial cell growth supplement
	Glial medium	DMEM with 10 % v/v foetal calf serum and 1% w/v penicillin/streptomycin.
	Neuronal change medium	Neurobasal medium with 5 % v/v plasma-derived serum, 1 % w/v penicillin/streptomycin, 1 % w/v glutamine and 2 % v/v B27 without antioxidants.
	Neuronal dissociation medium	Neuronal starve medium with 10 % w/v of trypsin and 417 U/ml DNase

	Neuronal seeding medium	Neurobasal medium with 5 % (v/v) plasma-derived serum, 1 % (w/v) penicillin/streptomycin, 1 % (w/v) glutamine and 2 % (v/v) B27 with antioxidants.
	Neuronal starve medium	DMEM supplemented with 1 % (w/v) penicillin/streptomycin
	Neutrophil buffer	0.1 % (w/v) BSA and 1 mM EDTA in 1x PBS filtered through a 0.22 µm filter.
Buffers	Cryoprotectant	30 % (v/v) ethylene glycol, 20 % (v/v) glycerol in 1x PBS
	ELISA buffers	Wash: 0.05 % (v/v) Tween-20 in 1x PBS
		Reagent diluent: 1 % (w/v) BSA in 1x BS
	Lysis buffer	For tissue: 50 mM Tris-HCl pH 7.5, 150 mM NaCl, 5 mM CaCl ₂ , 0.02 % (w/v) NaN ₃ , 1 % (v/v) Triton X-100 and 1x protease and phosphatase inhibitor cocktail (PIC).
		For cells: 50 mM Tris-HCl pH 7.5 with 1 % (v/v) Triton X-100 and 1x protease and phosphatase inhibitor cocktail (PIC).
	PCR lysis buffer	For earsnips: Tris HCl pH 8.5, 0.5 M EDTA pH 8, SDS 10% (v/v), 5 M NaCl, Proteinase K 10 mg/ml, H ₂ O.
		For embryos: 10 mM Tris pH 8.5, 50 mM KCl, 2 mM MgCl ₂ , 0.1 mg/ml gelatine, 0.45 (v/v) % NP-40, 0.45 % (v/v) Tween-20, 0.1 mg/ml proteinase K
	PCR master mix	H ₂ O, 10x NH ₄ , MgCl ₂ , dNTPs, primer Q17 (5' – AGCAATGCACCTCCCTGCGAT-3'), primer Q118 (5' – TCCTCGGTGGGATGAAGTCCA-3'), primer PGK (5' – CTGCTCTTTACTGAAGGCTC-3'), DMSO, Taq. PTX3 is recognised by Q117-Q118, and the mutation site by Q117-PGK
Primary diluent	20 mM sodium azide, 0.3 % (v/v) Triton-X in 1x PBS	

Table 5. Cell media and buffers.

References

Abbott NJ, Patabendige AAK, Dolman DEM, Yusof SR, Begley DJ (2010) Structure and function of the blood brain barrier. *Neurobiology of Disease* **37**: 13-25

Abrous DN, Koehl M, Le Moal M (2005) Adult neurogenesis: from precursors to network and physiology. *Physiol Rev* **85**: 523-569

Aktas O, Ullrich O, Infante-Duarte C, Nitsch R, Zipp F. (2007) Neuronal damage in brain inflammation. *Arch Neurol* **64**: 185-189.

Allan S, Pinteaux E (2003) The interleukin-1 system: an attractive and viable therapeutic target in neurodegenerative disease. *Current Drug Targets CNS and Neurological Disorders* **2**: 293-302

Allan SM, Rothwell NJ (2001) Cytokines and acute neurodegeneration. *Nat Rev Neurosci* **2**: 734-744

Allan SM, Tyrrell PJ, Rothwell NJ (2005) Interleukin-1 and neuronal injury. *Nat Rev Immunol* **5**: 629-640

Allen C, Thornton P, Denes A, McColl BW, Pierozynski A, Monestier M, Pinteaux E, Rothwell NJ, Allan SM (2012) Neutrophil cerebrovascular transmigration triggers rapid neurotoxicity through release of proteases associated with decondensed DNA. *The Journal of Immunology* **189**: 381-392

Andre R, Moggs JG, Kimber I, Rothwell NJ, Pinteaux E (2006) Gene regulation by IL-1 β independent of IL-1R1 in the mouse brain. *Glia* **53**: 477-483

Ara J, Fekete S, Zhu A, Frank M (2010) Characterization of neural stem/progenitor cells expressing VEGF and its receptors in the subventricular zone of newborn piglet brain. *Neurochem Res* **35**: 1455-1470

Arlicot N, Petit E, Katsifis A, Toutain J, Divoux D, Bodard S, Roussel S, Guilloteau D, Bernaudin M, Chalon S (2010) Detection and quantification of remote microglial activation in rodent models of focal ischaemia using the TSPO radioligand CLINDE. *European Journal of Nuclear Medicine and Molecular Imaging* **37**: 2371-2380

Aronowski J, Strong R, Grotta JC (1997) Reperfusion injury: demonstration of brain damage produced by reperfusion after transient focal ischemia in rats. *J Cereb Blood Flow Metab* **17**: 1048-1056

Baeten KM, Akassoglou K (2011) Extracellular matrix and matrix receptors in blood-brain barrier formation and stroke. *Dev Neurobiol* **71**: 1018-1039

- Balabanov R, Dore-Duffy P (1998) Role of the CNS microvascular pericyte in the blood-brain barrier. *J Neurosci Res* **53**: 637-644
- Baldini M, Maugeri N, Ramirez GA, Giacomassi C, Castiglioni A, Prieto-González S, Corbera-Bellalta M, Di Comite G, Papa I, Dell'Antonio G, Ammirati E, Cuccovillo I, Vecchio V, Mantovani A, Rovere-Querini P, Sabbadini MG, Cid MC, Manfredi AA (2011) Selective upregulation of the soluble pattern recognition receptor PTX3 and of VEGF in giant cell arteritis: Relevance for recent optic nerve ischemia. *Arthritis & Rheumatism* **64**: 854-865
- Balkaya M, Krober J, Gertz K, Peruzzaro S, Endres M (2013) Characterization of long-term functional outcome in a murine model of mild brain ischemia. *Journal of Neuroscience Methods* **213**: 179-187
- Banati RB, Gehrmann J, Schubert P, Kreutzberg GW (1993) Cytotoxicity of microglia. *Glia* **7**: 111-118
- Banz Y, Rieben R (2012) Role of complement and perspectives for intervention in ischemia-reperfusion damage. *Ann Med* **44**: 205-217
- Baranova NS, Inforzato A, Briggs DC, Tilakaratna V, Enghild JJ, Thakar D, Milner CM, Day AJ, Richter RP (2014) Incorporation of Pentraxin 3 into Hyaluronan Matrices is Tightly Regulated and Promotes Matrix Cross-Linking. *J Biol Chem* [Epub ahead of print]
- Bartels AL, Leenders KL (2007) Neuroinflammation in the pathophysiology of Parkinson's disease: Evidence from animal models to human in vivo studies with [11C]-PK11195 PET. *Movement Disorders* **22**: 1852-1856
- Bartels AL, Leenders KL (2009) Parkinson's disease: The syndrome, the pathogenesis and pathophysiology. *Cortex* **45**: 915-921
- Baruah P, Propato A, Dumitriu IE, Rovere-Querini P, Russo V, Fontana R, Accapezzato D, Peri G, Mantovani A, Barnaba V, Manfredi AA (2006) The pattern recognition receptor PTX3 is recruited at the synapse between dying and dendritic cells, and edits the cross-presentation of self, viral, and tumor antigens. *Blood* **107**: 151-158
- Basile A, Sica A, d'Aniello E, Breviario F, Garrido G, Castellano M, Mantovani A, Introna M (1997) Characterization of the promoter for the human long pentraxin PTX3. *The Journal of Biological Chemistry* **272**: 8172-8178
- Beck H, Plate KH (2009) Angiogenesis after cerebral ischemia. *Acta Neuropathol* **117**: 481-496
- Becker C, Jick SS, Meier CR (2010) Risk of stroke in patients with idiopathic Parkinson disease. *Parkinsonism & Related Disorders* **16**: 31-35

Block F, Dihné M, Loos M (2005) Inflammation in areas of remote changes following focal brain lesion. *Progress in Neurobiology* **75**: 342-365

Bolam JP, Smith Y (1990) The GABA and substance P input to dopaminergic neurones in the substantia nigra of the rat. *Brain Research* **529**: 57-78

Bonde C, Sarup A, Schousboe A, Gegelashvili G, Zimmer J, Norberg J (2003) Neurotoxic and neuroprotective effects of the glutamate transporter inhibitor DL-threo-beta-benzoyloxyaspartate (DL-TBOA) during physiological and ischemia-like conditions. *Neurochem Int* **43**: 371-380

Bonifati DM, Kishore U (2007) Role of complement in neurodegeneration and neuroinflammation. *Mol Immunol.* **44**: 999-1010

Bottazzi B, Doni A, Garlanda C, Mantovani A (2010) An integrated view of humoral innate immunity: pentraxins as a paradigm. *Annual Review of Immunology* **28**: 157-183

Bousser M-G (2012) Stroke prevention: an update. *Frontiers of Medicine* **6**: 22-34

Boutin H, LeFeuvre RA, Horai R, Asano M, Iwakura Y, Rothwell NJ (2001) Role of IL-1 alpha and IL-1 beta in ischemic brain damage. *The Journal of Neuroscience* **21**: 5528-5534

Breviario F, d'Aniello EM, Golay J, Peri G, Bottazzi B, Bairoch A, Saccone S, Marzella R, Predazzi V, Rocchi M (1992) Interleukin-1-inducible genes in endothelial cells. Cloning of a new gene related to C-reactive protein and serum amyloid P component. *The Journal of Biological Chemistry* **267**: 22190-22197

Buck BH, Liebeskind DS, Saver JL, Bang OY, Yun SW, Starkman S, Ali LK, Kim D, Villablanca JP, Salamon N, Razinia T, Ovbiagele B (2008) Early neutrophilia is associated with volume of ischemic tissue in acute stroke. *Stroke* **39**: 355-360

Bush TG, Puvanachandra N, Horner CH, Polito A, Ostensfeld T, Svendsen CN, Mucke L, Johnson MH, Sofroniew MV (1999) Leukocyte infiltration, neuronal degeneration, and neurite outgrowth after ablation of scar-forming, reactive astrocytes in adult transgenic mice. *Neuron* **23**: 297-308

Butovsky O, Talpalar AE, Ben-Yaakov K, Schwartz M (2005) Activation of microglia by aggregated beta-amyloid or lipopolysaccharide impairs MHC-II expression and renders them cytotoxic whereas IFN-gamma and IL-4 render them protective. *Molecular and Cellular Neuroscience* **29**: 381-393

Butovsky O, Ziv Y, Schwartz A, Landa G, Talpalar AE, Pluchino S, Martino G, Schwartz M (2006) Microglia activated by IL-4 or IFN-gamma differentially induce neurogenesis and oligodendrogenesis from adult stem/progenitor cells. *Molecular and Cellular Neuroscience* **31**: 149-160

Campanella M, Sciorati C, Tarozzo G, Beltramo M (2002) Flow cytometric analysis of inflammatory cells in ischemic rat brain. *Stroke* **33**: 586-592

Campos LS, Leone DP, Relvas JB, Brakebusch C, Fassler R, Suter U, French-Constant C. (2004) $\beta 1$ integrins activate a MAPK signalling pathway in neural stem cells that contributes to their maintenance. *Development* **131**: 3433-3444.

Ceciliani F, Giordano A, Spagnolo V (2002) The systemic reaction during inflammation: the acute-phase proteins. *Protein and Peptide Letters* **9**: 211-223

Chapman KZ, Dale VQ, Denes A, Bennett G, Rothwell NJ, Allan SM, McColl BW (2009) A rapid and transient peripheral inflammatory response precedes brain inflammation after experimental stroke. *J Cereb Blood Flow Metab* **29**: 1764-1768

Chen Y, Swanson RA (2003) Astrocytes and brain injury. *J Cereb Blood Flow Metab* **23**: 137-149

Cinamon G, Grabovsky V, Winter E, Franitza S, Feigelson S, Shamri R, Dwir O, Alon R (2001) Novel chemokine functions in lymphocyte migration through vascular endothelium under shear flow. *Journal of Leukocyte Biology* **69**: 860-866

Conover J, Notti R (2008) The neural stem cell niche. *Cell and Tissue Research* **331**: 211-224

Cuello F, Shankar-Hari M, Mayr U, Yin X, Marshall M, Suna G, Willeit P, Langley SR, Jayawardhana T, Zeller T, Terblanche M, Shah AM, Mayr M. (2014) Redox-state of pentraxin 3 as a novel biomarker for resolution of inflammation and survival in sepsis. *Mol Cell Proteomics*. [Epub ahead of print]

Cunningham C, Wilcockson DC, Campion S, Lunnon K, Perry VH (2005) Central and systemic endotoxin challenges exacerbate the local inflammatory response and increase neuronal death during chronic neurodegeneration. *The Journal of Neuroscience* **25**: 9275-9284

D'Angelo C, De Luca A, Zelante T, Bonifazi P, Moretti S, Giovannini G, Iannitti RG, Zagarella S, Bozza S, Campo S, Salvatori G, Romani L (2009) Exogenous pentraxin 3 restores antifungal resistance and restrains inflammation in murine chronic granulomatous disease. *The Journal of Immunology* **183**: 4609-4618

Dalkara T, Gursoy-Ozdemir Y, Yemisci M (2011) Brain microvascular pericytes in health and disease. *Acta Neuropathologica* **122**: 1-9

Deban L, Jaillon S, Garlanda C, Bottazzi B, Mantovani A (2010a) Pentraxins in innate immunity: lessons from PTX3. *Cell and Tissue Research* **343**: 1-13

Deban L, Russo RC, Sironi M, Moalli F, Scanziani M, Zambelli V, Cuccovillo I, Bastone A, Gobbi M, Valentino S, Doni A, Garlanda C, Danese S, Salvatori G, Sassano M, Evangelista V, Rossi B, Zenaro E, Constantin G, Laudanna C, Bottazzi B,

- Mantovani A (2010b) Regulation of leukocyte recruitment by the long pentraxin PTX3. *Nat Immunol* **11**: 328-334
- del Zoppo GJ, Milner R (2006) Integrin-matrix interactions in the cerebral microvasculature. *Arterioscler Thromb Vasc Biol* **26**: 1966-1975
- Denes A, Ferenczi S, Kovacs KJ (2011) Systemic inflammatory challenges compromise survival after experimental stroke via augmenting brain inflammation, blood-brain barrier damage and brain oedema independently of infarct size. *Journal of neuroinflammation* **8**: 164-176
- Denes A, Humphreys N, Lane TE, Grecis R, Rothwell N (2010a) Chronic systemic infection exacerbates ischemic brain damage via a CCL5 (regulated on activation, normal T-cell expressed and secreted)-mediated proinflammatory response in mice. *The Journal of Neuroscience* **30**: 10086-10095
- Denes A, Thornton P, Rothwell NJ, Allan SM (2010b) Inflammation and brain injury: Acute cerebral ischaemia, peripheral and central inflammation. *Brain, Behavior, and Immunity* **24**: 708-723
- Denes A, Vidyasagar R, Feng J, Narvainen J, McColl BW, Kauppinen RA, Allan SM (2007) Proliferating resident microglia after focal cerebral ischaemia in mice. *J Cereb Blood Flow Metab* **27**: 1941-1953
- Diamandis EP, Goodglick L, Planque C, Thornquist MD (2011) Pentraxin-3 is a novel biomarker of lung carcinoma. *Clinical Cancer Research* **17**: 2395-2399
- Dihné M, Block F (2001) Focal ischemia induces transient expression of IL-6 in the substantia nigra pars reticulata. *Brain Research* **889**: 165-173
- Diniz SN, Nomizo R, Cisalpino PS, Teixeira MM, Brown GD, Mantovani A, Gordon S, Reis LFL, Dias AAM (2004) PTX3 function as an opsonin for the dectin-1-dependent internalization of zymosan by macrophages. *Journal of Leukocyte Biology* **75**: 649-656
- Dole VS, Bergmeier W, Mitchell HA, Eichenberger SC, Wagner DD (2005) Activated platelets induce Weibel-Palade-body secretion and leukocyte rolling in vivo: role of P-selectin. *Blood* **106**: 2334-2339
- Doni A, Mantovani G, Porta C, Tuckermann J, Reichardt HM, Kleiman A, Sironi M, Rubino L, Pasqualini F, Nebuloni M, Signorini S, Peri G, Sica A, Beck-Peccoz P, Bottazzi B, Mantovani A (2008) Cell-specific Regulation of PTX3 by Glucocorticoid Hormones in Hematopoietic and Nonhematopoietic Cells. *The Journal of Biological Chemistry* **283**: 29983-29992
- Ducruet AF, Mocco J, Mack WJ, Coon AL, Marsh HC, Pinsky DJ, Hickman ZL, Kim GH, Connolly ES (2007) Pre-clinical evaluation of an sLe x-glycosylated complement inhibitory protein in a non-human primate model of reperfused stroke. *J Med Primatol* **36**: 375-380.

- Durukan A, Tatlisumak T (2007) Acute ischemic stroke: Overview of major experimental rodent models, pathophysiology, and therapy of focal cerebral ischemia. *Pharmacology Biochemistry and Behavior* **87**: 179-197
- Eisenhardt SU, Thiele JR, Bannasch H, Stark GB, Peter K (2009) C-reactive protein: how conformational changes influence inflammatory properties. *Cell Cycle* **8**: 3885-3892
- Elvington A, Atkinson C, Zhu H, Yu J, Takahashi K, Stahl GL, Kindy MS, Tomlinson S (2012) The alternative complement pathway propagates inflammation and injury in murine ischemic stroke. *J Immunol.* **189**: 4640-4647.
- Emsley HCA, Smith CJ, Georgiou RF, Vail A, Hopkins SJ, Rothwell NJ, Tyrrell PJ (2005) A randomised phase II study of interleukin-1 receptor antagonist in acute stroke patients. *Journal of neurology, neurosurgery and psychiatry* **76**: 1366-1372
- Forstreuter F, Lucius R, Mentlein R (2002) Vascular endothelial growth factor induces chemotaxis and proliferation of microglial cells. *J Neuroimmunol* **132**: 93-98
- Fukuda S, Fini CA, Mabuchi T, Koziol JA, Eggleston LL, Jr., del Zoppo GJ (2004) Focal cerebral ischemia induces active proteases that degrade microvascular matrix. *Stroke* **35**: 998-1004
- Garlanda C, Bottazzi B, Bastone A, Mantovani A (2005) Pentraxins at the crossroads between innate immunity, inflammation, matrix deposition, and female fertility. *Annual Review of Immunology* **23**: 337-366
- Garlanda C, Hirsch E, Bozza S, Salustri A, De Acetis M, Nota R, Maccagno A, Riva F, Bottazzi B, Peri G, Doni A, Vago L, Botto M, De Santis R, Carminati P, Siracusa G, Altruda F, Vecchi A, Romani L, Mantovani A (2002) Non-redundant role of the long pentraxin PTX3 in anti-fungal innate immune response. *Nature* **420**: 182-186
- Garlanda C, Maina V, Cotena A, Moalli F (2009) The soluble pattern recognition receptor pentraxin-3 in innate immunity, inflammation and fertility. *Journal of Reproductive Immunology* **83**: 128-133
- Girard S, Brough D, Lopez-Castejon G, Giles J, Rothwell NJ, Allan SM (2013) Microglia and macrophages differentially modulate cell death after brain injury caused by oxygen-glucose deprivation in organotypic brain slices. *Glia* **61**: 813-824
- Glass CK, Saijo K, Winner B, Marchetto MC, Gage FH (2010) Mechanisms Underlying Inflammation in Neurodegeneration. *Cell* **140**: 918-934
- Gout E, Moriscot C, Doni A, Dumestre-Perard C, Lacroix M, Perard J, Schoehn G, Mantovani A, Arlaud GJ, Thielens NM (2011) M-ficolin interacts with the long pentraxin PTX3: a novel case of cross-talk between soluble pattern-recognition molecules. *The Journal of Immunology* **186**: 5815-5822

Green AR, Odergren T, Ashwood T (2003) Animal models of stroke: do they have value for discovering neuroprotective agents? *Trends Pharmacol Sci* **24**: 402-408

Griffiths MR, Neal JW, Fontaine M, Das T, Gasque P (2009) Complement factor H, a marker of self protects against experimental autoimmune encephalomyelitis. *J Immunol* **182**: 4368-4377

Grossmann J (2002) Molecular mechanisms of "detachment-induced apoptosis--Anoikis". *Apoptosis* **7**: 247-260

Gupta R, Connolly ES, Mayer S, Elkind MS (2004) Hemispherectomy for massive middle cerebral artery territory infarction: a systematic review. *Stroke* **35**: 539-543

Hajos M, Greenfield SA (1994) Synaptic connections between pars compacta and pars reticulata neurones: electrophysiological evidence for functional modules within the substantia nigra. *Brain Research* **660**: 216-224

Hayashi T, Noshita N, Sugawara T, Chan PH (2003) Temporal profile of angiogenesis and expression of related genes in the brain after ischemia. *J Cereb Blood Flow Metab* **23**: 166-180

He H, Zhang S, Tighe S, Son J, Tseng SC. (2013) Immobilized heavy chain-hyaluronic acid polarizes lipopolysaccharide-activated macrophages toward M2 phenotype. *J Biol Chem* **288**: 25792-25803.

Her GJ, Wu HC, Chen MH, Chen MY, Chang SC, Wang TW (2013) Control of three-dimensional substrate stiffness to manipulate mesenchymal stem cell fate toward neuronal or glial lineages. *Acta Biomater* **9**: 5170-5180

Hicklin DJ, Ellis LM (2005) Role of the vascular endothelial growth factor pathway in tumor growth and angiogenesis. *J Clin Oncol* **23**: 1011-1027

Hineno A, Kaneko K, Yoshida K, Ikeda S (2011) Ceruloplasmin protects against rotenone-induced oxidative stress and neurotoxicity. *Neurochem Res* **36**: 2127-2135

Hosomi N, Ban CR, Naya T, Takahashi T, Guo P, Song XY, Kohno M (2005) Tumor necrosis factor-alpha neutralization reduced cerebral edema through inhibition of matrix metalloproteinase production after transient focal cerebral ischemia. *J Cereb Blood Flow Metab* **25**: 959-967

Hossmann K-A (2006) Pathophysiology and therapy of experimental stroke. *Cellular and Molecular Neurobiology* **26**: 1055-1081

Huang J, Kim LJ, Mealey R, Marsh HC Jr, Zhang Y, Tenner AJ, Connolly ES Jr, Pinsky DJ (1999) Neuronal protection in stroke by an sLex-glycosylated complement inhibitory protein. *Science* **285**: 595-599

Hughes RN (2004) The value of spontaneous alternation behavior (SAB) as a test of retention in pharmacological investigations of memory. *Neurosci Biobehav Rev* **28**: 497-505

Hunter AJ, Hatcher J, Virley D, Nelson P, Irving E, Hadingham SJ, Parsons AA (2000) Functional assessments in mice and rats after focal stroke. *Neuropharmacology* **39**: 806-816

Hynes RO (2002) Integrins: bidirectional, allosteric signaling machines. *Cell* **110**: 673-687

Iadecola C, Anrather J (2011) The immunology of stroke: from mechanisms to translation. *Nat Med* **17**: 796-808

Ievoli E, Lindstedt R, Inforzato A, Camaioni A, Palone F, Day AJ, Mantovani A, Salvatori G, Salustri A (2011) Implication of the oligomeric state of the N-terminal PTX3 domain in cumulus matrix assembly. *Matrix Biology* **30**: 330-337

Inforzato A, Baldock C, Jowitt TA, Holmes DF, Lindstedt R, Marcellini M, Riviuccio V, Briggs DC, Kadler KE, Verdoliva A, Bottazzi B, Mantovani A, Salvatori G, Day AJ (2010) The angiogenic inhibitor long pentraxin PTX3 forms an asymmetric octamer with two binding sites for FGF2. *Journal of Biological Chemistry* **285**: 17681-17692

Inforzato A, Bottazzi B, Garlanda C, Valentino S, Mantovani A, Lambris JD, Hajishengallis G (2012) Pentraxins in humoral innate immunity. *Current Topics in Innate Immunity II*. **946**: 1-20

Inforzato A, Peri G, Doni A, Garlanda C, Mantovani A, Bastone A, Carpentieri A, Amoresano A, Pucci P, Roos A, Daha MR, Vincenti S, Gallo G, Carminati P, De Santis R, Salvatori G (2006) Structure and function of the long pentraxin PTX3 glycosidic moiety: fine-tuning of the interaction with C1q and complement activation. *Biochemistry* **45**: 11540-11551

Inforzato A, Riviuccio V, Morreale AP, Bastone A, Salustri A, Scarchilli L, Verdoliva A, Vincenti S, Gallo G, Chiapparino C, Pacello L, Nucera E, Serlupi-Crescenzi O, Day AJ, Bottazzi B, Mantovani A, De Santis R, Salvatori G (2008) Structural characterization of PTX3 disulfide bond network and its multimeric status in cumulus matrix organization. *The Journal of Biological Chemistry* **283**: 10147-10161

Israeli D, Tanne D, Daniels D, Last D, Shneor R, Guez D, Landau E, Roth Y, Ocherashvili A, Bakon M, Hoffman C, Weinberg A, Volk T, Mardor Y (2010) The application of MRI for depiction of subtle blood brain barrier disruption in stroke. *Int J Biol Sci* **7**: 1-8

Jaillon S, Peri G, Delneste Y, Fremaux I, Doni A, Moalli F, Garlanda C, Romani L, Gascan H, Bellocchio S, Bozza S, Cassatella MA, Jeannin P, Mantovani A (2007) The humoral pattern recognition receptor PTX3 is stored in neutrophil granules and localizes in extracellular traps. *The Journal of Experimental Medicine* **204**: 793-804

- Jenny NS, Arnold AM, Kuller LH, Tracy RP, Psaty BM (2009) Associations of pentraxin 3 with cardiovascular disease and all-cause death: the cardiovascular health study. *Arteriosclerosis, Thrombosis, and Vascular Biology* **29**: 594-599
- Jeon H, Lee S, Lee W-H, Suk K (2010) Analysis of glial secretome: the long pentraxin PTX3 modulates phagocytic activity of microglia. *Journal of Neuroimmunology* **229**: 63-72
- Jiao H, Wang Z, Liu Y, Wang P, Xue Y (2011) Specific role of tight junction proteins claudin-5, occludin, and ZO-1 of the blood-brain barrier in a focal cerebral ischemic insult. *Journal of Molecular Neuroscience* **44**: 130-139
- Jin K, Zhu Y, Sun Y, Mao XO, Xie L, Greenberg DA (2002) Vascular endothelial growth factor (VEGF) stimulates neurogenesis in vitro and in vivo. *Proc Natl Acad Sci U S A* **99**: 11946-11950
- Jin R, Yang G, Li G (2010) Inflammatory mechanisms in ischemic stroke: role of inflammatory cells. *Journal of Leukocyte Biology* **87**: 779-789
- Joshi A, Perin DP, Gehle A, Nsiah-Kumi PA (2013) Feasibility of using C-reactive protein for point-of-care testing. *Technol Health Care* **21**: 233-240
- Juttler E, Bonmann E, Spranger M, Kolb-Bachofen V, Suschek CV (2007) A novel role of interleukin-1-converting enzyme in cytokine-mediated inducible nitric oxide synthase gene expression: Implications for neuroinflammatory diseases. *Mol Cell Neurosci* **34**: 612-620
- Kaess BM, Vasan RS (2011) Heart failure: Pentraxin 3-a marker of diastolic dysfunction and HF? *Nat Rev Cardiol* **8**: 246-248
- Kahle KT, Simard JM, Staley KJ, Nahed BV, Jones PS, Sun D (2009) Molecular mechanisms of ischemic cerebral edema: role of electroneutral ion transport. *Physiology* **24**: 257-265
- Kawano H, Kimura-Kuroda J, Komuta Y, Yoshioka N, Li H, Kawamura K, Li Y, Raisman G (2012) Role of the lesion scar in the response to damage and repair of the central nervous system. *Cell and Tissue Research* **349**: 169-180
- Kigerl KA, Gensel JC, Ankeny DP, Alexander JK, Donnelly DJ, Popovich PG (2009) Identification of two distinct macrophage subsets with divergent effects causing either neurotoxicity or regeneration in the injured mouse spinal cord. *The Journal of Neuroscience* **29**: 13435-13444
- Klouche M, Peri G, Knabbe C, Eckstein H-H, Schmid F-X, Schmitz G, Mantovani A (2004) Modified atherogenic lipoproteins induce expression of pentraxin-3 by human vascular smooth muscle cells. *Atherosclerosis* **175**: 221-228

- Kokuzawa J, Yoshimura S, Kitajima H, Shinoda J, Kaku Y, Iwama T, Morishita R, Shimazaki T, Okano H, Kunisada T, Sakai N (2003) Hepatocyte growth factor promotes proliferation and neuronal differentiation of neural stem cells from mouse embryos. *Molecular and Cellular Neuroscience* **24**: 190-197
- Komine-Kobayashi M, Chou N, Mochizuki H, Nakao A, Mizuno Y, Urabe T (2004) Dual role of Fcγ receptor in transient focal cerebral ischemia in mice. *Stroke* **35**: 958-963
- Kopell BH, Rezaei AR, Chang JW, Vitek JL (2006) Anatomy and physiology of the basal ganglia: Implications for deep brain stimulation for Parkinson's disease. *Movement Disorders* **21**: S238-S246
- Kreitzer AC, Malenka RC (2008) Striatal plasticity and basal ganglia circuit function. *Neuron* **60**: 543-554
- Kronenberg G, Wang LP, Synowitz M, Gertz K, Katchanov J, Glass R, Harms C, Kempermann G, Kettenmann H, Endres M (2005) Nestin-expressing cells divide and adopt a complex electrophysiologic phenotype after transient brain ischemia. *J Cereb Blood Flow Metab* **25**: 1613-1624
- Krupinski J, Kaluza J, Kumar P, Kumar S, Wang JM (1994) Role of angiogenesis in patients with cerebral ischemic stroke. *Stroke* **25**: 1794-1798
- Lambertsen KL, Biber K, Finsen B (2012) Inflammatory cytokines in experimental and human stroke. *J Cereb Blood Flow Metab* **32**: 1677-1698
- Latini R, Maggioni AP, Peri G, Gonzini L, Lucci D, Mocarelli P, Vago L, Pasqualini F, Signorini S, Soldateschi D, Tarli L, Schweiger C, Fresco C, Cecere R, Tognoni G, Mantovani A, on behalf of the Lipid Assessment Trial Italian Network I (2004) Prognostic significance of the long pentraxin PTX3 in acute myocardial infarction. *Circulation* **110**: 2349-2354
- Leali D, Inforzato A, Ronca R, Bianchi R, Belleri M, Coltrini D, Di Salle E, Sironi M, Norata GD, Bottazzi B, Garlanda C, Day AJ, Presta M (2012) Long pentraxin 3/tumor necrosis factor-stimulated gene-6 interaction. *Arteriosclerosis, Thrombosis, and Vascular Biology* **32**: 696-703
- Lee J-K, Tran T, Tansey M (2009) Neuroinflammation in Parkinson's Disease. *Journal of Neuroimmune Pharmacology* **4**: 419-429
- Lee MY, Ju WK, Cha JH, Son BC, Chun MH, Kang JK, Park CK (1999) Expression of vascular endothelial growth factor mRNA following transient forebrain ischemia in rats. *Neurosci Lett* **265**: 107-110
- Lee TH, Lee GW, Ziff EB, Vilcek J (1990) Isolation and characterization of eight tumor necrosis factor-induced gene sequences from human fibroblasts. *Mol Cell Biol* **10**: 1982-1988

- Ley K, Laudanna C, Cybulsky MI, Nourshargh S (2007) Getting to the site of inflammation: the leukocyte adhesion cascade updated. *Nat Rev Immunol* **7**: 678-689
- Li L, Harms KM, Ventura PB, Lagace DC, Eisch AJ, Cunningham LA (2010) Focal cerebral ischemia induces a multilineage cytogenic response from adult subventricular zone that is predominantly gliogenic. *Glia* **58**: 1610-1619
- Lin B, Levy S, Raval AP, Perez-Pinzon MA, DeFazio RA (2010) Forebrain ischemia triggers GABAergic system degeneration in substantia nigra at chronic stages in rats. *Cardiovascular Psychiatry and Neurology* **2010**: 1-16
- Lin CM, Lin JW, Chen YC, Shen HH, Wei L, Yeh YS, Chiang YH, Shih R, Chiu PL, Hung KS, Yang LY, Chiu WT. (2009) Hyaluronic acid inhibits the glial scar formation after brain damage with tissue loss in rats. *Surg Neurol* **72: suppl 2**: 50-44.
- Lindfors N, Brodin E, Tossman U, Segovia J, Ungerstedt U (1989) Tissue levels and in vivo release of tachykinins and GABA in striatum and substantia nigra of rat brain after unilateral striatal dopamine denervation. *Experimental Brain Research* **74**: 527-534
- Lindwall C, Olsson M, Osman AM, Kuhn HG, Curtis MA (2013) Selective expression of hyaluronan and receptor for hyaluronan mediated motility (Rhamm) in the adult mouse subventricular zone and rostral migratory stream and in ischemic cortex. *Brain Res.* **1503**: 62-77
- Lipton P (1999) Ischemic Cell Death in Brain Neurons. *Physiological Reviews* **79**: 1431-1568
- Liu F, Schafer DP, McCullough LD (2009) TTC, Fluoro-Jade B and NeuN staining confirm evolving phases of infarction induced by middle cerebral artery occlusion. *Journal of Neuroscience Methods* **179**: 1-8
- Lo Giudice P, Campo S, Verdoliva A, Rivieccio V, Borsini F, De Santis R, Salvatori G (2010) Efficacy of PTX3 in a rat model of invasive aspergillosis. *Antimicrobial Agents and Chemotherapy* **54**: 4513-4515
- Loddick SA, Rothwell NJ (1996) Neuroprotective effects of human recombinant interleukin-1 receptor antagonist in focal cerebral ischaemia in the rat. *J Cereb Blood Flow Metab* **16**: 932-940
- Loos M, Dihné M, Block F (2003) Tumor necrosis factor-[alpha] expression in areas of remote degeneration following middle cerebral artery occlusion of the rat. *Neuroscience* **122**: 373-380
- Love S (1999) Oxidative Stress in Brain Ischemia. *Brain Pathology* **9**: 119-131
- Lu J, Marnell LL, Marjon KD, Mold C, Du Clos TW, Sun PD (2008) Structural recognition and functional activation of FcgammaR by innate pentraxins. *Nature* **456**: 989-992

- Lunnon K, Teeling JL, Tutt AL, Cragg MS, Glennie MJ, Perry VH (2011) Systemic inflammation modulates Fc receptor expression on microglia during chronic neurodegeneration. *The Journal of Immunology* **186**: 7215-7224
- Ma SY, Rinne JO, Collan Y, Roytta M, Rinne UK (1996) A quantitative morphometrical study of neuron degeneration in the substantia nigra in Parkinson's disease. *Journal of the Neurological Sciences* **140**: 40-45
- Ma YJ, Doni A, Hummelshoj T, Honore C, Bastone A, Mantovani A, Thielens NM, Garred P (2009) Synergy between ficolin-2 and pentraxin 3 boosts innate immune recognition and complement deposition. *Journal of Biological Chemistry* **284**: 28263-28275
- Manfredi AA, Rovere-Querini P, Bottazzi B, Garlanda C, Mantovani A (2008) Pentraxins, humoral innate immunity and tissue injury. *Current Opinion in Immunology* **20**: 538-544
- Mantovani A, Garlanda C, Bottazzi B, Peri G, Doni A, Martinez de la Torre Y, Latini R (2006) The long pentraxin PTX3 in vascular pathology. *Vascular Pharmacology* **45**: 326-330
- Margheri F, Serrati S, Lapucci A, Chillà A, Bazzichi L, Bombardieri S, Kahaleh B, Calorini L, Bianchini F, Fibbi G, Del Rosso M (2010) Modulation of the angiogenic phenotype of normal and systemic sclerosis endothelial cells by gain-loss of function of pentraxin 3 and matrix metalloproteinase 12. *Arthritis & Rheumatism* **62**: 2488-2498
- Marti HH, Risau W (1998) Systemic hypoxia changes the organ-specific distribution of vascular endothelial growth factor and its receptors. *Proc Natl Acad Sci U S A* **95**: 15809-15814
- Marti HJ, Bernaudin M, Bellail A, Schoch H, Euler M, Petit E, Risau W (2000) Hypoxia-induced vascular endothelial growth factor expression precedes. *Am J Pathol* **156**: 965-976
- Martinez de la Torre Y, Fabbri M, Jaillon S, Bastone A, Nebuloni M, Vecchi A, Mantovani A, Garlanda C (2010) Evolution of the pentraxin family: the new entry PTX4. *The Journal of Immunology* **184**: 5055-5064
- Mathiisen TM, Lehre KP, Danbolt NC, Ottersen OP (2010) The perivascular astroglial sheath provides a complete covering of the brain microvessels: an electron microscopic 3D reconstruction. *Glia* **58**: 1094-1103
- Matsubara J, Sugiyama S, Nozaki T, Sugamura K, Konishi M, Ohba K, Matsuzawa Y, Akiyama E, Yamamoto E, Sakamoto K, Nagayoshi Y, Kaikita K, Sumida H, Kim-Mitsuyama S, Ogawa H (2011) Pentraxin 3 is a new inflammatory marker correlated with left ventricular diastolic dysfunction and heart failure with normal ejection fraction. *Journal of the American College of Cardiology* **57**: 861-869

- Mauborgne A, Javoy-Agid F, LeGrand JC, Agid Y, Cesselin F (1983) Decrease of substance P-like immunoreactivity in the substantia nigra and pallidum of parkinsonian brains. *Brain Research* **268**: 167-170
- Maugeri N, Rovere-Querini P, Slavich M, Coppi G, Doni A, Bottazzi B, Garlanda C, Cianflone D, Maseri A, Mantovani A, Manfredi AA (2011) Early and transient release of leukocyte pentraxin 3 during acute myocardial infarction. *The Journal of Immunology* **187**: 970-979
- McArthur KS, Quinn TJ, Dawson J, Walters MR (2011) Diagnosis and management of transient ischaemic attack and ischaemic stroke in the acute phase. *British Medical Journal* **342**: 1-12
- McColl BW, Rothwell NJ, Allan SM (2007) Systemic inflammatory stimulus potentiates the acute phase and CXC chemokine responses to experimental stroke and exacerbates brain damage via interleukin-1- and neutrophil-dependent mechanisms. *The Journal of Neuroscience* **27**: 4403-4412
- McEver RP (2010) Rolling back neutrophil adhesion. *Nat Immunol* **11**: 282-284
- McGeer PL, McGeer EG (2004) Inflammation and neurodegeneration in Parkinson's disease. *Parkinsonism & Related Disorders*. **10, suppl 1**: 3-7
- McMahon S, Grondin F, McDonald PP, Richard DE, Dubois CM (2005) Hypoxia-enhanced expression of the proprotein convertase furin is mediated by hypoxia-inducible factor-1: impact on the bioactivation of proproteins. *J Biol Chem* **280**: 6561-6569
- McNaull BBA, Todd S, McGuinness B, Passmore AP (2010) Inflammation and Anti-Inflammatory Strategies for Alzheimers Disease. A Mini-Review. *Gerontology* **56**: 3-14
- Medzhitov R (2010) Inflammation 2010: New adventures of an old flame. *Cell* **140**: 771-776
- Minami M, Satoh M (2003) Chemokines and their receptors in the brain: pathophysiological roles in ischemic brain injury. *Life Sci* **74**: 321-327
- Mocco J, Mack WJ, Ducruet AF, King RG, Sughrue ME, Coon AL, Sosunov SA, Sciacca RR, Zhang Y, Marsh HC Jr, Pinsky DJ, Connolly ES (2006) Preclinical evaluation of the neuroprotective effect of soluble complement receptor type 1 in a nonhuman primate model of reperfused stroke. *J Neurosurg* **105**: 595-601.
- Modo M, Stroemer RP, Tang E, Veizovic T, Sowniski P, Hodges H (2000) Neurological sequelae and long-term behavioural assessment of rats with transient middle cerebral artery occlusion. *J Neurosci Methods* **104**: 99-109

- Molina-Holgado E, Molina-Holgado F (2010) Mending the broken brain: neuroimmune interactions in neurogenesis. *Journal of Neurochemistry* **114**: 1277-1290
- Moroz E, Carlin S, Dyomina K, Burke S, Thaler HT, Blasberg R, Serganova I (2009) Real-time imaging of HIF-1 α stabilization and degradation. *PLoS ONE* **4**: e5077
- Moskowitz MA, Lo EH, Iadecola C (2010) The Science of stroke: mechanisms in search of treatments. *Neuron* **67**: 181-198
- Nagasawa H, Kogure K (1990) Exo-focal postischemic neuronal death in the rat brain. *Brain Research* **524**: 196-202
- Nakajima M, Hirano T, Terasaki T, Uchino M (2010) Signal change of the substantia nigra on diffusion-weighted imaging following striatal infarction. *Internal Medicine* **49**: 65-68
- Nakane M, Teraoka A, Asato R, Tamura A (1992) Degeneration of the ipsilateral substantia nigra following cerebral infarction in the striatum. *Stroke* **23**: 328-332
- Napoleone E, Di Santo A, Bastone A, Peri G, Mantovani A, de Gaetano G, Donati MB, Lorenzet R (2002) Long pentraxin PTX3 upregulates tissue factor expression in human endothelial cells: a novel link between vascular inflammation and clotting activation. *Arteriosclerosis, Thrombosis, and Vascular Biology* **22**: 782-787
- Napoleone E, Di Santo A, Peri G, Mantovani A, de Gaetano G, Donati MB, Lorenzet R (2004) The long pentraxin PTX3 up-regulates tissue factor in activated monocytes: another link between inflammation and clotting activation. *Journal of Leukocyte Biology* **76**: 203-209
- Nathan C, Ding A (2010) Nonresolving inflammation. *Cell* **140**: 871-882
- Nauta A, Bottazzi B, Mantovani A, Salvatori G, Kishore U, Schwaeble W, Gingras A, Tzima S, Vivanco F, Egido J, Tijssma O, Hack E, Daha M, Roos A (2003) Biochemical and functional characterization of the interaction between pentraxin 3 and C1q. *European Journal of Immunology* **33**: 465-473
- Nguyen L, Rothwell NJ, Pinteaux E, Boutin H (2011) Contribution of interleukin-1 receptor accessory protein b to interleukin-1 actions in neuronal cells. *Neurosignals* **19**: 222-230
- Norata GD, Marchesi P, Pulakazhi Venu VK, Pasqualini F, Anselmo A, Moalli F, Pizzitola I, Garlanda C, Mantovani A, Catapano AL (2009) Deficiency of the long pentraxin PTX3 promotes vascular inflammation and atherosclerosis. *Circulation* **120**: 699-708
- O'Connor TM, O'Connell J, O'Brien DI, Goode T, Bredin CP, Shanahan F (2004) The role of substance P in inflammatory disease. *Journal of Cellular Physiology* **201**: 167-180

- O'Neill LA, Greene C (1998) Signal transduction pathways activated by the IL-1 receptor family: ancient signaling machinery in mammals, insects, and plants. *J Leukoc Biol* **63**: 650-657
- Oberman L, Pascual-Leone A (2013) Changes in plasticity across the lifespan: cause of disease and target for intervention. *Prog Brain Res* **207**: 91-120
- Obrenovitch TP (1995) The ischaemic penumbra: twenty years on. *Cerebrovasc Brain Metab Rev* **7**: 297-323
- Ogawa T, Okudera T, Inugami A, Noguchi K, Kado H, Yoshida Y, Uemura K (1997) Degeneration of the ipsilateral substantia nigra after striatal infarction: evaluation with MR imaging. *Radiology* **204**: 847-851
- Ohab JJ, Carmichael ST (2008) Poststroke neurogenesis: emerging principles of migration and localization of immature neurons. *The Neuroscientist* **14**: 369-380
- Okun E, Griffioen KJ, Lathia JD, Tang S-C, Mattson MP, Arumugam TV (2009) Toll-like receptors in neurodegeneration. *Brain Research Reviews* **59**: 278-292
- Olesen R, Wejse C, Velez DR, Bisseye C, Sodemann M, Aaby P, Rabna P, Worwui A, Chapman H, Diatta M, Adegbola RA, Hill PC, Ostergaard L, Williams SM, Sirugo G (2007) DC-SIGN (CD209), pentraxin 3 and vitamin D receptor gene variants associate with pulmonary tuberculosis risk in West Africans. *Genes Immun* **8**: 456-467
- Orlowski P, Chappell M, Park CS, Grau V, Payne S (2011) Modelling of pH dynamics in brain cells after stroke. *Interface Focus* **1**: 408-416
- Perry VH, O'Connor V (2010) The role of microglia in synaptic stripping and synaptic degeneration: a revised perspective. *ASN Neuro* **2**: 281-291
- Piccinini AM, Midwood KS (2010) DAMPening inflammation by modulating TLR signalling. *Mediators of Inflammation* **2010**: 1-21
- Pinteaux E, Parker LC, Rothwell NJ, Luheshi GN (2002a) Expression of interleukin-1 receptors and their role in interleukin-1 actions in murine microglial cells. *Journal of Neurochemistry* **83**: 754-763
- Pinteaux E, Parker LC, Rothwell NJ, Luheshi GN (2002b) Expression of interleukin-1 receptors and their role in interleukin-1 actions in murine microglial cells. *Journal of neurochemistry* **83**: 754-763
- Pinteaux E, Trotter P, Simi A (2009) Cell-specific and concentration-dependent actions of interleukin-1 in acute brain inflammation. *Cytokine* **45**: 1-7
- Polazzi E, Monti B (2010) Microglia and neuroprotection: from in vitro studies to therapeutic applications. *Progress in Neurobiology* **92**: 293-315

Polentarutti N, Bottazzi B, Di Santo E, Blasi E, Agnello D, Ghezzi P, Introna M, Bartfai T, Richards G, Mantovani A (2000) Inducible expression of the long pentraxin PTX3 in the central nervous system. *Journal of Neuroimmunology* **106**: 87-94

Preston M, Sherman LS (2011) Neural stem cell niches: roles for the hyaluronan-based extracellular matrix. *Front Biosci* **3**:1165-1179

Price CJ, Menon DK, Peters AM, Ballinger JR, Barber RW, Balan KK, Lynch A, Xuereb JH, Fryer T, Guadagno JV, Warburton EA (2004) Cerebral neutrophil recruitment, histology, and outcome in acute ischemic stroke: an imaging-based study. *Stroke* **35**: 1659-1664

Rahpeymai Y, Hietala MA, Wilhelmsson U, Fotheringham A, Davies I, Nilsson AK, Zwirner J, Wetsel RA, Gerard C, Pekny M, Pekna M (2006) Complement: a novel factor in basal and ischemia-induced neurogenesis. *EMBO J*. **25**: 1364-74

Ravizza T, Moneta D, Bottazzi B, Peri G, Garlanda C, Hirsch E, Richards GJ, Mantovani A, Vezzani A (2001) Dynamic induction of the long pentraxin PTX3 in the CNS after limbic seizures: evidence for a protective role in seizure-induced neurodegeneration. *Neuroscience* **105**: 43-53

Reading PC, Bozza S, Gilbertson B, Tate M, Moretti S, Job ER, Crouch EC, Brooks AG, Brown LE, Bottazzi B, Romani L, Mantovani A (2008) Antiviral activity of the long chain pentraxin PTX3 against influenza viruses. *The Journal of Immunology* **180**: 3391-3398

Relton JK, Rothwell NJ (1992) Interleukin-1 receptor antagonist inhibits ischaemic and excitotoxic neuronal damage in the rat. *Brain Research Bulletin* **29**: 243-246

Reynolds BA, Weiss S (1992) Generation of neurons and astrocytes from isolated cells of the adult mammalian central nervous system. *Science* **255**: 1707-1710

Ribeiro Mde C, Hirt L, Bogousslavsky J, Regli L, Badaut J (2006) Time course of aquaporin expression after transient focal cerebral ischemia in mice. *J Neurosci Res* **83**: 1231-1240

Rodriguez-Grande B, Blackabey V, Gittens B, Pinteaux E, Denes A (2013) Loss of substance P and inflammation precede delayed neurodegeneration in the substantia nigra after cerebral ischemia. *Brain, Behavior, and Immunity* **29**: 51-61

Rodriguez-Grande B, Swana M, Nguyen L, Englezou P, Maysami S, Allan SM, Rothwell NJ, Garlanda C, Denes A, Pinteaux E (2014) The acute-phase protein PTX3 is an essential mediator of glial scar formation and resolution of brain edema after ischemic injury. *J Cereb Blood Flow Metab* **34**:480-488

Rolls A, Shechter R, Schwartz M (2009) The bright side of the glial scar in CNS repair. *Nat Rev Neurosci* **10**: 235-241

- Rolph MS, Zimmer S, Bottazzi B, Garlanda C, Mantovani A, Hansson GK (2002) Production of the long pentraxin PTX3 in advanced atherosclerotic plaques. *Arteriosclerosis, Thrombosis, and Vascular Biology* **22**: 10-14
- Rosenberg GA (2002) Matrix metalloproteinases in neuroinflammation. *Glia* **39**: 279-291
- Rovere P, Peri G, Fazzini F, Bottazzi B, Doni A, Bondanza A, Zimmermann VS, Garlanda C, Fascio U, Sabbadini MG, Rugarli C, Mantovani A, Manfredi AA (2000) The long pentraxin PTX3 binds to apoptotic cells and regulates their clearance by antigen-presenting dendritic cells. *Blood* **96**: 4300-4306
- Ruhul Amin AR, Senga T, Oo ML, Thant AA, Hamaguchi M (2003) Secretion of matrix metalloproteinase-9 by the proinflammatory cytokine, IL-1beta: a role for the dual signalling pathways, Akt and Erk. *Genes Cells* **8**: 515-523
- Rusnati M, Camozzi M, Moroni E, Bottazzi B, Peri G, Indraccolo S, Amadori A, Mantovani A, Presta M (2004) Selective recognition of fibroblast growth factor-2 by the long pentraxin PTX3 inhibits angiogenesis. *Blood* **104**: 92-99
- Rymo SF, Gerhardt H, Wolfhagen Sand F, Lang R, Uv A, Betsholtz C (2011) A two-way communication between microglial cells and angiogenic sprouts regulates angiogenesis in aortic ring cultures. *PLoS One* **6**: e15846
- Ryu W-S, Kim CK, Kim BJ, Kim C, Lee S-H, Yoon B-W (2012) Pentraxin 3: A novel and independent prognostic marker in ischemic stroke. *Atherosclerosis* **220**: 581-586
- Saklayen SS, Mabrouk OS, Pehek EA (2004) Negative feedback regulation of nigrostriatal dopamine release: mediation by striatal D1 receptors. *The Journal of Pharmacology and Experimental Therapeutics* **311**: 342-348
- Salazar J, Martinez MS, Chavez M, Toledo A, Anez R, Torres Y, Apruzzese V, Silva C, Rojas J, Bermudez V (2014) C-reactive protein: clinical and epidemiological perspectives. *Cardiol Res Pract* **2014**: 1-10
- Salio M, Chimenti S, De Angelis N, Molla F, Maina V, Nebuloni M, Pasqualini F, Latini R, Garlanda C, Mantovani A (2008) Cardioprotective function of the long pentraxin PTX3 in acute myocardial infarction. *Circulation* **117**: 1055-1064
- Salustri A, Garlanda C, Hirsch E, De Acetis M, Maccagno A, Bottazzi B, Doni A, Bastone A, Mantovani G, Peccoz PB, Salvatori G, Mahoney DJ, Day AJ, Siracusa G, Romani L, Mantovani A (2004) PTX3 plays a key role in the organization of the cumulus oophorus extracellular matrix and in in vivo fertilization. *Development* **131**: 1577-1586
- Savchenko AS, Inoue A, Ohashi R, Jiang S, Hasegawa G, Tanaka T, Hamakubo T, Kodama T, Aoyagi Y, Ushiki T, Naito M (2011) Long pentraxin 3 (PTX3) expression and release by neutrophils in vitro and in ulcerative colitis. *Pathology International* **61**: 290-297

- Scarchilli L, Camaioni A, Bottazzi B, Negri V, Doni A, Deban L, Bastone A, Salvatori G, Mantovani A, Siracusa G, Salustri A (2007) PTX3 Interacts with Inter- α -trypsin Inhibitor. *The Journal of Biological Chemistry* **282**: 30161-30170
- Schabitz WR, Steigleder T, Cooper-Kuhn CM, Schwab S, Sommer C, Schneider A, Kuhn HG (2007) Intravenous brain-derived neurotrophic factor enhances poststroke sensorimotor recovery and stimulates neurogenesis. *Stroke* **38**: 2165-2172
- Schilling M, Besselmann M, Leonhard C, Mueller M, Ringelstein EB, Kiefer R (2003) Microglial activation precedes and predominates over macrophage infiltration in transient focal cerebral ischemia: a study in green fluorescent protein transgenic bone marrow chimeric mice. *Exp Neurol* **183**: 25-33
- Schilling M, Besselmann M, Muller M, Strecker JK, Ringelstein EB, Kiefer R (2005) Predominant phagocytic activity of resident microglia over hematogenous macrophages following transient focal cerebral ischemia: an investigation using green fluorescent protein transgenic bone marrow chimeric mice. *Exp Neurol* **196**: 290-297
- Schwartz M (2003) Macrophages and microglia in central nervous system injury [colon] are they helpful or harmful? *J Cereb Blood Flow Metab* **23**: 385-394
- Schwindt TT, Motta FL, Filoso Barnabes G, Goncalves Massant C, de Oliveira Guimaraes A, Calcagnotto ME, Silva Conceisao F, Bosco Pesquero J, Rehen S, Mello LE (2009) Short-term withdrawal of mitogens prior to plating increases neuronal differentiation of human neural precursor cells. *PLoS ONE* **4**: e4642
- Sciacca P, Betta P, Mattia C, Li Volti G, Frigiola A, Curreri S, Amato M, Distefano G (2010) Pentraxin-3 in late-preterm newborns with hypoxic respiratory failure. *Front Biosci (Elite Ed)* **2**: 805-809
- Seaberg RM, van der Kooy D (2002) Adult Rodent Neurogenic Regions: The Ventricular Subependyma Contains Neural Stem Cells, But the Dentate Gyrus Contains Restricted Progenitors. *The Journal of Neuroscience* **22**: 1784-1793
- Shafer LL MJ, Young MR (2002) Brain activation of monocyte lineage cells: brain-derived soluble factors differentially regulate BV2 microglia and peripheral macrophage immune functions. *Neuroimmunomodulation* **10**: 283-294
- Sims JE, March CJ, Cosman D, Widmer MB, MacDonald HR, McMahan CJ, Grubin CE, Wignall JM, Jackson JL, Call SM, *et al.* (1988) cDNA expression cloning of the IL-1 receptor, a member of the immunoglobulin superfamily. *Science* **241**: 585-589
- Sinor AD, Irvin SM, Cobbs CS, Chen J, Graham SH, Greenberg DA (1998) Hypoxic induction of vascular endothelial growth factor (VEGF) protein in astroglial cultures. *Brain Res* **812**: 289-291

Skopal J, Turbucz P, Vastag M, Bori Z, Pek M, deChatel R, Nagy Z, Toth M, Karadi I (1998) Regulation of endothelin release from human brain microvessel endothelial cells. *J Cardiovasc Pharmacol* **31 suppl 1**: S370-372

Slevin M, Kumar P, Gaffney J, Kumar S, Krupinski J (2006) Can angiogenesis be exploited to improve stroke outcome? Mechanisms and. *Clin Sci (Lond)* **111**: 171-183

Smith CJ, Lawrence CB, Rodriguez-Grande B, Kovacs KJ, Pradillo JM, Denes A (2013) The immune system in stroke: clinical challenges and their translation to experimental research. *J Neuroimmune Pharmacol* **8**: 867-887

Soeki T, Niki T, Kusunose K, Bando S, Hirata Y, Tomita N, Yamaguchi K, Koshiba K, Yagi S, Taketani Y, Iwase T, Yamada H, Wakatsuki T, Akaike M, Sata M (2011) Elevated concentrations of pentraxin 3 are associated with coronary plaque vulnerability. *Journal of Cardiology* **58**: 151-157

Spasova MS, Sadowska GB, Threlkeld SW, Lim YP, Stonestreet BS. (2014) Ontogeny of inter-alpha inhibitor proteins in ovine brain and somatic tissues. *Exp Biol Med* **239**: 724-736

Stoll G, Jander S, Schroeter M (1998) Inflammation and glial responses in ischemic brain lesions. *Progress in Neurobiology* **56**: 149-171

Struve J, Maher PC, Li YQ, Kinney S, Fehlings MG, Kuntz C 4th, Sherman LSS (2005) Disruption of the hyaluronan-based extracellular matrix in spinal cord promotes astrocyte proliferation. *Glia* **52**: 16-24.

Sun X, Zhang Q-W, Xu M, Guo J-J, Shen S-W, Wang Y-Q, Sun F-Y (2011) New striatal neurons form projections to substantia nigra in adult rat brain after stroke. *Neurobiology of Disease* **45**: 601-609

Swanson RA, Farrell K, Stein BA (1997) Astrocyte energetics, function, and death under conditions of incomplete ischemia: a mechanism of glial death in the penumbra. *Glia* **21**: 142-153

http://swissmodel.expasy.org/repository/?pid=smr03&mid=md1b620c5796649222ad44fffd826a84e_s182_e375_t3pvn&query_1_input=P26022

Tanaka J, Toku K, Zhang B, Ishihara K, Sakanaka M, Maeda N (1999) Astrocytes prevent neuronal death induced by reactive oxygen and nitrogen species. *Glia* **28**: 85-96

Tansey MG, McCoy MK, Frank-Cannon TC (2007) Neuroinflammatory mechanisms in Parkinson's disease: potential environmental triggers, pathways, and targets for early therapeutic intervention. *Experimental Neurology* **208**: 1-25

Thornton E, Vink R (2012) Treatment with a substance P receptor antagonist is neuroprotective in the intrastriatal 6-hydroxydopamine model of early Parkinson's disease. *PLoS ONE* **7**: e34138

- Thyboll J, Korttesmaa J, Cao R, Soininen R, Wang L, Iivanainen A, Sorokin L, Risling Mr, Cao Y, Tryggvason K (2002) Deletion of the laminin α 4 chain leads to impaired microvessel maturation. *Molecular and cellular Biology* **22**: 1194-1202
- Todd G, Kimber TE, Ridding MC, Semmler JG (2010) Reduced motor cortex plasticity following inhibitory rTMS in older adults. *Clin Neurophysiol* **121**: 441-447
- Tranguch S, Chakrabarty A, Guo Y, Wang H, Dey SK (2007) Maternal pentraxin 3 deficiency compromises implantation in mice. *Biology of Reproduction* **77**: 425-432
- Tropepe V, Sibilina M, Ciruna BG, Rossant J, Wagner EF, van der Kooy D (1999) Distinct neural stem cells proliferate in response to EGF and FGF in the developing mouse telencephalon. *Developmental Biology* **208**: 166-188
- Turner RJ, Blumbergs PC, Sims NR, Helps SC, Rodgers KM, Vink R (2006) Increased substance P immunoreactivity and edema formation following reversible ischemic stroke. *Acta Neurochir Suppl* **96**: 263-266
- Turner RJ, Helps SC, Thornton E, Vink R (2011) A substance P antagonist improves outcome when administered 4 h after onset of ischaemic stroke. *Brain Research* **1393**: 84-90
- Uchida H, Yokoyama H, Kimoto H, Kato H, Araki T (2010) Long-term changes in the ipsilateral substantia nigra after transient focal cerebral ischaemia in rats. *International Journal of Experimental Pathology* **91**: 256-266
- Wang MY, Ji SR, Bai CJ, El Kebir D, Li HY, Shi JM, Zhu W, Costantino S, Zhou HH, Potempa LA, Zhao J, Filep JG, Wu Y (2011) A redox switch in C-reactive protein modulates activation of endothelial cells. *Faseb j* **25**: 3186-3196
- Wheeler RD, Boutin H, Touzani O, Luheshi GN, Takeda K, Rothwell NJ (2003) No role for interleukin-18 in acute murine stroke-induced brain injury. *J Cereb Blood Flow Metab* **23**: 531-535
- Whitney NP, Eidem TM, Peng H, Huang Y, Zheng JC (2009) Inflammation mediates varying effects in neurogenesis: relevance to the pathogenesis of brain injury and neurodegenerative disorders. *Journal of Neurochemistry* **108**: 1343-1359
- Whitty CJ, Paul MA, Bannon MJ (1997) Neurokinin receptor mRNA localization in human midbrain dopamine neurons. *The Journal of Comparative Neurology* **382**: 394-400
- Wilson JX (1997) Antioxidant defense of the brain: a role for astrocytes. *Can J Physiol Pharmacol* **75**: 1149-1163
- Windgassen EB, Funtowicz L, Lunsford TN, Harris LA, Mulvagh SL (2011) C-reactive protein and high-sensitivity C-reactive protein: an update for clinicians. *Postgrad Med* **123**: 114-119

- Wissel J, Olver J, Sunnerhagen KS (2011) Navigating the poststroke continuum of care. *Journal of Stroke and Cerebrovascular Diseases* **22**: 1-8
- Wuestefeld R, Chen J, Meller K, Brand-Saberi B, Theiss C (2012) Impact of vegf on astrocytes: analysis of gap junctional intercellular communication, proliferation, and motility. *Glia* **60**: 936-947
- Yamada K, Goto S, Yoshikawa M, Ushio Y (1996) Gabaergic transmission and tyrosine hydroxylase expression in the nigral dopaminergic neurons: an in vivo study using a reversible ischemia model of rats. *Neuroscience* **73**: 783-789
- Yemisci M, Gursoy-Ozdemir Y, Vural A, Can A, Topalkara K, Dalkara T (2009) Pericyte contraction induced by oxidative-nitrative stress impairs capillary reflow despite successful opening of an occluded cerebral artery. *Nat Med* **15**: 1031-1037
- Zanier E, Brandi G, Peri G, Longhi L, Zoerle T, Tettamanti M, Garlanda C, Sigurtà A, Valaperta S, Mantovani A, De Simoni M, Stocchetti N (2010) Cerebrospinal fluid pentraxin 3 early after subarachnoid hemorrhage is associated with vasospasm. *Intensive Care Medicine* **37**: 302-309
- Zaremba J, Losy J (2002) Adhesion molecules of immunoglobulin gene superfamily in stroke. *Folia Morphol (Warsz)* **61**: 1-6
- Zelenina M (2010) Regulation of brain aquaporins. *Neurochem Int* **57**: 468-488
- Zhang RL, Zhang ZG, Chopp M (2005) Neurogenesis in the adult ischemic brain: generation, migration, survival, and restorative therapy. *The Neuroscientist* **11**: 408-416
- Zhang S, Zhu YT, Chen SY, He H, Tseng SC (2014) Constitutive expression of pentraxin 3 (PTX3) protein by human amniotic membrane cells leads to formation of the heavy chain (HC)-hyaluronan (HA)-PTX3 complex. *J Biol Chem* **289**: 13531-13542
- Zhang ZG, Zhang L, Jiang Q, Zhang R, Davies K, Powers C, Bruggen N, Chopp M (2000) VEGF enhances angiogenesis and promotes blood-brain barrier leakage in the ischemic brain. *J Clin Invest* **106**: 829-838
- Zhao Y, Rempe DA (2010) Targeting astrocytes for stroke therapy. *Neurotherapeutics* **7**: 439-451
- Zhou J, van Zijl PC (2011) Defining an acidosis-based ischemic penumbra from pH-weighted MRI. *Transl Stroke Res* **3**: 76-83
- Ziv Y, Schwartz M (2008) Orchestrating brain-cell renewal: the role of immune cells in adult neurogenesis in health and disease. *Trends in Molecular Medicine* **14**: 471-478

